SERI/STR-253-3212
DE87012281

September 1987

Mean and Peak Wind Load Reduction on Heliostats

Colorado State University
Fort Collins, Colorado

Prepared under Subcontract No. XK-6-06034-1

Solar Energy Research Institute
A Division of Midwest Research Institute

1617 Cole Boulevard
Golden, Colorado 80401-3393

Operated for the
U.S. Department of Energy
under Contract No. DE-AC02-83CH10093

SERI/STR-253-3212
UC Category: 62a
DE87012281

Mean and Peak Wind Load Reduction on Heliostats

Colorado State University
Fort Collins, Colorado

September 1987

Prepared under Subcontract No. XK-6-06034-1

SERI Technical Monitor: Al Lewandowski

Solar Energy Research Institute
A Division of Midwest Research Institute

1617 Cole Boulevard
Golden, Colorado 80401-3393

Prepared for the
U.S. Department of Energy
Contract No. DE-AC02-83CH10093

NOTICE

Printed in the United States of America
Available from:
National Technical Information Service
U.S. Department of Commerce
5285 Port Royal Road
Springfield, VA 22161

Price: Microfiche A01
Printed Copy A11

Codes are used for pricing all publications. The code is determined by the number of pages in the publication. Information pertaining to the pricing codes can be found in the current issue of the following publications, which are generally available in most libraries. *Energy Research Abstracts, (ERA); Government Reports, Announcements* and Index (*GRA* and I): *Scientific and Technical Abstract Reports (STAR);* and publication NTIS-PR-360 available from NTIS at the above address.

FOREWORD

The research and development described in this document was conducted within the U.S. Department of Energy's Solar Thermal Technology Program. The goal of this program is to advance the engineering and scientific understanding of solar thermal technology and to establish the technology base from which private industry can develop solar thermal power production options for introduction into the competitive energy market.

Solar thermal technology concentrates the solar flux using tracking mirrors or lenses onto a receiver where the solar energy is absorbed as heat and converted into electricity or incorporated into products as process heat. The two primary solar thermal technologies, central receivers and distributed receivers, employ various point and line-focus optics to concentrate sunlight. Current central receiver systems use fields of heliostats (two-axis tracking mirrors) to focus the sun's radiant energy onto a single, tower-mounted receiver. Point focus concentrators up to 17 meters in diameter track the sun in two axes and use parabolic dish mirrors or Fresnel lenses to focus radiant energy onto a receiver. Troughs and bowls are line-focus tracking reflectors that concentrate sunlight onto receiver tubes along their focal lines. Concentrating collector modules can be used alone or in a multimodule system. The concentrated radiant energy absorbed by the solar thermal receiver is transported to the conversion process by a circulating working fluid. Receiver temperatures range from 100°C in low-temperature troughs to over 1500°C in dish and central receiver systems.

The Solar Thermal Technology Program is directing efforts to advance and improve each system concept through solar thermal materials, components, and subsystems research and development and by testing and evaluation. These efforts are carried out with the technical direction of DOE and its network of field laboratories that works with private industry. Together they have established a comprehensive, goal-directed program to improve performance and provide technically proven options for eventual incorporation into the Nation's energy supply.

To successfully contribute to an adequate energy supply at reasonable cost, solar thermal energy must be economically competitive with a variety of other energy sources. The Solar Thermal Program has developed components and system-level performance targets as quantitative program goals. These targets are used in planning research and development activities, measuring progress, assessing alternative technology options, and developing optimal components. These targets will be pursued vigorously to ensure a successful program.

This report presents the results of wind-tunnel tests supported through the Solar Energy Research Institute (SERI) by the Office of Solar Thermal Technology of the U.S. Department of Energy as part of the SERI research effort on innovative concentrators. As gravity loads on drive mechanisms are reduced through stretched-membrane technology, the wind-load contribution of the required drive capacity increases in percentage. Reduction of wind loads can provide economy in support structure and heliostat drive. Wind-tunnel tests have been directed at finding methods to reduce wind loads on heliostats. The tests investigated primarily the mean and peak forces and moments. A significant increase in ability to predict peak heliostat wind loads and their reduction within a heliostat field was achieved.

The work reported here was monitored by L. M. Murphy and A. Lewandowski of SERI.

This report was authored by J.A. Peterka, Professor; Z. Tan, Graduate Student; B. Bienkiewicz, Assistant Professor; and J.E. Cermak, University Distinguished Professor; Fluid Mechanics and Wind Engineering Program, Fluid Dynamics and Diffusion Laboratory, Colorado State University, Fort Collins, Colorado.

Approved for

SOLAR ENERGY RESEARCH INSTITUTE

L. M. Murphy, Manager
Thermal Systems Research Branch

A. Lewandowski
Thermal Systems Research Branch

G. C. Groff, Director
Solar Heat Research Division

SUMMARY

The purpose of this study was to define wind load reduction factors for heliostats within a field of heliostats. The wind load reduction factors applied to both mean and peak wind loads and account for the protective effects of upwind heliostats, wind protective fences, or other blockage elements. The reason for finding methods to reduce wind loads is to improve the economy of heliostat support structures and drive mechanisms. These elements will become more sensitive to wind loads as gravity loads decrease through stretched membrane or other innovative technology. The method used in the study was to generalize wind load data obtained during tests on model heliostats placed in a modeled atmospheric wind in a boundary-layer wind tunnel.

Previous wind-tunnel test results had shown that mean wind load decreases due to upwind blockage from nearby heliostats or wind-protective fences could be systematically accounted for with a simple 'generalized blockage area' concept. In this study, the results were extended to include peak wind loads and to include more field geometries. In addition, results were extended to round as well as square shaped heliostats to demonstrate the use of the wind load reduction factors for stretched membrane modules. The use of porosity at the edge of a heliostat was investigated as a possible load reduction mechanism.

Wind loads on isolated heliostats were determined for a range of approach wind turbulence intensities characteristic of those found in open-country environments. The results of this test were expected to show small variations in load with turbulence intensity. However, the drag and lift components showed a high and unexpected sensitivity to turbulence level when the heliostat was within about 45 degrees of perpendicular to the wind.

A key finding was that heliostats in operational orientations have higher wind loads than for survival winds in stow position if the heliostats are properly oriented to the wind. A review of past wind load analyses for parabolic solar collectors was made to determine whether or not additional measurements were required for parabolic collectors. Insufficient data for adequate design decisions were found. The following conclusions were drawn from the study:

- The influence of upwind blockage of heliostats or wind fences can be accounted for by defining a generalized blockage area (GBA) so that the specific geometry may be ignored.

- Both mean and peak wind loads decrease significantly with increasing GBA except for very small GBA characteristic of heliostats in very open fields or of heliostats in the first two rows at the field edge.

- Wind fences at 45 degrees to the approach wind are less effective than wind fences perpendicular to the wind. Wind blockage elements (fences) whose length to height ratio is one or two are likely to be more effective than longer ones.

- Wind drag and lift on isolated heliostats have shown a surprising sensitivity to turbulence in the wind within the range expected for open-country environments.

- Square and circular heliostats have similar mean and peak wind load coefficients.

- Peak wind loads on operational heliostats are larger than those on heliostats in survival stow position provided that the heliostat in stow is rotated so that the elevation rotation axis points into the wind.

- Fluctuating loads about a near zero mean load in stow position may create fatigue loading more severe than for operational loads for some load components.

- Heliostats with porous edges do not provide effective load reductions for either mean or peak wind loads.

- Some data in uniform flow exists for wind loads on parabolic collectors, but insufficient data is available for adequate design decisions.

The following recommendations for future work were made:

- The effects of approach wind turbulence should be explored to determine the range of isolated collector load expected in typical installation environments. This recommendation is in response to the unexpected sensitivity to turbulence uncovered in this study.

- With resolution of the turbulence issue, a simplified design guide should be prepared for use in preliminary field design.

- Peak wind loads on flat heliostats in stow position should be examined more closely to determine the nature of fatigue loading.

- Mean and peak wind loads on parabolic collectors should be obtained in both isolated and field environments to determine differences between flat and parabolic shapes.

ACKNOWLEDGEMENTS

The authors wish to express their gratitude to the staff and personnel of the Fluid Dynamics and Diffusion Laboratory at Colorado State University. Special thanks go to Mr. Q. Roberts, who drafted most of the illustrations found in this report, and Mr. D. Boyajian, who offered great assistance with data acquisition. Sincere gratitude is extended to Mrs. Gloria Burns for typing and compiling this report.

Appreciation is herewith presented to the Solar Energy Research Institute (SERI) operated for the U. S. Department of Energy under Contract No. XK-6-06034-1.

TABLE OF CONTENTS

LIST OF TABLES

LIST OF FIGURES

Figure | Page

NOMENCLATURE

Symbol	Definition
A	1) actual surface area, and 2) constant
A_B	area of blockage elements projected onto a plane perpendicular to approach wind direction
A_F	field area containing blocking elements used for A_B
A_{fence}	fence solid area
$A_{gross,actual,mirror}$	gross, actual or mirror area for edge-porous model
A_{ref}	reference area for force and moment coefficients
B	constant
BL	boundary layer
C	constant
C_{cp}	eccentricity coefficient
$C_{Fx,y,z,N}(HCL)$	force coefficient, $\frac{Fx,y,z,N}{(q(HCL))(A)}$
$C_{Mx,y,z,Hx,Hy}(HCL,H)$	moment coefficient, $\frac{Mx,y,z,Hx,Hy}{(q(HCL))(A)(HCL)}$
$C_{Mx,y,z,Hx,Hy}(HCL,HCL)$	moment coefficient, $\frac{Mx,y,z,Hx,Hy}{(q(HCL))(A)(HCL)}$
d	diameter of parabolic collector
D	distance between EF and heliostats at the first row
E	hot-wire output voltage
EF	external fence
f	frequency, Hz
$F_{x,y,z,N}$	measured force along axis x, y, z or heliostat surface normal N
GBA	generalized blockage area
h	depth of parabolic collector
H	heliostat chord

Symbol	Definition
H_f	height of external fence
H_{mirror}	heliostat chord of mirror area for edge-porous model
H_o	heliostat unit under consideration
Hx,Hy,z	coordinate system at the hinge
HCL	height of heliostat centerline (heliostat center)
IF	internal fence
K	constant
L_1	distance between heliostats in the EF direction
L_2	distance between heliostats across EF direction
L_x	integral length scale for turbulent flow
L_{ref}	reference length
M_o,M_p	moments for parabolic collector
$M_{x,y,z,Hx,Hy}$	measured moment about axis x, y, z, Hx and Hy
n	exponent of velocity profile
NN,N,W	gaps between heliostat rows
p	porosity of fences, fraction of total area which is open
q(HCL)	dynamic pressure of wind at height HCL, $\frac{1}{2} \rho U^2(HCL)$
SCT, SCT1, SCT2	data files listed in Appendix D
T	thickness of heliostat plate
Tu	turbulence intensity, percent; $(U_{rms}/U) \times 100$
U	mean wind velocity
$\frac{UD}{\nu}$	Reynolds number
U(HCL)	wind velocity at height HCL
U(z)	wind velocity at height z above ground
U_{ref}	wind velocity at reference height
U_{rms}	root-mean-square of velocity about U

Symbol	Definition
U_*	surface friction velocity
x,y,z	coordinate system at the base
z	height above ground
Z_0	roughness length
α	elevation angle
β	wind direction
$\gamma_{Fx,Fz,MHy,Mz}$	ratio of field load to isolated load for force or moment component
δ	boundary-layer thickness
ρ	density of air
ν	kinematic viscosity

Symbol Subscript	Definition
mean	mean value
peak	peak value
rms	root-mean-square about mean
ref	reference

SECTION 1.0

INTRODUCTION

An important knowledge base needed for the design and development of fields of tracking solar collectors is an understanding of mean and peak wind loads which act on individual units within the field. This knowledge base provides an important input into the cost effective design of conventional concentrators and low-cost designs which can be less resistant to wind loads than conventional designs. This input can provide a basis for systems studies aimed at optimizing energy production per unit cost. Thus, the effects of collector size, component strength for resisting wind loads, field density, and protective wind fences can be traded during field design to produce the most economical field.

Wind loads for current heliostat designs which support the heliostat at a single point are particularly critical since the tracking drive system also must support the gravity and applied wind loads. Thus, the magnitudes of forces and moments at the drive/support location are important.

Previous studies of heliostat wind loads have concentrated on measurement in a boundary layer wind tunnel of mean wind loads on isolated units and on units within a field. However, it is the peak loads which must be resisted. It is not evident that peak loads can be obtained by a quasi-static analysis using a peak gust speed in conjunction with load coefficients determined from mean wind and measured mean load. In this study, peak wind loads were measured directly.

A need has existed for a wind load formulation for fields of heliostats which will permit meaningful systems studies and preliminary field designs. This study has addressed that need by finding a set of load coefficient reductions which can be applied to a heliostat anywhere within a field and which predicts the reduction in wind load which is expected to occur due to protection of surrounding heliostats and protective wind fences. The load reduction coefficients were determined for both mean and peak wind loads for operational orientations of the heliostat.

Some experiments were made in this study to extend the range of wind turbulence intensity to the full range expected for an open-country environment. The purpose was to verify that this range of turbulence intensity would cause only minor changes in wind load. These experiments revealed an unexpected sensitivity to turbulence intensity in the range of typical atmospheric turbulence for drag and lift forces and suggest the need for additional study.

Structural failure due to wind load can be due to different mechanisms. One type is overstressing in which the peak stresses induced by the wind exceed the material capacity. Measurement of peak loads in this study provide a method for design against this type of failure. A second type of failure is fatigue in which a large number of loading cycles at less than material capacity can cause failure. Measurements of mean and peak loads partially solves that loading problem.

All experimental measurements in this report are for flat concentrator shapes. Parabolic concentrator shapes are expected to have somewhat different loading than flat plate geometries. A review of past wind load measurements is included in this report as a starting point for future work.

The main purpose of this study was to investigate the mean and peak wind loads on a single flat plate heliostat and a heliostat in a field of similar structures. The intent was to determine methods for decreasing the wind loads on heliostats below those values for an isolated heliostat. Both mean and peak loads were measured in a boundary layer wind tunnel capable of modeling the atmospheric boundary layer winds. No inertial response of the heliostats was assumed in this study. Six load components (three forces and three moments) are presented in non-dimensional coefficient form: C_{Fx}, C_{Fy}, C_{Fz}, C_{Mx}, C_{My} and C_{Mz}. The hinge moments (C_{MHy}) and centers of pressure (C_{cp}) are developed from these results.

Wind loads on a heliostat in a field are a function of heliostat orientation, field density, wind direction, and the presence of wind blockage elements other than the heliostats themselves. The wind load on a heliostat fluctuates about a mean value due to gusting in the approach winds, due to turbulence generated by upwind heliostats or fences and due to turbulence generated in the wake of the heliostat itself. For a structure which has little resonant response to the fluctuating wind load, peak design stresses will result from the peaks in the fluctuating wind load acting as a quasi-static load assuming that the bulk of the wind energy is at frequencies below the heliostat natural frequency. For a heliostat or collector which can undergo resonant response, the stresses to which the collector can be subjected will be larger than those induced by a quasi-static wind load since inertially driven stresses are present. For those cases, analysis beyond that presented herein would be necessary.

1.1 A REVIEW OF PREVIOUS WORK

The study of wind loads on ground based solar collectors has been extensive during recent years, [references 1 to 14]. These studies include: heliostats [references 1 and 2], photovoltaic collectors [references 3, 5 to 7, and 10 to 14] and parabolic trough collectors [references 4, 8 and 9]. Some other related studies have investigated roof mounted collectors [references 15 to 18] and dish antennas [references 19 to 21, and 40 to 42]. Reviews of some previous wind load studies are given in references [22 and 39].

The most recent study pertaining to the work in this report was performed by Peterka et al. [23] at the Fluid Dynamics and Diffusion Laboratory at Colorado State University. In that study, mean wind loads on heliostats within a field were compared to those for an isolated heliostat to determine load reductions to be expected within the field. In order to avoid explicitly analyzing the large number of dependent variables (heliostat azimuth and elevation angles, field layout geometry, protective wind fence geometry, and wind direction), a generalized blockage area (GBA) was defined to account for all upwind blockage in a single variable. While not all possible geometries were explored, the concept of a generalized blockage area appeared to work well for mean loads.

That report also measured some fluctuating loads -- sufficient to show that peak loads decreased within a field.

The current study expands upon and extends the work of Peterka [23]. Additional mean load cases were studied to expand the range of conditions for which the GBA concept is valid and extended the study to also cover measured peak loads.

1.2 DEFINITION OF THE GENERALIZED BLOCKAGE AREA (GBA)

The generalized blockage is defined as follows:

$GBA = A_B/A_F$ When the test array is deeper into the field than the second row or when an external fence is in place.

A_B = solid blockage area of a representative set of upwind heliostats added to the area of protective wind fences or other blockage elements projected onto a plane normal to the approach wind direction (see Figure 1-1).

A_F = the ground area occupied by the upwind blockage arrays included in the calculation of A_B.

Special cases are:

GBA = 0.01 When the test array is in the first row with no external fence.

GBA = 0.02 When the test array is in the second row with no external fence.

Because the generalized blockage area does not work strictly for the first two rows without fence, values of 0.01 and 0.02 were selected arbitrarily. These values provided a convenient method of representing these two rows in relation to the interior rows.

The definition of GBA can be simplified for the case when the external fence is not constructed (see Figure 1-2):

(a) Without internal fence,

A_B = the projection of the heliostat on to the normal to the approach wind direction.

A_F = the field area surrounding the arrays under consideration (see Figure 1-2).

(b) With internal fence,

A_B = the projection of the heliostats and the internal fence.

A_F = field area containing two heliostats and an internal fence (see Figure 1-2).

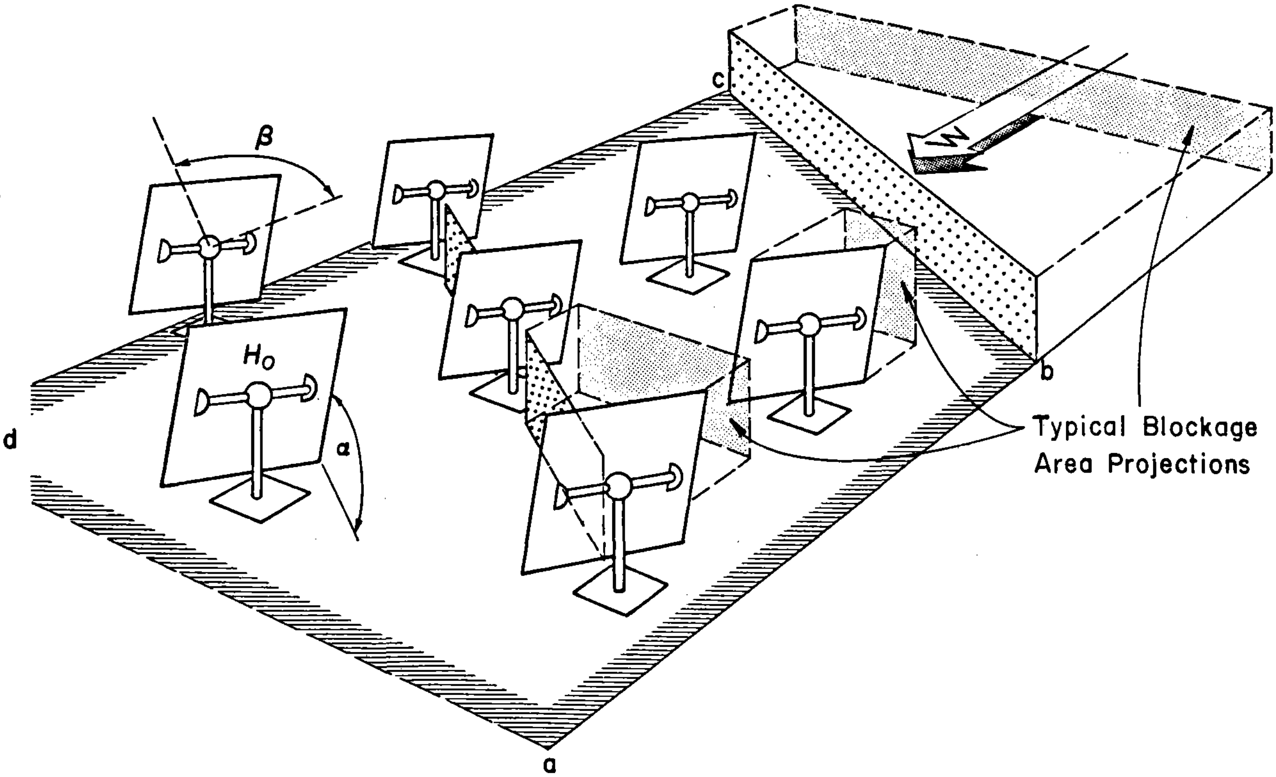

typ.

- Internal Fence
- External Fence
- Blockage Area for $H_O = A_B$
- Field Area (= a b c d) for $H_O = A_F$

A_B = Blockage Area Projected on Plane Perpendicular to Wind of all Blockage Elements in A_F

A_F = Field Area Containing Blocking Elements Used for A_B

Unit Under Consideration, H_O

H_O at First Row without External Fence, GBA = 0.01

H_O at Second Row without External Fence, GBA = 0.02

$$GBA = \text{Blockage Area } A_B / \text{Field Area } A_F$$

FIGURE 1-1. Definition of Generalized Blockage Area (GBA)

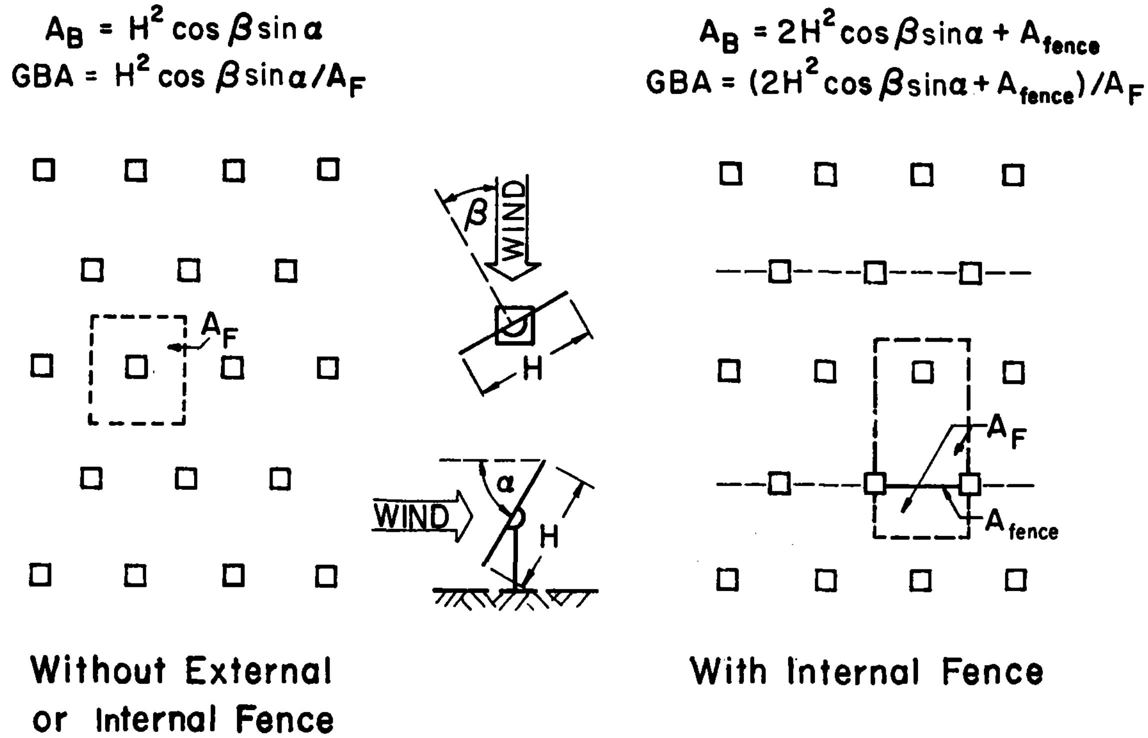

FIGURE 1-2. GBA Calculation Without External Fence

A special case arises for the case of a heliostat in the first or second row with an external fence. In that event, the calculation of GBA is performed as shown in Figure 1-3. For more details refer to the example calculations in Appendix C-2.

1.3 SIMULATION OF WIND LOADS IN THE WIND TUNNEL

Modeling of the aerodynamic loading on a structure requires special consideration of flow conditions in order to obtain similitude between model and prototype. In general, the requirements are that the model and prototype be geometrically similar, that the approach mean velocity have a vertical profile shape similar to the full-scale flow, that the turbulence characteristics of the flows be similar, and that the Reynolds number for the model and prototype be equal.

These criteria are satisfied by constructing a scale model of the structure and its surroundings and performing the wind tests in a wind tunnel specifically designed to model atmospheric boundary-layer flows. At large model scales of 1:20 to 1:100, some problems are encountered with exact modeling of the turbulence intensity. Further discussion of this issue and its impact on measured loads appears in following sections.

First Row

D = Distance between EF and Heliostat

L_1 = Distance between Heliostats in the EF Direction

H_f = EF Height, P = Porosity of EF

$$GBA = \frac{L_1 \times H_f \times (1-P)}{L_1 \times D} = \frac{H_f(1-P)}{D}$$

Second Row

L_2 = Distance between Heliostats Across EF Direction

H = Side Length of Square Heliostat

$$GBA = \frac{L_1 \times H_f \times (1-P) + H^2 \cos\beta \sin\alpha}{L_1(L_2 + D)}$$

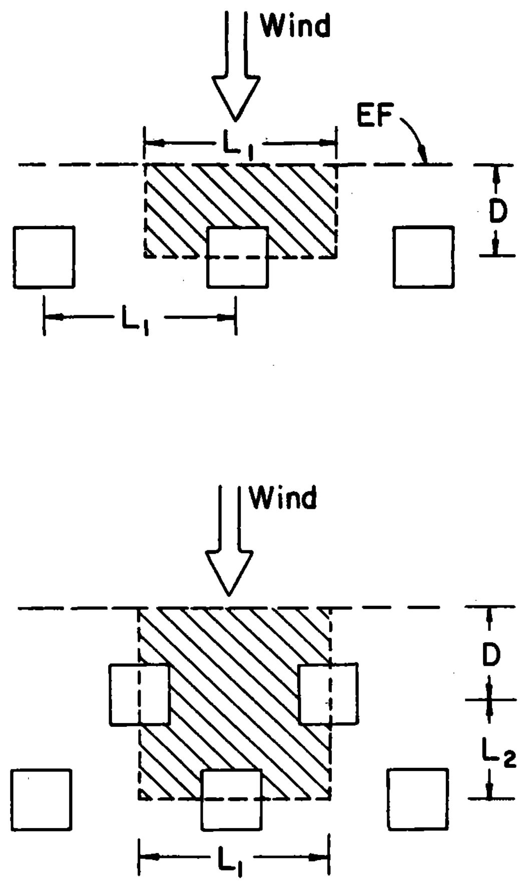

FIGURE 1-3. GBA Calculation With External Fence

Reynolds number similarity requires that the quantity UD/ν be similar for model and prototype. Since ν, the kinematic viscosity of air, is identical for both, Reynolds numbers cannot be made precisely equal with reasonable wind velocities. To accomplish this the air velocity in the wind tunnel would have to be as large as the model scale factor times the prototype wind velocity, a velocity which would introduce unacceptable compressibility effects. However, for sufficiently high Reynolds numbers ($>2\times10^4$) the pressure coefficient at any location on the structure will be essentially constant for a large range of Reynolds numbers.[6] Typical values encountered are 10^7-10^8 for the full-scale and 10^5-10^6 for the wind-tunnel model. In this range acceptable flow similarity is achieved without precise Reynolds number equality.

SECTION 2.0

EXPERIMENTAL APPARATUS AND PROCEDURES

2.1 THE WIND TUNNEL AND FORCE BALANCE

This study was performed at the Fluid Dynamics and Diffusion Laboratory of the Engineering Research Center at Colorado State University. All the data was collected in the Industrial Wind Tunnel, Figure 2-1.

The closed circuit Industrial Wind Tunnel is powered by a 56 kw electric induction motor connected to a sixteen blade propeller. The useful mean flow velocity may be varied from 0.3 to 25 m/s. A flexible roof permits a boundary layer flow to be developed with a zero pressure gradient to approximate the zero pressure gradient in atmospheric flows. Roughness elements on the wind tunnel floor and four spires at the entrance to the working section develop a velocity profile comparable to that found in an open country environment.

The force balance is a strain sensing apparatus mounted on the test section turntable, Figures 2-2 and 2-3. The lower strain gauges, Figure 2-2, are mounted in the base of the force balance and the upper gauges (see Figure 2-3) are mounted to the heliostat support post. Each set of gauges measures fluctuating moments about two horizontal and perpendicular axes through the gauge location. Differences in the moments at two elevations permit the forces to be obtained. Placing the upper gauges on the heliostat support post permits a more precise measurement of the hinge moment than can be obtained if both sets of gauges are below floor level. The vertical position of the plate centerline is given in this report as HCL (height of centerline = 152 mm). This centerline height represents 6.08 m if the model scale is taken as 1:40.

The turntable was mcunted to prevent contact with the wind-tunnel walls so that fan induced vibrations were minimized. In this study the turntable and balance maintained a constant orientation to the stationary wind tunnel. Variations in wind direction were achieved by rotating the heliostat on the fixed support pole. Thus the coordinate system used was wind-fixed, not body-fixed. Prior to presentation, the data was rotated to a body-fixed coordinate system.

A pitot-static tube was mounted upwind of the heliostat models to record the approach wind speed. The velocity was measured at the HCL height of 152 mm, the heliostat centerline. This velocity was used in the calculation of wind load coefficients.

2.2 THE MODELS AND FENCES

The three models shown in Figures 2-3 and 2-4 were made of 1/8 inch thick plywood: a square solid plate, a round solid plate and a square plate with porous edges. The solid square plate was used in both the single and in-field studies. The round plate was only used for a comparison with the single, square plate results. Similarly the porous-edged plate was only used to determine the effect of porosity for the single case when compared to the

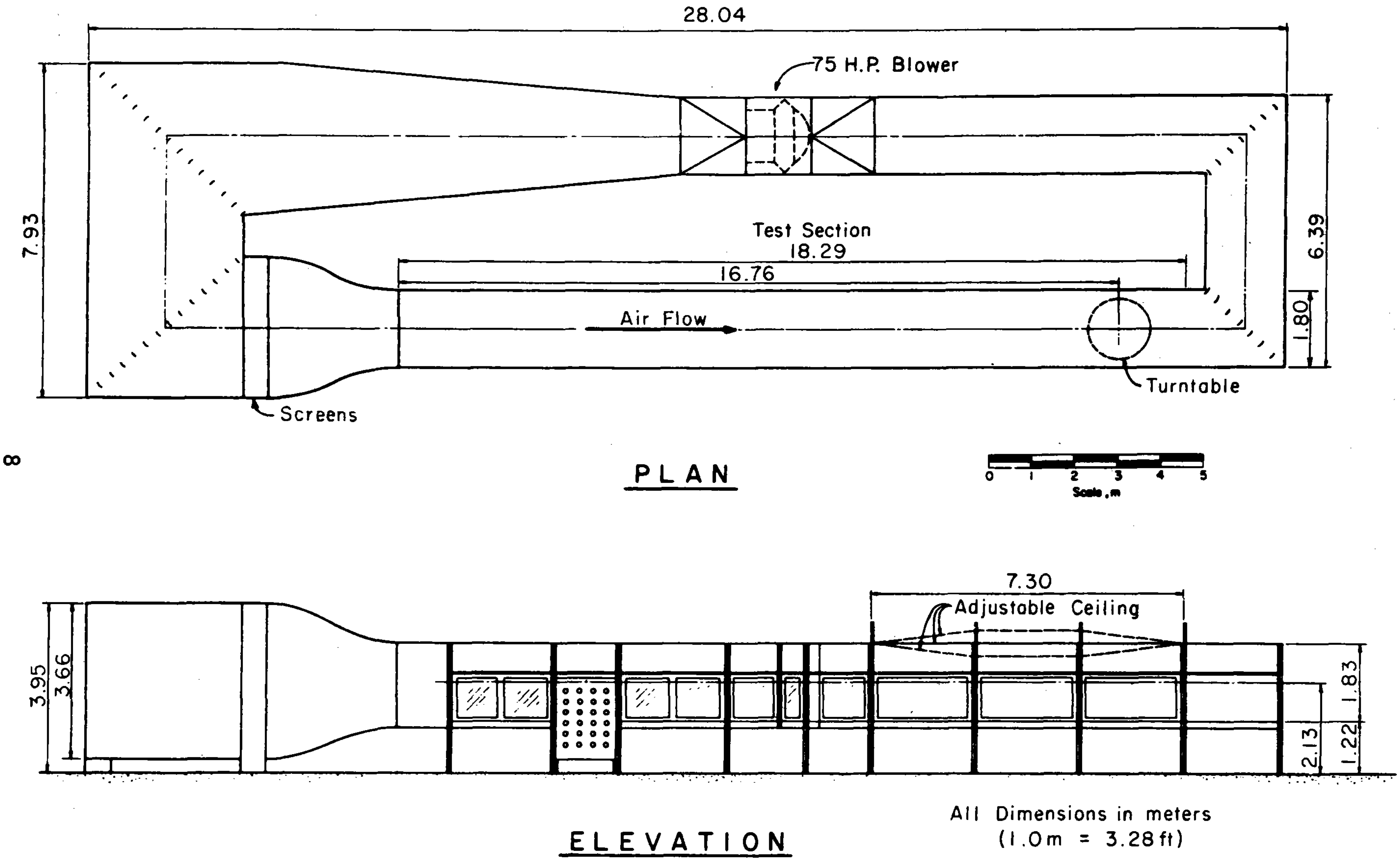

FIGURE 2-1. Industrial Aerodynamics Wind Tunnel, FDDL

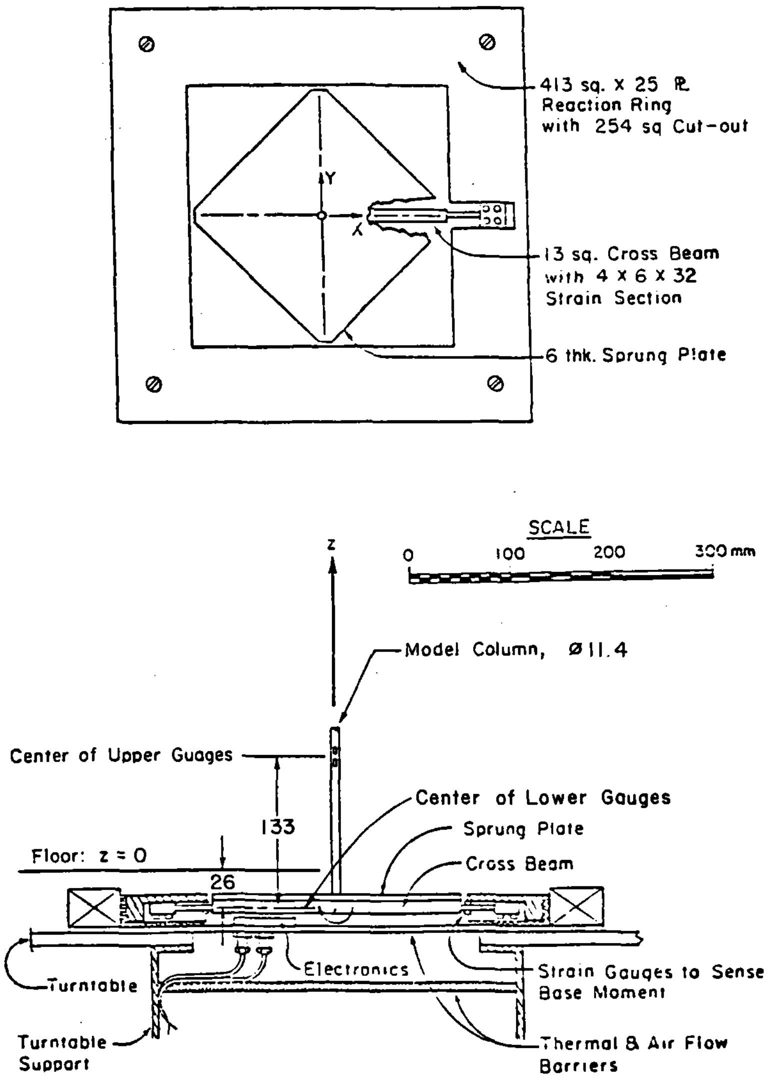

FIGURE 2-2. Force and Moment Balance

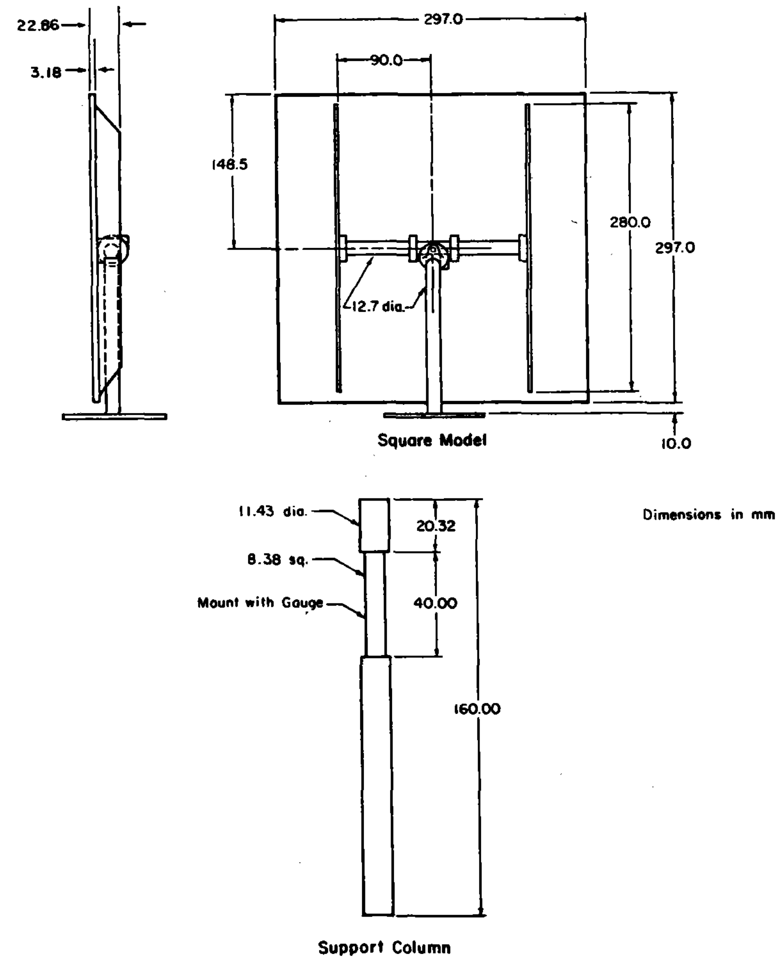

FIGURE 2-3. Square Model and Support Column

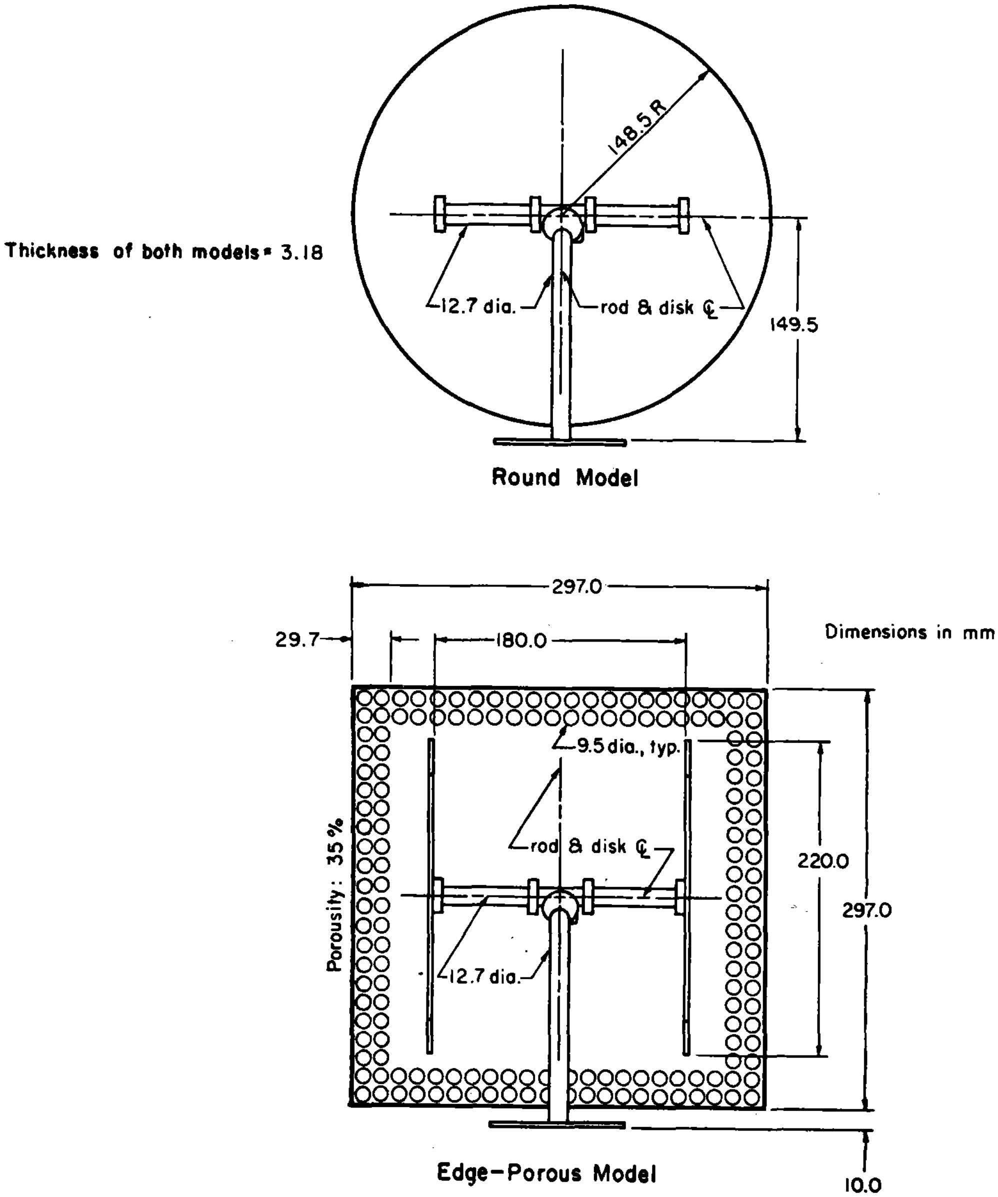

FIGURE 2-4. Round Model and Edge-porous Model

solid, square plate. The vertical post in all cases was aluminum (with strain gauges mounted near the top) and this was attached, via a standard clamp, to a horizontal plexiglass rod at the back of each plate.

Internal (within-field) and external (edge-of-field) fences (IF and EF) were made of the same material: a steel mesh with a porosity of approximately 40% (see Figure 2-5). A 20% change in the porosity of the fence gives a change of about 8% maximum in GBA value for heliostats in the 3rd row or deeper in the field. In the first or second row, the GBA changes in direct proportion to the porosity. The internal fence height was 159 mm (0.534 of the plate length, H) and the external fence height was 240 mm (0.80 of the plate length, H).

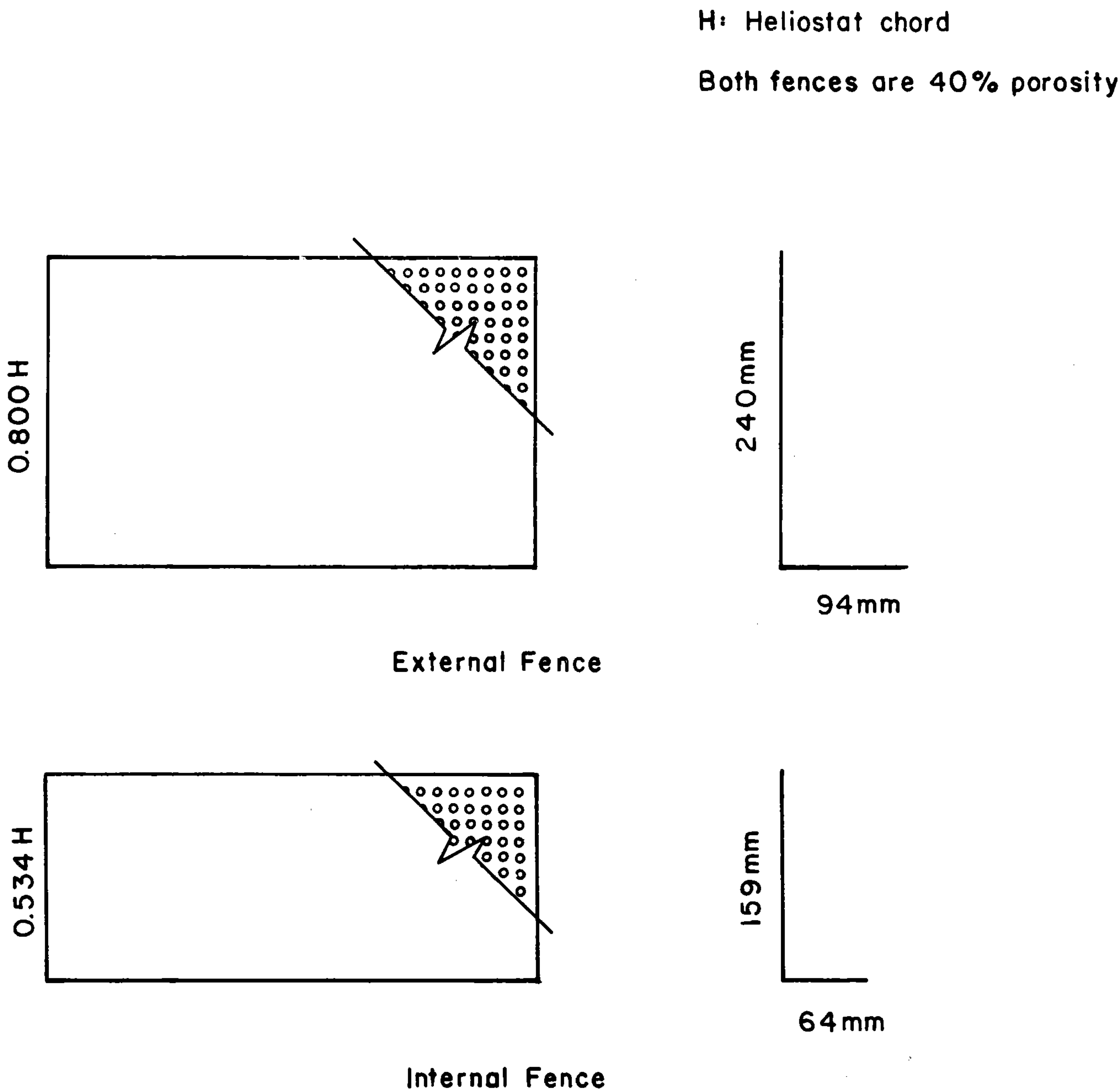

FIGURE 2-5. Dimensions for Fences

2.3 THE SPECTRA AND VELOCITY PROFILES

By using a light-weight plywood material for the plates, the natural frequency of the balance/model combination could be kept as high as possible.

1. The solid, square plate had a fundamental natural frequency on the balance of 41 Hz (see Figure 2-6a). The cutoff filter frequency was chosen as 32 Hz and the resulting moment spectrum in wind is shown in Figure 2-6b.

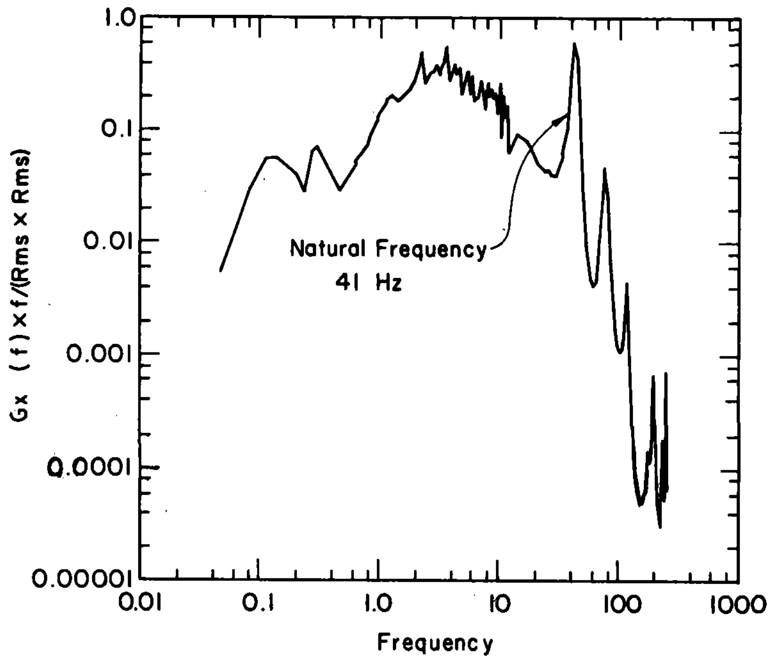

(a) Unfiltered

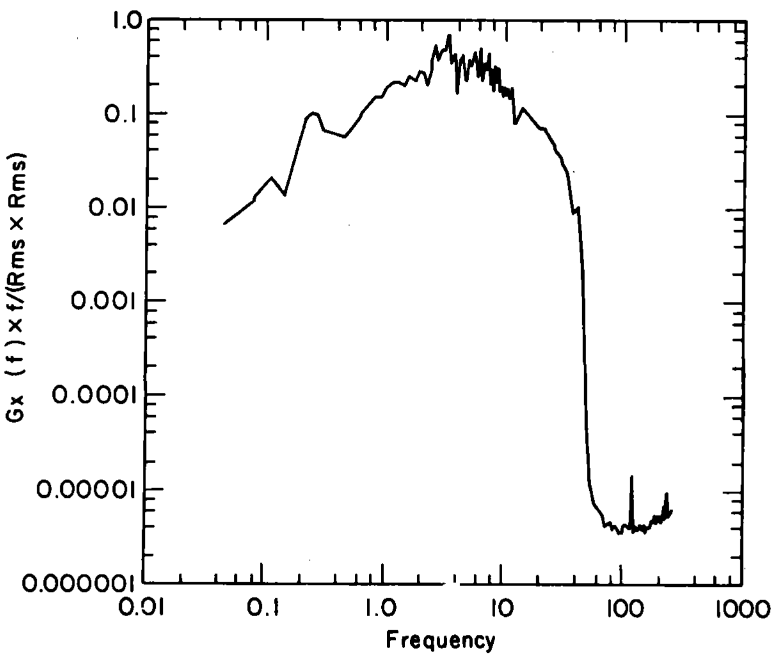

(b) Filtered

FIGURE 2-6. Base Moment Wind Load Spectra for the Square Heliostat

2. The round plate had a fundamental natural frequency on the balance of 53 Hz (see Figure 2-7a). The cutoff filter frequency was chosen as 35 Hz and the resulting moment spectrum in wind is shown in Figure 2-7b.

3. The edge-porous, square plate had a fundamental natural frequency on the balance of 48 Hz (see Figure 2-8a). The cutoff filter frequency was chosen as 35 Hz and the resulting moment spectrum in wind is shown in Figure 2-8b.

It has been shown by Cochran [24] that peak loads obtained using the frequency responses of Figures 2-6 to 2-8 are accurate.

A typical velocity spectrum from the modeled atmospheric wind with no model present is compared, in Figure 2-9, with atmospheric spectra measured by Harris [34], Davenport [35] and Simiu [32]. In this case the data fits most closely to the function developed by Simiu.

Two boundary layer flows were used in the wind tunnel as shown in Figure 2-10. Both had open-country mean velocity profile shapes with a power-law exponent of 0.14. Both profiles also fit well to a log-law relationship with an effective open-country roughness length of 0.01-0.03 meters. Two turbulence profiles were used, one with turbulence intensities of 15-20 percent over the heliostat height simulating that expected in an open-country environment and one with lower turbulence intensities. The lower turbulence profile was naturally developed. The higher turbulence profile was generated using a 380 mm high two dimensional barrier 9 m upstream from the model location. Most data were acquired using the lower percent turbulence intensity; only comparison data were acquired with the larger turbulence level. The implications of these profiles on the wind load data are discussed in Sections 3.3 and 4.1.

2.4 CALIBRATION AND REYNOLDS NUMBER INDEPENDENCE

The six electronic signals coming from the balance during testing were directed to an on-line data acquisition system. The balance was calibrated with standard loads prior to any experimental studies. The interaction between channels was small (<1%) and linear. The channel interactions were small enough to ignore. The calibration coefficients were subsequently used in the data collection program. The necessary load coefficients were developed using measured loads and wind velocity in a computer program installed in an IBM PC-XT based data acquisition system. The software packages are discussed in more detail in Section 3.0.

The independence of the load coefficients to variations in Reynolds number is shown in Figure 2-11. The Reynolds number independence assumption is valid over the range from 11.4×10^4 to 34.1×10^4. Thus the testing velocities were kept within the range of 6 to 18 m/s which corresponds to this range.

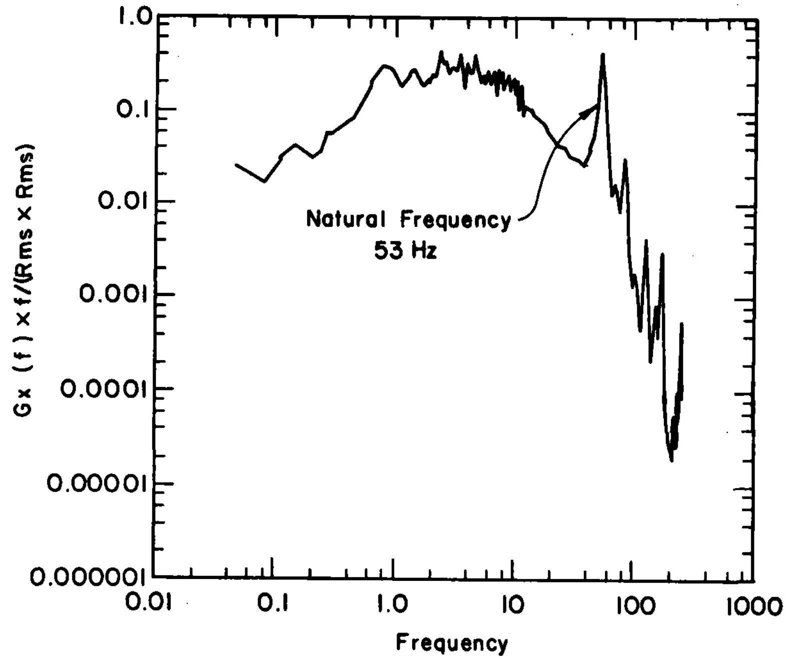

(a) Unfiltered

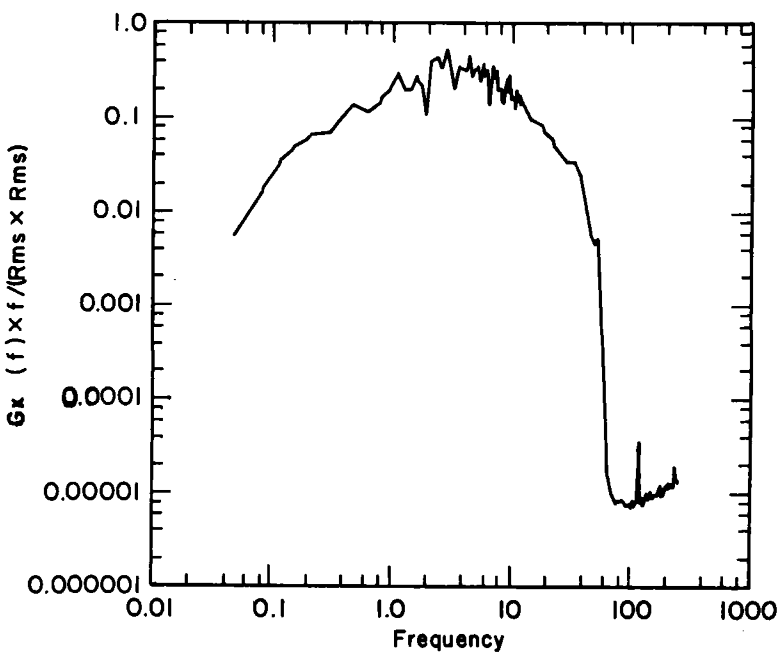

(b) Filtered

FIGURE 2-7. Base Moment Wind Load Spectra for the Round Heliostat

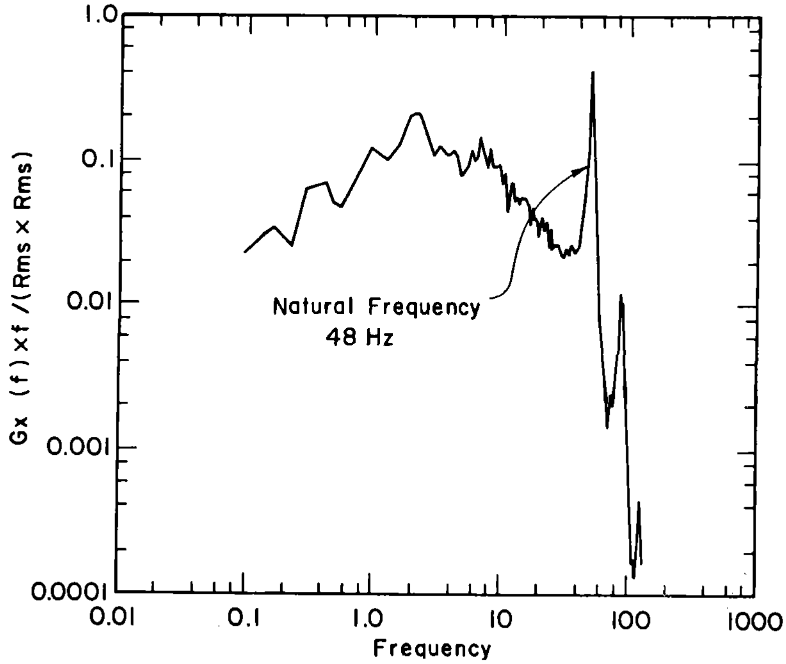

(a) Unfiltered

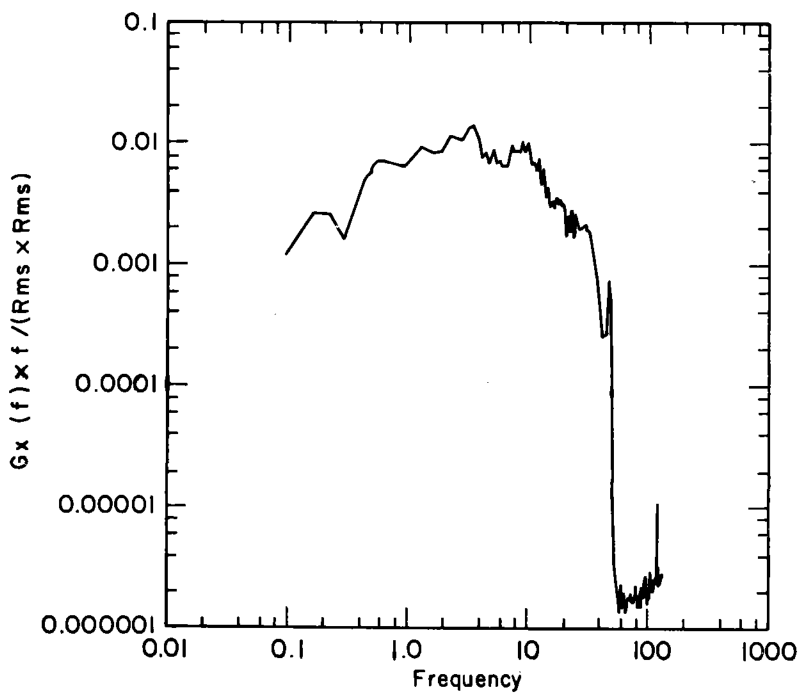

(b) Filtered

FIGURE 2-8. Base Moment Wind Load Spectra for the Edge-porous Heliostat

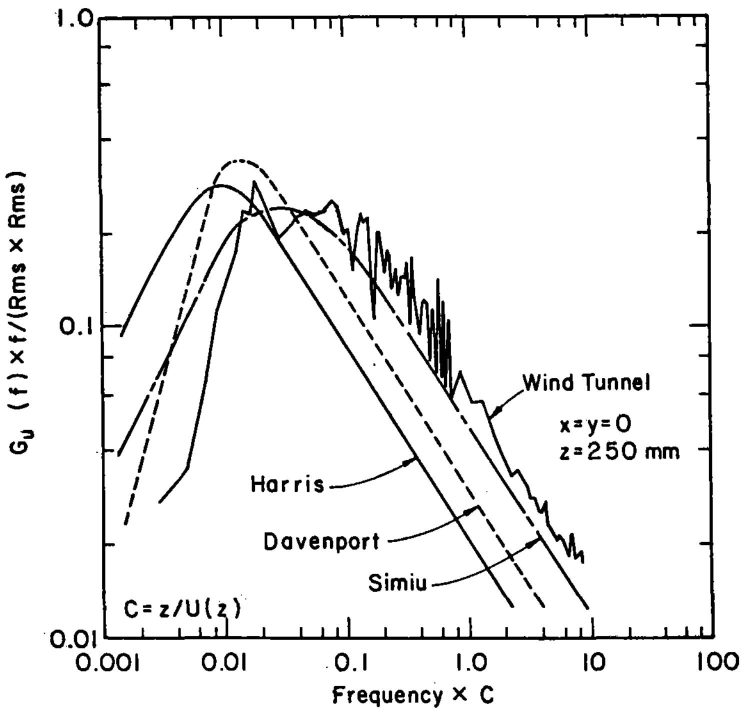

FIGURE 2-9. Comparison Between the Wind Tunnel and Atmospheric Spectra

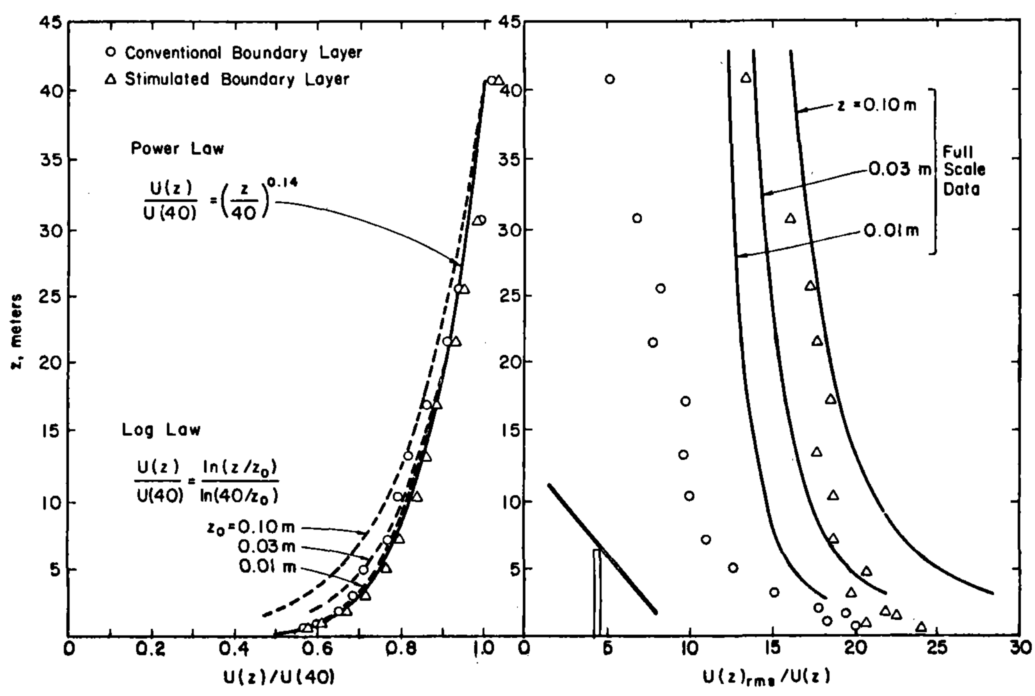

FIGURE 2-10. Mean Velocity and Turbulence Intensity Profiles

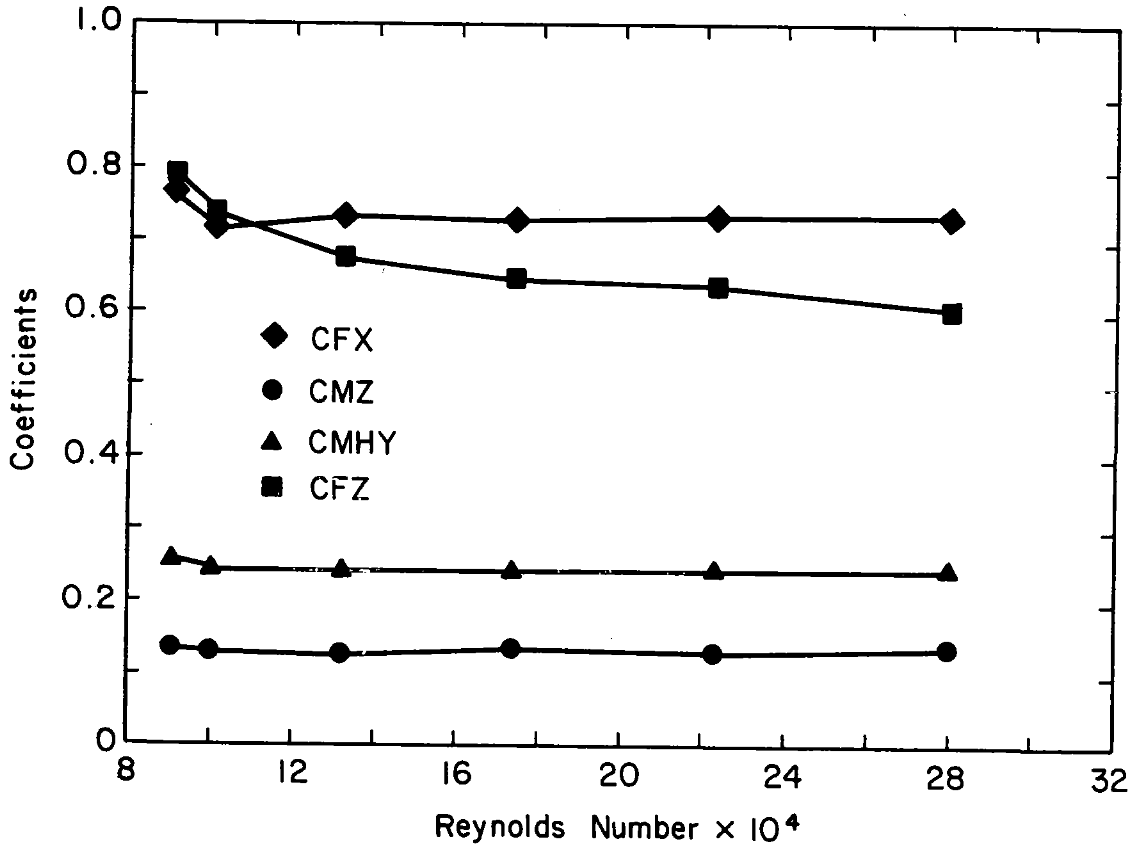

FIGURE 2-11. Reynolds Number Independence Study

2.5 TEST PLAN

The test program can be divided into two general areas:

1. Wind loads on an isolated heliostat.

2. Wind loads on a heliostat as part of a field of similar structures.

A set of generic field geometries were selected as shown in Figure 2-12. These field geometries were selected on the basis of previous experience in order to locate conditions yielding the largest loads on field heliostats. There were two row arrangements relative to the external fence used in this study; 0 and 45°. The 0° case gives the results when the wind approaches perpendicular to the rows of arrays while the other case is taken at 45° to the array rows (see Figure 2-12). These two directions were selected on the basis of previous results to define the largest loads which are likely to act on a heliostat in the field. The field layout geometry was generically similar to that used by Peterka et al. [23] which used the "solar one field" at Barstow with variations in density of that field. These two row arrangements have roughly the same GBA values and exactly the same field densities.

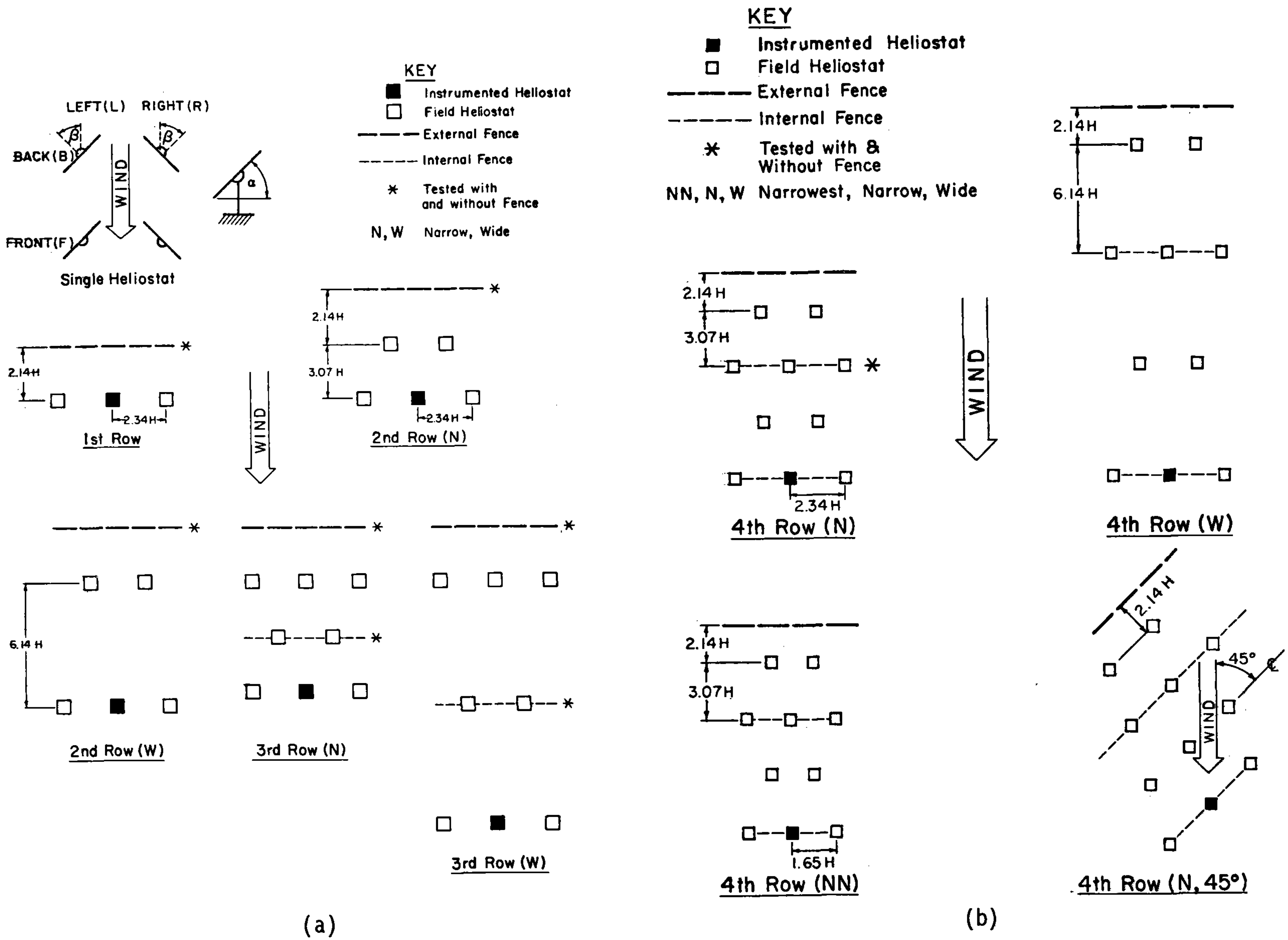

FIGURE 2-12. Test Plan

The fields were modified by changing the following variables:

1. Generalized Blockage Area (GBA)

   GBA is a function of the physical parameters listed below. Calculation of GBA is shown in Section 1.2. The GBA values used in this study are shown in Table 2-1 to provide some intuitive feel to the range of values. Variables in the table are discussed below.

TABLE 2-1. Values of GBA for Test Data

A: 0^0 row arrangement, gap = N, $\alpha = 90^0$, $\beta = 0^0$

Fence Configuration	Row under consideration			
	1	**2**	**3**	**4**
No fence	0.01	0.02	0.139	0.139
Internal fence	---	---	0.168	0.168
External fence	0.224	0.174	0.213	0.193
External fence and Internal fence	---	---	0.235	0.225

B: 0^0 row arrangement, gap = W, $\alpha = 90^0$, $\beta = 0^0$

Fence Configuration	Row under consideration			
	1	**2**	**3**	**4**
No fence	0.01	0.02	0.070	0.070
Internal fence	---	---	0.084	0.084
External fence	0.224	0.110	0.122	0.106
External fence and Internal fence	---	---	0.135	0.124

2. Field density without fences (row gaps of W, N, NN).

   Field densities ranged from very open to densities typical of the Barstow heliostat field. When there is no fence present the GBA may be calculated using the method shown in Section 1.2. The GBA varies with field density (W,N,NN), with heliostat orientation within the field, and with wind direction. In this report three densities were studied for the case with heliostats vertical ($\alpha = 90^o$) and perpendicular to the wind ($\beta = 0, 180^o$). α and β are defined in Figure 2-13. The widest (W) gap gave GBA = 0.070, the narrow (N) gap gave GBA = 0.139, and the narrowest gap (NN) produced GBA = 0.197 with $\alpha = 90^o$, $\beta = 0, 180^o$. Figure 2-12 shows the use of the symbols W, N and NN in presenting the data.

3. Wind direction (beta).

   Three wind directions were used in this study, 0, 20 and 45 degrees. Refer to Figure 2-13 for definition of β.

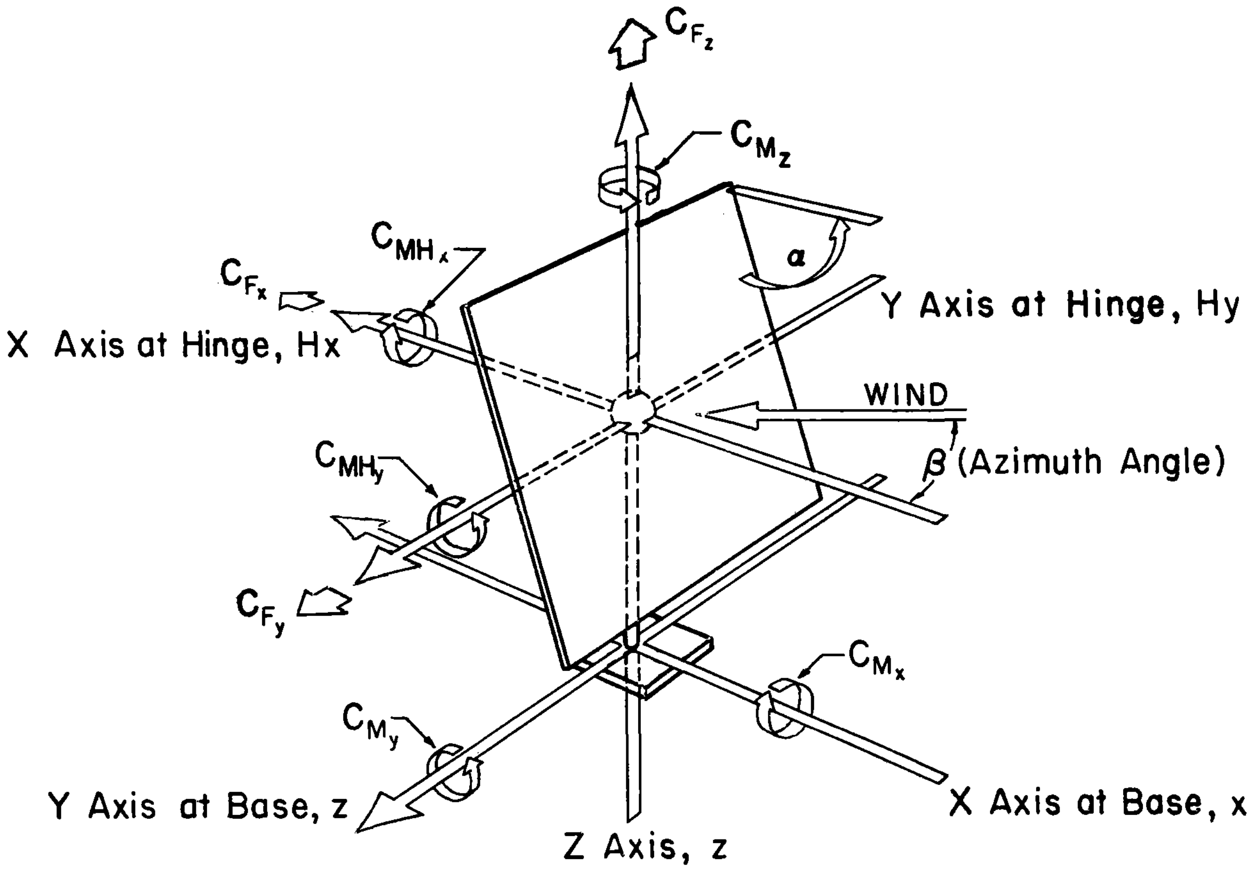

FIGURE 2-13. Definition of Coordinate System

4. Tilt angle (alpha).

   Refer to Figure 2-13 for definition of the elevation angle alpha.

5. Number of rows upstream.

   For a field with constant density, loads do not change significantly past the fourth row into the field. Hence, only rows 1-4 were tested here. For rows 1 and 2 without the external fence, the GBA is not effective and values of 0.01 and 0.02 were used.

6. External fence (EF).

   The external fence was always placed at a distance two times the heliostat chord H (i.e. 2H = 0.594 m) from the first row.

7. Internal fence (IF).

   The internal fences were located at the even row numbers only; that is rows two, four, six, etc.

Figure 2-12 shows the entire test plan for this study including both the isolated and in-field heliostats. Wind loads on the first and second rows were measured with and without external fences and in the narrow (N) and wide (W) density configurations. The third and fourth rows were tested with and without the internal and external fences as well as with an angular variation of 45°. A few runs were made with the narrow field density (NN) at an approach angle of 0°. In the third and fourth row studies there were always four runs due to the combinations of internal and external fencing.

The output data files (SCT, SCT1 and SCT2) show over 400 runs and cover the single and in-field results. A more detailed interpretation of the results is presented by matrix tables in Appendix C.

Photographs of the models in the wind tunnel are shown in Figures 2-14 to 2-21.

2.6 ACCURACY OF DATA

The following three areas effect the accuracy of the test results:

1. Modeling of the wind environment.

2. Accuracy of the instruments.

3. Precise modeling of the heliostat and fence geometry.

Two boundary layer simulations were used, one of which provided a more turbulent flow simulation than boundary layer models used in previous studies. Minor changes in results were expected. The change in boundary layer, however, revealed an unexpected sensitivity to the level of turbulence intensity over the range of turbulence expected in the full scale. This is discussed more thoroughly in Section 4.1.

The accuracy of the instruments could be effected by calibration variation and temperature changes. The accuracy of the measurement is believed to be within about 5% of a representative maximum load measurement on any channel.

The heliostat dimensions are representative of heliostats currently under design. Current designs are virtually solid with no large gaps to enable a face-down stow position. The thickness of the heliostat as a plate was too here. For rows 1 and 2 without the external fence, the GBA is not effective and values of 0.01 and 0.02 were used.

6. External fence (EF).

   The external fence was always placed at a distance two times the heliostat chord H (i.e. 2H = 0.594 m) from the first row.

7. Internal fence (IF).

   The internal fences were located at the even row numbers only; that is rows two, four, six, etc.

Figure 2-12 shows the entire test plan for this study including both the isolated and in-field heliostats. Wind loads on the first and second rows were measured with and without external fences and in the narrow (N) and wide (W) density configurations. The third and fourth rows were tested with and without the internal and external fences as well as with an angular variation of 45^{o}. A few runs were made with the narrow field density (NN) at an approach angle of 0^{o}. In the third and fourth row studies there were always four runs due to the combinations of internal and external fencing.

The output data files (SCT, SCT1 and SCT2) show over 400 runs and cover the single and in-field results. A more detailed interpretation of the results is presented by matrix tables in Appendix C.

Photographs of the models in the wind tunnel are shown in Figures 2-14 to 2-21.

2.6 ACCURACY OF DATA

The following three areas effect the accuracy of the test results:

1. Modeling of the wind environment.
2. Accuracy of the instruments.
3. Precise modeling of the heliostat and fence geometry.

Two boundary layer simulations were used, one of which provided a more turbulent flow simulation than boundary layer models used in previous studies. Minor changes in results were expected. The change in boundary layer, however, revealed an unexpected sensitivity to the level of turbulence intensity over the range of turbulence expected in the full scale. This is discussed more thoroughly in Section 4.1.

The accuracy of the instruments could be effected by calibration variation and temperature changes. The accuracy of the measurement is believed to be within about 5% of a representative maximum load measurement on any channel.

The heliostat dimensions are representative of heliostats currently under design. Current designs are virtually solid with no large gaps to enable a face-down stow position. The thickness of the heliostat as a plate was too

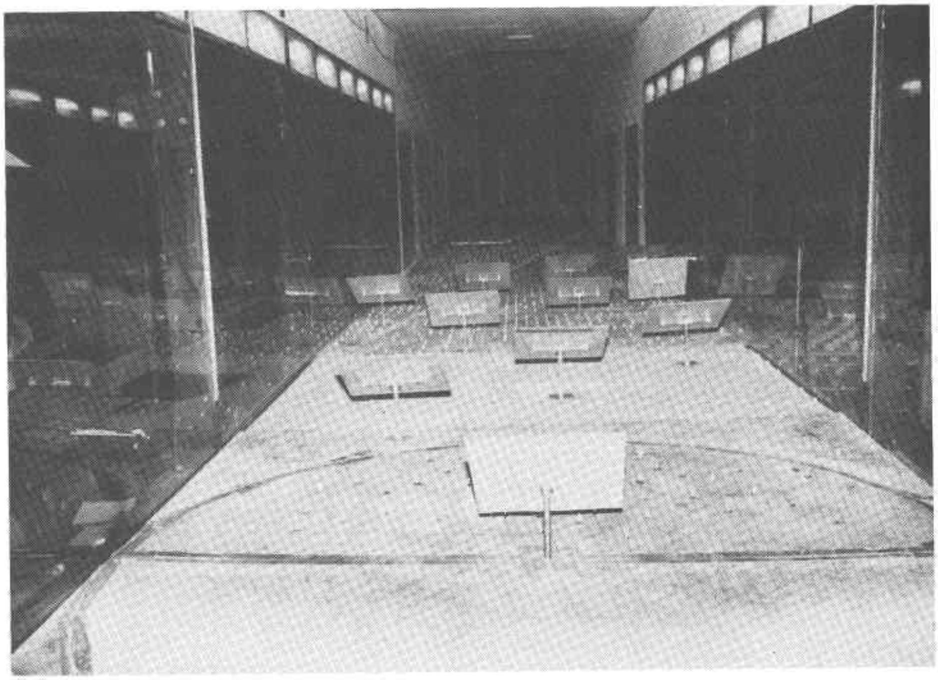

FIGURE 2-14. Test Section of the Industrial Wind Tunnel with Heliostats

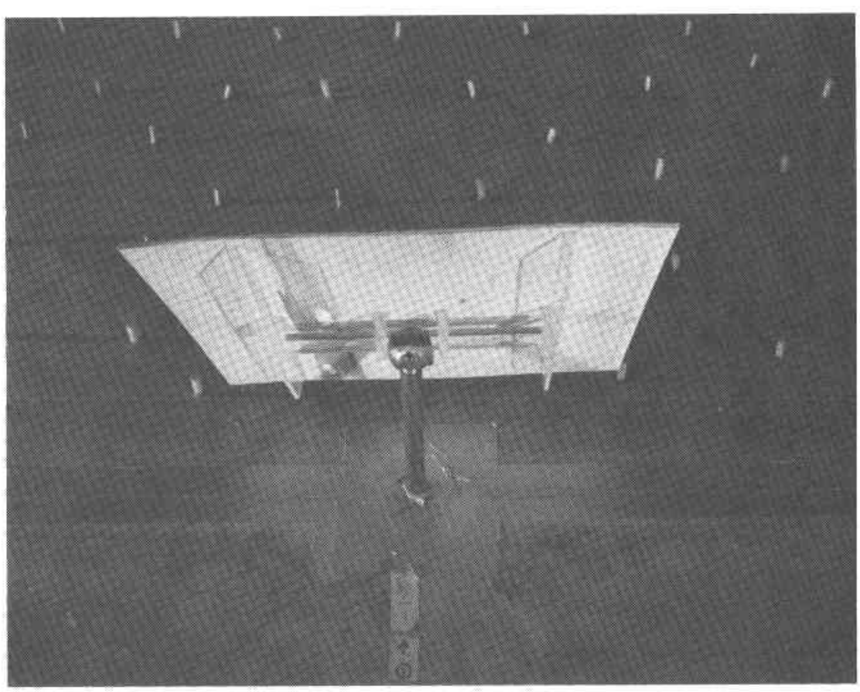

FIGURE 2-15. Back View of the Heliostat

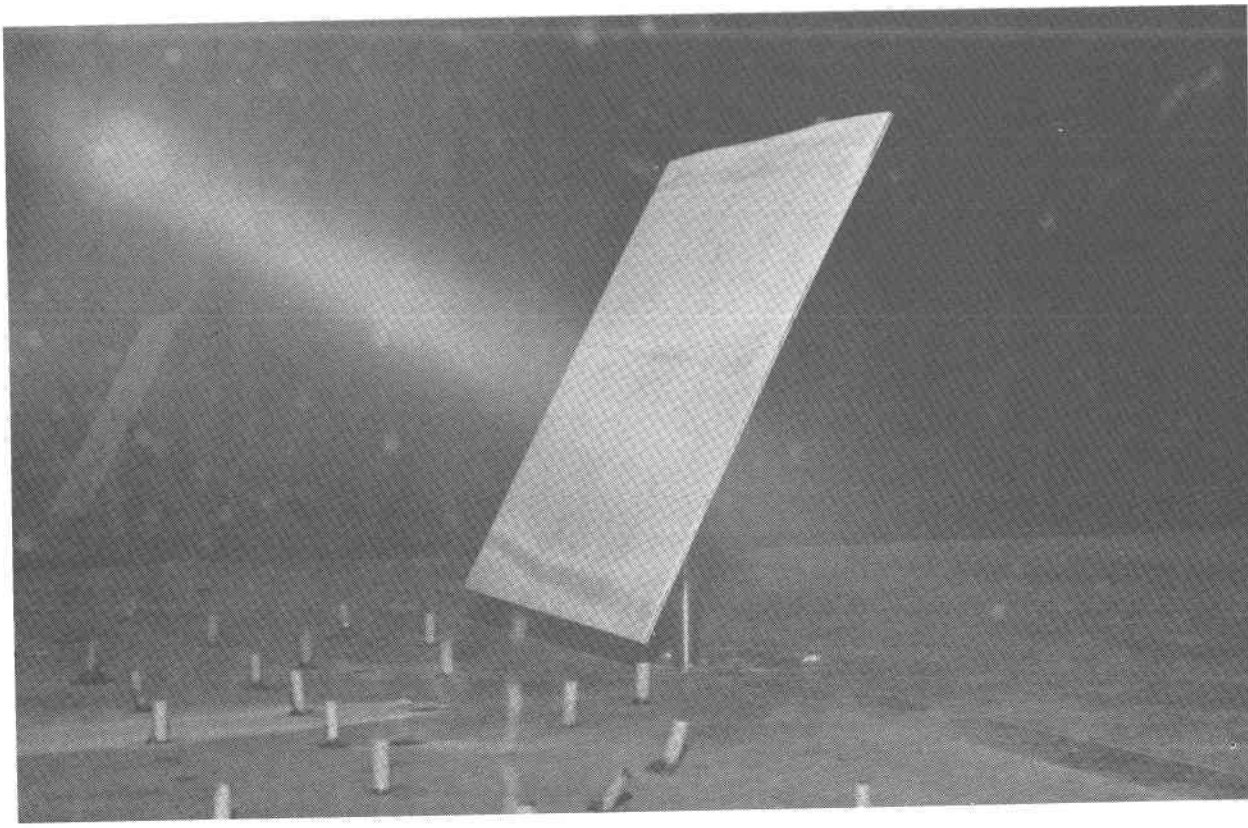

FIGURE 2-16. Single Heliostat under Testing

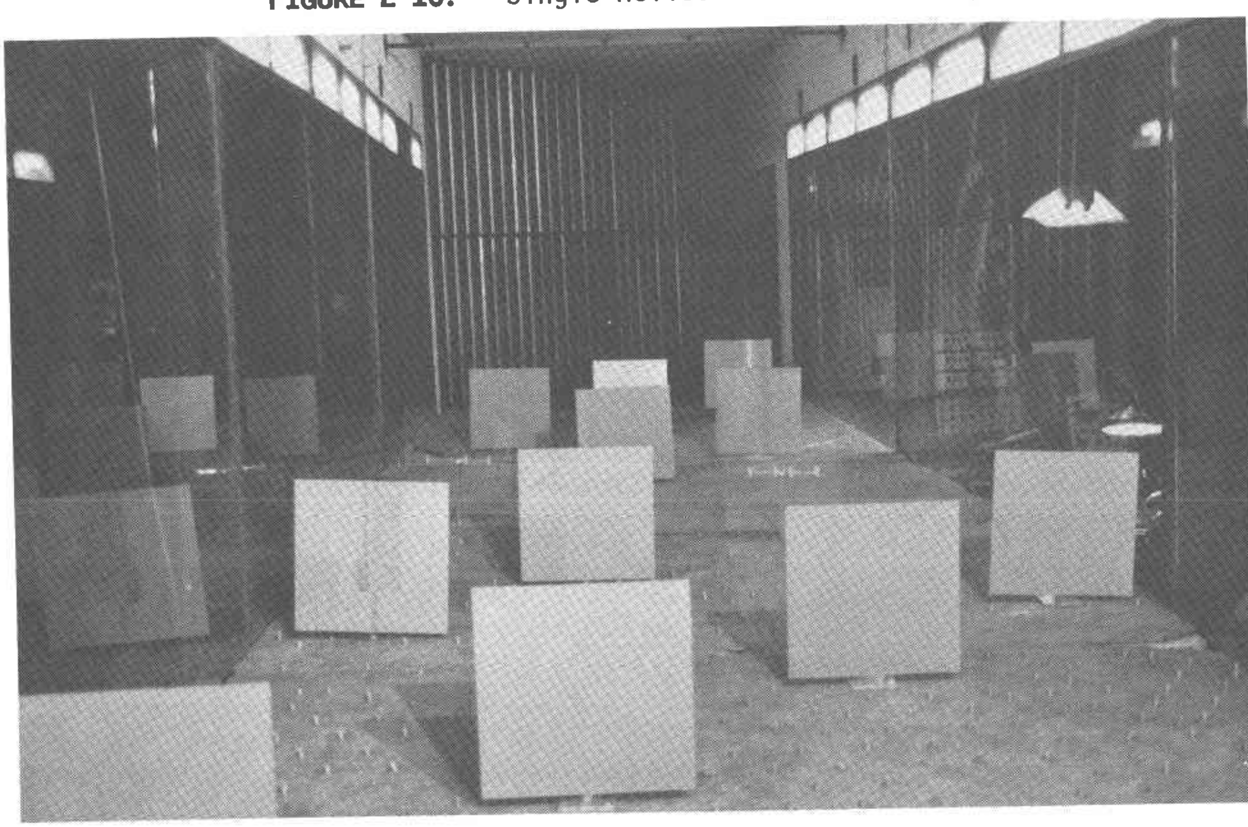

FIGURE 2-17. In-field Study of Heliostats Without Fences

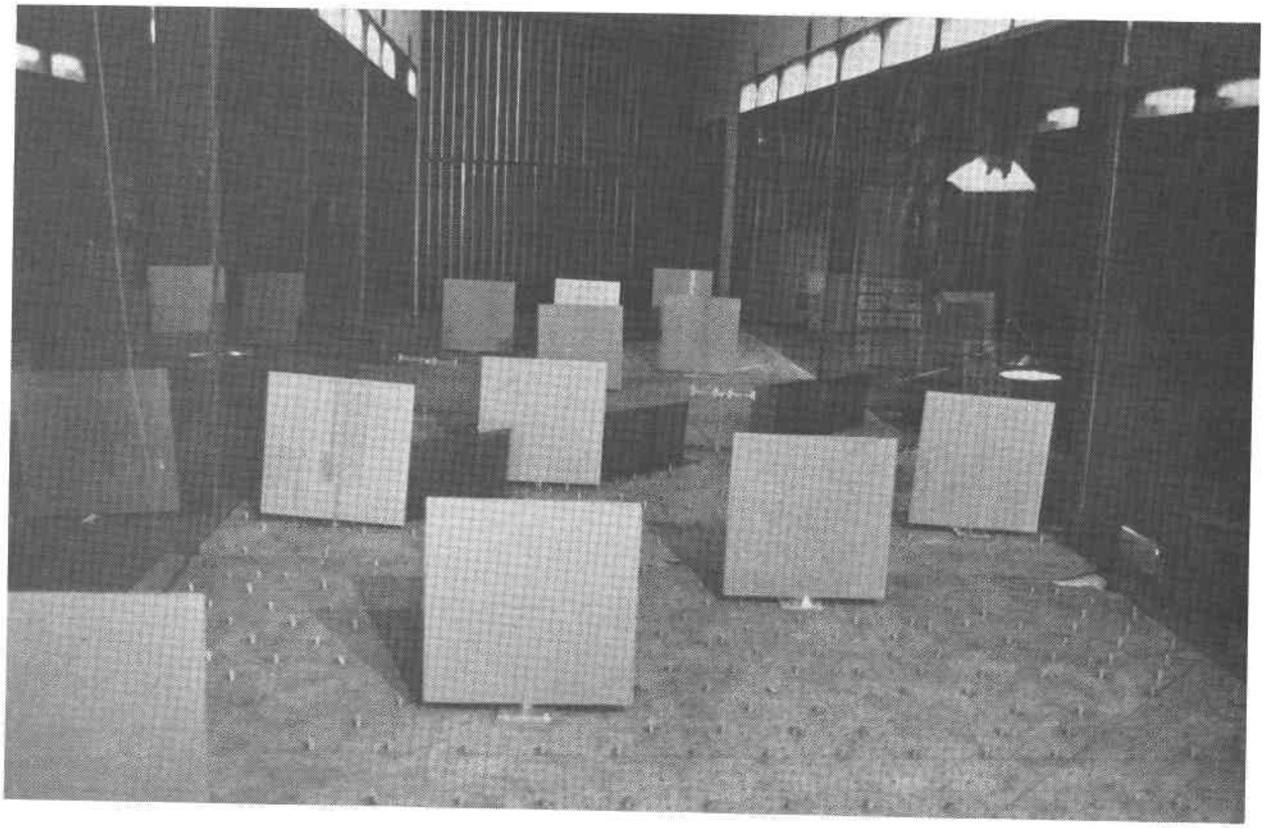

FIGURE 2-18. In-field Study of Heliostats with Internal Fences

FIGURE 2-19. In-field Study of Heliostats with Both Internal and External Fences

FIGURE 2-20. Flow Visualization of an Inclined Heliostat

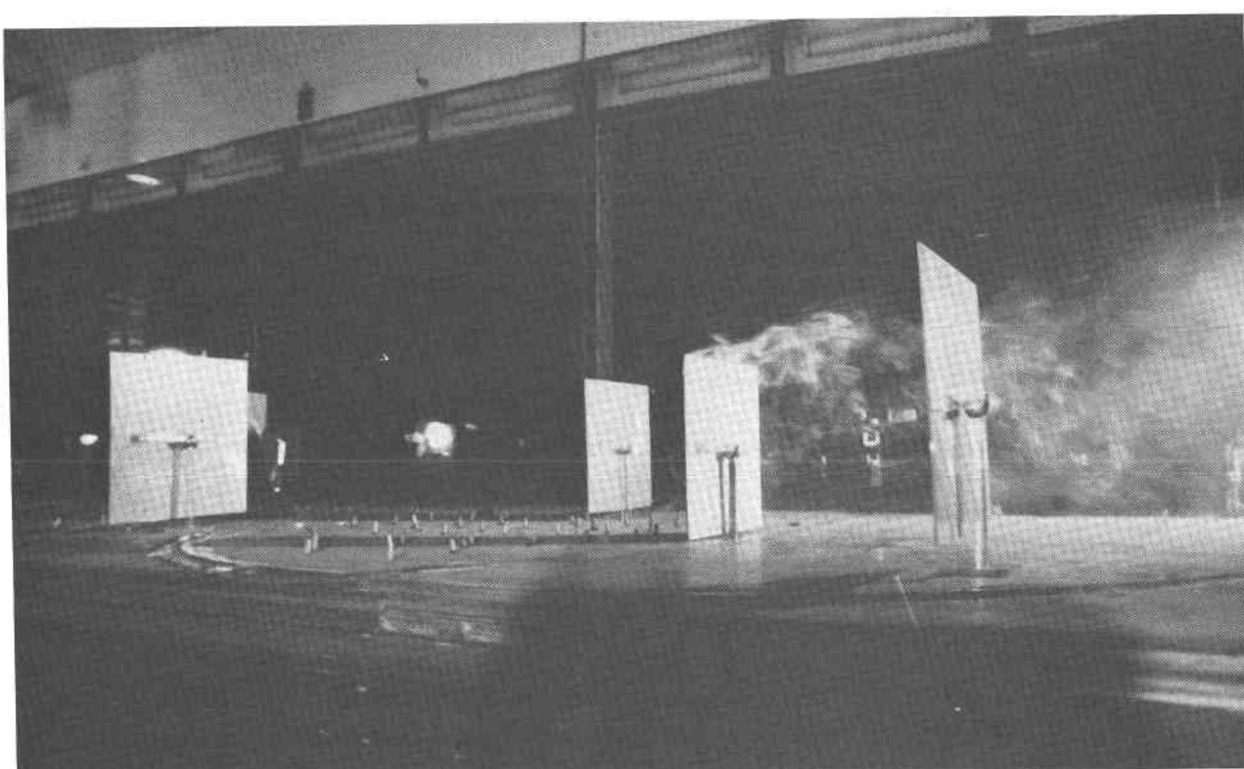

FIGURE 2-21. Flow Visualization of a Vertical Heliostat

large in the model (3.2 mm model = 127 mm full scale at 1:40 scale) in order to maintain adequate model stiffness. However, since the ratio of thickness T to chord H is small (T/H = 0.011), the thickness is not expected to have an influence on measured loads. Fence porosity was set at 40 percent, in the middle of the 30-50 percent range which provides excellent protection with minimum materials. Previous work [23] showed that a berm could be effectively treated as a fence with no porosity for calculation of GBA.

SECTION 3.0

DATA ACQUISITION, PROCESSING AND REDUCTION

3.1 HARDWARE DESCRIPTION

Most data collection was performed by an IBM personal computer fitted with a Data Translation analog to digital converter. Only the velocity spectra and velocity profiles were obtained using an older Hewlett Packard 1000 computer with a Preston Scientific analogue to digital converter.

The six signals from the high frequency force balance passed through six Accudata 118 amplifiers and Wavetek hi/lo filters (model number 852) to the IBM personal computer via an analogue to digital converter. The low-pass filters cut out the natural resonance of the system described in Section 2.3. Each channel recorded 4032 samples over a period of 40 seconds at a rate of about 100 Hz. From this record, mean, rms, peak maximum and peak minimum values on each channel were obtained. This data acquisition procedure has been shown, Cochran [24], to provide an adequate definition of the mean, rms and peak loads for a heliostat which is not in resonant response to the applied fluctuating load.

3.2 SOFTWARE ROUTINES

"FORCA" is a data collection routine which receives signals from the force balance, via the electronic equipment described in Section 3.1, and then converts the voltages to force or moment coefficients (defined below) at a prescribed position on the structure. These dimensionless coefficients are stored in files for later inspection.

"SETRF" is a routine that was primarily used in the calibration process. When a static, known load is applied the computer reads the voltage difference produced across the strain gauge bridges. Thus a plot of force or moment can be developed as a function of voltage. The slope of these straight lines is then used in the load matrix of "FORCA."

3.3 VELOCITY MEASUREMENTS

The velocity and turbulence measurements were obtained using a hot-film anemometer mounted on a traverse mechanism. Calibration of the hot-film anemometer was achieved by comparison with a pitot-static tube in the airflow of the Industrial Wind Tunnel. The resulting data was fitted to the King's law relationship:

$$E^2 = A + BU^c \quad . \tag{3.1}$$

In Equation (3.1) E is the hot-wire output voltage, U is the wind velocity and A, B and C are curve fitting coefficients. During tests, the mean velocity was obtained from 3.1 using measured voltage and previously calculated calibration coefficients. The fluctuating velocity was obtained from:

$$U_{rms} = \frac{2\ E\ E_{rms}}{B\ C\ U^{C-1}} \tag{3.2}$$

in which rms means root-mean-square about the mean.

The mean velocity profile in the simulated atmospheric wind can be described as a power law:

$$\frac{U(z)}{U_{ref}} = \left[\frac{z}{z_{ref}}\right]^n \tag{3.3}$$

or as a logarithmic law:

$$U(z) = \frac{1}{K}\, U_{*}\, \ln\left(\frac{z}{z_0}\right) \tag{3.4}$$

In Equation (3.3) U_{ref} was the velocity at a height of z_{ref} = 1.016 m in the boundary layer (40 m full scale). The constant n describes the upwind roughness; n = 0.14 is typical of an open-country site. In Equation (3.4), K is a constant (= 0.4), z_0 is a roughness length dependent on upwind surface roughness and u_* is a surface friction velocity related to the upstream roughness and ambient wind speed. The log law can be rewritten to relate velocities at one elevation to those at a reference elevation as:

$$\frac{U(z)}{U_{ref}} = \frac{\ln(z/z_0)}{\ln(z_{ref}/z_0)} \tag{3.5}$$

The turbulence intensity as a percent is defined as:

$$T_u = \frac{U_{rms}}{U(z)} \times 100 \tag{3.6}$$

The mean velocity and turbulence profiles used in this study are shown in Figure 2-10. Two boundary layer configurations were used, denoted by circle and triangle symbols. The mean velocity profiles for both configurations compare well to a typical open-country profile (n = 0.14 or z_0 = 0.03 m) also plotted in the figure. Two turbulence profiles were used which had turbulence intensities of 10-12 percent and 17-20 percent respectively over the height range of the heliostats. The solid lines in the turbulence intensity plot in Figure 2-16 are typical values of turbulence obtained from field measurements for a range of open-country environments (z_0 = 0.01 - 0.1 meters). The triangle data best fit the field data. Since most previous data were obtained at lower turbulence levels and since the influence of turbulence was expected to be small, only a limited amount of data was obtained at the higher turbulence level.

The lower turbulence intensity profile is a naturally developed boundary layer and can be shown to correctly model an open country site at a scale of about 1:300. The higher turbulence intensity profile was generated by installing a passive turbulence generator well upstream from the model. The generator was experimentally tuned to obtain the appropriate turbulence level.

Load data were acquired for a single heliostat both with the lower turbulence intensity of 12 percent, for comparison with previous results which typically used this lower turbulence intensity profile, and with the higher turbulence level of 18 percent. Data available in the literature [38] for turbulence intensities up to 9 percent predicted that the difference in drag due to the change in profile in this experiment from 12 to 18 percent would be less than 5 percent. Load measurements discussed below showed a much larger difference than the 5 percent expected.

3.4 FORCE AND MOMENT MEASUREMENTS

Program "FORCA" produced the six force and moment coefficients: C_{Fx}, C_{Fy}, C_{Fz}, C_{Mx} or C_{MHx}, C_{My} or C_{MHy}, and C_{Mz}. All the C's were omitted in the data files for simplicity. The coefficients are defined as follows:

The coefficient of the force along the x-axis,

$$C_{Fx} = \frac{F_x}{\frac{1}{2}\rho U^2 A_{ref}} \tag{3.7}$$

The coefficient of the force along the y-axis,

$$C_{Fy} = \frac{F_y}{\frac{1}{2}\rho U^2 A_{ref}} \tag{3.8}$$

The coefficient of the force along the z-axis,

$$C_{Fz} = \frac{F_z}{\frac{1}{2}\rho U^2 A_{ref}} \tag{3.9}$$

The coefficient of the moment about the x-axis at the base,

$$C_{Mx} = \frac{M_x}{\frac{1}{2}\rho U^2 A_{ref} L_{ref}} . \qquad (3.10)$$

The coefficient of the moment about the y-axis at the base,

$$C_{My} = \frac{M_y}{\frac{1}{2}\rho U^2 A_{ref} L_{ref}} . \qquad (3.11)$$

The coefficient of the moment about the z-axis,

$$C_{Mz} = \frac{M_z}{\frac{1}{2}\rho U^2 A_{ref} L_{ref}} . \qquad (3.12)$$

The coefficient of the moment about the x-axis at the hinge,

$$C_{MHx} = \frac{M_{Hx}}{\frac{1}{2}\rho U^2 A_{ref} L_{ref}} . \qquad (3.13)$$

The coefficient of the moment about the y-axis at the hinge,

$$C_{MHy} = \frac{M_{Hy}}{\frac{1}{2}\rho U^2 A_{ref} L_{ref}} . \qquad (3.14)$$

Where,

U = reference mean velocity at hinge level at HCL = .152 m above floor for model at scale of 1:40, 6.08 m in full scale [m/s].

ρ = air density [kg/m^3].

A_{ref} = reference area of 0.088 m^2 for the model at scale of 1:40, 141.1 m^2 full scale [m^2].

L_{ref} = reference length, chord of 0.297 m at a scale of 1:40, 11.88 m full scale [m].

F_x, F_y, F_z = measured forces along given axes [N].

$M_x, M_y, M_z, M_{Hx}, M_{Hy}$ = measured moments about given axes [N.M].

All the moments conform to the right hand rule and the hinge moments may be derived from the base moments in the following manner. The relationship between C_{My} and C_{MHy} is:

$$C_{My} = C_{MHy} + C_{Fx} \left[\frac{HCL}{H}\right] \tag{3.15}$$

In data file "SCT", MX, MY refer to C_{Mx} and C_{My}; however, in the data files "SCT1" and "SCT2," they refer to C_{MHx} and C_{MHy}.

The data files also list the gust and peak factors. The gust factor is the peak recorded value divided by the mean. The peak factor is the difference between the peak and the mean divided by the measured rms (the number of standard deviations from the mean). Thus the reported information given in each file is, in coefficient form:

mean = time average,

rms = root-mean-square of the fluctuating values about the mean,

peak = largest and smallest values recorded during each 40 second run,

Gust factor = peak divided by the mean, and

Peak factor = (peak-mean)/rms.

These factors relate to the way peak loads are often specified in code formulations and may be useful for later analysis related to codified formats of data presentation.

SECTION 4.0

RESULTS AND DISCUSSION

4.1 THE SINGLE FLAT PLATE

The plots given in Appendix A give the available wind data for an isolated flat plate. The following studies are referenced: Heliostat 85 [23], Heliostat 78 [1], ASCE report of 1961 [36] and a NASA report [37]. The drag, lift and normal force coefficients are given as functions of the tilt angle in Figures A-1, A-2 and A-3. The normal force is a projection of both the drag and lift forces to the normal taken from the plate surface:

$$C_{Fn}\,(HCL) = C_{Fx}\,(HCL)\,\sin\alpha + C_{Fz}\,(HCL)\,\cos\alpha \quad . \tag{4.1}$$

HCL here indicates that C was calculated using U at height HCL. The normal force may not precisely be equal to the resultant of the drag and lift forces since a small component of force may act parallel to the surface.

The data presented in Appendix A indicates that the drag and lift forces measured in this study with the higher turbulence intensity are generally larger than in previous work. The turbulence intensity is at a more realistic level (18% at centerline height HCL) in the current work, whereas the heliostat 85 data used 14% and the heliostat 78 work used 12%. This would suggest that the shear flow and the turbulence intensity influence the resulting loads significantly. In fact, when compared to the uniform flow case there is an increase in the drag coefficient of more than 50% in the high turbulent shear flow. This is a very large change which was not expected.

Figure 4-1 shows the variation of mean drag coefficient with turbulence intensity at height HCL for wind approaching perpendicular to a heliostat in the current study, in studies [1] and [23], and for turbulent air flow behind a grid in Bearman [38]. Figure 4-2 shows a similar trend for peak drag coefficients. This sharp increase in drag coefficient with turbulence intensities above 10 percent has not, to our knowledge, been previously documented. Integral length scale, L_x, of the turbulence is included to show that no systematic changes are evident. L_x represents a typical length scale of the eddy size of the turbulent fluctuations.

Figure 4-3 shows the influence of turbulence on drag in the form presented by Bearman [38]. He postulated that a turbulence parameter

$$\frac{U_{rms}}{U(z)} \, \frac{L_x^2}{A_{ref}} \tag{4.2}$$

would govern the variation of base pressure (pressure on the rear face) for a flat plate perpendicular to a turbulent flow. Recent data from tests on heliostats shown in Figure 4-1 are shown on the figure. The portion of total drag attributable to base pressure was estimated using Bearman's data. No regular pattern for the data emerge from that data presentation.

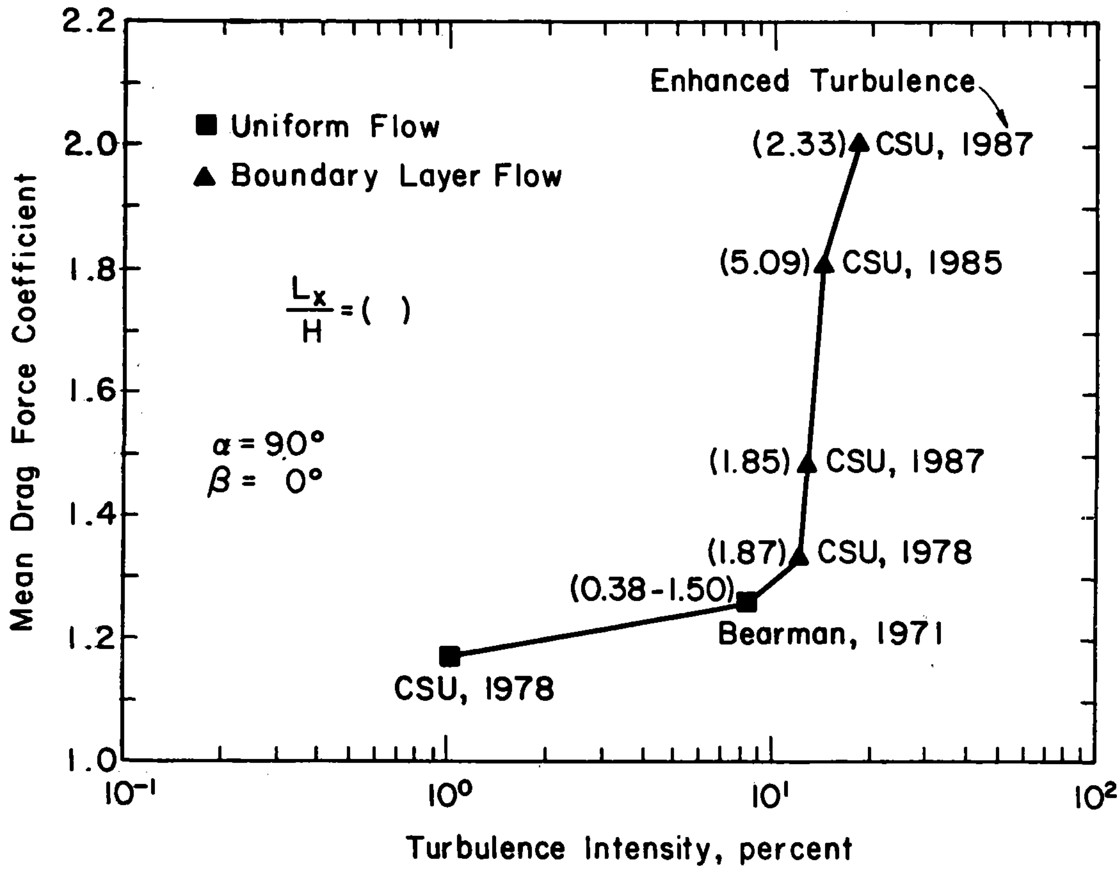

FIGURE 4-1. Mean Drag Force Coefficient Variation with Turbulence Intensity

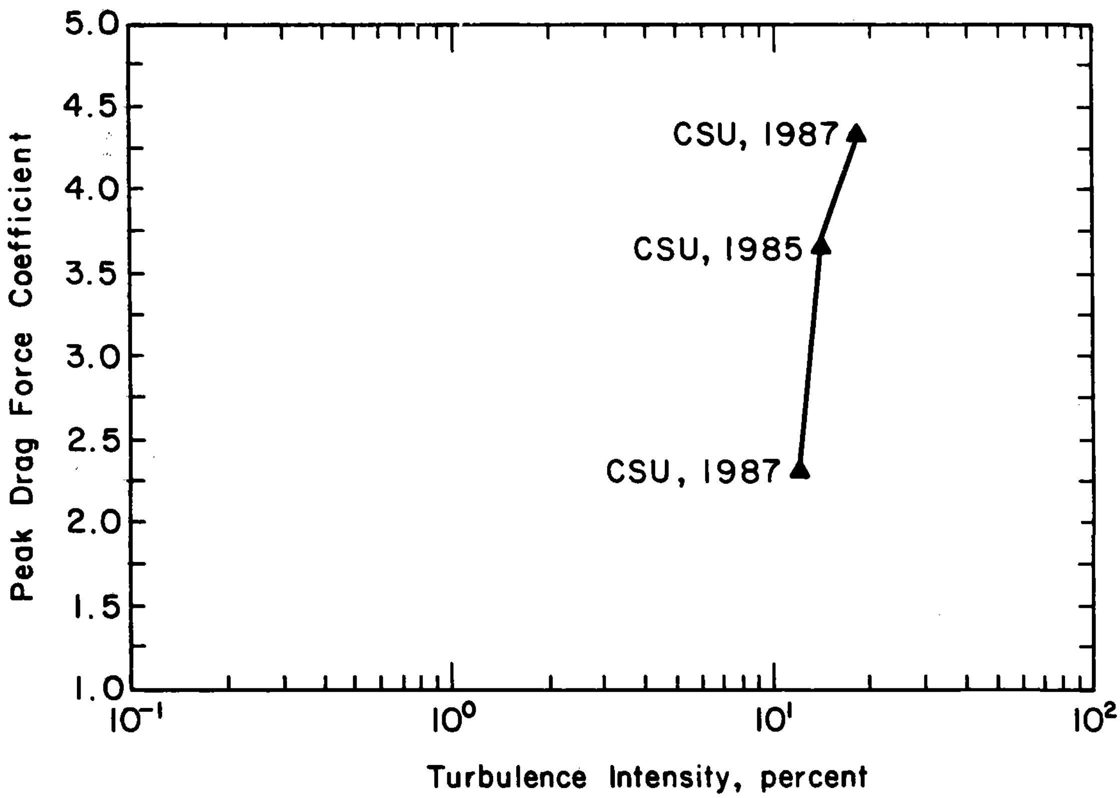

FIGURE 4-2. Peak Drag Force Coefficient Variation with Turbulence Intensity

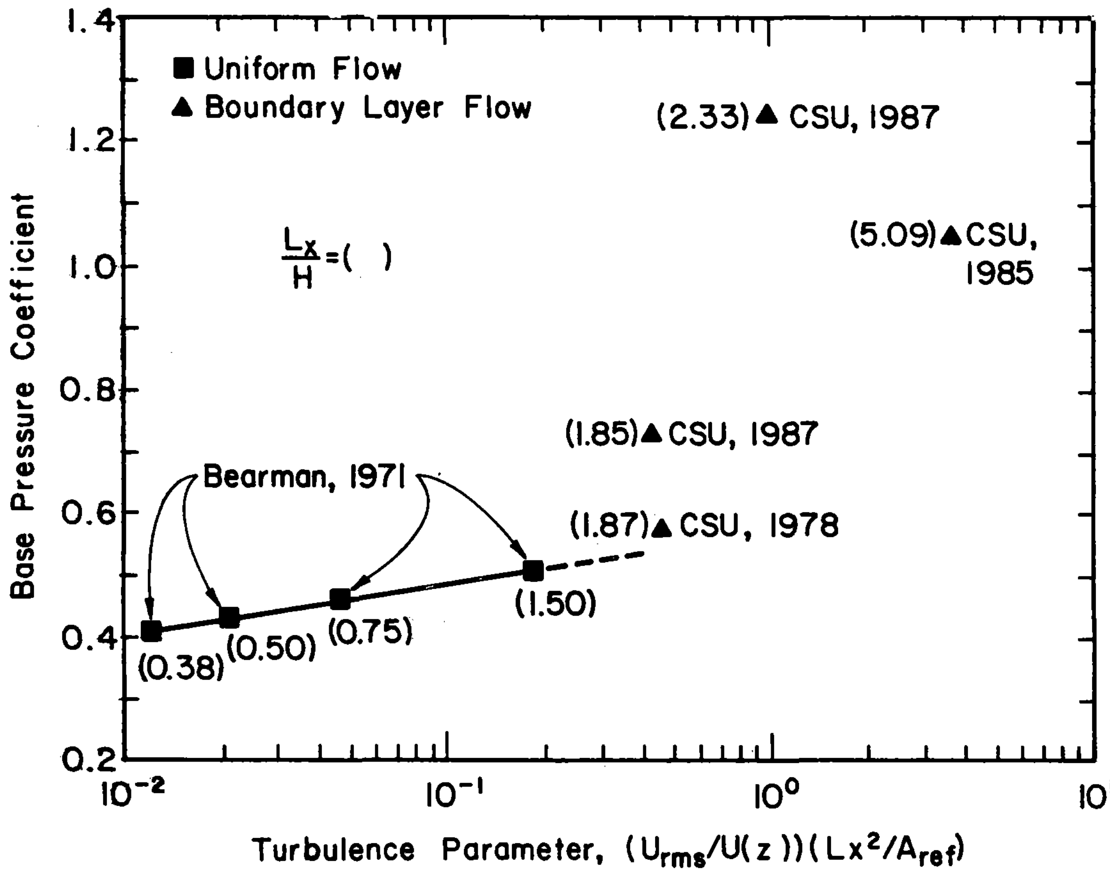

FIGURE 4-3. Mean Base Pressure Coefficient Variation with Turbulence Parameter

Data presented in Appendix A show that the influence of turbulence in inducing large load increases is maximum for a vertical heliostat perpendicular to the wind. The effects decrease in magnitude as the elevation angle α decreases from 90 degrees. For this reason, the largest effects are seen in the drag force. Maximum lift force is affected, but to a lesser extent since peak lift occurs for α = 30-40 degrees. For similar reasons, maximum pitching moment and maximum azimuth torque are also affected less. However, all load components are increased due to turbulence above those predicted by uniform flow.

Figure A-4 shows the base moment increase above the uniform flow case from a 12 percent, 14 percent and 18 percent turbulence level. According to Bearman's data and the additional moment expected from a center-of-pressure shift due to the shear flow we would expect the load increase for 18 percent turbulence to fall about where the 12 percent data falls. The extra increase due to turbulence is not now explained. Design load increases above those predictable from Bearman's data appear to be restricted to the maximum drag and base moment due to drag.

Additional study is needed to determine why the rapid increase in drag force occurs for turbulence intensities above 10 percent. Pertinent variables include turbulence intensity, integral scale of turbulence, vertical gradient of turbulence, vertical gradient of mean velocity, and proximity of the ground plane. It can be hypothesized that increased mixing in the separated shear layer at the heliostat edge caused by increased turbulence intensity caused a larger shear layer curvature and consequently a larger base pressure and drag. However, the reason for the sharp change in slope above 10 percent turbulence intensity in Figure 4-1 is not known.

Figure A-5 shows the hinge moment data. The hinge moment peaks for an elevation angle of 20 to 30 degrees at a value of 0.20 to 0.25 depending on turbulence intensity. These values are twice the value predicted from uniform flow results. The effects of turbulence within the range of typical applications appears to be small.

The position of center of pressure (location of resultant force) is shown in Figure A-6. The variation with turbulence intensity is small. The center of pressure is positioned above the centerline due to the shear flow which causes higher pressures near the top of the heliostat.

Figures A-7 and A-8 show the mean azimuth moment coefficient (C_{MZ}). It appears to reach a peak between 0.2 and 0.25 when the wind angle (β) ranges from 60^o to 70^o. These load values and angles to the flow are very similar to those for the maximum elevation hinge moment.

Figure A-9 presents the mean drag force (resolved normal to the plate) as a function of wind direction (β) for the current data set with the higher turbulence intensity.

Peak loads on an isolated heliostat are shown in Figures A-10 to A-13. The data shows a variation with turbulence intensity similar to that for the mean wind loads. The largest peak loads are 2 to 3 times the value of largest mean loads. Peak values of 2 times the mean are consistent with gust loading from the approaching wind. Values much greater than two times the mean are consistent with gust loading augmented by wake excitation. This appears to be the case for the elevation and azimuth moments. In addition, the peak loads for these two moments are not symmetrical about the mean, an indication of highly correlated wake pressure fluctuations. This feature has recently been observed also by Cochran et al. [24].

The data in A-10 to A-13 permit an examination of the relative magnitudes of maximum wind loads in operational orientations versus stow orientation. If we use 90 mph for survival stow position loads and 55 mph for maximum survivable operational loads in any position, then wind loads can be calculated for both operational and stow conditions. Comparing the ratio of peak wind loads at any orientation in A-10 to A-13 with those at stow (α = 0) to 1.0 will reveal whether operational loads are larger than stow position loads. The relevant peak load ratios are:

Load Component	Fx	Fz	MHy	Mz
Peak Operational Load (55 mph) / Peak Stow Load (90 mph)	2.0	1.1	0.6	>>1.0

Load coefficient ratios greater than 1.0 indicate that operational loads at 55 mph are greater than stow loads at 90 mph. Only for MHy do stow loads control the design. However, if the heliostat were rotated in azimuth relative to the wind in stow position so that the elevation rotation axis aligns with the wind, then the MHy can be lowered below operational load maximum. This orientation is easily achieved with a computer-controlled field and will significantly reduce design loads on the elevation drive. Since the stow MHy loads cycle about a low or zero mean, the implications of a high cyclic load rate on system fatigue needs further examination. Positive/negative load cycling causes fatigue with fewer cycles than loads which cycle between values of the same sign. Positive/negative load cycling can be expected, for example, at $\alpha = 0$ degrees in Figure A-12.

An interesting feature of this study is that the round and square models produce very similar force and moment coefficients as shown in Figures A1-A13. This feature allows data obtained from earlier studies on square shapes to be used for circular heliostats.

The results of the edge-porous study are given in Figures A-14 to A-20. Results are presented for an isolated heliostat for mean force coefficient (Figure A-14), mean lift coefficient (Figure A-15), mean normal force (Figure A-16) and mean elevation hinge moment (Figure A-17). Some results are presented for three values of reference area: the 'gross area' which includes the total solid area plus the area of the porosity, the 'actual area' which includes all solid area of the heliostat, and the 'mirror area' which is the solid area inside the porous edge which is suitable for a mirror surface. Comparison of Figure A-14 for the drag of a heliostat with a porous edge to that of a solid heliostat in Figure A-9 shows that the porosity decreases the drag coefficient from about 2.1 to about 1.7 based on gross area. However, based on actual area, the drag coefficient increases to about 2.0. Based on mirror area, the drag coefficient rises to about 2.6. Thus the presence of porosity is a net drag producer based on a realistic energy production mirror area. Comparison of Figure A-17 for hinge moment with Figure A-4 shows that the hinge moment based on mirror area is not decreased due to presence of edge porosity. Peak load coefficients are presented in Figures A-18 to A-20. Comparison of peak loads with edge porosity to those without edge porosity shows that, based on the mirror area, the loads are as large or larger than those of a solid heliostat without porosity. It thus appears that edge porosity is not a beneficial addition to heliostat geometry.

Porous edges were the only 'spoiler' concept tested in this study. Insufficient effort was available to test a variety of devices. It cannot be determined with resources available to date whether or not a spoiler exists which might reduce peak loads.

4.2 THE FLAT PLATE AS PART OF A FIELD

In these studies the influence of nearby collectors on the drag (C_{Fx}), the lift (C_{Fz}), the hinge moment (C_{MHy}) and the azimuth moment (C_{Mz}) was studied in detail. The resulting load reductions for both the mean and peak loads are presented in Appendix B as a function of GBA. Data plotted in Appendix B is listed in Appendix C. In each figure of Appendix B the x-axis represents the generalized blockage area and the y-axis is the ratio of each component value (mean or peak) to the maximum value of that component found in the corresponding single heliostat study. The single-heliostat load used for the denominator of the load ratio is shown in the figure. The 12 percent turbulence level data were used.

The four components noted above are presented in Figures B-1 to B-8 in mean and peak plots: Figures B-1 and B-2 the mean and peak drag, Figures B-3 and B-4 the mean and peak lift, Figures B-5 and B-6 the mean and peak hinge moment and Figures B-7 and B-8 the mean and peak azimuth moment.

Solid data points occur on the graphs of Appendix B. These data points reflect the load on a heliostat in row 1 or 2 with a fence present, but plotted for the GBA without the fence. These data were used in assessing the impact of the external fence and could otherwise be omitted from those graphs without loss of content.

Also presented in Figures B-9 to B-14 are the results from other studies such as Heliostat 85 [23] and Heliostat 78 [1]. The data is presented in the same manner; mean and peak coefficients (C_{Fx}, C_{Fz}, and C_{MHy}).

The old and new data were combined and an enveloping curve defined. This information is presented in Figures B-15 to B-22 and the upperbound equation that gives the wind load limits is given on each figure.

All the mean load data for all load components are combined in Figure B-23 and all the peak load data are combined in a similar manner in Figure B-24. The merging of these two results (Figure B-25) provides a "total wind load reduction curve."

The data and bounding curves of Appendix B show that significant reductions in both mean and peak wind loads result from the blockage induced by upwind heliostats and fences if the GBA is sufficiently high. Very open portions of fields such as Solar 1 at Barstow, California may have GBA values as low as 0.1 while the dense portions may be as high as 0.25 to 0.3 based on a calculation without wind fences. None of the load components in Appendix B for either mean or peak load have a significant load reduction for GBA = 0.1. For GBA less than 0.1, for example in the first two rows of a field with no wind fences, the load may be higher than that of an isolated heliostat. For a GBA of 0.25, a fairly easily obtained value if wind fences are included or if the heliostats are fairly tightly packed, the load may be reduced by 20 percent for peak drag force, by 65 percent for peak hinge moment, and by 80 percent for peak azimuth moment.

The load reduction charts of Appendix B used the maximum isolated heliostat load associated with a 12 percent turbulence intensity. This was done because all in-field studies were performed at a 12 percent turbulence intensity. The load reduction curves might be somewhat different in an 18 percent turbulence intensity environment. However, since the drag force is the only component which is highly sensitive to turbulence intensity, only the load reduction charts for drag may change significantly. It is expected that the load on a heliostat at a GBA of 0.2 to 0.25 would be fairly insensitive to approach turbulence since the local in-field turbulence intensity generated by upwind heliostats is quite high. Thus, use of the curves with a drag value for turbulence of 12 percent for an isolated heliostat for any approach wind will give a correct answer for GBA ~ 0.2 regardless of the actual approach conditions. For GBA ~ 0.1, the reduction in load may not be completely dominated by local turbulence, and use of the 18 percent turbulence drag coefficient for an isolated heliostat might be more appropriate and would be conservative. Additional study is recommended to resolve this issue, since the use of the lower isolated drag coefficient may, in fact, give a reasonable result in this case.

The next step in use of the curves of Appendix B is to construct a users guide which simplifies as much as possible the use of the data. Such a guide is planned and is in development.

The external fence is a critical mechanism to the reduction of first and second row heliostat loads. The load reduction from an external fence is less significant in the third row and not apparent for rows further back than number four. This result is confirmed by the Heliostat 85 data [23].

The impact of decreasing row spacing for rows near the edge of the field with an external fence is shown in Figures 4-4 and 4-5. These figures show that the mean and peak wind loads decrease with increasing GBA (decreased row spacing) and increase with distance from the fence. The reason for the increase with distance from the fence is that the region immediately behind the fence is better protected than areas farther from the fence (interior to the field) where the external fence is not effective in providing protection. For very dense fields this effect would not occur.

Figures 4-6 through 4-9 show the influence of internal and external fences on wind loads in row 4 for various combinations of row spacing and approach wind direction. The important conclusions from these figures are that closer row spacing is beneficial (increased GBA) and that flow crossing a fence at 45 degrees to the fence is less effective than flow crossing perpendicular to a fence.

All of the effects shown in Figures 4-4 through 4-9 are included in the load reduction charts of Appendix B. Further research into effects such as improving the protective influence of a fence at 45 degrees to the wind flow might enable a further decrease in load in the position of the bounding load reduction curves.

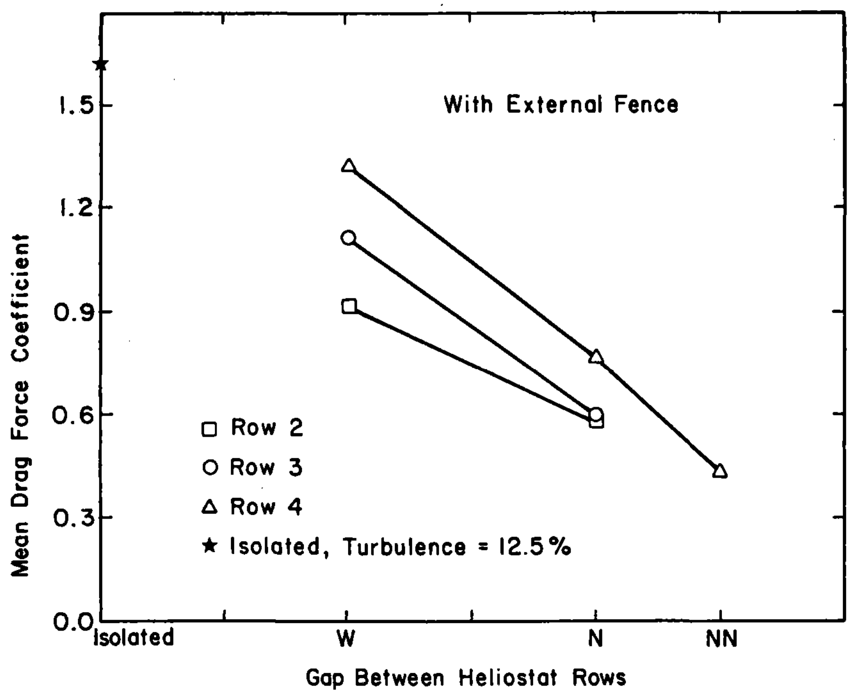

FIGURE 4-4. Influence of Row Spacing on Mean Drag Force

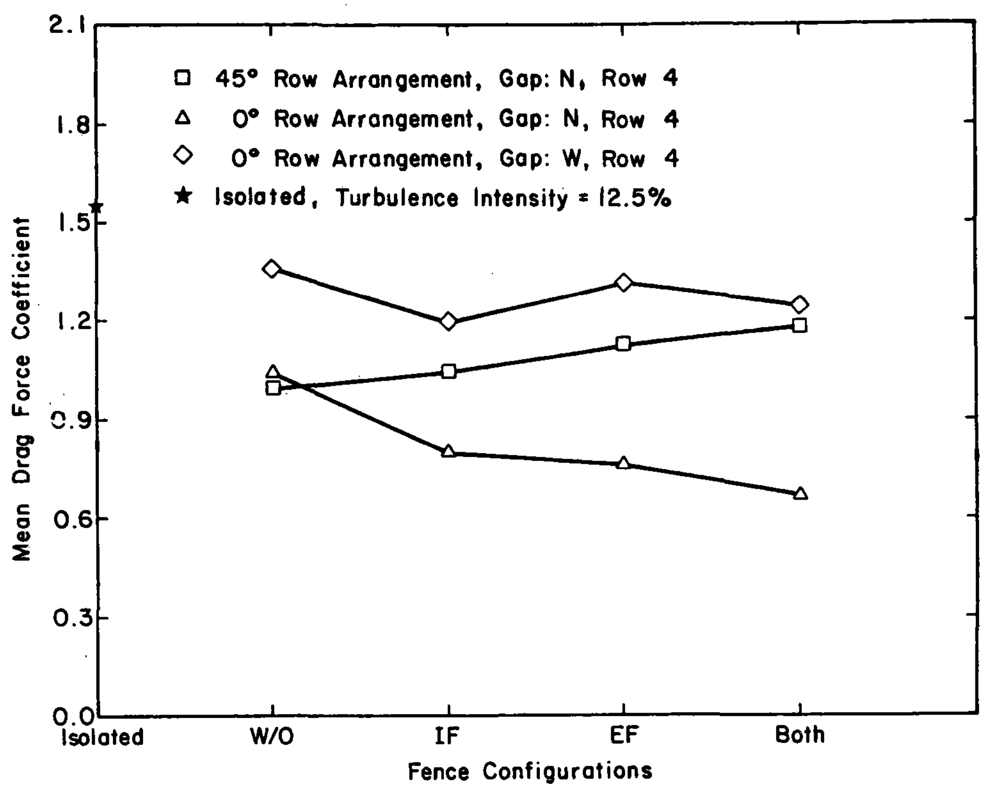

FIGURE 4-5. Influence of Row Spacing on Peak Drag Force

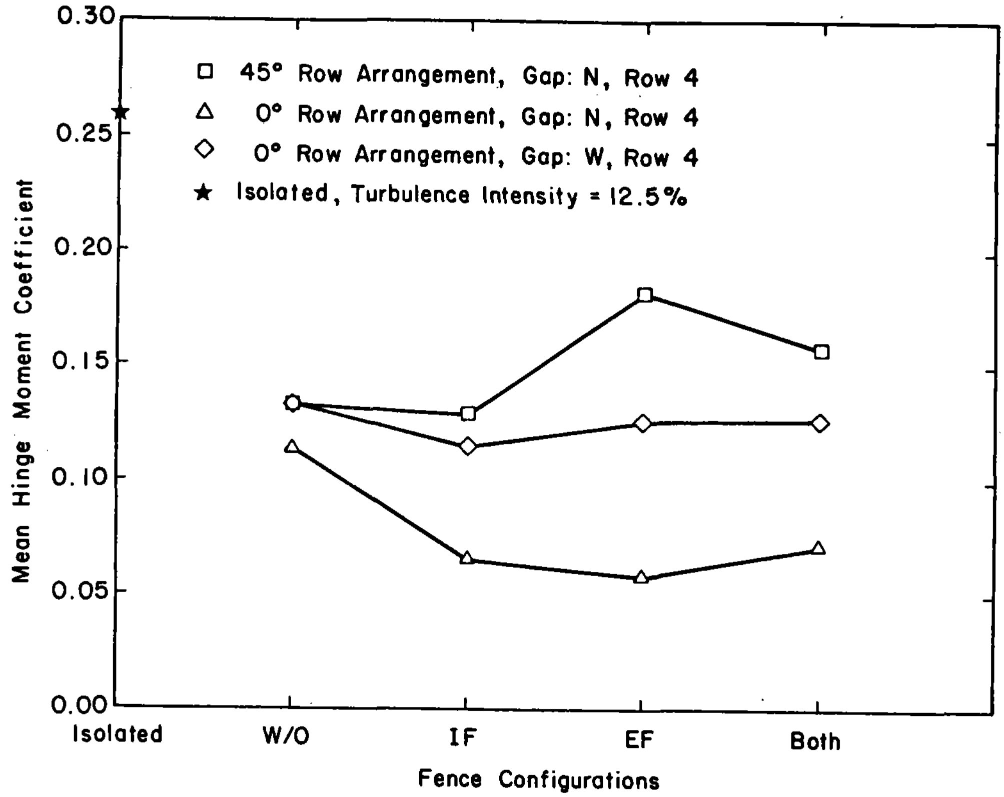

FIGURE 4-6. Influence of Fences and Wind Angle on Fourth Row Mean Drag Force

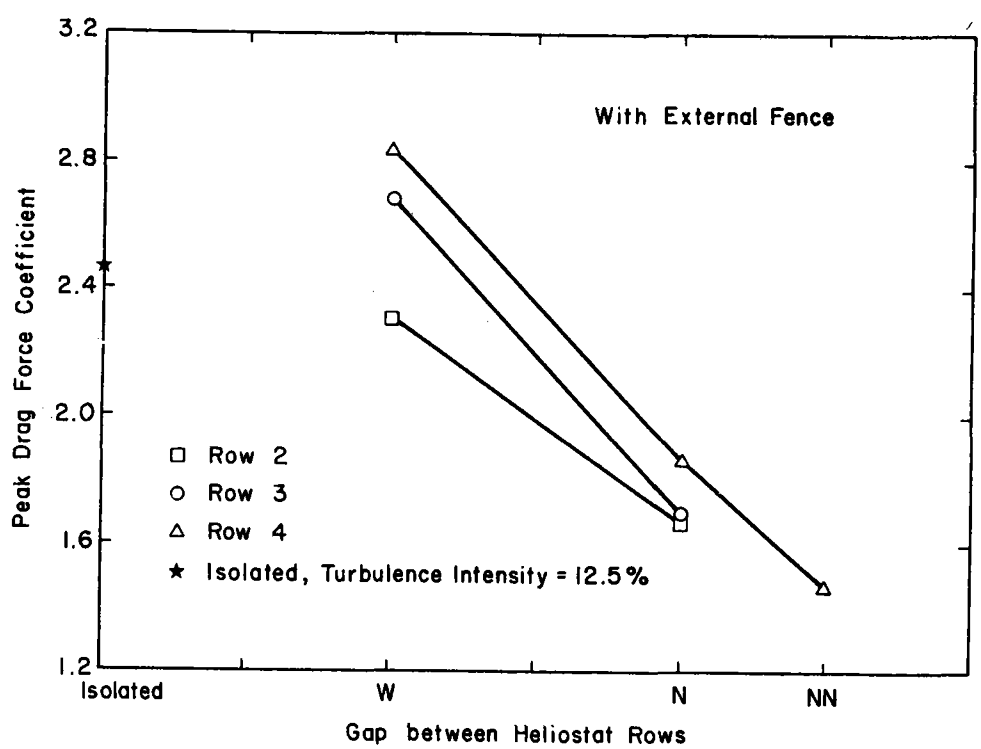

FIGURE 4-7. Influence of Fences and Wind Angle on Fourth Row Mean Hinge Moment

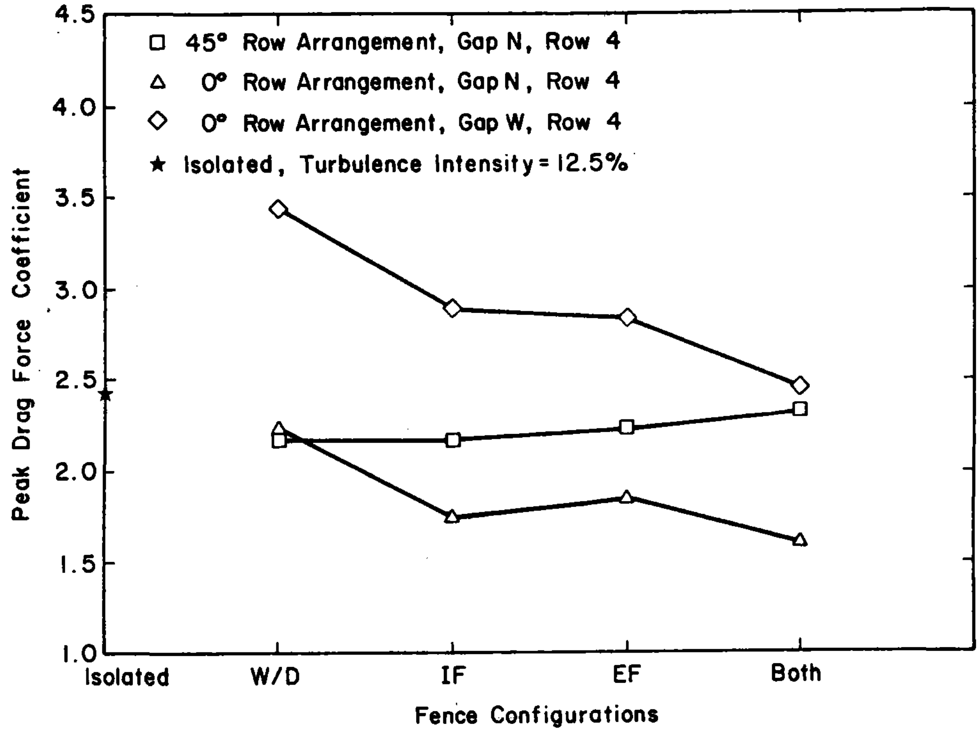

FIGURE 4-8. Influence of Fences and Wind Angle on Fourth Row Peak Drag Force

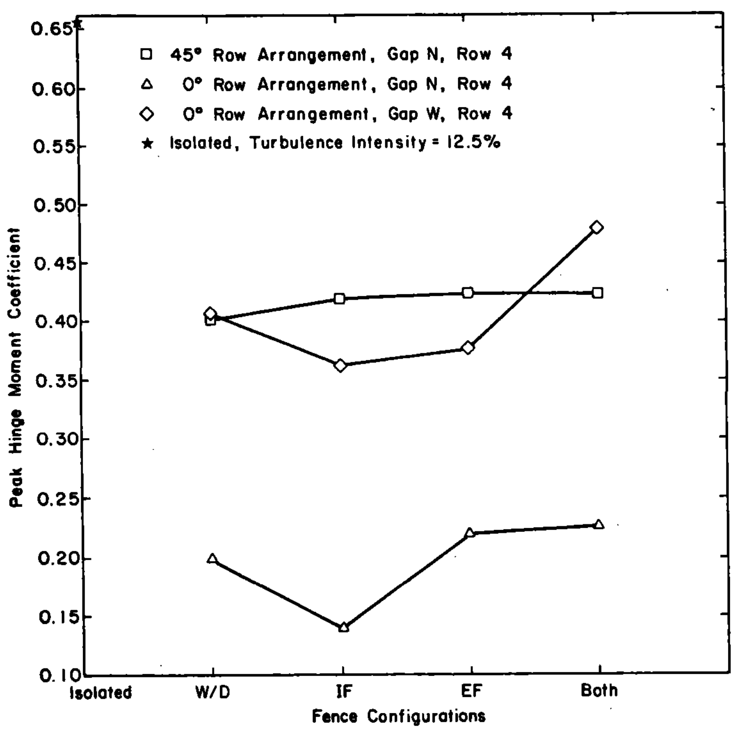

FIGURE 4-9. Influence of Fences and Wind Angle on Fourth Row Peak Hinge Moment

SECTION 5.0

REVIEW OF WIND LOADS ON PARABOLIC COLLECTORS

The bluff geometry of parabolic concentrators results in complex flow patterns which are impossible to predict analytically. As with flat collectors, experimental results are used to provide data necessary for prediction of the wind-induced aerodynamic loads on and responses of the collectors. The data is based on wind-tunnel and full-scale experiments. In most cases only the wind-tunnel data is available.

The scope of available data related to wind loading on three-dimensional parabolic collectors is rather limited. Parabolic troughs and trough field arrays have been studied in a simulated atmospheric boundary layer [8], but the majority of wind loading data for three-dimensional parabolic reflectors were obtained from model studies on radio antennas [39]. Most of the earlier theoretical and experimental studies were performed for isolated (single) reflectors in uniform non-turbulent flows. As shown earlier in this report, the lack of turbulence and shear in the approach flow can seriously underpredict wind loads on collectors in a real atmospheric wind.

Wind-tunnel data for parabolic antenna models were presented by Blaylock et al. [40]. Models with different surface porosities (uniform porosity ranging from zero to 50 percent and edge-only porosity) and various depth-to-diameter ratios were tested. The overall aerodynamic forces and moments were measured for various orientations of the antenna model relative to the approach flow. Only the mean (static) loads were reported. Most of the tests were conducted in uniform flow.

The results presented in reference [40] included the sensitivity of the aerodynamic data to changes in such parameters as: the center of rotation of the antenna, the depth-to-diameter ratio, the surface porosity, edge spoilers, support structure, ground plane interference. The effects of the atmospheric velocity profile were evaluated through a series of tests in 1/7th power-law boundary-layer profile. No turbulence characteristics such as intensity, spectra, or scale were reported for these shear flow tests so that it is not possible to determine how well the flow modeled the atmospheric boundary layer. The influence of the boundary layer in these tests was small, a possible indication of too low a turbulence intensity.

Use of data of [40] for wind loading specifications for prototype parabolic reflectors is limited due to the fact that most of the data was extracted in a uniform flow. Also, the data obtained in boundary-layer flow should be treated with caution. Therefore extrapolation of the model data to prototype conditions cannot be made without significant uncertainties.

Wind effects on parabolic antennas were also analyzed by Cohen and Vellozzi [41]. Their study was limited to an analysis of static effects. The authors synthesized earlier experimental results for parabolic antennas, obtained for small models in uniform flow. They summarized the effects of several design parameters (depth-to-diameter ratio, surface solidity ratio, details of surface geometry) on mean aerodynamic forces and moments. The effects were discussed for the operational ranges of the altitude and azimuth angles.

The experimental data was supplemented by theoretical analysis for pressure distribution and lift coefficient for antenna at low angles of attack. A potential flow theory developed for a circular arc and flat plate was extended and used to estimate pressure distribution and lift coefficient for a parabolic (solid and porous) reflector. For higher angles of attack, empirical relations were proposed by the authors. The agreement between the theoretical predictions and the experimental data was not satisfactory; however, trends in the results were similar and the agreement was improved by adjustments in the theoretical results to account for viscous effects and flow separation.

The authors also discussed in some detail ground effects and shielding effects for a parabolic reflector. Based on the data for the effects of ground proximity on aerodynamic characteristics of rectangular cambered wings of low aspect ratio, they conducted that the ground effects for a solid circular reflector in a vertical position should be negligible for gap-to-diameter ratio greater than 0.35. (The gap is the minimum distance from the reflector to the ground.) Limited experimental data was also used to estimate the shielding effects by an upwind reflector. An empirical relation was proposed for the shielding factor downstream of a reflector of porosity equal to or higher than 0.20.

The presented data did not address the effects of the boundary-layer flow approaching the reflectors. Only static wind effects were analyzed. These constraints limit the application of the presented data in design of prototype parabolic solar collectors.

A recent discussion [39] of uniform flow wind-tunnel results for parabolic reflectors suggests the following observations:

1. The minimum drag occurs at zero angle of attack. It increases with the depth-to-diameter ratio.

2. Maximum lift occurs at a positive angle of attack of 30 degrees. The lift is low and directed upwards for negative angles of attack.

3. Support structures generally have a tendency to reduce peak loads.

A wind-tunnel study has been performed at CSU on a LaJet parabolic collector in a turbulent boundary layer flow which modeled atmospheric winds [42]. A comparison of these data with uniform flow data on parabolic collectors was made as part of this study. Differences were expected because of the large porosity of the LaJet collector and due to the presence of turbulence and shear in the wind flow.

The results of the comparison of LaJet data with uniform flow data are given in Figures 5-1 to 5-4. These figures show drag, lift, and moments about two locations for two sets of data: (1) a summary of uniform flow lift, drag and moment obtained from pages 13-38 and 13-39 of Roschke [39], and (2) data from reference [42] which lists data for turbulent boundary layer flow for the LaJet collector. Data were converted to the coordinate reference system used

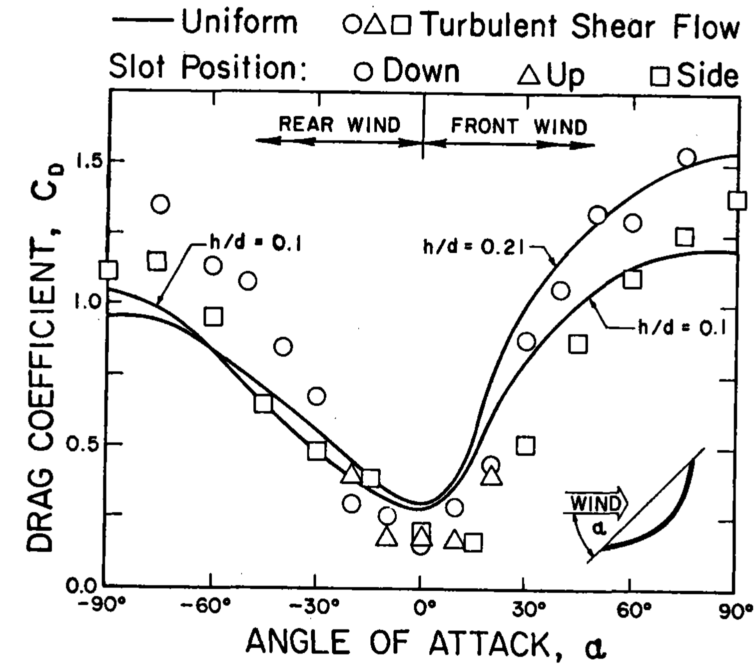

FIGURE 5-1. Comparison of LaJet Collector Drag with Uniform Flow Dish Collectors from Reference 6

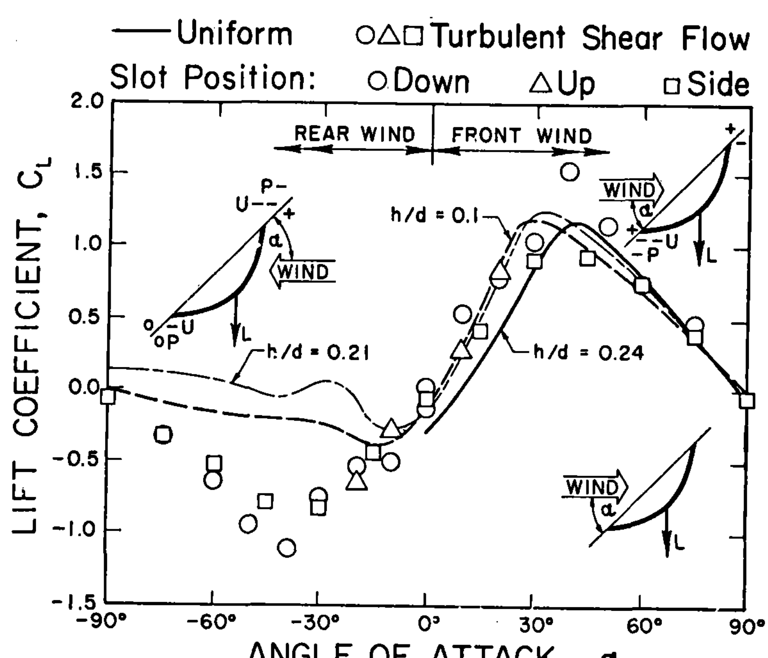

FIGURE 5-2. Comparison of LaJet Collector Lift with Uniform Flow Dish Collectors from Reference 6

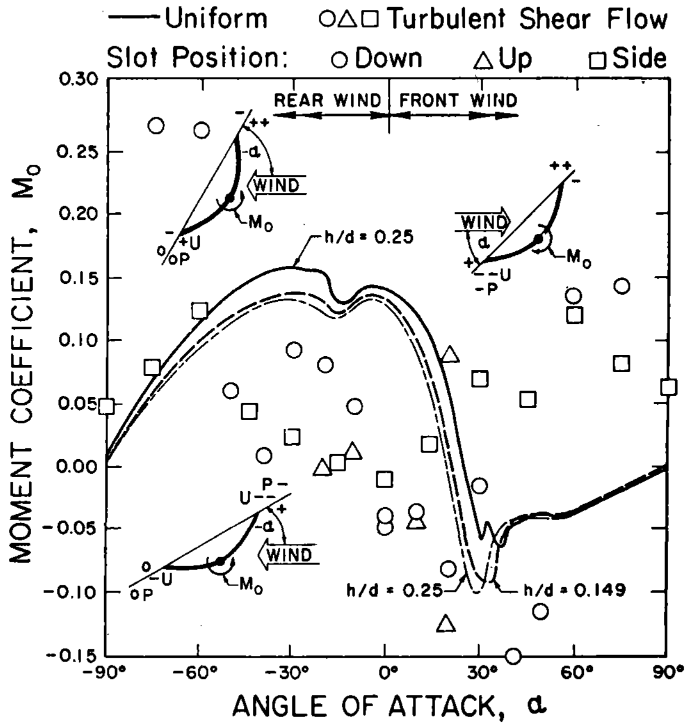

FIGURE 5-3. Comparison of LaJet Collector Moment at O with Uniform Flow Dish Collectors from Reference 39

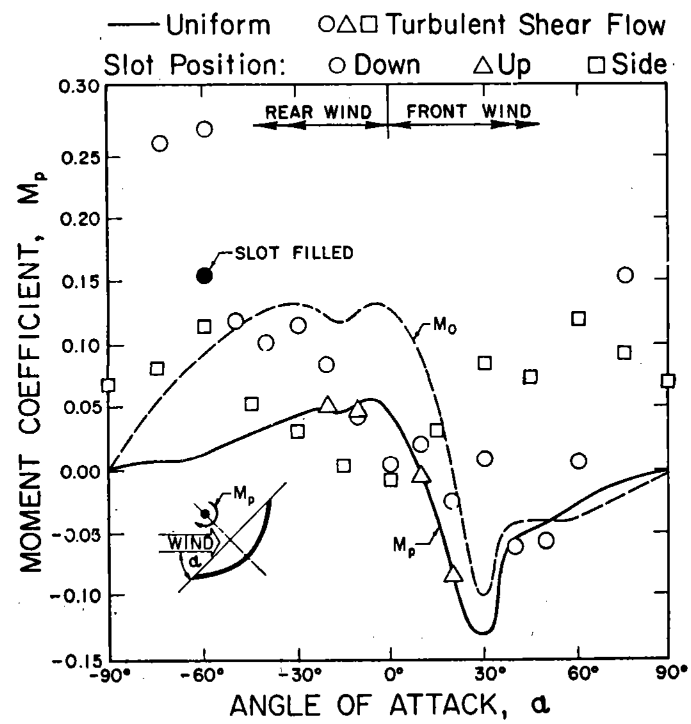

FIGURE 5-4. Comparison of LaJet Collector Moment at P with Uniform Flow Dish Collectors from Reference 39

by Roschke for convenience. The reference area used in the coefficients was based on a circle with diameter of the LaJet collector at the midpoint of the six flat sides bounding the periphery of the collector and with 1/6 of the area removed to account for the missing 1/6 sector of the collector (called slot in the figures). Porosity was ignored in calculating collector area, since porosity is not always effective in reducing loads by the fraction of porosity existing and because estimated area of the supporting truss work accounted for more than half of the area represented by porosity. The variable h/d in the figures represents depth of collector dish h divided by the diameter d. This value was about 0.1 for the LaJet collector.

Several factors contribute to differences between the LaJet collector of reference [42] and the collectors of reference [39]: one set is porous, one solid; one set has a slot, the other none; one set was tested in a turbulent boundary layer, the other in a uniform, non-turbulent flow. The differences in load coefficients in Figures 5-1 to 5-4 can be attributed to these differences. The increase in drag coefficient of Figure 5-1 for the LaJet data indicates increase in drag due to turbulence, although uncertainty in applicable reference area is of the same size as differences in drag coefficient.

In Figure 5-2, the apparent good agreement between data sets for $\alpha > 0$ is the result of two factors influencing the LaJet collector: increased turbulence is expected to increase lift while the collector porosity should adjust pressure distributions across the surface in a way which should decrease lift. The cancellation of these effects leaves the data essentially unchanged from the uniform flow case. For $\alpha < 0$, balancing forces at opposite rims in the uniform flow case are disrupted in the LaJet case resulting in a significantly higher lift. In Figures 5-2 to 5-4, + and - local pressure indications near the lips are labeled with U for uniform flow or P for porous. The speculated changes in the local pressure distribution from one case to the other can provide an explanation of differences between the data sets. These local pressure indications are conjecture based on experience and has no basis in actual local pressure measurements.

The moment comparisons of Figures 5-3 and 5-4 show large variations between uniform flow and the LaJet data. The LaJet data above 0.25 in moment coefficient are due in major part to the shift in center of pressure caused by the missing sector in the slot down configuration. Filling the slot or turning it to the side caused a dramatic decrease in moment. Other differences between uniform flow and LaJet data can be explained by conjectured local pressure distribution differences as shown by drawings on the figures. The overall precision of the measurements of the LaJet data is much better than the general scatter of LaJet data. Differences in geometry between the various LaJet configurations is sufficient to cause this.

The difference which might be expected between two identical solid dish collectors placed in uniform or turbulent boundary layer flow is difficult to assess from the comparisons shown above. An indication of the differences might be provided by the one equivalent comparison shown by Roschke on pages 13-37, reproduced here as Figure 5-5. The differences shown are modest; however, the modeled boundary layer was not developed over a long fetch and its ability to duplicate atmospheric turbulence effects has not been established.

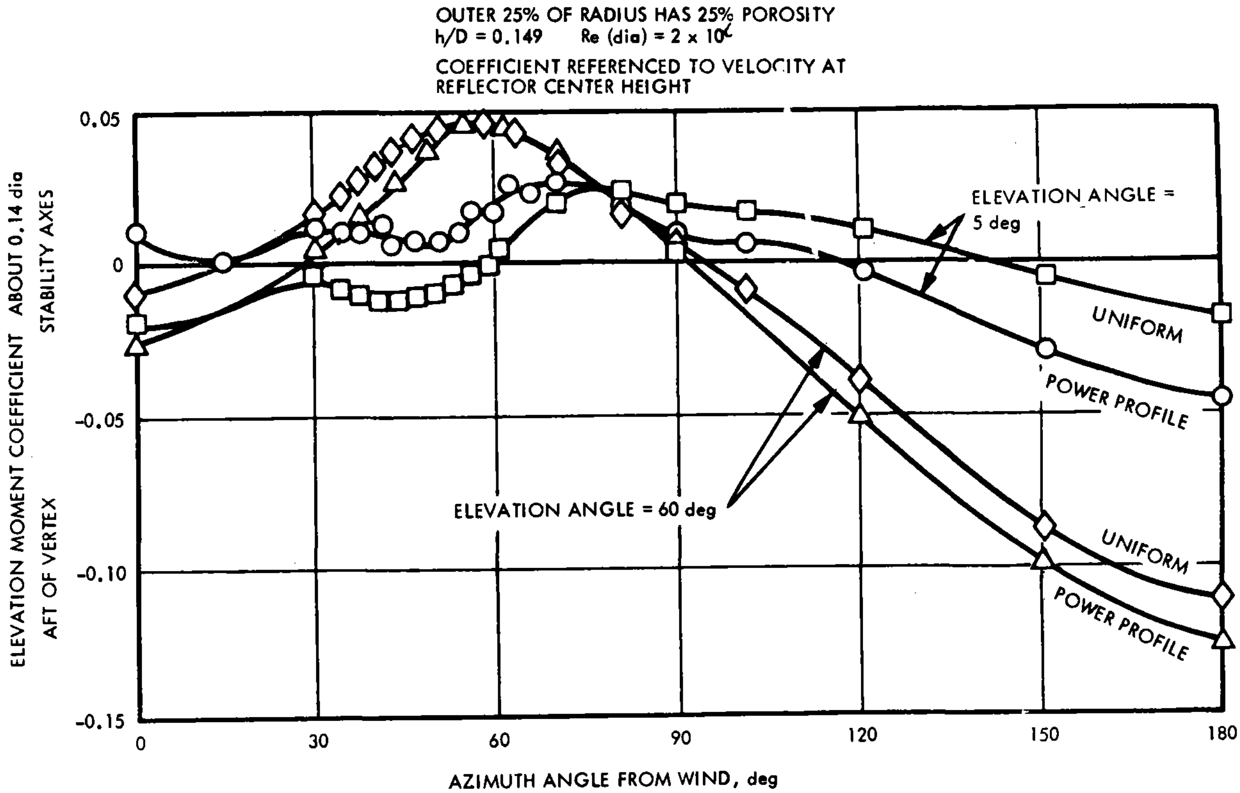

FIGURE 5-5. Effect of a Turbulent Boundary Layer on Dish Collector Moments from Reference 39

The conclusion from the foregoing analysis of parabolic collectors is that uniform flow results increased by 10-20 percent may be a valid starting point for load estimation for solid disks in an atmospheric boundary layer. However, changes in geometry to the disk (or support structure) may cause large and unpredictable variations from the uniform flow case. Systematic studies of dish collectors in an atmospheric boundary layer flow are needed to define isolated collector loads and to determine the influence of nearby collectors in a field.

SECTION 6.0

CONCLUSIONS AND RECOMMENDATIONS

In this study, fluctuating wind loads on model heliostats were obtained in a boundary layer wind tunnel capable of simulating wind flows at model scale. Based on data presented, the following conclusions can be drawn:

- The influence of upwind blockage of heliostats or wind fences can be accounted for by defining a generalized blockage area (GBA) so that the specific geometry may be ignored.

- Both mean and peak wind loads decrease significantly with increasing GBA except for very small GBA, characteristic of heliostats in very open fields, or of heliostats in the first two rows at the field edge.

- Wind fences at 45 degrees to the approach wind are less effective than wind fences perpendicular to the wind. Wind blockage elements (fences) which do not represent a long continuous fence may be more effective than a single long fence.

- Wind drag and lift on isolated heliostats have shown a surprising sensitivity to turbulence in the wind within the range expected for open-country environments.

- Square and circular heliostats have similar mean and peak wind load coefficients.

- Peak wind loads on operational heliostats are larger than those on heliostats in survival stow position provided that the heliostat in stow is rotated so that the axis of elevation rotation points into the wind.

- Fluctuating loads about a near zero mean load in stow position may create fatigue loading more severe than for operational loads for some load components. This result is based on conjecture and not on experimental measurements in this study.

- Heliostats with porous edges do not provide effective load reductions for either mean or peak wind loads.

- Some data in uniform flow exists for wind loads on parabolic collectors, but insufficient data is available for adequate design decisions.

On the basis of the data and the conclusions presented herein, the following recommendations for further work are set forth:

- The effects of approach wind turbulence should be explored to determine the range of isolated collector load expected in typical installation environments. This recommendation is in response to the unexpected sensitivity to turbulence uncovered in this study.

- With resolution of the turbulence issue, a simplified design guide should be prepared for use in preliminary field design.

- Peak wind loads on flat heliostats in stow position should be examined more closely to determine the nature of fatigue loading.

- Mean and peak wind loads on parabolic collectors should be obtained in both isolated and field environments to determine differences between flat and parabolic shapes.

- Research to improve the effectiveness of wind fences oriented 45 degrees to approach winds might reduce the loads on heliostats in a field below those reported herein.

REFERENCES

1. Cermak, J. E., J. A. Peterka and A. Kareem, "Heliostat Field-Array Wind Tunnel Test," Technical Report for McDonnell Douglas Astronautics Company, Huntington Beach, California, Report No. CER78-79JEC-JAP-AK2, July 1978, 55 pages.

2. Ewald, R. L., J. A. Peterka and J. E. Cermak, "Heliostat-Array Wind Tunnel Study," Technical Report for Martin Marietta Aerospace, Report No. CER78-79RLE-JAP-JEC31, January 1979.

3. Peterka, J. A., J. J. Lou and J. E. Cermak, "Wind-Tunnel Test of a Photovoltaic Concentrator Array," Technical Report for Martin Marietta, Denver, Colorado, Report No. CER78-79JAP-JJL-JEC62, June 1979, 34 pages.

4. Peterka, J. A., J. M. Sinou and J. E. Cermak, "Mean Wind Forces on Parabolic-Trough Solar Collectors," Technical Report for Sandia Laboratories, Albuquerque, New Mexico, Report No. CER79-80JAP-JMS-JEC4, July 1979, 109 pages.

5. Franklin, H. A., "Wind Design of Flat-Panel Photovoltaic Array Structures -- Final Report," Report No. SAND 79-7057, 83 pages.

6. Miller, R. and D. Zimmerman, "Wind Loads on Flat Plate Photovoltaic Array Fields, Phase II: Final Report," Report No. DOE/JPL 954833-79/2, September 1979, 111 pages.

7. Poreh, M., J. A. Peterka and J. E. Cermak, "Wind-Tunnel Study of Wind Loads on Photovoltaic Structures," Technical Report for Bechtel National, San Francisco, California, Report No. CER79-80MP-JAP-JEC11, September 1979, 83 pages.

8. Peterka, J. A., J. M. Sinou and J. E. Cermak, "Mean Wind Forces on Parabolic-Trough Solar Collectors," Sandia Laboratories, Albuquerque, New Mexico, Report No. SAND 80-7023, May 1980, 109 pages.

9. Randall, D. E., D. D. McBride and R. E. Tate, "Steady-State Wind Loading on Parabolic-Trough Solar Collectors," Report No. SAND 79-2134, August 1980, 21 pages.

10. Hosoya, N., J. A. Peterka, M. Poreh and J. E. Cermak, "Wind Pressures and Forces on Flat-Plate Photovoltaic Solar Arrays," Technical Report for Boeing Eng., Seattle, Washington, Report No. CER80-81NH-JAP-MP-JEC13, September 1980, 81 pages.

11. Hosoya, N., J. A. Peterka, M. Poreh and J. E. Cermak, "Wind Pressures and Forces on Flat-Plate Photovoltaic Solar Arrays Data Supplement: Appendix," Technical Report for Boeing Eng., Seattle, Washington, Report No. CER80-81NH-JAP-MP-JEC13a, September 1980, 182 pages.

12. Miller, R. D. and D. K. Zimmerman, "Wind Loads on Flat Plate Photovoltaic Array Fields, Phase III, Final Report," Report No. DOE/JPL 954833-81/3, April 1981, 250 pages.

13. Hosoya, N., J. A. Peterka and J. E. Cermak, "Wind Pressures and Forces on Flat-Plate Photovoltaic Solar Arrays - Cross-Spectral Analysis," Technical Report for Boeing Eng., Seattle, Washington, Report No. CER80-81NH-JAP-JEC57, June 1981, 47 pages.

14. Miller, R. D. and D. K. Zimmerman, "Wind Loads on Flat Plate Photovoltaic Array Fields (Nonsteady Winds)," Report No. DOE/JPL 954833-81/4, August 1981, 100 pages.

15. Tieleman, H. W., P. R. Sparks and R. E. Akins, "Wind Loads on Flat Plate Solar Collectors," Preprint No. 3632, ASCE Convention and Exposition, Atlanta, Georgia, 23-25 October 1979, 21 pages.

16. Tieleman, H. W., R. E. Akins and P. R. Sparks, "An Investigation of Wind Loads on Solar Collectors," Report No. VPI-E-80-1, January 1980, 155 pages.

17. Tieleman, H. W., R. E. Akins and P. R. Sparks, "An Investigation of Wind Loads on Solar Collectors, Appendix I - Data Listing for Top and Bottom of Collector," Report No. VPI-E-80-1, January 1980, 307 pages

18. Tieleman, H. W., R. E. Akins and P. R. Sparks, "An Investigation of Wind Loads on Solar Collectors, Appendix II - Net Pressure Coefficients," Report No. VPI-E-80-1, January 1980, 165 pages.

19. Mar, J. W. and H. Liebowitz (ed.), Structures Technology for Large Radio and Radar Telescope Systems, The MIT Press, 1969.

20. Cohen, E. (ed.), Large Steerable Radio Antennas - Climatological and Aerodynamic Considerations, Annals of the New York Academy of Science, Vol. 116, October 1964, pp. 1-355.

21. Jet Propulsion Laboratory, "Wind Loads on Dish Antenna," Technical Report CP-6 (unpublished).

22. Murphy L. M., "An Assessment of Existing Studies of Wind Loading on Solar Collectors," Report No. SERI/TR-632-812, February 1981, 43 pages.

23. Peterka, J. A., N. Hosoya, B. Bienkiewicz and J. E. Cermak, "Wind Load Reduction for Heliostats," Solar Energy Research Institute Report, SERI/STR-253-2859, May 1986.

24. Cochran, L. S., J. A. Peterka and J. E. Cermak, "Influence of Porosity on the Mean and Peak Wind Loads for Three Concentrator Photovoltaic Arrays," Technical Report prepared for Sandia National Laboratories, Albuquerque, New Mexico, September 1986, CER86-87LC-JAP-JEC6.

25. Raine, J. K. and D. C. Stevenson, "Wind Protection by Model Fences in a Simulated Atmospheric Boundary Layer, J. Indust. Aero., Vol. 2, 1977, pp. 159-180.

26. Perara, M.D.A.E.S., "Shelter Behind Two-Dimensional Solid and Porous Fences," J. Wind Eng. and Indust. Aero., Vol. 8, 1981, pp. 93-104.

27. Bradley, E. F. and P. J. Mulhearn, "Development of Velocity and Shear Stress Distributions in the Wake of a Porous Shelter Fence," J. Wind Eng. and Indust. Aero., Vol. 15, 1983, pp. 145-156.

28. Cermak, J. E., "Laboratory Simulation of the Atmospheric Boundary Layer," AIAA Jl., Vol. 9, 1971.

29. Cermak, J. E., " Applications of Fluid Mechanics to Wind Engineering," A Freeman Scholar Lecture, ASME Jl. of Fluids Engineering, Vol. 97, No. 1, 1975.

30. Cermak, J. E., "Aerodynamics of Buildings," Annual Review of Fluid Mech., Vol. 8, 1976, pp. 75-106.

31. Green, H. J., letter with data addressed to Clay Mavis, Sandia National Laboratories, Livermore, California, 23 April 1985.

32. Simiu, E. and R. H. Scanlan, "Wind Effects on Structures: An Introduction to Wind Engineering," John Wiley and Sons, New York, 1978.

33. Simiu, E., "Wind Spectra and Dynamic Along Wind Response," ASCE, Jl. of the Structural Division, Vol. 100, NO. ST9, September 1974.

34. Harris, R. I., "On the Spectrum and Auto-correlation Function of Gustiness in High Winds," British Electrical Research Association, Report No. 5273, October 1968.

35. Davenport, A. G., "The Relationship of Wind Structure to Wind Loading," Proc. of Conference on Wind Effects on Structures, NLP, HMSO, 1965.

36. ASCE, "Wind Forces on Structures," Final Report of the Task Committee on Wind Forces of the Committee on Loads and Stresses of the Structural Division, Paper No. 3269, reprinted from Transactions, Vol. 126, Part II, 1961, p. 1124.

37. Peglow, S. G., "Wind Tunnel Test of a Full-Scale Heliostat," Prepared by Sandia Laboratories, Albuquerque, New Mexico, 87115 and Livermore, California 94550 for the U.S. Department of Energy under Contract DE-AC04-76OP00789, printed June 1979.

38. Bearman, P. W., "An Investigation of the Forces on Flat Plates Normal to a Turbulent Flow," Jl. of Fluid Mech., Vol. 46, Part 1, 1971, pp. 177-198.

39. Roschke, E. J., "Wind Loadings on Solar Concentrators: Some General Considerations," Jet Propulsion Laboratory, Pasadena, California, Technical Report DOE/JPL-1060-66 (DE85000337), 1984.

40. Blaylock, R. B., Dayman B. and Fox, N. L., "Wind Tunnel Testing of Antenna Models," Annals New York Academy of Sciences, Vol. 116, pp. 239-272, 1964.

41. Cohen, E. and Vellozzi, J., "Calculation of Wind Forces and Pressures on Antennas," Annals New York Academy of Sciences, Vol. 116, pp. 161-121, 1964.

42. Thoroddsen, S. T., J. A. Peterka and J. E. Cermak, "Wind-Tunnel Study of Wind Loads on LaJet Solar Collector Module," Fluid Mechanics and Wind Engineering Program, Colorado State University, Technical Report CER85-86SST-JAP-JEC12, 1985.

APPENDIX A

Plotted Results for a Single Flat Plate

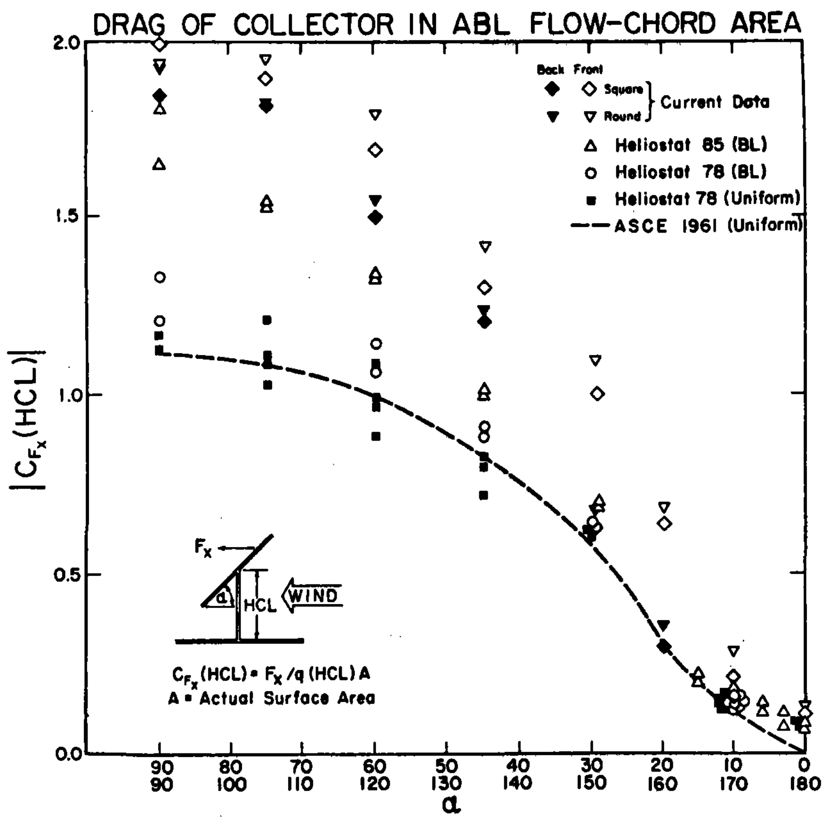

FIGURE A-1. Mean Drag Force Coefficient Variation with α

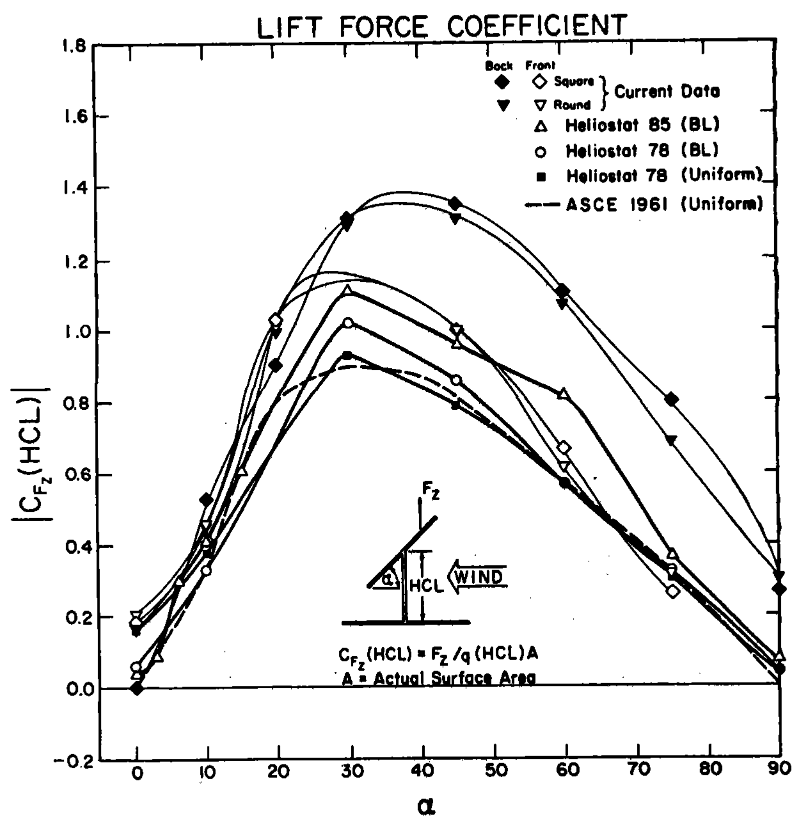

FIGURE A-2. Mean Lift Force Coefficient Variation with α

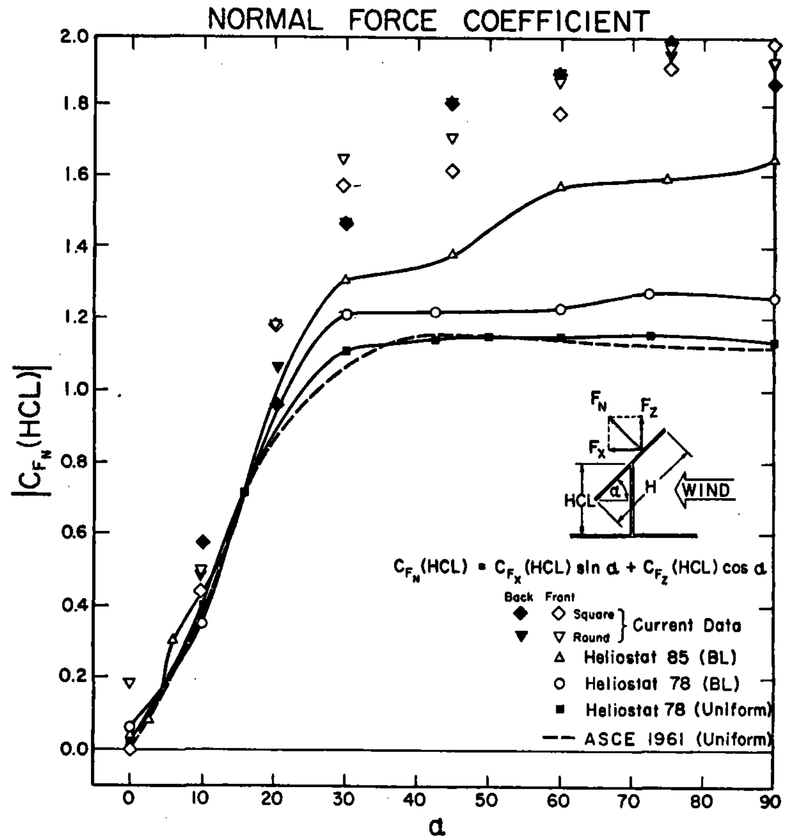

FIGURE A-3. Mean Normal Force Coefficient Variation with α

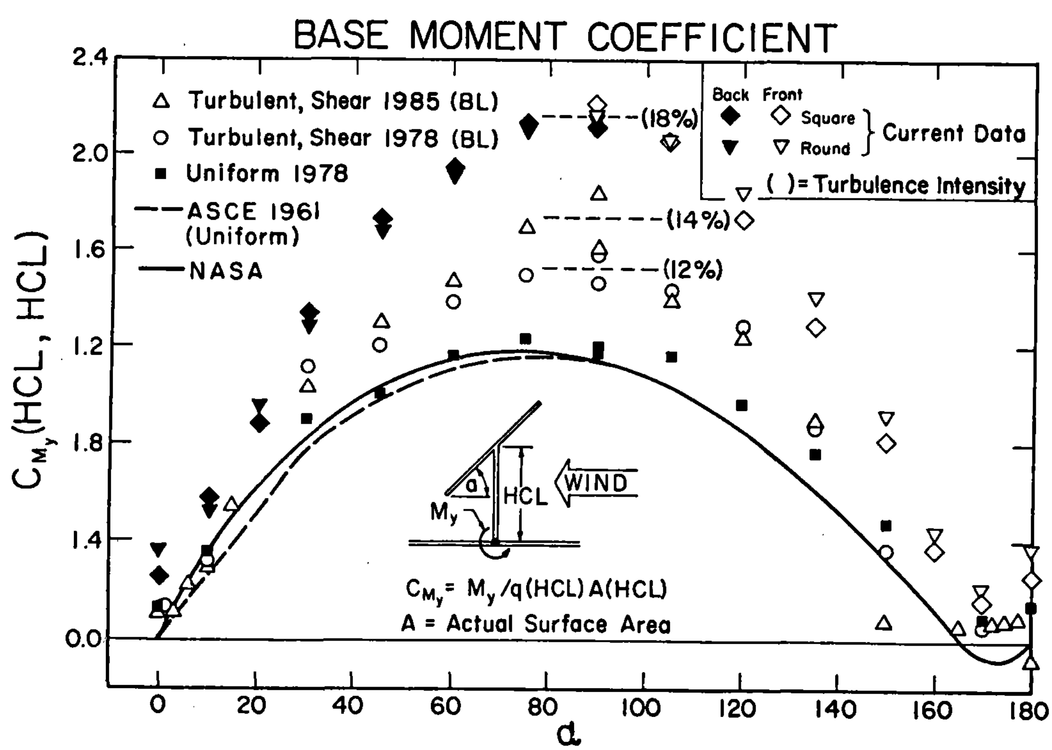

FIGURE A-4. Mean Base Moment Coefficient Variation with α

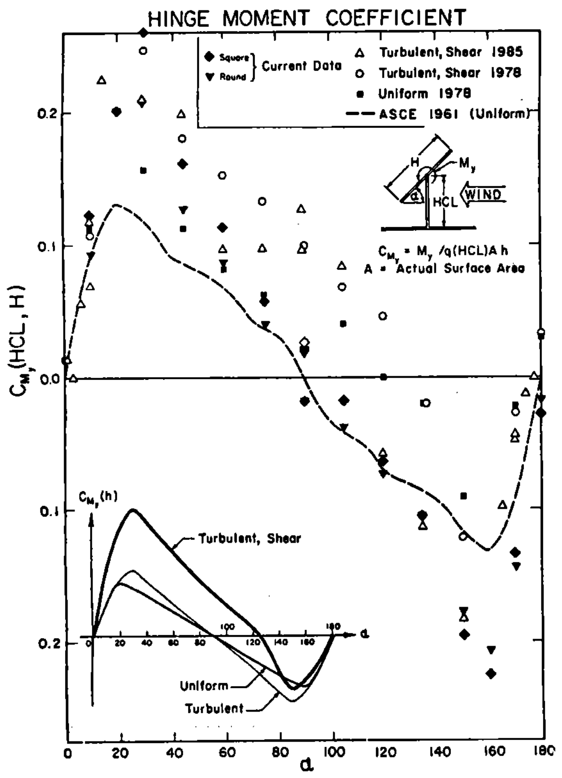

FIGURE A-5. Mean Hinge Moment Variation with α

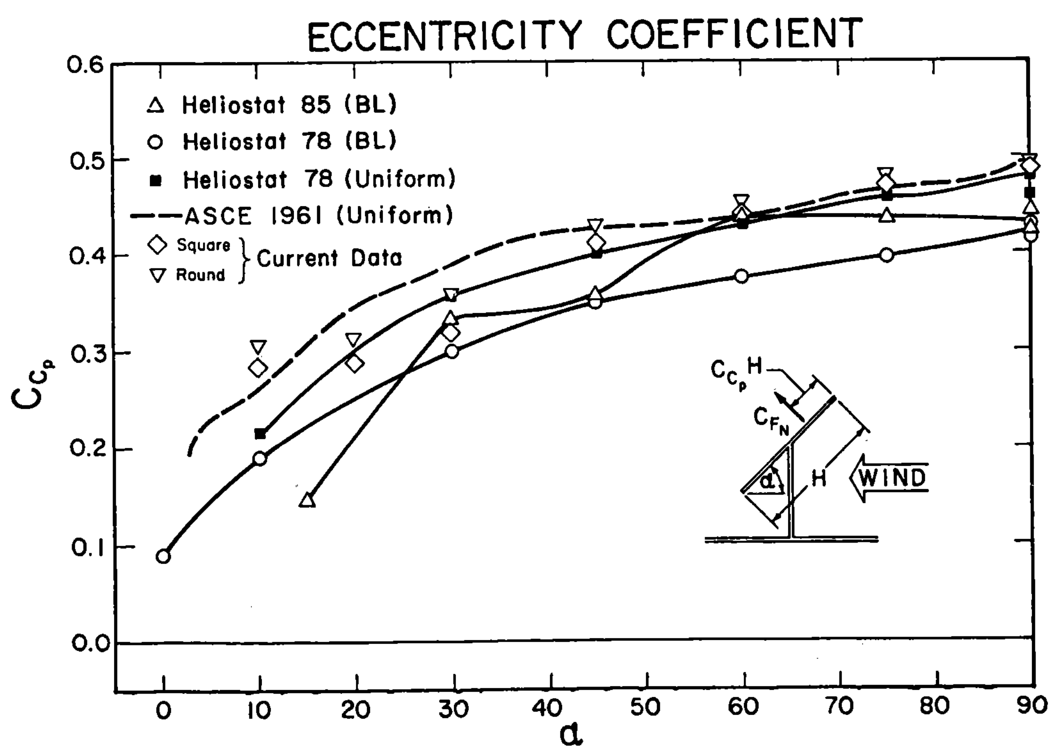

FIGURE A-6. Mean Eccentricity Coefficient Variation with α

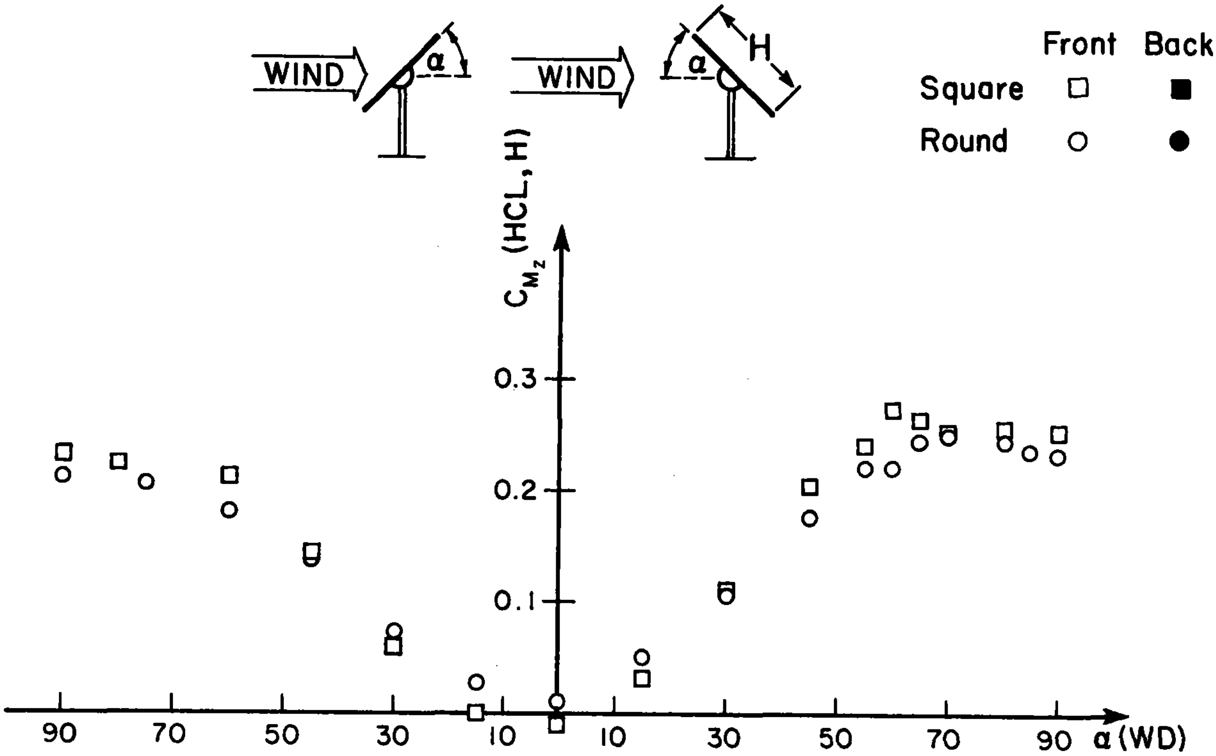

FIGURE A-7. Mean Azimuth Moment Coefficient at β = 65° -- Variation with α

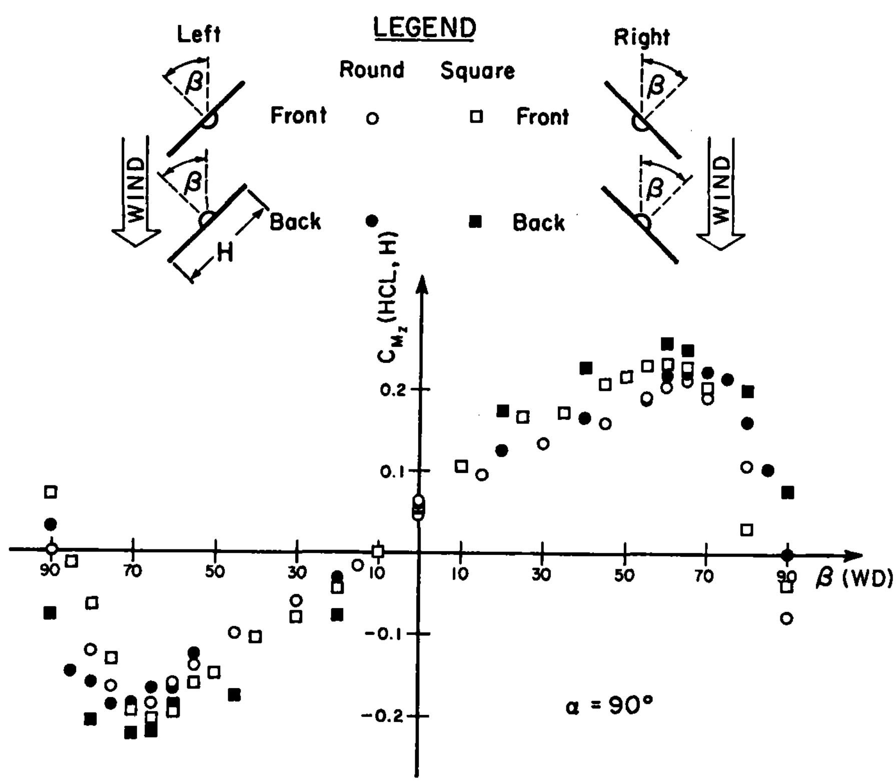

FIGURE A-8. Mean Azimuth Moment Coefficient Variation with β

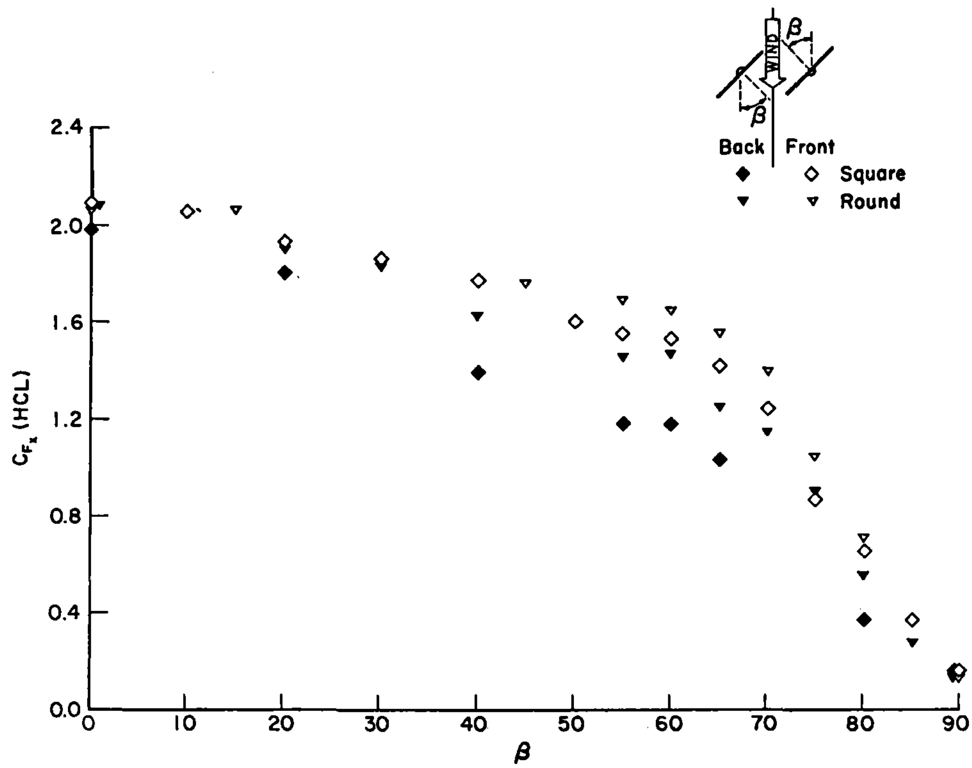

FIGURE A-9. Mean Drag Force Variation with Wind Direction at $\alpha = 90^0$

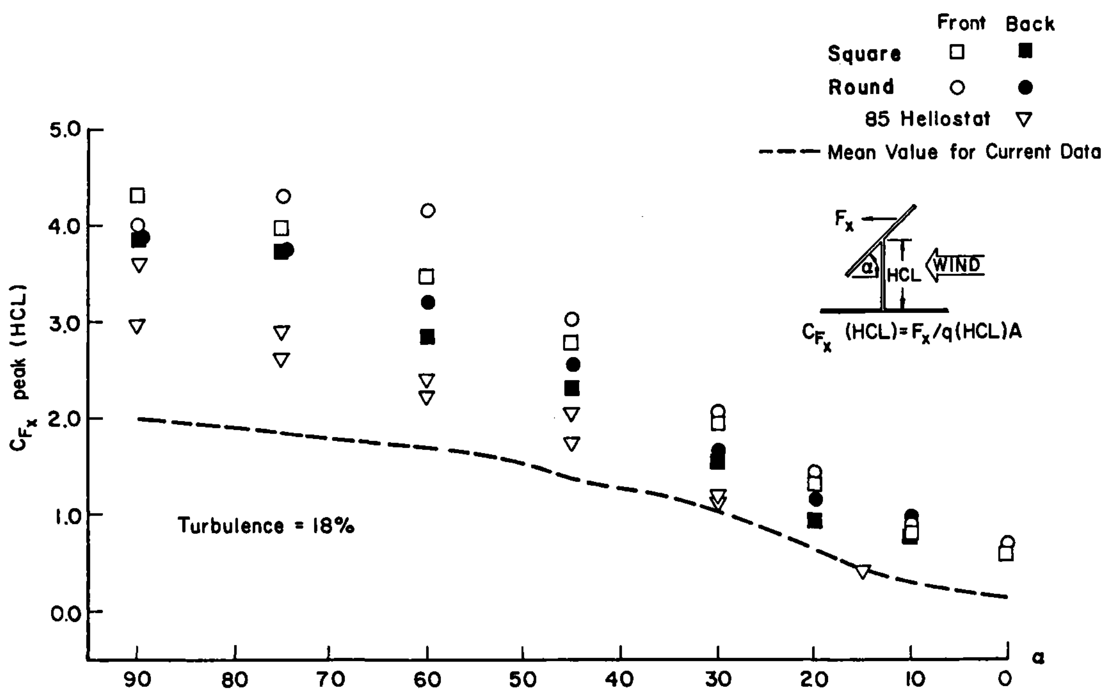

FIGURE A-10. Peak Drag Force Coefficient Variation with α

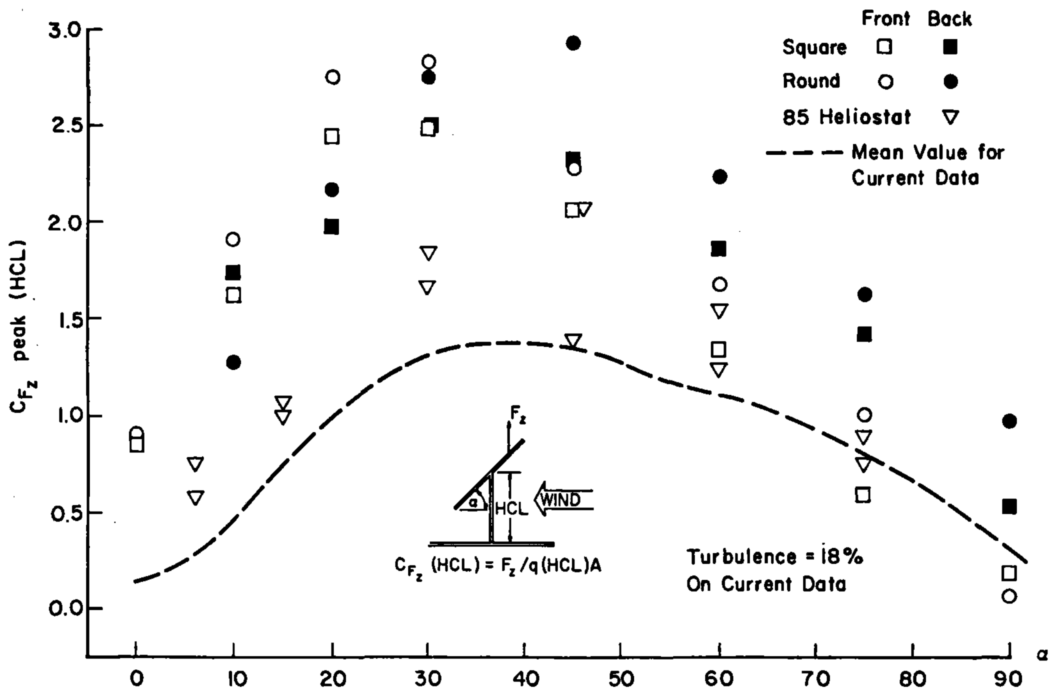

FIGURE A-11. Peak Lift Force Ceofficient Variation with α

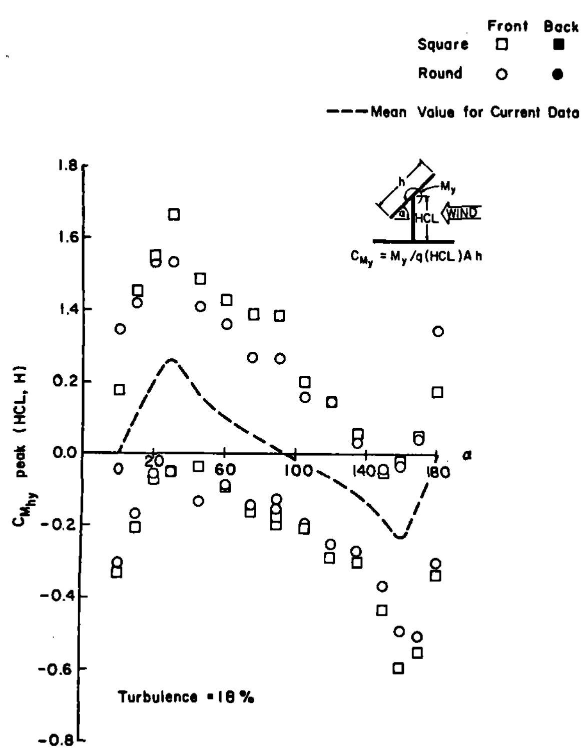

FIGURE A-12. Peak Hinge Moment Coefficient Variation with α

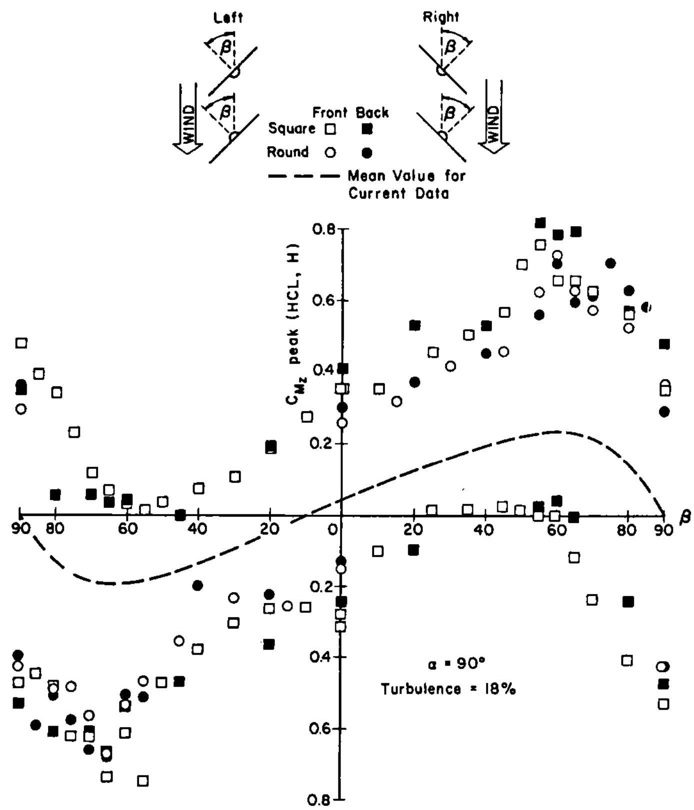

FIGURE A-13. Peak Azimuth Moment Coefficient Variation with β

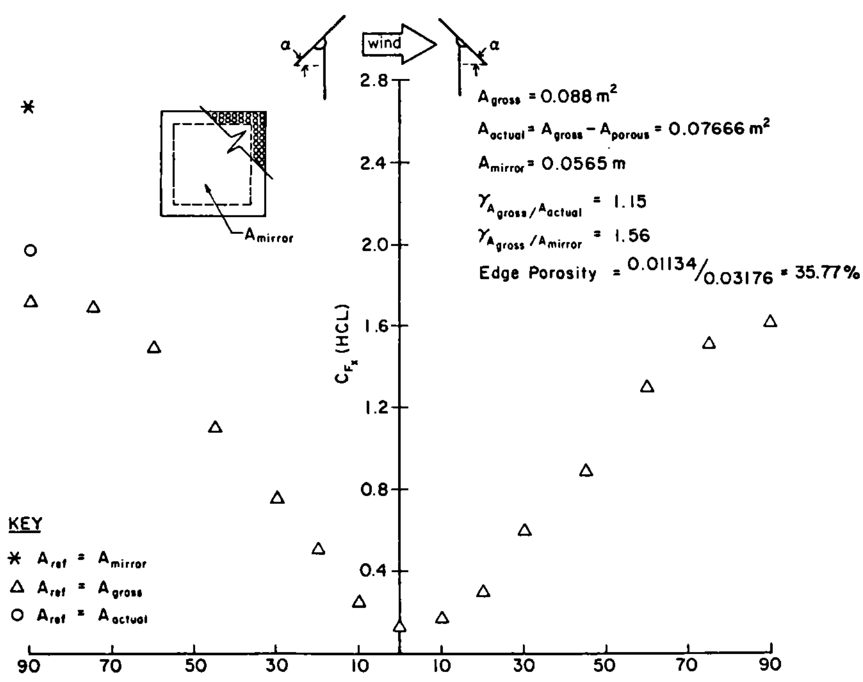

FIGURE A-14. Mean Drag Force on Edge-porous Model

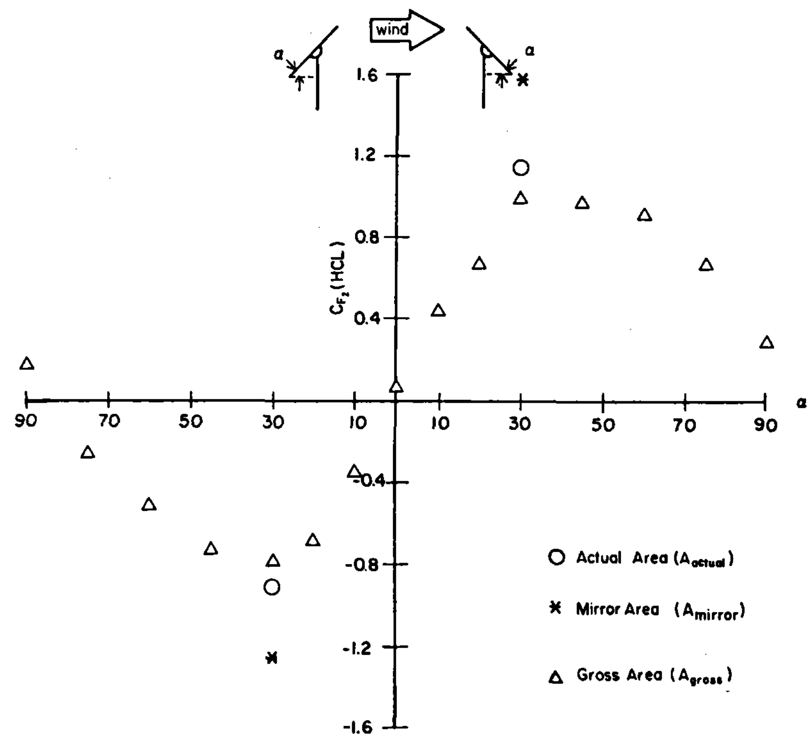

FIGURE A-15. Mean Lift Force on Edge-porous Model

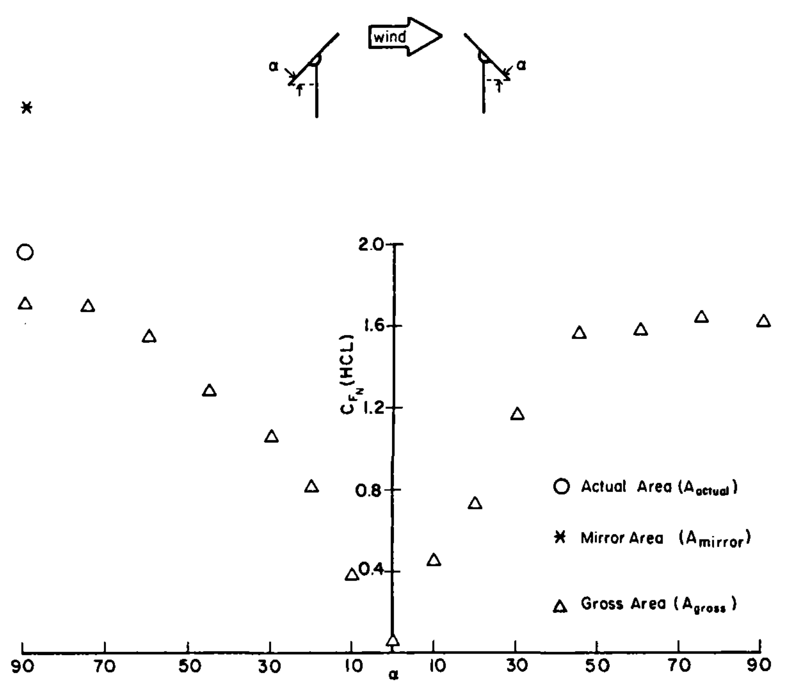

FIGURE A-16. Mean Normal Force on Edge-porous Model

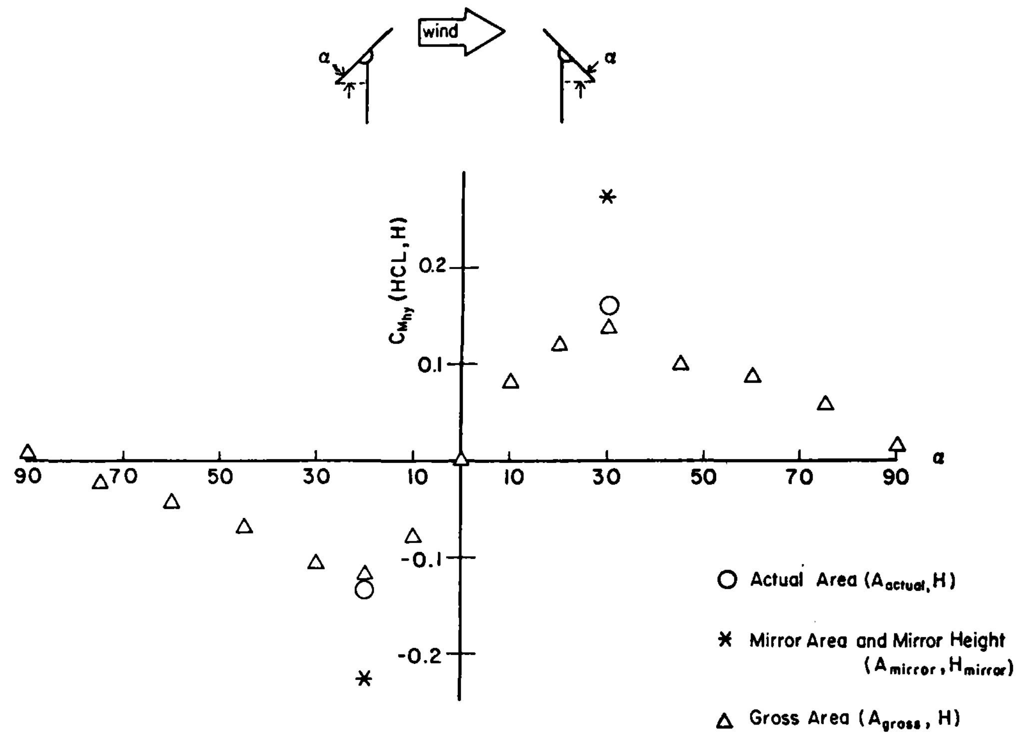

FIGURE A-17. Mean Hinge Moment on Edge-porous Model

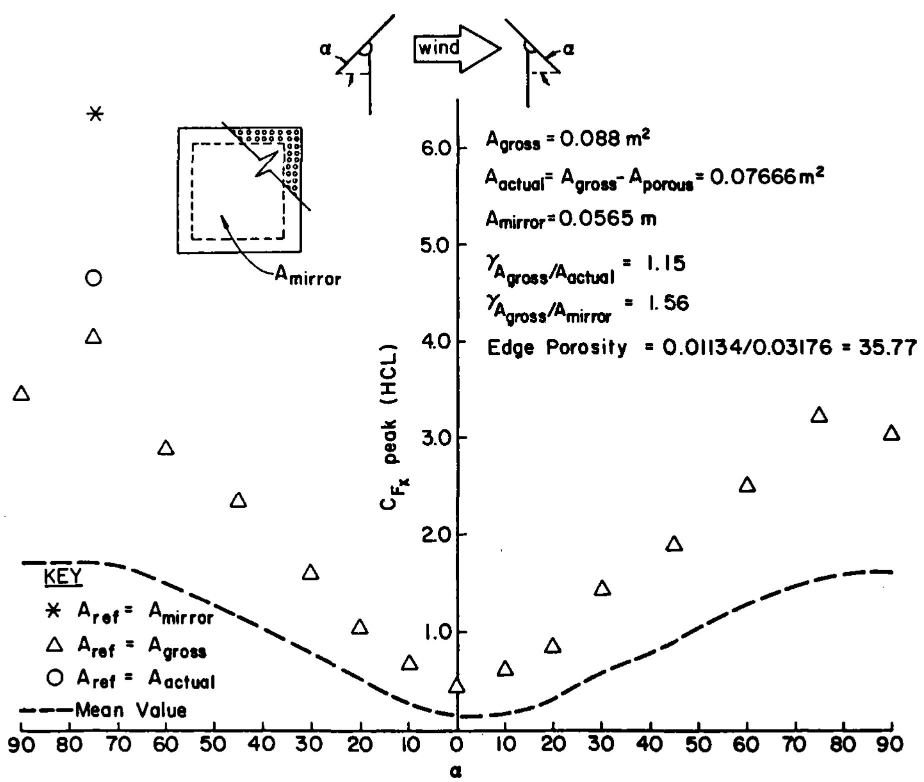

FIGURE A-18. Peak Drag Force on Edge-porous Model

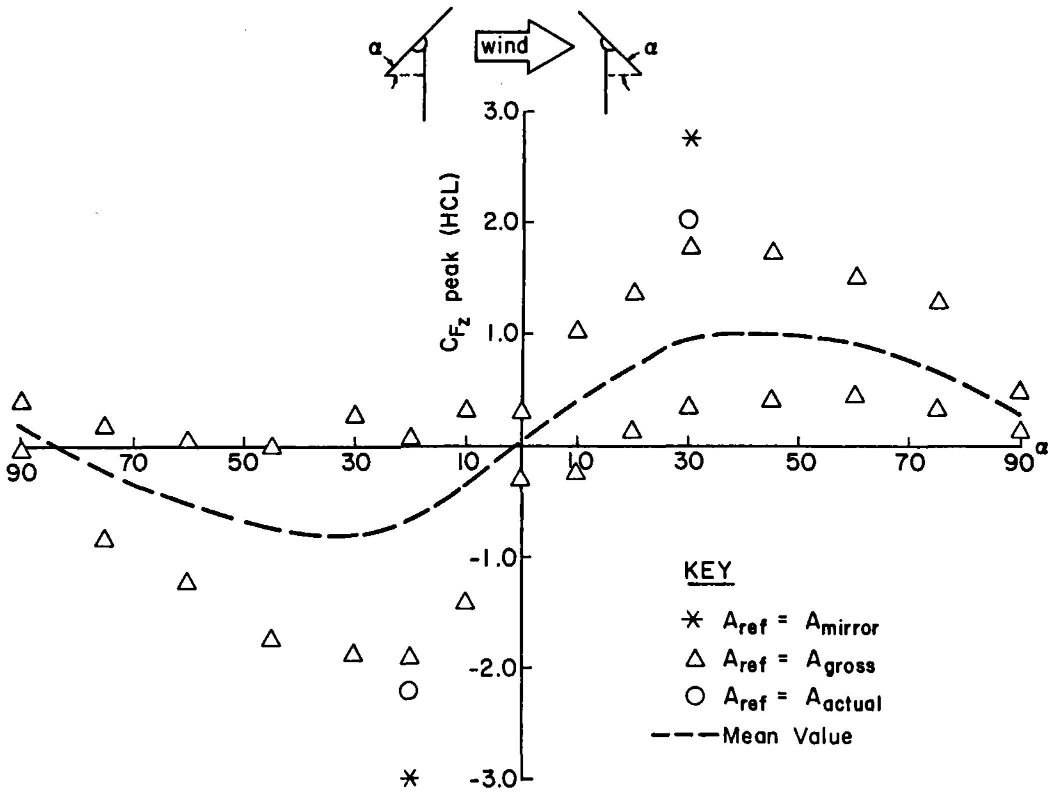

FIGURE A-19. Peak Lift Force on Edge-porous Model

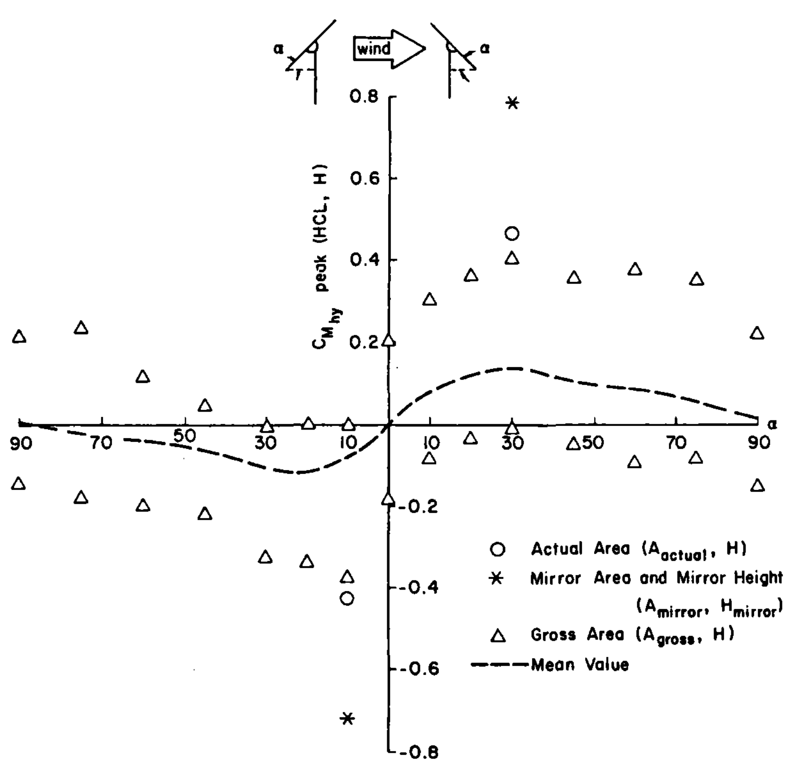

FIGURE A-20. Peak Hinge Moment on Edge-porous Model

APPENDIX B

Plotted Results for a Flat Plate as Part of a Field

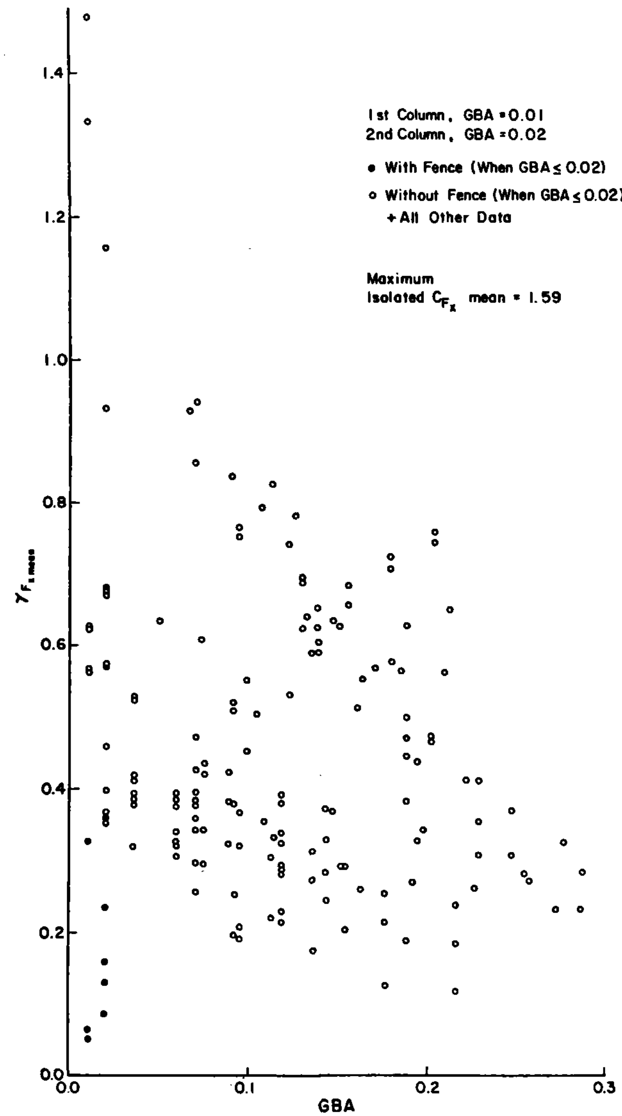

FIGURE B-1. Mean Drag Force Ratio in Current Study

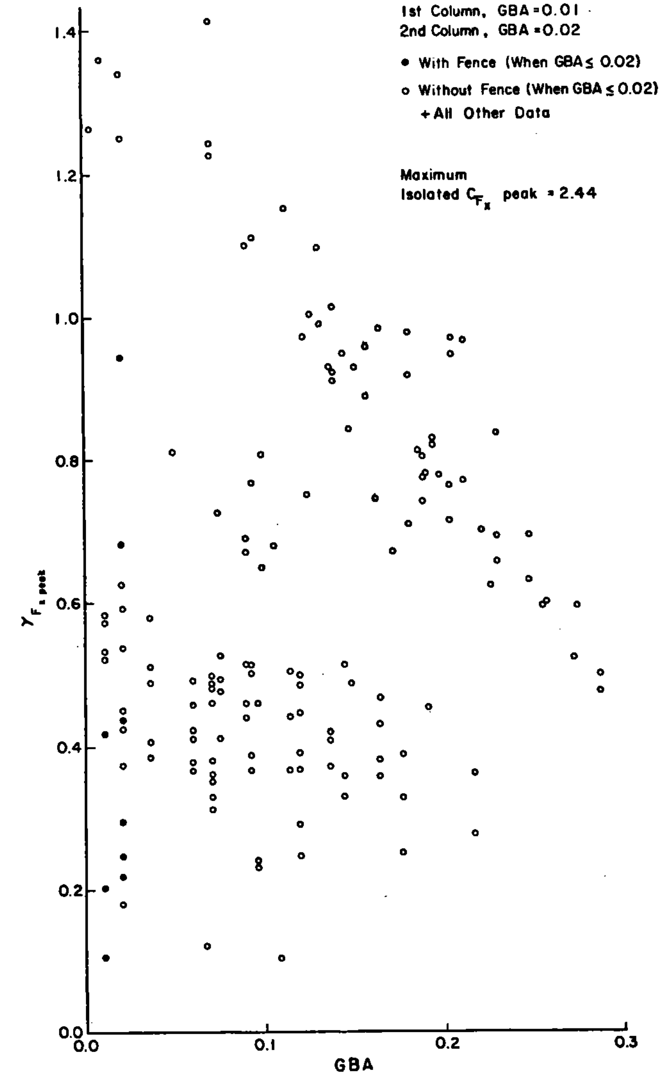

FIGURE B-2. Peak Drag Force Ratio in Current Study

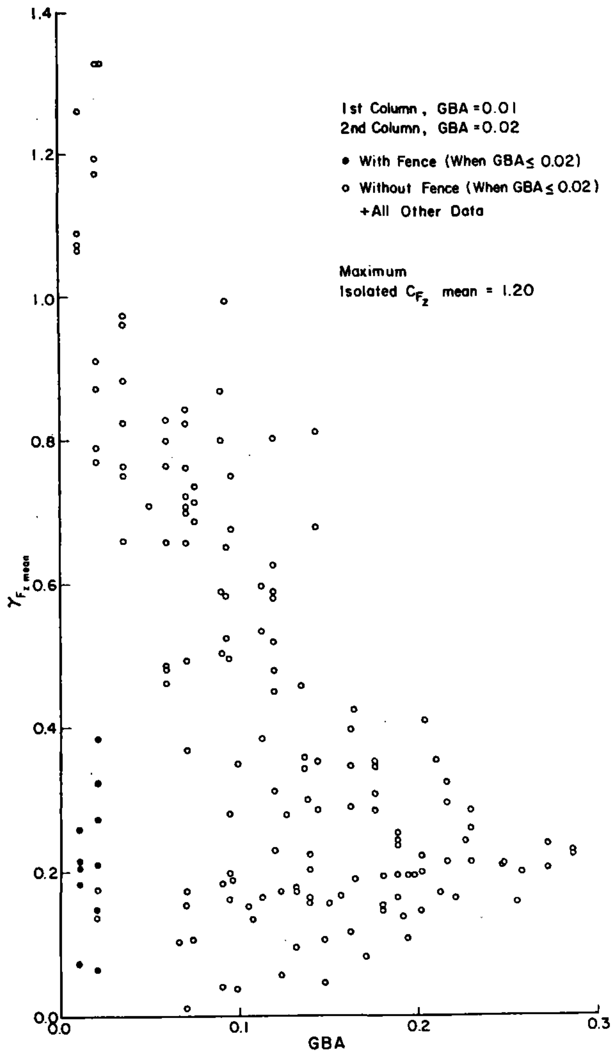

FIGURE B-3. Mean Lift Force Ratio in Current Study

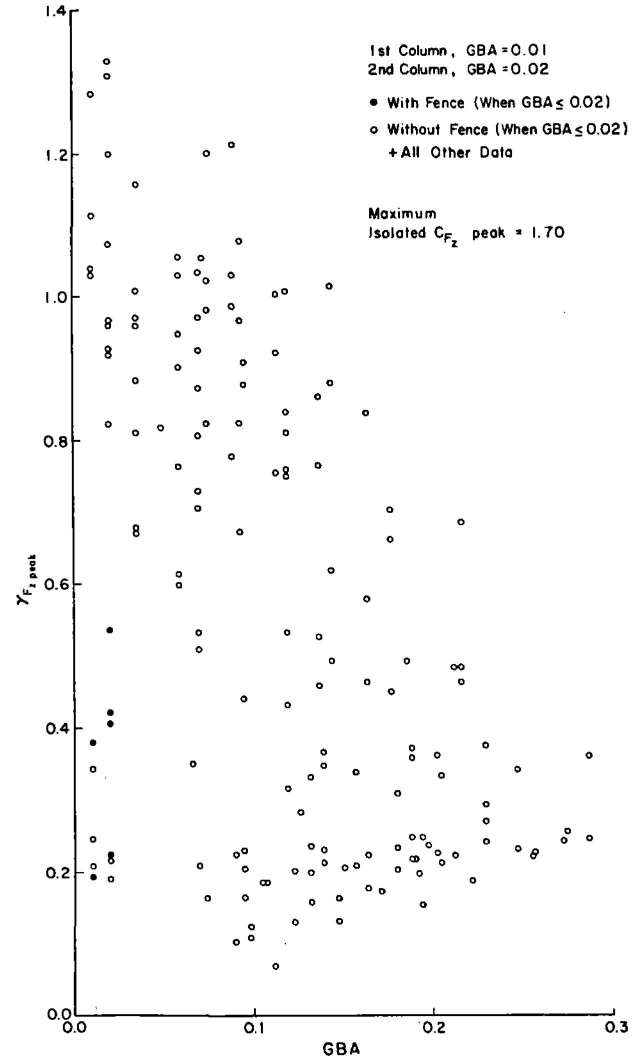

FIGURE B-4. Peak Lift Force Ratio in Current Study

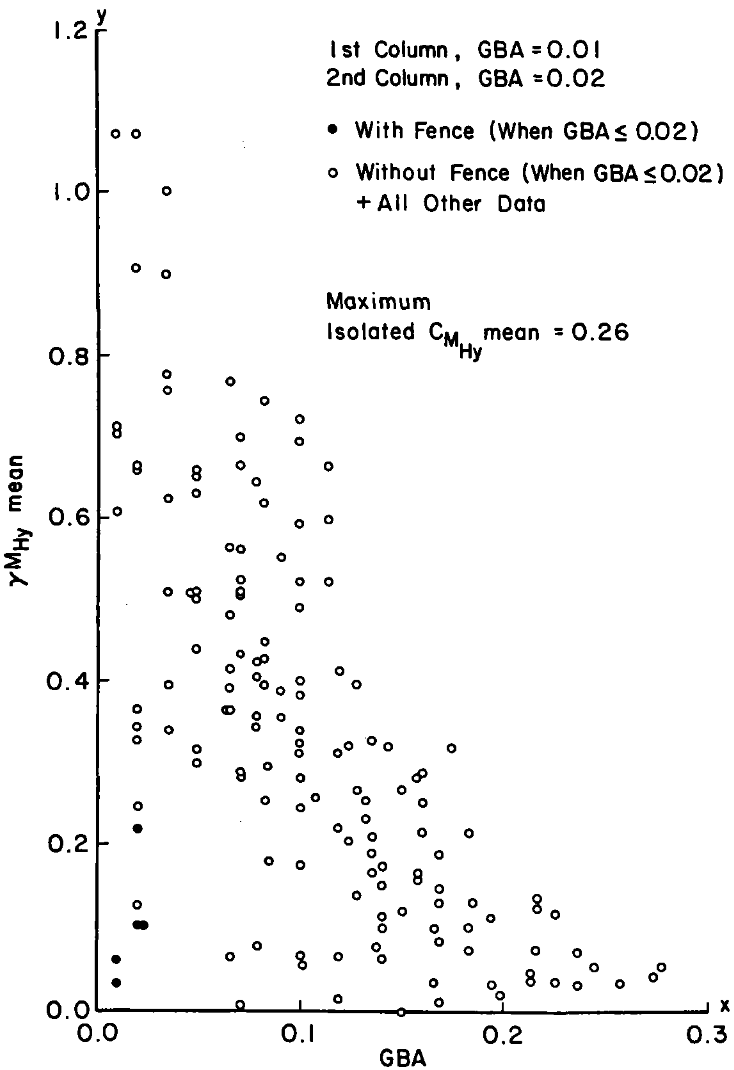

FIGURE B-5. Mean Hinge Moment Ratio in Current Study

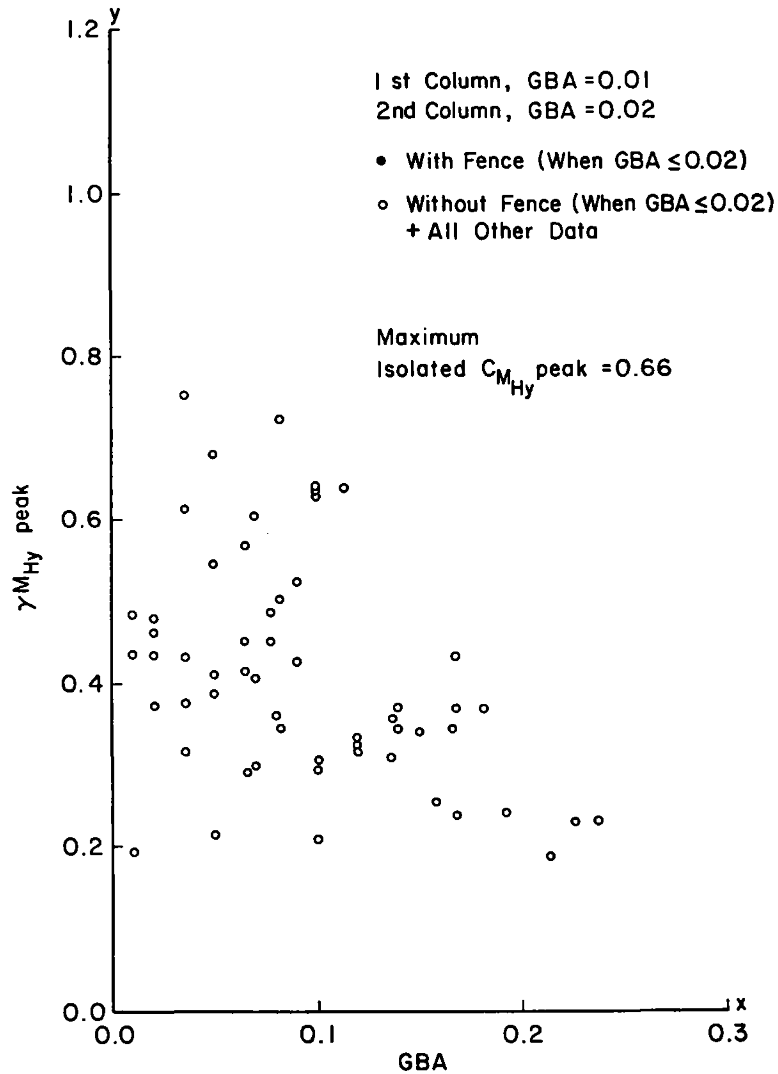

FIGURE B-6. Peak Hinge Moment Ratio in Current Study

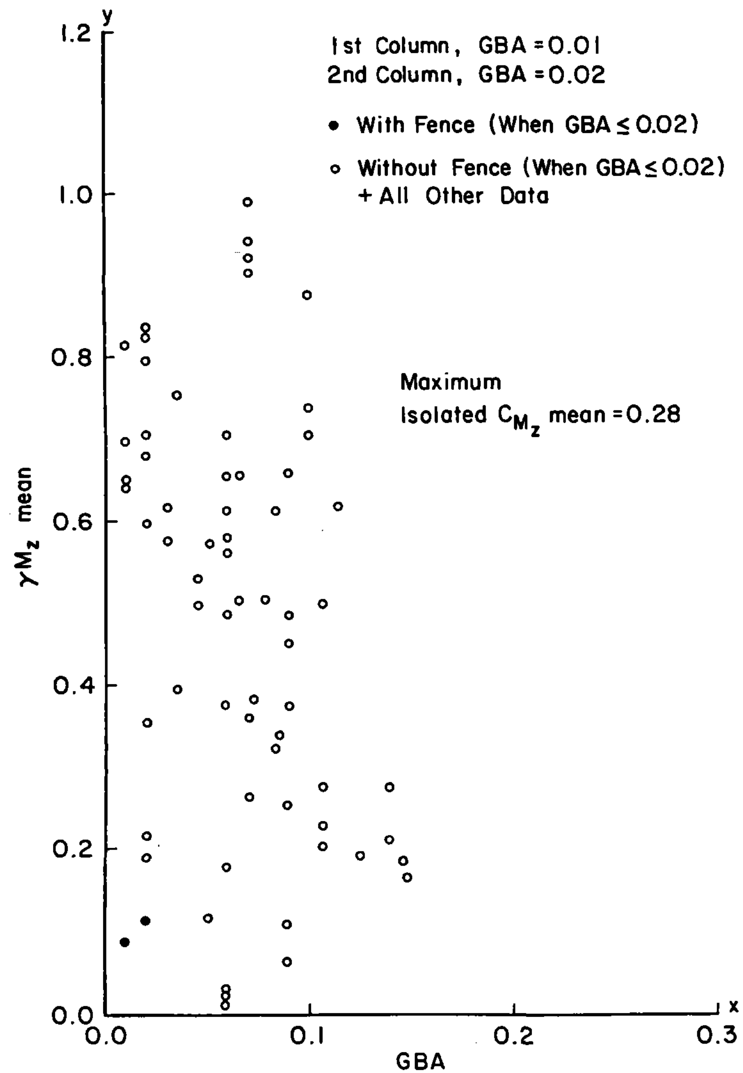

FIGURE B-7. Mean Azimuth Moment Ratio in Current Study

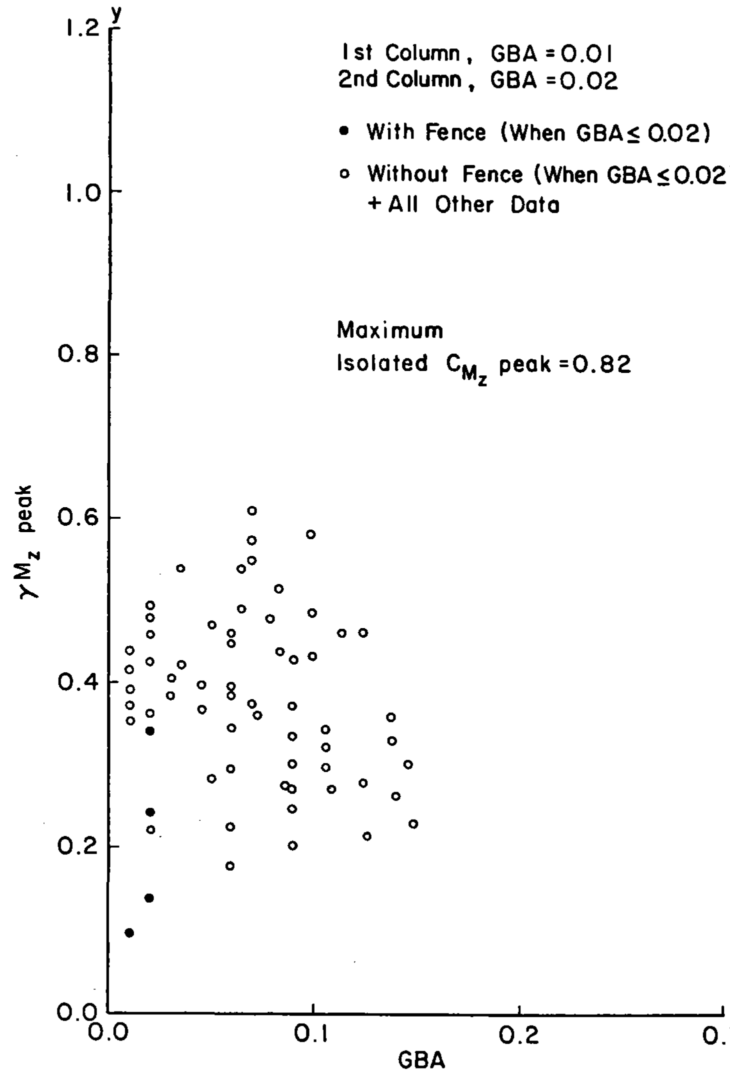

FIGURE B-8. Peak Azimuth Moment Ratio in Current Study

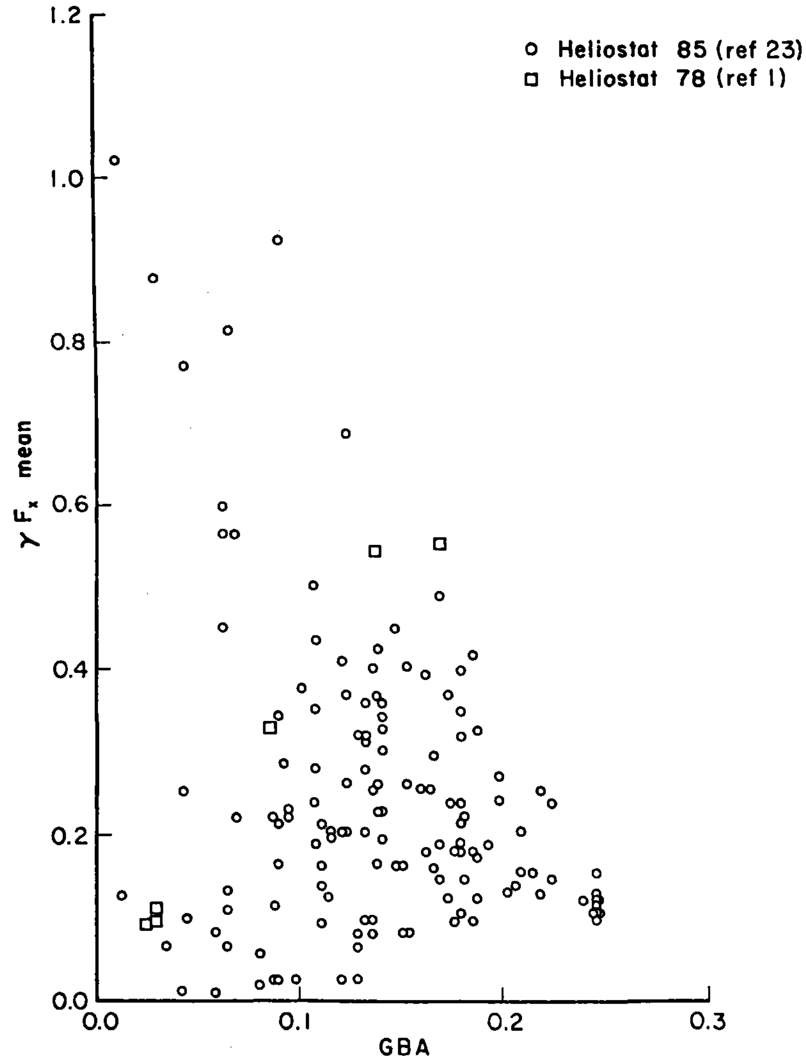

FIGURE B-9. Mean Drag Force Ratio from Previous Studies

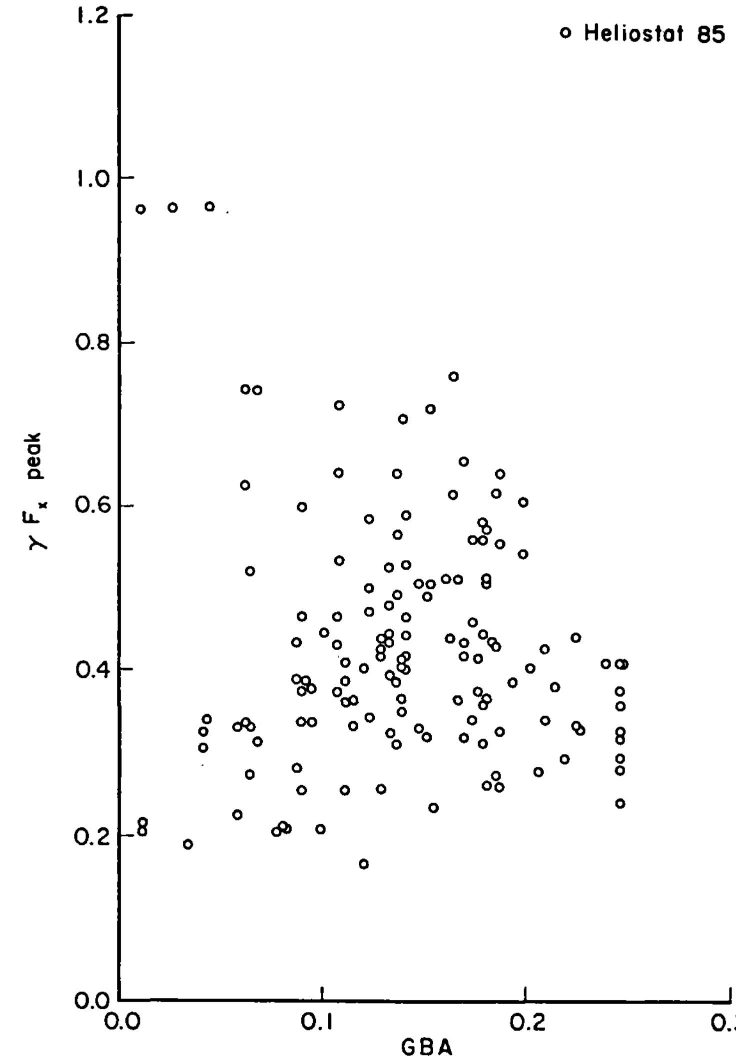

FIGURE B-10. Peak Drag Force Ratio from Previous Studies

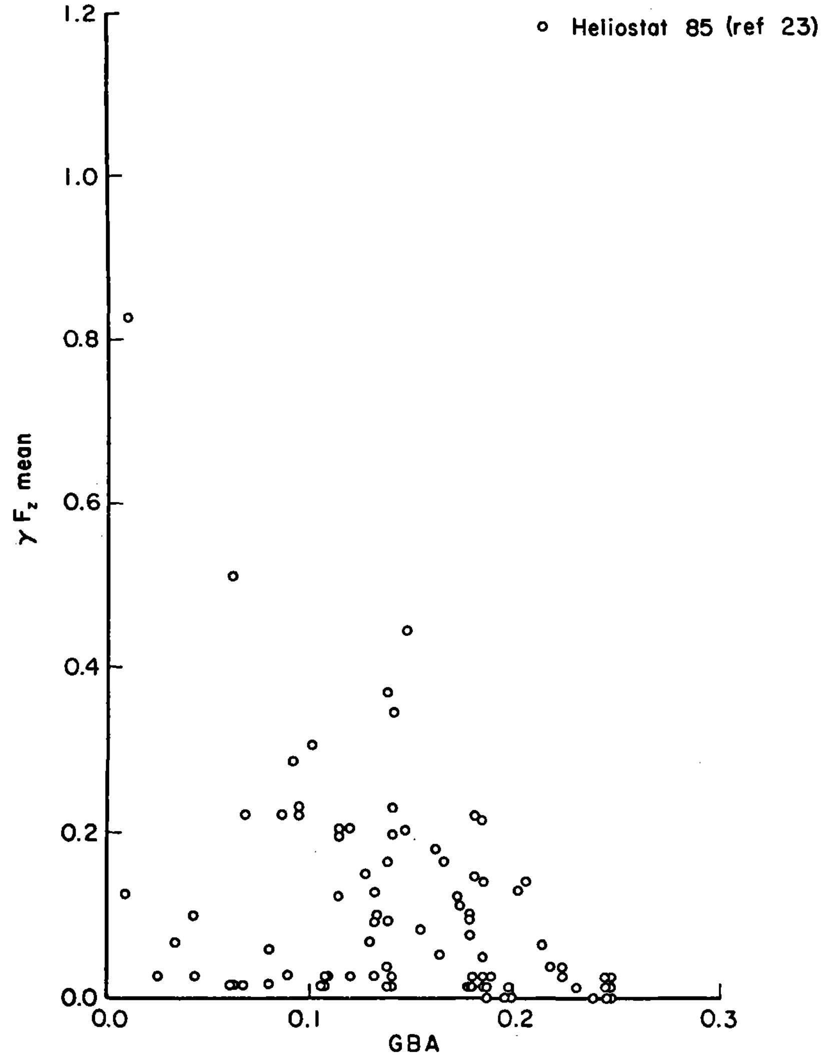

FIGURE B-11. Mean Lift Force Ratio from Previous Studies

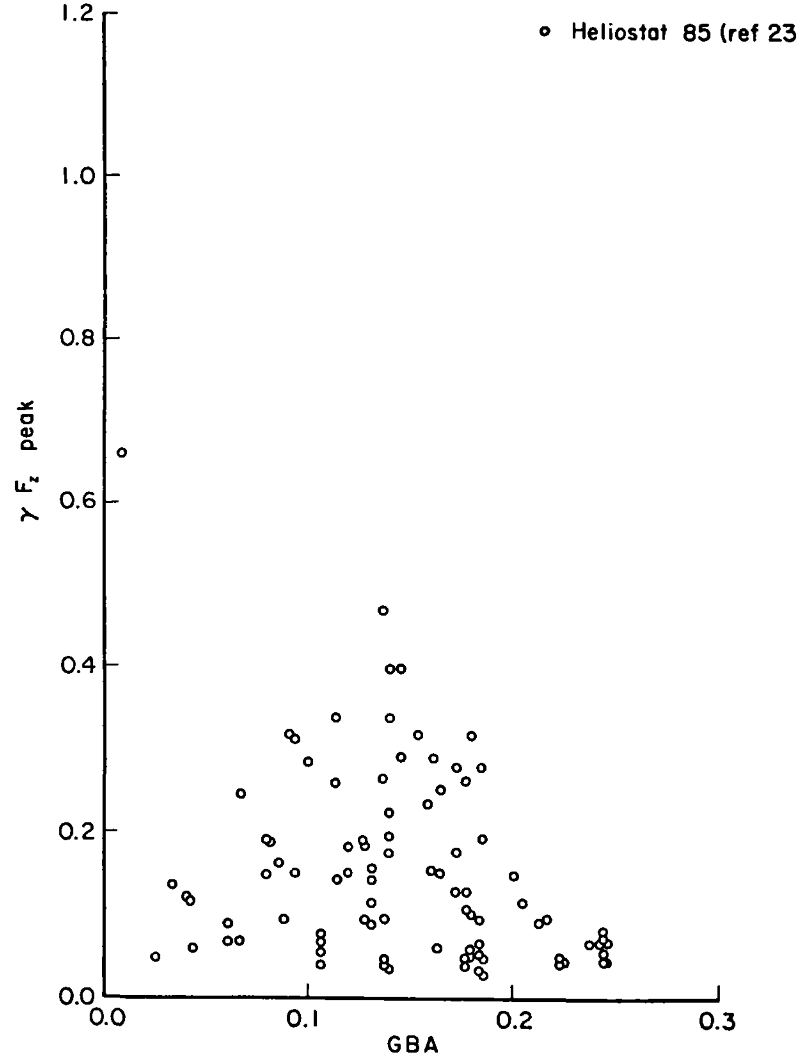

FIGURE B-12. Peak Lift Force Ratio from Previous Studies

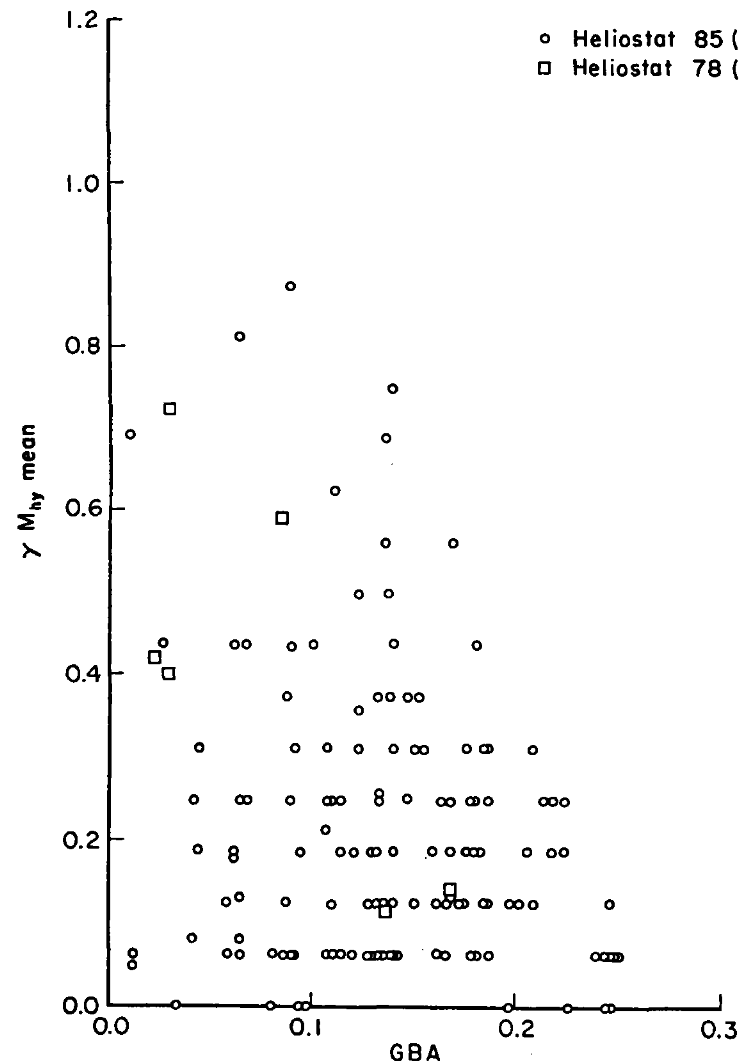

FIGURE B-13. Mean Hinge Moment Ratio from Previous Studies

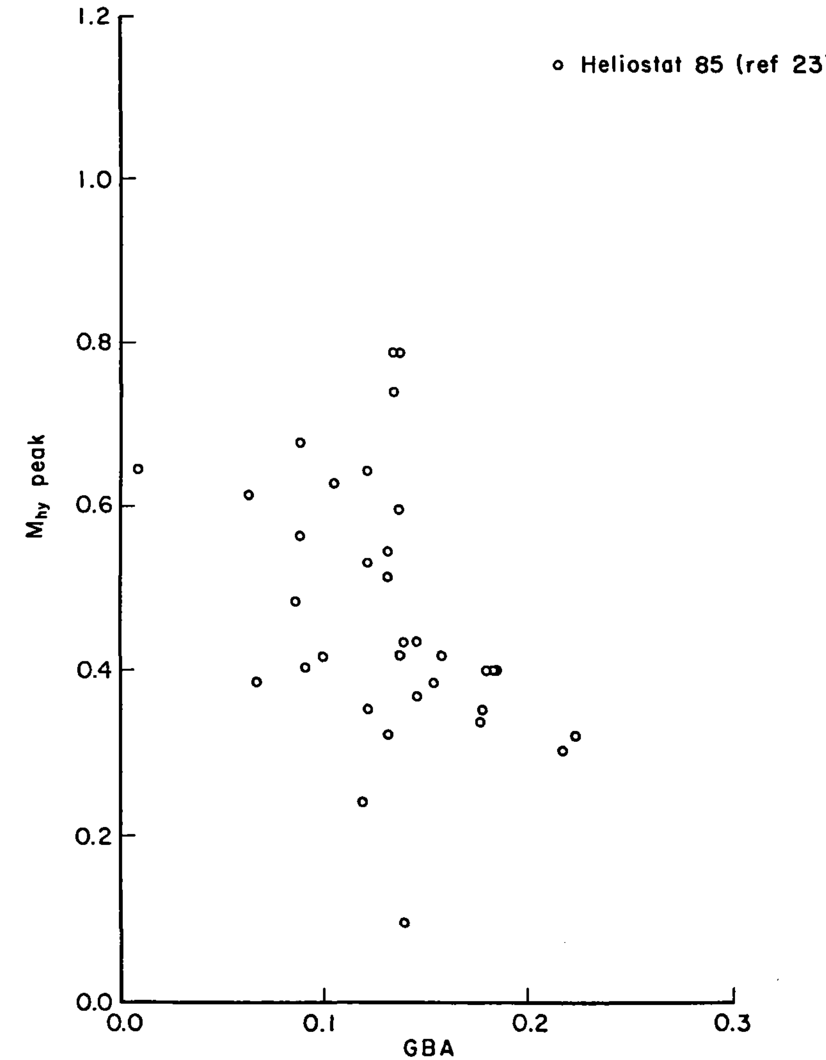

FIGURE B-14. Peak Hinge Moment Ratio from Previous Studies

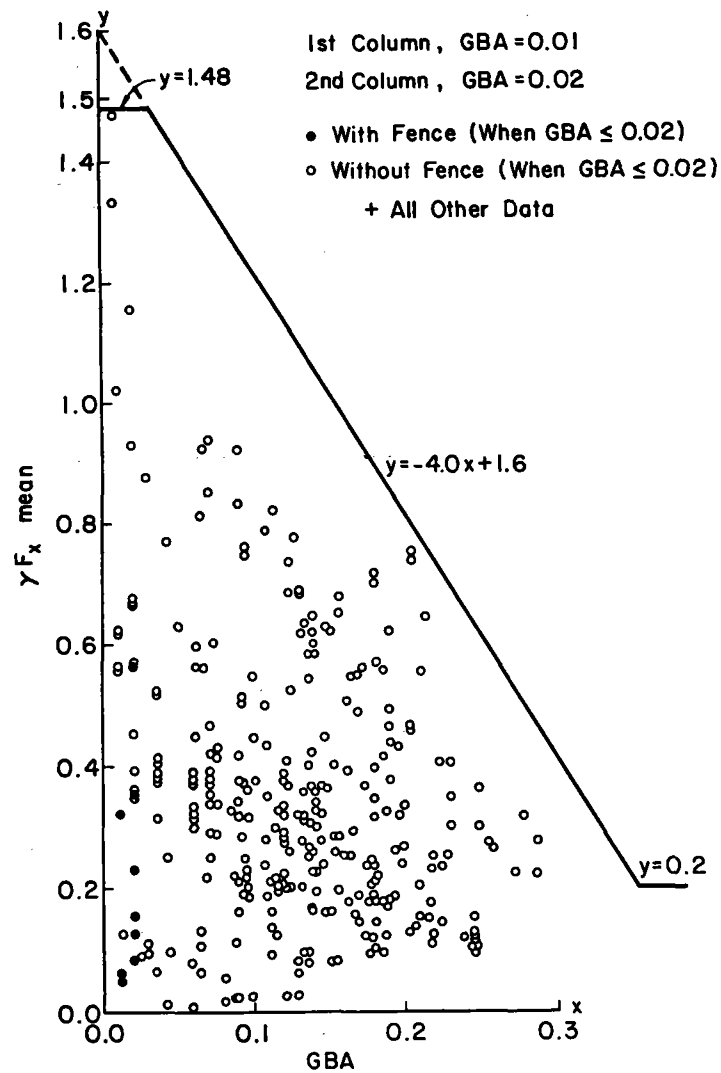

FIGURE B-15. Mean Drag Force Ratio with Bounding Curve

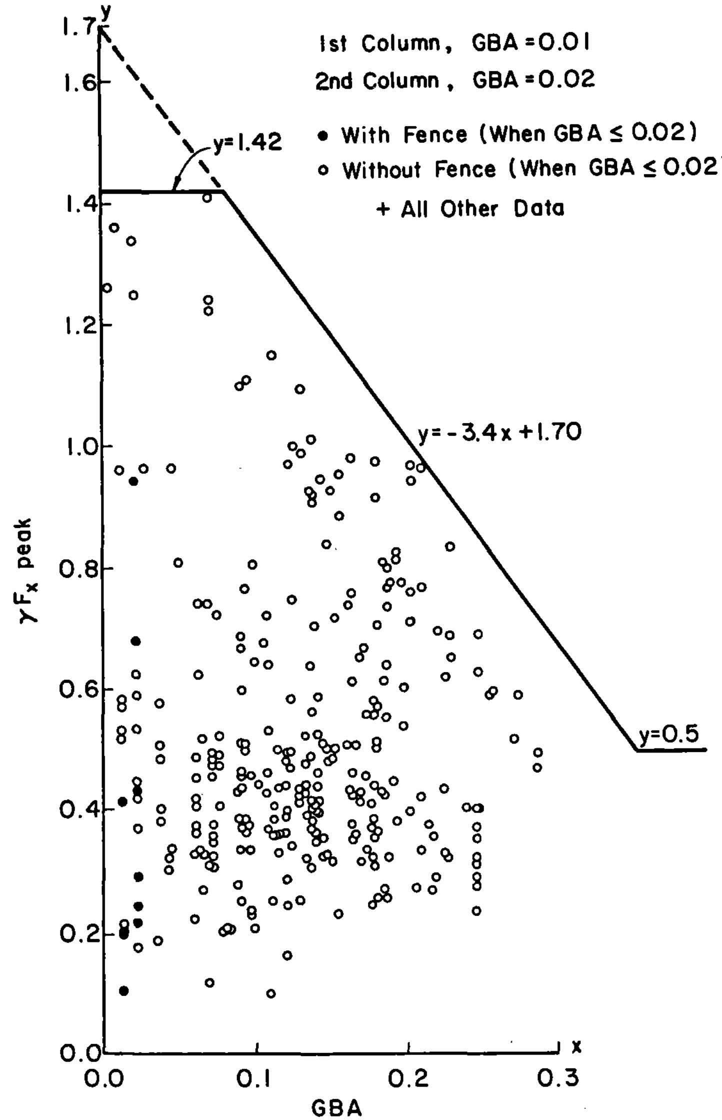

FIGURE B-16. Peak Drag Force Ratio with Bounding Curve

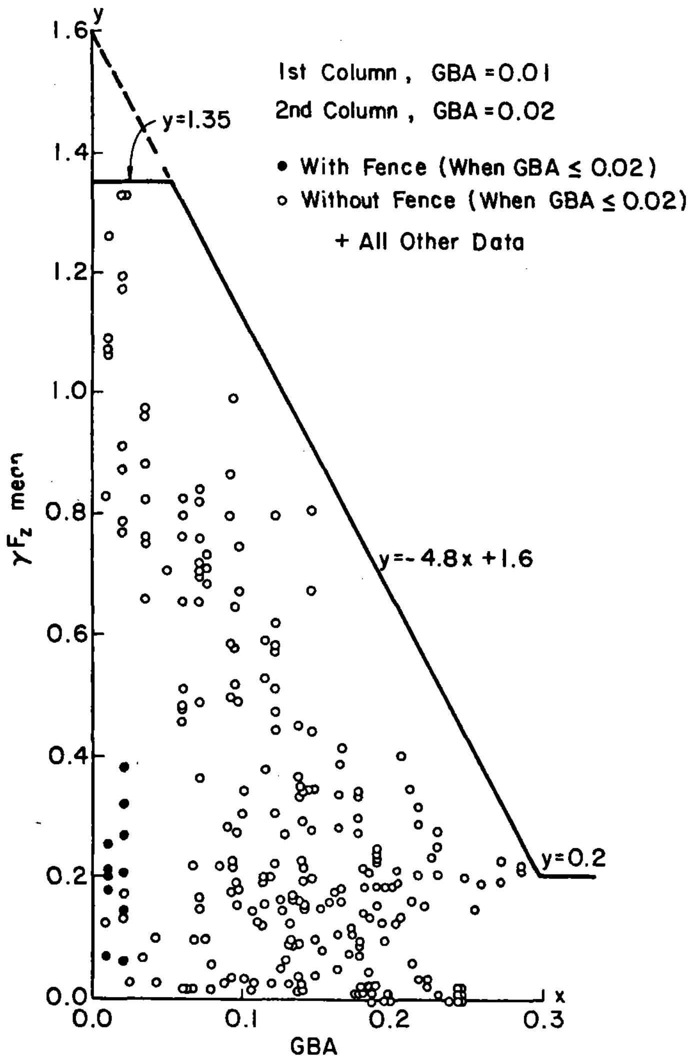

FIGURE B-17. Mean Lift Force Ratio with Bounding Curve

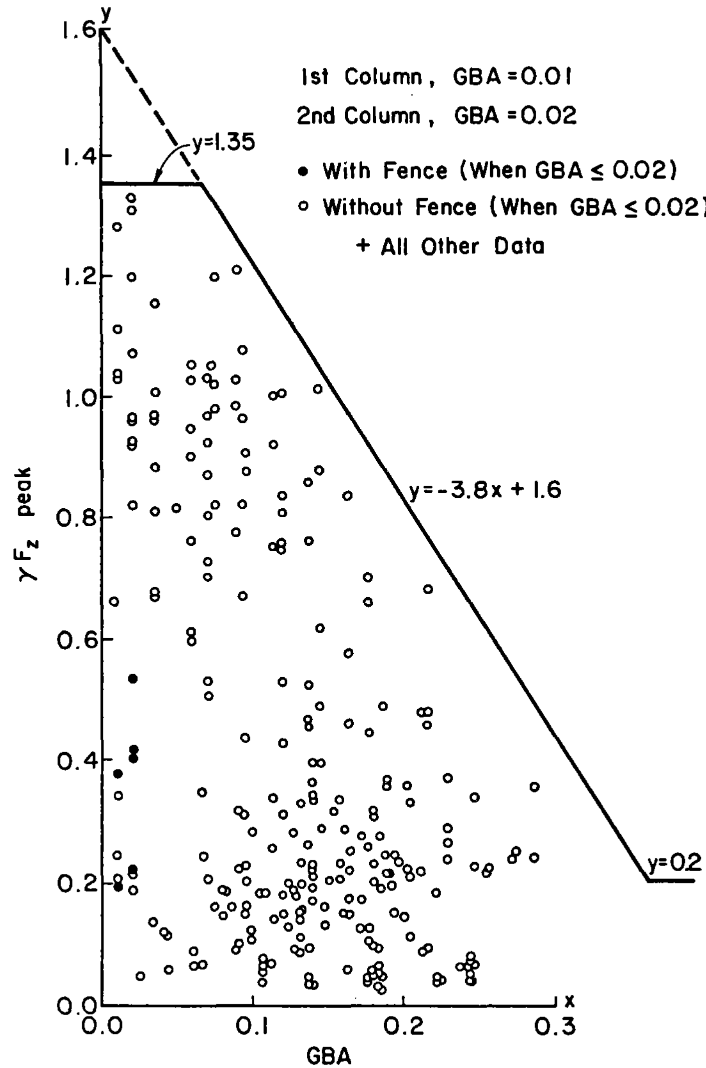

FIGURE B-18. Peak Lift Force Ratio with Bounding Curve

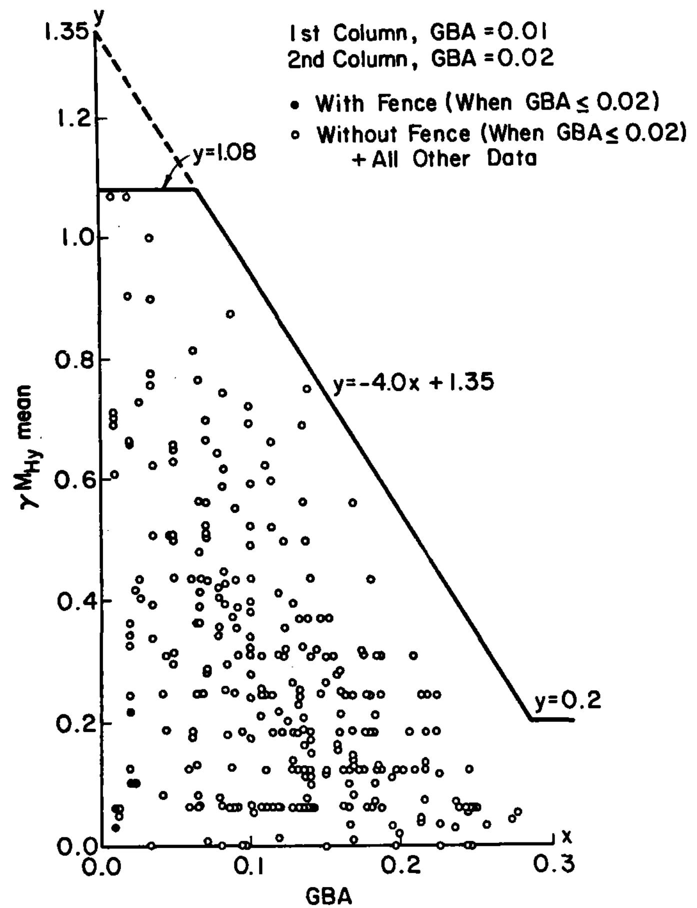

FIGURE B-19. Mean Hinge Moment Ratio with Bounding Curve

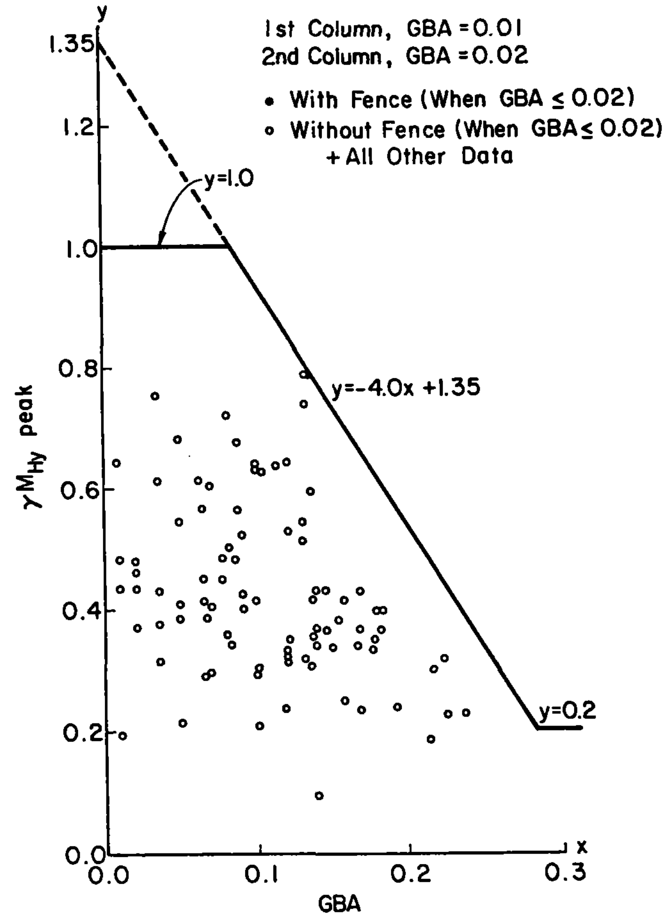

FIGURE B-20. Peak Hinge Moment Ratio with Bounding Curve

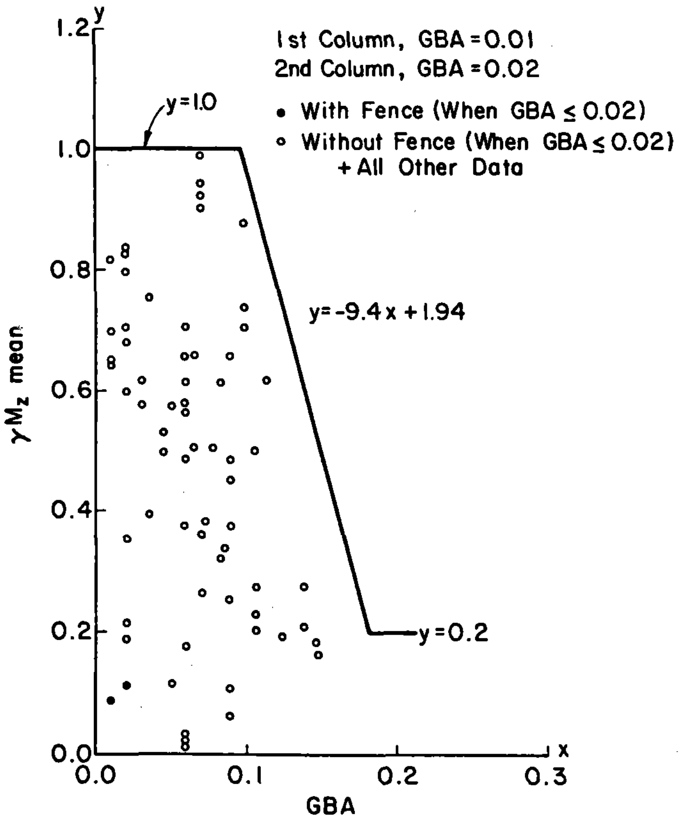

FIGURE B-21. Mean Azimuth Moment Ratio with Bounding Curve

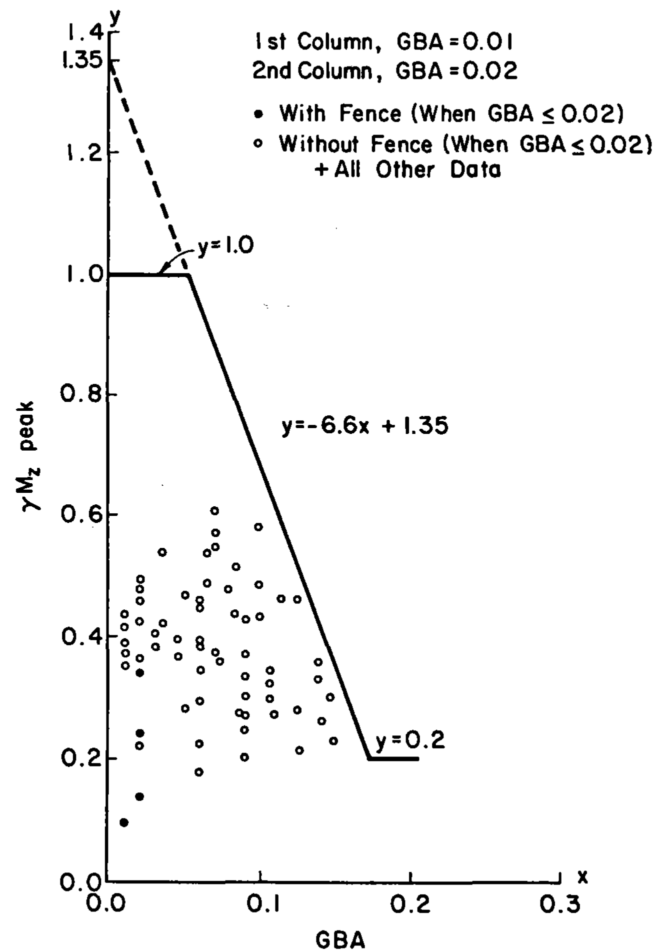

FIGURE B-22. Peak Azimuth Moment Ratio with Bounding Curve

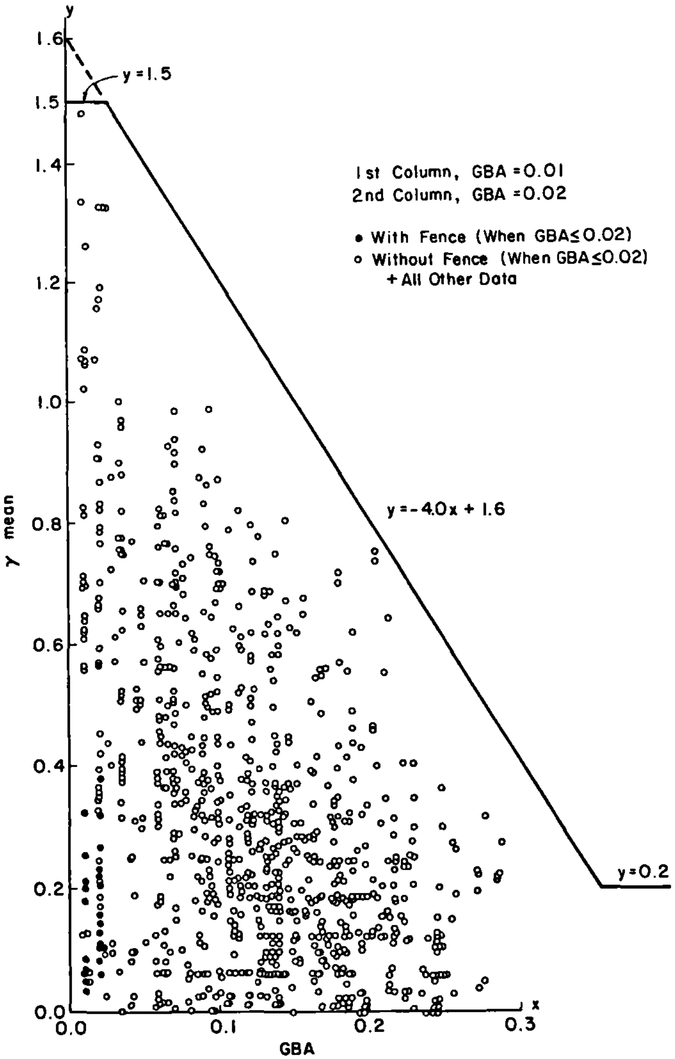

FIGURE B-23. Summary of Mean In-field to Maximum Mean Isolated Load

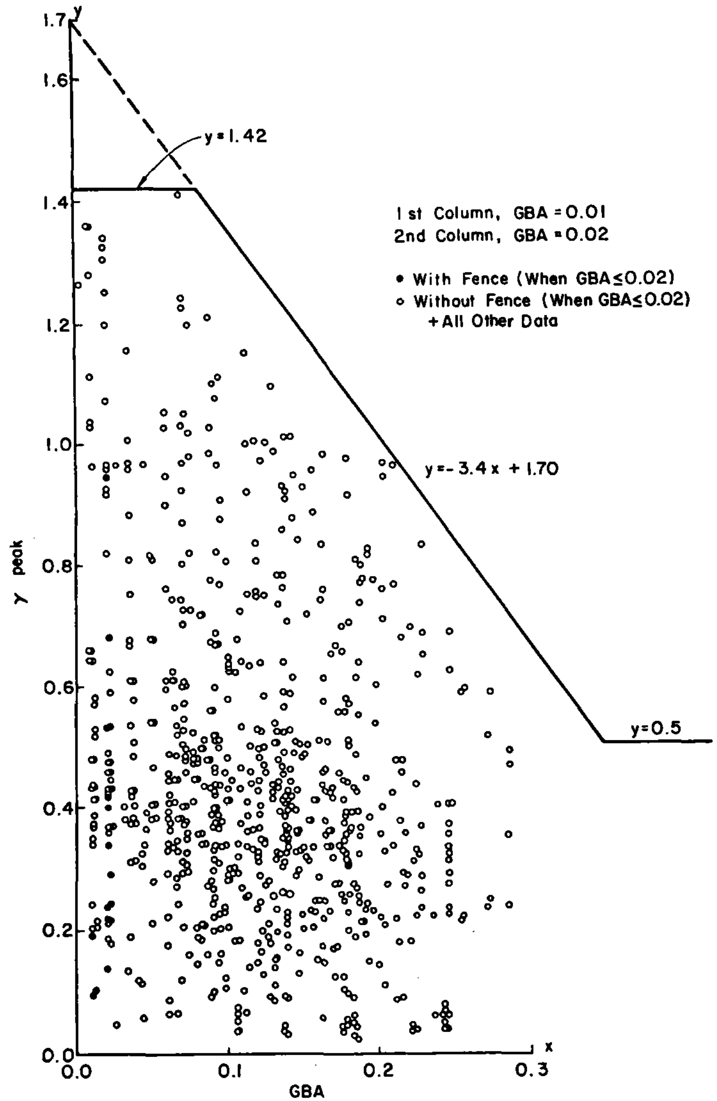

FIGURE B-24. Summary of Peak In-field to Maximum Peak Isolated Load

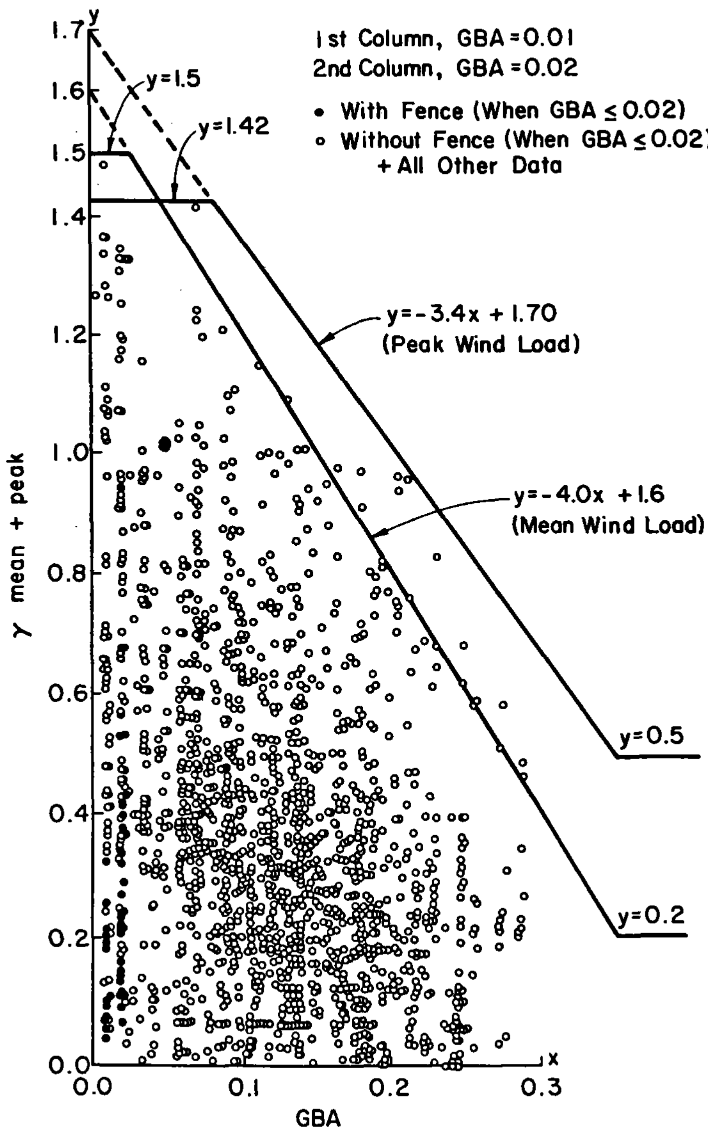

FIGURE B-25. Wind Load Reduction Summary for Mean and Peak Wind Loads

APPENDIX C

Test Interpretation

C.1. Test Plan
C.2. Calculation of GBA
C.3. In-field Case as a Function of GBA Values

C.1. TEST PLAN

TABLE. C-1-1. Test Plan -- Single Study

(Comment: Repeated run numbers don't mean they are the same run.)

Postscripts F, B, L, R, see Figure 2-12

Square Model Run #	α	β	Round Model Run #	α	β	Edge-porous Model Run #	α	β
Data File: SCT1								
254	90F	0	270	90F	0	271	90F	0
255	75F	0	271	75F	0	272	75F	0
256	60F	0	272	60F	0	273	60F	0
257	45F	0	273	45F	0	274	45F	0
258	30F	0	274	30F	0	275	30F	0
259	20F	0	275	20F	0	276	20F	0
260	10F	0	276	10F	0	277	10F	0
261	0	0	277	0	0	278	0	0
262	10B	0	278	10B	0	279	10B	0
263	20B	0	279	20B	0	280	20B	0
264	30B	0	280	30B	0	281	30B	0
265	45B	0	281	45B	0	282	45B	0
266	60B	0	282	60B	0	283	60B	0
267	75B	0	283	75B	0	284	75B	0
268	90B	0	284	90B	0	285	90B	0
Data File: SCT2								
8	90F	0	57	90F	0			
9	90F	10L	58	90F	15L			
10	90F	20L	59	90F	30L			
11	90F	30L	60	90F	45L			
12	90F	40L	61	90F	55L			
13	90F	50L	62	90F	60L			
14	90F	60L	63	90F	70L			
15	90F	70L	64	90F	65L			
3	90F	80L	65	90F	75L			
4	90F	90L	66	90F	80L			
5	90F	85L	67	90F	90L			
7	90F	65L	68	90F	15R			
8	90F	55L	69	90F	30R			
9	90F	65L	70	90F	45R			
10	90F	0	71	90F	55R			
11	90F	10R	72	90F	60R			
12	90F	25R	73	90F	65R			
13	90F	45R	75	90F	70R			

TABLE. C-1-1. Test Plan -- Single Study (con't)

(Comment: Repeated run numbers don't mean they are the same run.)

Postscripts F, B, L, R, see Figure 2-12

Square Model			Round Model			Edge-porous Model		
Run #	α	β	Run #	α	β	Run #	α	β
14	90F	50R	76	90F	80R			
15	90F	55R	77	90F	90R			
16	90F	60R	78	90B	0			
17	90F	65R	79	90B	20L			
18	90F	70R	80	90B	40L			
19	90F	80R	81	90B	55L			
20	90F	90R	82	90B	60L			
21	90F	65R	83	90B	65L			
22	90B	65L	84	90B	70L			
24	90B	65R	85	90B	75L			
25	90B	65R	86	90B	80L			
26	90B	0	87	90B	90L			
27	90B	20L	88	90B	85L			
28	90B	45L	89	90B	20R			
29	90B	80L	90	90B	40R			
30	90B	20R	91	90B	55R			
31	90B	40R	92	90B	60R			
32	90B	80R	93	90B	65R			
33	80F	60R	94	90B	70R			
34	60F	60R	95	90B	75R			
35	45F	60R	96	90B	80R			
36	30F	60R	97	90B	85R			
37	15F	60R	98	75F	65L			
38	0	60R	99	60F	65L			
39	15B	65R	100	45F	65L			
40	30B	65R	101	30F	65L			
41	45B	65R	102	15F	65L			
42	60B	65R	103	0	65L			
43	80B	65R	104	15B	65L			
44	65B	65R	105	30B	65L			
45	55B	65R	106	45B	65L			
47	65B	65R	107	55B	65L			
48	70B	65R	108	60B	65L			
49	90B	55R	109	65B	65L			
50	90B	60L	110	70B	65L			
51	90B	60L	111	75B	65L			
54	90F	75L	112	80B	65L			
56	90F	35R	113	85B	65L			

TABLE. C-1-2A. Test Plan -- Field Study

Key = Row Arr., Degree (0 and 45 degrees); Gap: W, N, NN;
Row #: 1, 2, 3, 4

(Refer to Section 2.5 and Figure 2-12)

1. Data File: SCT

Run #	Row Arr.	Gap	Row #	α	β	EF	IF
13	0	-	1	90F	0	W/O	-
14	0	-	1	90F	0	W	-
17	0	N	2	90F	0	W/O	-
20	0	N	2	90F	0	W	-
21	0	W	2	90F	0	W/O	-
22	0	W	2	90F	0	W	-
23	0	N	3	90F	0	W	W/O
24	0	N	3	90F	0	W/O	W/O
25	0	N	3	90F	0	W/O	W
26	0	N	3	90F	0	W	W
27	0	N	3	30F	0	W	W
28	0	N	3	30F	0	W	W/O
29	0	N	3	30F	0	W/O	W
30	0	N	3	30F	0	W/O	W/O
31	0	N	2	30F	0	W/O	-
32	0	N	2	30F	0	W	-
33	0	-	1	30F	0	W/O	-
34	0	-	1	30F	0	W	-
35	0	W	2	30F	0	W/O	-
36	0	W	2	30F	0	W	-
37	0	W	3	30F	0	W/O	W/O
38	0	W	3	30F	0	W	W/O
39	0	W	3	30F	0	W	W
40	0	W	3	30F	0	W/O	W
41	0	W	3	90F	0	W/O	W
42	0	W	3	90F	0	W	W
43	0	W	3	90F	0	W	W/O
44	0	W	3	90F	0	W/O	W/O
45	0	W	4	90F	0	W/O	W/O
46	0	W	4	90F	0	W	W/O
47	0	W	4	90F	0	W	W
48	0	W	4	90F	0	W/O	W
49	0	W	4	30F	0	W/O	W
50	0	W	4	30F	0	W	W
51	0	W	4	30F	0	W	W/O
52	0	W	4	30F	0	W/O	W/O
53	0	W	4	30B	0	W/O	W/O
54	0	W	4	30B	0	W	W/O
55	0	W	4	30B	0	W	W

TABLE. C-1-2A. Test Plan -- Field Study (con't)

Key = Row Arr., Degree (0 and 45 degrees); Gap: W, N, NN;
Row #: 1, 2, 3, 4

(Refer to Section 2.5 and Figure 2-12)

1. Data File: SCT

Run #	Row Arr.	Gap	Row #	α	β	EF	IF
56	0	W	4	30B	0	W/O	W
58	0	W	4	90F	20L	W/O	W
59	0	W	4	90F	20L	W	W
60	0	W	4	90F	20L	W	W/O
61	0	W	4	90F	20L	W/O	W/O
62	0	W	4	90F	45L	W/O	W/O
63	0	W	4	90F	45L	W	W/O
64	0	W	4	90F	45L	W	W
65	0	W	4	90F	45L	W/O	W
66	0	N	4	90F	0	W/O	W
67	0	N	4	90F	0	W	W
68	0	N	4	90F	0	W	W/O
69	0	N	4	90F	0	W/O	W/O
70	0	N	4	30B	0	W/O	W/O
71	0	N	4	30B	0	W	W/O
72	0	N	4	30B	0	W	W
73	0	N	4	30B	0	W/O	W
74	0	N	4	30F	0	W/O	W
75	0	N	4	30F	0	W	W
76	0	N	4	30F	0	W	W/O
77	0	N	4	30F	0	W/O	W/O
78	0	N	4	90F	20L	W/O	W/O
79	0	N	4	90F	20L	W/O	W
80	0	N	4	90F	20L	W	W
81	0	N	4	90F	20L	W	W/O
82	0	N	4	90F	45L	W	W/O
83	0	N	4	90F	45L	W	W
84	0	N	4	90F	45L	W/O	W
85	0	N	4	90F	45L	W/O	W/O
86	0	N	3	30B	0	W/O	W/O
87	0	N	3	30B	0	W	W/O
88	0	N	3	30B	0	W	W
89	0	N	3	30B	0	W/O	W
90	0	N	2	30B	0	W/O	-
91	0	N	2	30B	0	W	-
92	0	-	1	30B	0	W	-
93	0	-	1	30B	0	W/O	-
94	0	W	2	30B	0	W/O	-
95	0	W	2	30B	0	W	-

TABLE. C-1-2A. Test Plan -- Field Study (con't)

Key = Row Arr., Degree (0 and 45 degrees); Gap: W, N, NN;
Row #: 1, 2, 3, 4

(Refer to Section 2.5 and Figure 2-12)

1. Data File: SCT

Run #	Row Arr.	Gap	Row #	α	β	EF	IF
96	0	W	3	30B	0	W	W/O
97	0	W	3	30B	0	W/O	W/O
98	45	N	4	30B	0	W	W
99	45	N	4	30B	0	W/O	W
100	45	N	4	30B	0	W/O	W/O
101	45	N	4	30B	0	W	W/O
102	45	N	4	30F	0	W	W/O
103	45	N	4	30F	0	W	W
104	45	N	4	30F	0	W/O	W
105	45	N	4	30F	0	W/O	W/O
106	45	N	4	90F	0	W/O	W/O
107	45	N	4	90F	0	W/O	W
108	45	N	4	90F	0	W	W
109	45	N	4	90F	0	W	W/O
110	45	N	4	90F	20L	W/O	W/O
111	45	N	4	90F	20L	W/O	W
112	45	N	4	90F	20L	W	W
113	45	N	4	90F	20L	W	W/O
115	45	N	4	90F	45L	W	W/O
116	45	N	4	90F	45L	W	W
117	45	N	4	90F	45L	W/O	W
118	45	N	4	90F	45L	W/O	W/O
119	0	NN	4	90F	0	W/O	W
120	0	NN	4	90F	0	W	W
121	0	NN	4	90F	0	W	W/O
122	0	NN	4	90F	0	W/O	W/O
123	0	NN	4	80F	0	W/O	W/O
124	0	NN	4	80F	0	W/O	W
125	0	NN	4	80F	0	W	W
126	0	NN	4	80F	0	W	W/O

TABLE. C-1-2B. Test Plan -- Field Study

Key = Row Arr., Degree (0 and 45 degrees); Gap: W, N, NN;
Row #: 1, 2, 3, 4

(Refer to Section 2.5 and Figure 2-12)

2. Data File: SCT1

Run #	Row Arr.	Gap	Row #	α	β	EF	IF
197	0	W	4	30F	0	W/O	W/O
198	0	W	4	30F	0	W	W/O
199	0	W	4	30F	0	W	W
200	0	W	4	30F	0	W/O	W
201	0	W	4	30B	0	W/O	W
202	0	W	4	30B	0	W	W
203	0	W	4	30B	0	W	W/O
204	0	W	4	30B	0	W/O	W/O
205	0	W	3	30B	0	W/O	W/O
206	0	W	3	30B	0	W	W/O
207	0	W	3	30B	0	W	W
208	0	W	3	30B	0	W/O	W
209	0	W	3	30F	0	W/O	W
210	0	W	3	30F	0	W	W
211	0	W	3	30F	0	W	W/O
212	0	W	3	30F	0	W/O	W/O
213	0	W	2	30F	0	W/O	-
214	0	W	2	30B	0	W/O	-
215	0	-	1	30B	0	W/O	-
216	0	-	1	30F	0	W/O	-
217	0	-	1	90F	0	W/O	-
218	0	N	2	30F	0	W/O	-
219	0	N	2	30B	0	W/O	-
220	0	N	3	30F	0	W/O	-
221	0	N	3	30F	0	W	W/O
222	0	N	3	30F	0	W	W
223	0	N	3	30F	0	W/O	W
224	0	N	3	90F	0	W/O	W
225	0	N	3	90F	0	W	W
226	0	N	3	90F	0	W	W/O
227	0	N	3	90F	0	W/O	W/O
228	0	N	4	90F	0	W	W/O
229	0	N	4	90F	0	W	W
230	0	N	4	90F	0	W/O	W
231	0	N	4	90F	0	W/O	W/O
232	0	N	4	30F	0	W/O	W/O
233	0	N	4	30F	0	W	W/O
234	0	N	4	30F	0	W	W

TABLE. C-1-2B. Test Plan -- Field Study (con't)

Key = Row Arr., Degree (0 and 45 degrees); Gap: W, N, NN;
Row #: 1, 2, 3, 4

(Refer to Section 2.5 and Figure 2-12)

2. Data File: SCT1

Run #	Row Arr.	Gap	Row #	α	β	EF	IF
235	0	N	4	30F	0	W/O	W
237	45	N	4	80B	0	W/O	W
238	45	N	4	80B	0	W	W
239	45	N	4	80B	0	W	W/O
240	45	N	4	80B	0	W/O	W/O
241	45	N	4	30B	0	W/O	W/O
242	45	N	4	30B	0	W	W/O
243	45	N	4	30B	0	W	W
244	45	N	4	30B	0	W/O	W
245	45	N	4	30F	0	W/O	W/O
246	45	N	4	30F	0	W	W/O
247	45	N	4	30F	0	W	W
248	45	N	4	30F	0	W/O	W
250	45	N	4	90F	20L	W/O	W/O
251	45	N	4	90F	20L	W	W/O
252	45	N	4	90F	20L	W	W
253	45	N	4	90F	20L	W/O	W

TABLE. C-1-2c. Test Plan -- Field Study (con't)

Key = Row Arr., Degree (0 and 45 degrees); Gap: W, N, NN;
Row #: 1, 2, 3, 4

(Refer to Section 2.5 and Figure 2-12)

3. Data File: SCT2

Run #	Row Arr.	Gap	Row #	α	β	EF	IF
129	0	-	1	60B	60R	W/O	-
130	0	-	1	60B	60R	W	-
131	0	N	2	60B	60R	W/O	-
132	0	N	2	60B	60R	W	-
133	0	N	3	60B	60R	W/O	W/O
134	0	N	3	60B	60R	W	W/O
135	0	N	3	60B	60R	W	W
136	0	N	3	60B	60R	W/O	W
137	0	N	4	60B	60R	W/O	W/O
138	0	N	4	60B	60R	W	W/O
139	0	N	4	60B	60R	W	W
140	0	N	4	60B	60R	W/O	W
141	0	W	2	60B	60R	W/O	-
142	0	W	2	60B	60R	W	W/O
143	0	W	3	60B	60R	W/O	W/O
144	0	W	3	60B	60R	W	W/O
145	0	W	3	60B	60R	W	W
146	0	W	3	60B	60R	W/O	W
147	0	W	4	60B	60R	W/O	W/O
148	0	W	4	60B	60R	W	W/O
149	0	W	4	60B	60R	W	W
137	0	W	4	60B	60R	W/O	W
138	0	W	4	90B	60R	W/O	W
139	0	W	4	90B	60R	W	W
140	0	W	4	90B	60R	W	W/O
141	0	W	4	90B	60R	W/O	W/O
142	0	W	4	90F	60R	W/O	W/O
143	0	W	4	90F	60R	W	W/O
144	0	W	4	90F	60R	W	W
145	0	W	4	90F	60R	W/O	W
146	0	N	4	90F	65R	W/O	W
147	0	N	4	90F	65R	W	W
148	0	N	4	90F	65R	W	W/O
149	0	N	4	90F	65R	W/O	W/O
150	0	N	3	90F	65R	W/O	W/O
151	0	N	3	90F	65R	W	W/O
152	0	N	3	90F	65R	W	W
153	0	N	3	90F	65R	W/O	W

TABLE. C-1-2c. Test Plan -- Field Study (con't)

Key = Row Arr., Degree (0 and 45 degrees); Gap: W, N, NN;
Row #: 1, 2, 3, 4

(Refer to Section 2.5 and Figure 2-12)

3. Data File: SCT2

Run #	Row Arr.	Gap	Row #	α	β	EF	IF
154	0	N	4	90F	65L	W/O	W
155	0	N	4	90F	65L	W	W
156	0	N	4	90F	65L	W	W/O
157	0	N	4	90F	65L	W/O	W/O
158	45	N	4	60B	60R	W/O	W/O
159	45	N	4	60B	60R	W	W/O
160	45	N	4	60B	60R	W	W
161	45	N	4	60B	60R	W/O	W
162	45	N	4	90B	60R	W/O	W
163	45	N	4	90B	60R	W	W
164	45	N	4	90B	60R	W	W/O
165	45	N	4	90B	60R	W/O	W/O
166	45	N	3	90B	60R	W/O	W/O
167	45	N	3	90B	60R	W/O	W
168	45	N	3	90B	60R	W	W
169	45	N	3	90B	60R	W	W/O
170	45	N	2	90B	60R	W/O	-
171	45	N	2	90B	60R	W	-
172	45	-	1	90B	60R	W/O	-
173	45	-	1	90F	65L	W/O	-
174	45	N	2	90F	65L	W/O	-
175	45	N	3	90F	65L	W/O	W/O
176	45	N	4	90F	65L	W/O	W/O
177	45	N	4	90F	60R	W/O	W/O
178	45	N	3	90F	60R	W/O	W/O
179	45	N	2	90F	60R	W/O	-
180	45	-	1	90F	60R	W/O	-
181	45	-	1	90B	60R	W/O	W/O
182	45	N	2	90B	60R	W/O	W/O
183	45	N	3	90B	60R	W/O	W/O
184	45	N	4	90B	60R	W/O	W/O
185	45	N	4	90B	65L	W/O	W/O
186	45	N	3	90B	65L	W/O	W/O
187	45	N	2	90B	65L	W/O	W/O

C.2. CALCULATION OF GBA

Examples of calculation of GBA (α = 90, β = 0). Fence porosity is 40%. EF height is 0.8H, while IF height is 0.534H. For this section, refer to the test plan and Figure 2-12.

A. Third row at 0^0 row arrangement (N).

1. Without EF, without IF

$$GBA = \frac{H^2 \sin \alpha \cos \beta}{3.07H \times 2.34H} = \frac{H^2}{3.07H \times 2.34H} = 0.139$$

2. Without EF, with IF

$$GBA = \frac{2H^2 + 1.32H \times 0.534H \times 60\%}{2.34 \times 2 \times 3.07H} = 0.168$$

3. With EF, without IF

$$GBA = \frac{3H^2 + 2.34H \times 0.8H \times 60\%}{2.34H \times (2 \times 3.07H + 2.14H)} = 0.213$$

4. With EF, with IF

$$GBA = \frac{3H^2 + 2.34H \times 0.8H \times 60\% + 1.32H \times 0.534H \times 60\%}{2.34H \times (2 \times 3.07H + 2.14H)} = 0.235$$

B. Fourth row at 45^0 row arrangement (N)

1. Without EF, without IF

$$GBA = \frac{H^2}{3.07H \times 2.34H} = 0.139$$

2. Without EF, with IF

$$GBA = \frac{2H^2 + 1.32H \times 0.534H \times 60\%}{2.34H \times 2 \times 3.07H} = 0.168$$

3. With EF, without IF

The field from EF is 4.87 m long - 16.4H

$$GBA = \frac{14H^2 + 6.15H \times 0.8H \times 60\%}{16.4H \times 6.15H} = 0.168$$

4. With EF, with IF

$$GBA = \frac{14H^2 + 6.15H \times 0.8H \times 0.6 + 1.32H \times 0.534H \times 60\% \times 5 \times \cos 45^o}{16.4H \times 6.15H}$$

$$= 0.183$$

TABLE C-2-1. GBA Values for In-Field Study

Row Arr.	Gap	Row #	α	β	EF	IF	GBA
0	N	4	90	0	W/O	W/O	0.139
0	N	4	90	0	W/O	W	0.168
0	N	4	90	0	W	W/O	0.193
0	N	4	90	0	W	W	0.225
0	N	4	30	0	W/O	W/O	0.070
0	N	4	30	0	W/O	W	0.099
0	N	4	30	0	W	W/O	0.118
0	N	4	30	0	W	W	0.149
0	N	4	90	20	W/O	W/O	0.131
0	N	4	90	20	W/O	W	0.160
0	N	4	90	20	W	W/O	0.184
0	N	4	90	20	W	W	0.216
0	N	4	90	45	W/O	W/O	0.098
0	N	4	90	45	W/O	W	0.128
0	N	4	90	45	W	W/O	0.149
0	N	4	90	45	W	W	0.181
0	W	4	90	0	W/O	W/O	0.070
0	W	4	90	0	W/O	W	0.084
0	W	4	90	0	W	W/O	0.106
0	W	4	90	0	W	W	0.124
0	W	4	30	0	W/O	W/O	0.035
0	W	4	30	0	W/O	W	0.049
0	W	4	30	0	W	W/O	0.065
0	W	4	30	0	W	W	0.082
0	W	4	90	20	W/O	W/O	0.066
0	W	4	90	20	W/O	W	0.080
0	W	4	90	20	W	W/O	0.101
0	W	4	90	20	W	W	0.119
0	W	4	90	45	W/O	W/O	0.049
0	W	4	90	45	W/O	W	0.064
0	W	4	90	45	W	W/O	0.082
0	W	4	90	45	W	W	0.100
0	N	3	90	0	W/O	W/O	0.139
0	N	3	90	0	W/O	W	0.168
0	N	3	90	0	W	W/O	0.213
0	N	3	90	0	W	W	0.235
0	N	3	30	0	W/O	W/O	0.070
0	N	3	30	0	W/O	W	0.099
0	N	3	30	0	W	W/O	0.135
0	N	3	30	0	W	W	0.157
0	W	3	90	0	W/O	W/O	0.070
0	W	3	90	0	W/O	W	0.084
0	W	3	90	0	W	W/O	0.122
0	W	3	90	0	W	W	0.135
0	W	3	30	0	W/O	W/O	0.035
0	W	3	30	0	W/O	W	0.049
0	W	3	30	0	W	W/O	0.078

TABLE C-2-1. GBA Values for In-Field Study (con't)

Row Arr.	Gap	Row #	α	β	EF	IF	GBA
0	W	3	30	0	W	W	0.090
0	NN	4	90	0	W/O	W/O	0.197
0	NN	4	90	0	W/O	W	0.216
0	NN	4	90	0	W	W/O	0.256
0	NN	4	90	0	W	W	0.276
0	NN	4	80	0	W/O	W/O	0.194
0	WN	4	80	0	W/O	W	0.213
0	NN	4	80	0	W	W/O	0.253
0	NN	4	80	0	W	W	0.273
45	N	4	90	0	W/O	W/O	0.139
45	N	4	90	0	W/O	W	0.168
45	N	4	90	0	W	W/O	0.168
45	N	4	90	0	W	W	0.183
45	N	4	30	0	W/O	W/O	0.070
45	N	4	30	0	W/O	W	0.099
45	N	4	30	0	W	W/O	0.099
45	N	4	30	0	W	W	0.113
45	N	4	80	0	W/O	W/O	0.137
45	N	4	80	0	W/O	W	0.166
45	N	4	80	0	W	W/O	0.166
45	N	4	80	0	W	W	0.181
45	N	4	90	20	W/O	W/O	0.131
45	N	4	90	20	W/O	W	0.160
45	N	4	90	20	W	W/O	0.160
45	N	4	90	20	W	W	0.174
45	N	4	90	45	W/O	W/O	0.098
45	N	4	90	45	W/O	W	0.128
45	N	4	90	45	W	W/O	0.127
45	N	4	90	45	W	W	0.142
0	N	3	60	60	W/O	W/O	0.060
0	N	3	60	60	W/O	W	0.090
0	N	3	60	60	W	W/O	0.126
0	N	3	60	60	W	W	0.148
0	N	3	90	60	W/O	W/O	0.070
0	N	3	90	60	W/O	W	0.099
0	N	3	90	60	W	W/O	0.136
0	N	3	90	60	W	W	0.158
0	N	3	90	65	W/O	W/O	0.059
0	N	3	90	65	W/O	W	0.089
0	N	3	90	65	W	W/O	0.124
0	N	3	90	65	W	W	0.146
0	N	4	60	60	W/O	W/O	0.060
0	N	4	60	60	W/O	W	0.090
0	N	4	60	60	W	W/O	0.108
0	N	4	60	60	W	W	0.140
0	N	4	90	60	W/O	W/O	0.070
0	N	4	90	60	W/O	W	0.099

TABLE C-2-1. GBA Values for In-Field Study (con't)

Row Arr.	Gap	Row #	α	β	EF	IF	GBA
0	N	4	90	60	W	W/O	0.118
0	N	4	90	60	W	W	0.150
0	N	4	90	65	W/O	W/O	0.059
0	N	4	90	65	W/O	W	0.089
0	N	4	90	65	W	W/O	0.106
0	N	4	90	65	W	W	0.138
0	W	3	60	60	W/O	W/O	0.030
0	W	3	60	60	W/O	W	0.045
0	W	3	60	60	W	W/O	0.072
0	W	3	60	60	W	W	0.085
0	W	3	90	60	W/O	W/O	0.035
0	W	3	90	60	W/O	W	0.050
0	W	3	90	60	W	W/O	0.078
0	W	3	90	60	W	W	0.091
0	W	3	90	65	W/O	W/O	0.029
0	W	3	90	65	W/O	W	0.045
0	W	3	90	65	W	W/O	0.071
0	W	3	90	65	W	W	0.084
0	W	4	60	60	W/O	W/O	0.030
0	W	4	60	60	W/O	W	0.045
0	W	4	60	60	W	W/O	0.060
0	W	4	60	60	W	W	0.078
0	W	4	90	60	W/O	W/O	0.035
0	W	4	90	60	W/O	W	0.050
0	W	4	90	60	W	W/O	0.065
0	W	4	90	60	W	W	0.083
0	W	4	90	65	W/O	W/O	0.029
0	W	4	90	65	W/O	W	0.045
0	W	4	90	65	W	W/O	0.059
0	W	4	90	65	W	W	0.077
45	N	3	60	60	W/O	W/O	0.060
45	N	3	60	60	W/O	W	0.090
45	N	3	60	60	W	W/O	0.100
45	N	3	60	60	W	W	0.117
45	N	3	90	60	W/O	W/O	0.070
45	N	3	90	60	W/O	W	0.099
45	N	3	90	60	W	W/O	0.110
45	N	3	90	60	W	W	0.126
45	N	3	90	65	W/O	W/O	0.059
45	N	3	90	65	W/O	W	0.089
45	N	3	90	65	W	W/O	0.099
45	N	3	90	65	W	W	0.115
45	N	4	60	60	W/O	W/O	0.060
45	N	4	60	60	W/O	W	0.090
45	N	4	60	60	W	W/O	0.090
45	N	4	60	60	W	W	0.105
45	N	4	90	60	W/O	W/O	0.070

TABLE C-2-1. GBA Values for In-Field Study (con't)

Row Arr.	Gap	Row #	α	β	EF	IF	GBA
45	N	4	90	60	W/O	W	0.099
45	N	4	90	60	W	W/O	0.099
45	N	4	90	60	W	W	0.114
45	N	4	90	65	W/O	W/O	0.059
45	N	4	90	65	W/O	W	0.089
45	N	4	90	65	W	W/O	0.088
45	N	4	90	65	W	W	0.103

C.3. IN-FIELD CASE AS A FUNCTION OF GBA VALUES

TABLE C-3-1A. Current Heliostat Data According to GBA

1. Data File: SCT

Run #	GBA	γ_{Fx}	γ_{Fz}	γ_{MHy}	$\gamma_{Fx\ peak}$	$\gamma_{Fz\ peak}$
126	0.255	0.279	0.159	0.059	0.593	0.222
125	0.272	0.237	0.204	0.046	0.519	0.243
124	0.226	0.265	0.242	0.050	0.623	0.271
123	0.194	0.332	0.196	0.037	0.829	0.251
122	0.197	0.346	0.194	0.027	0.777	0.237
121	0.257	0.269	0.200	0.037	0.599	0.230
120	0.274	0.233	0.237	0.059	0.593	0.258
119	0.229	0.312	0.286	0.142	0.837	0.294
118	0.098	0.561	0.035	0.315	0.807	0.111
117	0.123	0.534	0.056	0.269	0.749	0.132
116	0.171	0.573	0.078	0.324	0.670	0.172
115	0.147	0.639	0.045	0.402	0.841	0.132
113	0.180	0.727	0.150	0.292	0.977	0.205
112	0.204	0.761	0.144	0.324	0.970	0.215
111	0.156	0.684	0.167	0.256	0.958	0.208
110	0.131	0.643	0.094	0.256	0.991	0.160
109	0.188	0.630	0.162	0.192	0.804	0.220
108	0.212	0.651	0.169	0.215	0.967	0.223
107	0.164	0.556	0.188	0.132	0.982	0.223
106	0.139	0.629	0.155	0.114	1.136	0.233
105	0.070	0.254	0.009	0.525	0.311	0.705
104	0.095	0.192	0.281	0.402	0.240	0.443
103	0.143	0.249	0.353	0.525	0.327	0.619
102	0.119	0.292	0.520	0.594	0.369	0.839
101	0.119	0.396	0.823	0.721	1.149	0.971
100	0.070	0.369	0.752	0.507	1.051	0.911
99	0.095	0.332	0.679	0.493	0.949	0.883
98	0.143	0.384	0.825	0.667	1.152	0.969
97	0.035	0.522	0.994	0.758	1.389	1.054
96	0.092	0.256	0.524	0.347	0.389	0.672
89	0.119	0.282	0.587	0.342	0.501	0.759
88	0.216	0.122	0.323	0.169	0.276	0.463
87	0.176	0.127	0.307	0.192	0.250	0.452
86	0.070	0.347	0.708	0.562	0.481	0.872
85	0.098	0.453	0.036	0.178	0.650	0.124
84	0.147	0.372	0.106	0.142	0.487	0.164
83	0.191	0.268	0.136	0.105	0.454	0.200
82	0.164	0.289	0.113	0.123	0.466	0.178
81	0.194	0.438	0.107	0.132	0.819	0.154
80	0.221	0.415	0.162	0.128	0.701	0.190
79	0.180	0.580	0.192	0.219	0.917	0.233
78	0.131	0.692	0.173	0.237	1.129	0.236

TABLE C-3-1A. Current Heliostat Data According to GBA (con't)

1. Data File: SCT

Run #	GBA	γ_{Fx}	γ_{Fz}	γ_{MHy}	$\gamma_{Fx\ peak}$	$\gamma_{Fz\ peak}$
77	0.070	0.375	0.657	0.667	0.380	0.711
76	0.136	0.314	0.460	0.416	0.421	0.863
75	0.163	0.291	0.422	0.452	0.430	0.840
74	0.119	0.231	0.311	0.384	0.247	0.432
73	0.119	0.341	0.579	0.068	0.498	0.763
72	0.163	0.204	0.398	0.000	0.357	0.582
71	0.136	0.176	0.343	0.014	0.372	0.529
70	0.070	0.417	0.721	0.009	0.498	0.807
69	0.139	0.657	0.165	0.174	1.098	0.213
68	0.202	0.479	0.200	0.119	0.763	0.227
67	0.229	0.418	0.214	0.119	0.691	0.246
66	0.188	0.501	0.240	0.151	0.739	0.251
65	0.074	0.613	0.104	0.365	0.725	0.164
64	0.104	0.507	0.151	0.283	0.680	0.187
63	0.090	0.513	0.041	0.256	0.691	0.104
62	0.049	0.637	0.710	0.320	0.811	0.819
61	0.066	0.934	0.101	0.365	1.232	0.349
60	0.107	0.769	0.132	0.279	1.056	0.189
59	0.121	0.746	0.172	0.315	0.971	0.205
58	0.090	0.837	0.185	0.425	1.102	0.223
56	0.059	0.395	0.800	0.511	0.490	0.949
55	0.089	0.425	0.869	0.452	0.673	1.212
54	0.075	0.346	0.687	0.416	0.480	0.824
53	0.035	0.384	0.749	0.338	0.492	0.885
52	0.035	0.414	0.765	0.776	0.382	0.811
51	0.075	0.436	0.739	0.767	0.546	1.201
50	0.089	0.383	0.590	0.744	0.514	0.984
49	0.059	0.339	0.486	0.658	0.382	0.764
48	0.094	0.754	0.198	0.301	0.772	0.230
47	0.126	0.784	0.280	0.324	1.003	0.285
46	0.112	0.829	0.162	0.260	1.160	0.068
45	0.070	0.858	0.153	0.292	1.247	0.210
44	0.070	0.942	0.171	0.283	1.411	0.205
43	0.130	0.698	0.173	0.205	1.093	0.198
42	0.150	0.630	0.154	0.169	0.933	0.203
41	0.094	0.768	0.159	0.183	1.116	0.205
40	0.059	0.389	0.658	0.653	0.458	0.903
39	0.113	0.337	0.534	0.553	0.507	1.050
38	0.092	0.382	0.651	0.644	0.501	1.078
37	0.035	0.527	0.962	1.000	0.578	0.677
30	0.070	0.474	0.842	0.699	0.463	0.925
29	0.119	0.390	0.622	0.525	0.392	0.754
28	0.176	0.261	0.351	0.329	0.388	0.705
27	0.216	0.235	0.296	0.283	0.362	0.688
26	0.286	0.285	0.231	0.078	0.498	0.248

TABLE C-3-1A. Current Heliostat Data According to GBA (con't)

1. Data File: SCT

Run #	GBA	γ_{Fx}	γ_{Fz}	γ_{MHy}	$\gamma_{Fx\ peak}$	$\gamma_{Fz\ peak}$
25	0.188	0.470	0.194	0.132	0.774	0.220
24	0.139	0.651	0.206	0.155	0.924	0.232
23	0.247	0.373	0.208	0.078	0.692	0.232
95	0.020	0.161	0.384	0.219	0.294	0.536
94	0.020	0.397	0.789	0.247	0.443	0.822
93	0.010	0.559	1.072	0.708	0.519	1.039
92	0.010	0.064	0.260	0.032	0.204	0.380
91	0.020	0.085	0.273	0.105	0.217	0.405
90	0.020	0.457	0.912	0.224	0.451	0.930
36	0.020	0.234	0.323	0.329	0.437	0.918
35	0.020	0.670	1.326	1.073	0.181	1.310
34	0.010	0.050	0.074	0.064	0.107	0.207
33	0.010	0.622	1.257	1.073	0.582	1.282
32	0.020	0.131	0.065	0.100	0.247	0.420
31	0.020	0.679	1.326	0.904	0.624	1.328
22	0.020	0.573	0.147	0.128	0.944	0.189
21	0.020	0.933	0.136	0.347	1.250	0.192
20	0.020	0.360	0.211	0.105	0.680	0.222
17	0.020	1.160	0.174	0.324	1.347	0.217
14	0.010	0.331	0.184	0.137	0.418	0.195
13	0.010	1.467	0.214	0.502	1.362	0.245

Table C-3-1b. Current Heliostat Data According to GBA

2. Data File: SCT1

Run #	GBA	γ_{Fx}	γ_{Fz}	γ_{MHy}	$\gamma_{Fx\ peak}$	$\gamma_{Fz\ peak}$	$\gamma_{MHy\ peak}$
197	0.035	0.395	0.661	0.510	0.386	0.672	0.327
198	0.075	0.421	0.714	0.483	0.529	0.982	0.451
199	0.089	0.356	0.503	0.430	0.460	0.780	0.502
200	0.059	0.321	0.462	0.441	0.368	0.614	0.386
201	0.059	0.323	0.831	0.632	0.423	1.056	0.546
202	0.089	0.323	0.800	0.621	0.443	1.029	0.721
203	0.075	0.295	0.737	0.563	0.416	1.023	0.567
204	0.035	0.320	0.765	0.513	0.405	0.959	0.614
205	0.035	0.419	0.973	0.900	0.490	1.158	0.751
206	0.092	0.195	0.500	0.360	0.368	0.824	0.452
207	0.113	0.221	0.598	0.391	0.370	0.923	0.523
208	0.059	0.306	0.763	0.659	0.492	1.031	0.680
209	0.059	0.374	0.479	0.502	0.413	0.599	0.410
210	0.113	0.304	0.386	0.356	0.441	0.757	0.427
211	0.092	0.383	0.582	0.410	0.515	0.967	0.484
212	0.035	0.524	0.885	0.625	0.512	1.008	0.431
213	0.020	0.675	1.194	0.663	0.591	1.075	0.480
214	0.020	0.364	0.770	0.295	0.425	0.962	0.373
215	0.010	0.566	1.089	0.713	0.531	1.116	0.486
216	0.010	0.623	1.066	0.701	0.570	1.039	0.436
217	0.010	1.340	0.205	0.061	1.264	0.343	0.196
218	0.020	0.569	1.173	0.667	0.538	1.200	0.463
219	0.020	0.354	0.872	0.368	0.375	0.986	0.434
220	0.070	0.383	0.700	0.521	0.361	0.729	0.407
221	0.176	0.213	0.286	0.211	0.328	0.666	0.308
222	0.216	0.185	0.215	0.165	0.276	0.487	0.255
223	0.119	0.291	0.478	0.326	0.290	0.534	0.297
224	0.188	0.445	0.252	0.084	0.779	0.373	0.370
225	0.286	0.235	0.223	0.034	0.471	0.362	0.235
226	0.247	0.310	0.211	0.042	0.632	0.348	0.189
227	0.139	0.605	0.206	0.107	1.016	0.351	0.342
228	0.188	0.383	0.235	0.034	0.756	0.360	0.240
229	0.229	0.356	0.260	0.038	0.655	0.381	0.232
230	0.202	0.466	0.221	0.015	0.713	0.365	0.238
231	0.139	0.590	0.224	0.065	0.915	0.368	0.371
232	0.070	0.344	0.493	0.437	0.326	0.509	0.300
233	0.136	0.273	0.358	0.222	0.407	0.766	0.330
234	0.163	0.260	0.290	0.272	0.379	0.581	0.339
235	0.119	0.215	0.229	0.249	0.244	0.317	0.210
237	0.161	0.513	0.346	0.103	0.747	0.467	0.431
238	0.210	0.563	0.366	0.077	0.770	0.486	0.368
239	0.185	0.565	0.345	0.038	0.809	0.494	0.345
240	0.137	0.591	0.302	0.080	0.931	0.461	0.354
241	0.070	0.361	0.763	0.510	0.489	1.033	0.605
242	0.119	0.381	0.801	0.697	0.485	1.008	0.638

TABLE C-3-1B. Current Heliostat Data According to GBA (con't)

2. Data File: SCT1

Run #	GBA	γ_{Fx}	γ_{Fz}	γ_{MHy}	$\gamma_{Fx\ peak}$	$\gamma_{Fz\ peak}$	$\gamma_{MHy\ peak}$
243	0.143	0.375	0.810	0.602	0.508	1.017	0.637
244	0.095	0.321	0.673	0.494	0.457	0.875	0.636
245	0.070	0.296	0.370	0.398	0.351	0.533	0.318
246	0.119	0.326	0.450	0.395	0.448	0.813	0.415
247	0.143	0.283	0.284	0.398	0.361	0.495	0.344
248	0.095	0.208	0.190	0.300	0.228	0.166	0.217
250	0.131	0.626	0.171	0.065	0.997	0.332	0.290
251	0.180	0.710	0.144	0.054	0.914	0.310	0.305
252	0.204	0.745	0.410	0.069	0.947	0.337	0.321
253	0.156	0.660	0.166	0.080	0.889	0.340	0.362

TABLE C-3-1c. Current Heliostat Data According to GBA

3. Data File: SCT2

Run #	GBA	γ_{Mz}	$\gamma_{Mz\ peak}$
129	0.010	0.815	0.415
130	0.010	0.084	0.094
131	0.020	0.796	0.425
132	0.020	0.113	0.138
133	0.060	0.611	0.394
134	0.126	0.189	0.215
135	0.148	0.167	0.231
136	0.090	0.451	0.336
137	0.060	0.484	0.346
138	0.108	0.287	0.283
139	0.140	0.276	0.264
140	0.090	0.375	0.272
141	0.020	0.705	0.360
142	0.020	0.215	0.241
143	0.030	0.575	0.403
144	0.072	0.382	0.361
145	0.085	0.338	0.276
146	0.045	0.495	0.393
147	0.030	0.615	0.382
148	0.060	0.560	0.385
149	0.078	0.505	0.477
137	0.045	0.527	0.364
138	0.050	0.571	0.469
139	0.083	0.611	0.514
140	0.065	0.655	0.540
141	0.035	0.753	0.538
142	0.035	0.396	0.420
143	0.065	0.502	0.490
144	0.083	0.324	0.438
145	0.050	0.116	0.283
146	0.089	0.062	0.203
147	0.138	0.211	0.331
148	0.106	0.229	0.324
149	0.059	0.022	0.227
150	0.059	0.375	0.327
151	0.124	0.193	0.278
152	0.146	0.185	0.302
153	0.089	0.255	0.302
154	0.089	0.109	0.248
155	0.138	0.211	0.360
156	0.106	0.204	0.299
157	0.059	0.178	0.295
158	0.060	0.705	0.459
159	0.090	0.484	0.374
160	0.105	0.498	0.341

TABLE C-3-1c. Current Heliostat Data According to GBA (con't)

3. Data File: SCT2

Run #	GBA	γ_{Mz}	$\gamma_{Mz\ peak}$
161	0.090	0.658	0.430
162	0.099	0.876	0.582
163	0.114	0.618	0.464
164	0.099	0.705	0.487
165	0.070	0.989	0.611
166	0.070	0.942	0.573
167	0.099	0.738	0.435
168	0.126	0.436	0.337
169	0.110	0.498	0.407
170	0.020	0.825	0.477
171	0.020	0.353	0.339
172	0.010	0.644	0.354
173	0.010	0.698	0.389
174	0.020	0.189	0.220
175	0.059	0.029	0.177
176	0.059	0.011	0.221
177	0.070	0.265	0.374
178	0.070	0.360	0.376
179	0.020	0.680	0.457
180	0.010	0.640	0.438
181	0.010	0.651	0.371
182	0.020	0.836	0.492
183	0.070	0.920	0.552
184	0.070	0.902	0.575
185	0.059	0.655	0.448
186	0.059	0.578	0.381
187	0.020	0.596	0.365

TABLE C-3-2. 85 Heliostat and 78 Heliostat Data According to GBA

Note: Coefficient values are as defined in refs. 23 and 1, not as in this report.

85 Heliostat: Maximum values in single study in ref. 23

Mean: $C_{Fx} = 1.72$ $C_{Fz} = 1.11$ $C_{MHy} = 0.16$

Peak: $C_{Fx\ peak} = 2.56$ $C_{Fz\ peak} = 1.47$ $C_{MHy\ peak} = 0.62$

78 Heliostat: Maximum values in single study in ref. 1

Mean: $C_{Fx} = 1.38$ $C_{MHy} = 0.215$

Config.	α	β	GBA	γ_{Fx}	γ_{Fz}	γ_{MHy}	$\gamma_{Fx\ peak}$	$\gamma_{Fz\ peak}$	$\gamma_{MHy\ peak}$
H5000	80	5.0	0.138	0.426	0.089	0.750	0.707	0.095	0.790
	80	5.0	0.138	0.262	0.013	0.438	0.352	0.048	0.419
	70	2.5	0.132	0.361	0.127	0.375	0.480	0.156	0.548
	90	5.0	0.140	0.328	0.025	0.438	0.590	0.177	0.097
H5001	90	5.0	0.186	0.328	0.025	0.250	0.641	0.194	
	80	5.0	0.184	0.180	0.025	0.125	0.434	0.054	
	65	2.5	0.173	0.369	0.216	0.125	0.559	0.279	
	45	2.5	0.146	0.451	0.445	0.375	0.504	0.401	0.435
H5100	45	2.5	0.100	0.377	0.305	0.438	0.445	0.286	0.419
	65	2.5	0.127	0.320	0.152	0.063	0.422	0.190	
	90	5.0	0.140	0.303	0.013	0.125	0.418	0.034	
	70	2.5	0.132	0.205	0.089	0.250	0.324	0.116	0.323
	80	5.0	0.138	0.230	0.013	0.375	0.406	0.034	0.419
	80	5.0	0.138	0.230	0.038	0.063	0.414	0.048	
H5101	45	2.5	0.146	0.164	0.203	0.250	0.332	0.293	0.371
	65	2.5	0.173	0.238	0.114	0.125	0.461	0.177	
	90	5.0	0.186	0.123	0.013	0.063	0.328	0.027	
	70	2.5	0.178	0.164	0.102	0.250	0.313	0.129	0.355
	80	5.0	0.184	0.238	0.051	0.313	0.430	0.068	0.403
	80	5.0	0.184	0.107	0.013	0.125	0.273	0.034	
H5102	80	5.0	0.223	0.238	0.038	0.188	0.441	0.048	
	80	5.0	0.223	0.148	0.025	0.250	0.332	0.041	0.323
	70	2.5	0.217	0.131	0.038	0.188	0.293	0.095	0.306
	90	5.0	0.225	0.123	0.013	0.000	0.328	0.048	
	65	2.5	0.213	0.156	0.064	0.250	0.379	0.095	
	45	2.5	0.185	0.098	0.140	0.313	0.258	0.279	0.403
H3100	90	0.0	0.245	0.123	0.000	0.063	0.410	0.068	

TABLE C-3-2. 85 Heliostat and 78 Heliostat Data According to GBA (con't)

Note: Coefficient values are as defined in refs. 23 and 1, not as in this report.

85 Heliostat: Maximum values in single study in ref. 23

Mean: $C_{Fx} = 1.72$ $C_{Fz} = 1.11$ $C_{MHy} = 0.16$

Peak: $C_{Fx\ peak} = 2.56$ $C_{Fz\ peak} = 1.47$ $C_{MHy\ peak} = 0.62$

78 Heliostat: Maximum values in single study in ref. 1

Mean: $C_{Fx} = 1.38$ $C_{MHy} = 0.215$

Config.	α	β	GBA	γ_{Fx}	γ_{Fz}	γ_{MHy}	$\gamma_{Fx\ peak}$	$\gamma_{Fz\ peak}$	$\gamma_{MHy\ peak}$
H3200	90	0.0	0.245	0.115	0.000	0.063	0.410	0.068	
	90	0.0	0.245	0.107	0.000	0.063	0.281	0.075	
	90	0.0	0.245	0.107	0.025	0.125	0.359	0.048	
	90	0.0	0.245	0.098	0.013	0.000	0.293	0.068	
	90	0.0	0.245	0.107	0.013	0.000	0.238	0.048	
	90	0.0	0.245	0.131	0.025	0.063	0.375	0.082	
	90	0.0	0.245	0.156	0.025	0.000	0.320	0.068	
	90	0.0	0.245	0.123	0.013	0.063	0.328	0.054	
H3300	90	0.0	0.238	0.123	0.000	0.063	0.450	0.068	
	90	0.0	0.131	0.279	0.025	0.188	0.527	0.088	
	90	0.0	0.067	0.566	0.013	0.438	0.742	0.068	
	90	0.0	0.044	0.770	0.025	0.313	0.965	0.061	
	90	0.0	0.026	0.877	0.025	0.438	0.965	0.048	
H3400	90	0.0	0.061	0.566	0.013	0.438	0.742	0.068	
	90	0.0	0.061	0.451	0.013	0.188	0.625	0.122	
H3401	90	0.0	0.107	0.434	0.025	0.313	0.723	0.054	
	90	0.0	0.107	0.352	0.025	0.063	0.531	0.075	
H3402	90	0.0	0.179	0.402	0.025	0.188	0.574	0.048	
	90	0.0	0.179	0.320	0.013	0.188	0.512	0.054	
H3405	90	0.0	0.197	0.270	0.000	0.125	0.605	0.054	
	90	0.0	0.197	0.238	0.013	0.000	0.543	0.041	
H3406	90	0.0	0.179	0.213	0.000	0.063	0.582	0.048	
	90	0.0	0.179	0.213	0.000	0.063	0.508	0.054	
H3500	90	0.0	0.061	0.598	0.051	0.180	0.625	0.088	
H3501	90	0.0	0.107	0.189	0.013	0.063	0.375	0.068	

TABLE C-3-2. 85 Heliostat and 78 Heliostat Data According to GBA (con't)

Note: Coefficient values are as defined in refs. 23 and 1, not as in this report.

85 Heliostat: Maximum values in single study in ref. 23

Mean: $C_{Fx} = 1.72$ $C_{Fz} = 1.11$ $C_{MHy} = 0.16$

Peak: $C_{Fx\ peak} = 2.56$ $C_{Fz\ peak} = 1.47$ $C_{MHy\ peak} = 0.62$

78 Heliostat: Maximum values in single study in ref. 1

Mean: $C_{Fx} = 1.38$ $C_{MHy} = 0.215$

Config.	α	β	GBA	γ_{Fx}	γ_{Fz}	γ_{MHy}	$\gamma_{Fx\ peak}$	$\gamma_{Fz\ peak}$	$\gamma_{MHy\ peak}$
H3502	90	00.0	0.179	0.180	0.013	0.063	0.445	0.061	
H3503	90	00.0	0.163	0.254	0.051	0.250	0.758	0.061	
H3504	90	00.0	0.107	0.279	0.013	0.250	0.641	0.041	
H3505	90	00.0	0.186	0.172	0.000	0.125	0.555	0.048	
Hel. 85	80	00.0	0.010	1.020	0.825	1.750	0.961	0.660	0.806
			0.010	0.186	0.126	0.690	0.543	0.218	0.645
Hel. 78	10	00.0	0.029	0.096		0.721			
	30	00.0	0.084	0.331		0.591			
	90	00.0	0.168	0.555		0.140			
	10	00.0	0.029	0.111		0.400			
	10	00.0	0.024	0.093		0.420			
	90	00.0	0.136	0.544		0.116			
H5000	80	50.0	0.089	0.344	0.036	0.438	0.465	0.061	0.565
	80	27.5	0.122	0.369	0.054	0.500	0.586	0.088	0.645
	80	17.5	0.132	0.313	0.027	0.254	0.395	0.020	0.516
	80	40.0	0.106	0.500	0.018	0.213	0.430	0.062	0.629
	80	62.5	0.064	0.063	0.018	0.082	0.273	0.048	
	80	62.5	0.064	0.813	0.027	0.131	0.336	0.088	0.613
	80	85.0	0.012	0.125	0.018	0.049	0.203	0.048	
	80	72.5	0.041	0.250	0.036	0.082	0.305	0.068	
	80	50.0	0.089	0.875	0.081	0.434	0.602	0.102	0.677
	80	27.5	0.122	0.688	0.054	0.361	0.500	0.088	0.532
H5001	80	50.0	0.135	0.402	0.063	0.563	0.641	0.109	0.790
	80	17.5	0.178	0.189	0.009	0.188	0.578	0.048	
	80	40.0	0.152	0.402	0.036	0.375	0.719	0.088	
	80	62.5	0.110	0.139	0.027	0.125	0.363	0.061	
	80	62.5	0.110	0.213	0.036	0.625	0.410	0.061	0.548

TABLE C-3-2. 85 Heliostat and 78 Heliostat Data According to GBA (con't)

Note: Coefficient values are as defined in refs. 23 and 1, not as in this report.

85 Heliostat: Maximum values in single study in ref. 23

Mean: $C_{Fx} = 1.72$ $C_{Fz} = 1.11$ $C_{MHy} = 0.16$

Peak: $C_{Fx\ peak} = 2.56$ $C_{Fz\ peak} = 1.47$ $C_{MHy\ peak} = 0.62$

78 Heliostat: Maximum values in single study in ref. 1

Mean: $C_{Fx} = 1.38$ $C_{MHy} = 0.215$

Config.	α	β	GBA	γ_{Fx}	γ_{Fz}	γ_{MHy}	$\gamma_{Fx\ peak}$	$\gamma_{Fz\ peak}$	$\gamma_{MHy\ peak}$
H5001	80	85.0	0.058	0.008	0.000	0.063	0.223	0.048	
(con't)	80	72.5	0.087	0.115	0.018	0.375	0.281	0.054	0.484
	80	50.0	0.135	0.254	0.045	0.688	0.492	0.082	0.742
	80	27.5	0.168	0.189	0.027	0.250	0.434	0.054	
H5100	80	27.5	0.122	0.205	0.027	0.313	0.344	0.048	0.355
	80	50.0	0.089	0.164	0.018	0.250	0.375	0.041	
	80	72.5	0.041	0.008	0.009	0.250	0.324	0.068	
	80	85.0	0.012	0.041	0.009	0.063	0.215	0.088	
	80	62.5	0.064	0.131	0.018	0.250	0.520	0.075	
	80	62.5	0.064	0.107	0.009	0.063	0.332	0.034	
	80	40.0	0.106	0.238	0.027	0.313	0.465	0.054	
	80	17.5	0.132	0.320	0.036	0.063	0.445	0.054	
	80	27.5	0.122	0.262	0.027	0.188	0.473	0.048	
	80	50.0	0.089	0.213	0.027	0.063	0.336	0.054	
H5101	80	27.5	0.168	0.148	0.000	0.188	0.320	0.027	
	80	50.0	0.135	0.082	0.000	0.125	0.309	0.034	
	80	72.5	0.087	0.025	0.027	0.125	0.391	0.075	
	80	85.0	0.058	0.082	0.018	0.125	0.332	0.061	
	80	62.5	0.110	0.164	0.018	0.250	0.387	0.068	
	80	62.5	0.110	0.094	0.018	0.063	0.254	0.068	
	80	40.0	0.152	0.262	0.018	0.313	0.508	0.041	
	80	17.5	0.178	0.180	0.009	0.188	0.359	0.041	
	80	27.5	0.168	0.164	0.009	0.135	0.418	0.048	
	80	50.0	0.135	0.098	0.027	0.063	0.387	0.041	
H5102	80	72.5	0.127	0.082	0.027	0.125	0.418	0.048	
	80	85.0	0.098	0.025	0.018	0.000	0.207	0.041	
	80	62.5	0.150	0.164	0.036	0.313	0.492	0.061	
	80	62.5	0.150	0.082	0.018	0.125	0.320	0.095	
	80	40.0	0.192	0.189	0.018	0.186	0.387	0.041	
	80	27.5	0.208	0.156	0.018	0.125	0.340	0.048	
	80	50.0	0.175	0.098	0.009	0.188	0.414	0.034	

TABLE C-3-2. 85 Heliostat and 78 Heliostat Data According to GBA (con't)

Note: Coefficient values are as defined in refs. 23 and 1, not as in this report.

85 Heliostat: Maximum values in single study in ref. 23

Mean: $C_{Fx} = 1.72$ $C_{Fz} = 1.11$ $C_{MHy} = 0.16$

Peak: $C_{Fx\ peak} = 2.56$ $C_{Fz\ peak} = 1.47$ $C_{MHy\ peak} = 0.62$

78 Heliostat: Maximum values in single study in ref. 1

Mean: $C_{Fx} = 1.38$ $C_{MHy} = 0.215$

Config.	α	β	GBA	γ_{Fx}	γ_{Fz}	γ_{MHy}	$\gamma_{Fx\ peak}$	$\gamma_{Fz\ peak}$	$\gamma_{MHy\ peak}$
H5001	65	50.0	0.128	0.025	0.050	0.063	0.441	0.184	
	65	27.5	0.159	0.254	0.175	0.188	0.512	0.238	
	65	25.0	0.161	0.393	0.225	0.063	0.617	0.293	
	65	20.0	0.165	0.295	0.175	0.063	0.512	0.252	
	65	42.5	0.140	0.361	0.213	0.063	0.531	0.224	
H5100	65	42.5	0.094	0.221	0.100	0.000	0.340	0.150	
	65	20.0	0.119	0.205	0.075	0.063	0.402	0.150	
	65	25.0	0.115	0.197	0.100	0.063	0.367	0.143	
	65	47.5	0.086	0.221	0.088	0.063	0.434	0.163	
	65	70.0	0.043	0.098	0.038	0.188	0.340	0.116	
H5101	65	42.5	0.140	0.230	0.125	0.063	0.465	0.197	
	65	20.0	0.165	0.164	0.075	0.125	0.367	0.150	
	65	25.0	0.161	0.180	0.050	0.125	0.438	0.156	
	65	47.5	0.132	0.098	0.025	0.125	0.434	0.141	
	65	70.0	0.089	0.025	0.013	0.063	0.254	0.095	
H5102	65	70.0	0.129	0.066	0.038	0.188	0.254	0.095	
	65	47.5	0.172	0.123	0.075	0.125	0.293	0.129	
	65	25.0	0.201	0.131	0.050	0.125	0.402	0.150	
	65	20.0	0.205	0.139	0.063	0.188	0.277	0.116	
	65	42.5	0.180	0.227	0.125	0.250	0.367	0.102	
H5001	45	70.0	0.080	0.016	0.013	0.000	0.211	0.190	
	45	47.5	0.114	0.205	0.238	0.250	0.355	0.340	
	45	25.0	0.137	0.369	0.413	0.500	0.566	0.469	0.597
	45	20.0	0.140	0.344	0.363	0.313	0.500	0.401	0.435
H5100	45	20.0	0.094	0.230	0.213	0.188	0.379	0.313	
	45	25.0	0.091	0.287	0.288	0.313	0.387	0.320	0.403
	45	47.5	0.068	0.221	0.200	0.250	0.313	0.245	0.387
	45	70.0	0.034	0.066	0.075	0.000	0.188	0.136	

TABLE C-3-2. 85 Heliostat and 78 Heliostat Data According to GBA (con't)

Note: Coefficient values are as defined in refs. 23 and 1, not as in this report.

85 Heliostat: Maximum values in single study in ref. 23

Mean: $C_{Fx} = 1.72$ $C_{Fz} = 1.11$ $C_{MHy} = 0.16$

Peak: $C_{Fx\ peak} = 2.56$ $C_{Fz\ peak} = 1.47$ $C_{MHy\ peak} = 0.62$

78 Heliostat: Maximum values in single study in ref. 1

Mean: $C_{Fx} = 1.38$ $C_{MHy} = 0.215$

Config.	α	β	GBA	γ_{Fx}	γ_{Fz}	γ_{MHy}	$\gamma_{Fx\ peak}$	$\gamma_{Fz\ peak}$	$\gamma_{MHy\ peak}$
H5101	45	20.0	0.140	0.197	0.213	0.188	0.445	0.340	
	45	25.0	0.137	0.164	0.125	0.125	0.367	0.265	
	45	47.5	0.114	0.123	0.113	0.188	0.332	0.265	
	45	70.0	0.080	0.057	0.088	0.063	0.207	0.150	
H5102	45	70.0	0.120	0.025	0.038	0.188	0.168	0.184	0.242
	45	47.5	0.154	0.082	0.138	0.313	0.234	0.320	0.387
	45	25.0	0.177	0.098	0.150	0.250	0.203	0.265	0.339
	45	20.0	0.180	0.148	0.225	0.438	0.262	0.320	0.403

APPENDIX D

Output Data Files (SCT, SCT1 and SCT2)

Data File: SCT

For Field Study

In the file labelled "SCT" the coefficient denoted by "MX" and "MY" are the base moment coefficients. However, in the files labelled "SCT1" and "SCT2" the coefficient of "MX" and "MY" are the hinge moment coefficients about the y-axis at the motor drive level.

Comments: 1. Because of system lift force, $F_{z\ actual} = F_z - 0.273$

(e.g. $F_z = 0.529$ (Run # 13), $F_{z\ actual} = 0.529 - 0.273 = 0.256$)

2. MY is the base moment coefficient, C_{My} in data file: SCT

DATA FILE: SCT

RUN #	WIND	TILT	VELOCITY	COMP:	FX	FY	FZ	MX	MY	MZ
13	.0	90.0	9.2	Mean	2.332	.076	.529	-.075	1.186	.018
				Max	3.321	.135	.689	-.045	1.696	.150
				Min	1.600	.023	.367	-.111	.823	-.104
				Rms	.265	.016	.044	.009	.139	.033
				GFAC	1.424	1.769	1.303	1.478	1.430	8.243
				PFAC	3.736	3.766	3.627	3.787	3.677	4.058
14	.0	90.0	9.3	Mean	.525	.088	.492	-.042	.262	.018
				Max	1.018	.147	.603	-.018	.530	.079
				Min	.191	.038	.392	-.069	.092	-.048
				Rms	.106	.016	.030	.007	.056	.016
				GFAC	1.937	1.665	1.226	1.642	2.026	4.433
				PFAC	4.626	3.755	3.702	3.981	4.789	3.862
17	.0	90.0	9.2	Mean	1.845	.075	.481	-.063	.954	.032
				Max	3.284	.252	.642	.011	1.631	.287
				Min	.344	-.077	.316	-.170	.184	-.181
				Rms	.377	.049	.045	.025	.194	.065
				GFAC	1.780	3.377	1.335	2.695	1.710	9.020
				PFAC	3.816	3.643	3.578	4.261	3.499	3.907
20	.0	90.0	9.3	Mean	.572	.063	.524	-.032	.294	.031
				Max	1.660	.131	.648	-.007	.880	.166
				Min	.133	-.001	.400	-.074	.068	-.063
				Rms	.184	.018	.035	.009	.101	.029
				GFAC	2.902	2.080	1.237	2.294	2.989	5.404
				PFAC	5.918	3.784	3.575	4.643	5.790	4.703
21	.0	90.0	9.2	Mean	1.482	.079	.435	-.053	.747	.025
				Max	3.049	.182	.599	-.008	1.553	.251

DATA FILE: SCT

RUN #	WIND	TILT	VELOCITY	COMP:	FX	FY	FZ	MX	MY	MZ
				Min	.578	-.016	.280	-.116	.289	-.142
				Rms	.302	.025	.044	.013	.162	.047
				GFAC	2.057	2.295	1.378	2.188	2.079	10.230
				PFAC	5.193	4.126	3.719	4.914	4.976	4.834
22	.0	90.0	9.2	Mean	.910	.059	.449	-.037	.477	.036
				Max	2.303	.163	.593	.000	1.157	.191
				Min	.227	-.020	.292	-.090	.093	-.103
				Rms	.258	.022	.041	.011	.139	.039
				GFAC	2.530	2.750	1.322	2.425	2.426	5.314
				PFAC	5.395	4.762	3.549	4.760	4.895	3.953
23	.0	90.0	9.1	Mean	.593	.068	.522	-.035	.312	.021
				Max	1.687	.168	.666	-.005	.926	.153
				Min	.069	-.009	.365	-.074	.053	-.106
				Rms	.201	.021	.041	.011	.110	.032
				GFAC	2.845	2.466	1.275	2.142	2.970	7.372
				PFAC	5.437	4.695	3.478	3.716	5.571	4.126
24	.0	90.0	9.2	Mean	1.035	.071	.519	-.045	.540	.034
				Max	2.255	.201	.667	.004	1.172	.215
				Min	.217	-.030	.385	-.117	.105	-.185
				Rms	.322	.031	.044	.016	.169	.045
				GFAC	2.179	2.827	1.287	2.592	2.169	6.276
				PFAC	3.790	4.221	3.403	4.492	3.731	4.033
25	.0	90.0	9.3	Mean	.747	.066	.505	-.037	.386	.031
				Max	1.885	.167	.645	.009	.928	.261
				Min	-.132	-.064	.341	-.099	-.066	-.150
				Rms	.273	.025	.043	.013	.148	.042

DATA FILE: SCT

RUN #	WIND	TILT	VELOCITY	COMP:	FX	FY	FZ	MX	MY	MZ
				GFAC	2.523	2.520	1.277	2.644	2.405	8.348
				PFAC	4.165	4.002	3.233	4.796	3.653	5.486
26	.0	90.0	9.2	Mean	.454	.072	.549	-.033	.235	.020
				Max	1.213	.141	.693	-.007	.638	.131
				Min	-.079	.001	.415	-.068	-.026	-.071
				Rms	.168	.017	.039	.009	.092	.025
				GFAC	2.670	1.956	1.263	2.077	2.718	6.687
				PFAC	4.510	4.003	3.657	4.075	4.367	4.437
27	.0	30.0	9.3	Mean	.374	.105	-.080	-.049	.146	.013
				Max	.881	.231	.380	.068	.356	.094
				Min	.080	.023	-.896	-.143	.007	-.032
				Rms	.118	.030	.187	.025	.050	.016
				GFAC	2.357	2.209	11.216	2.916	2.438	7.022
				PFAC	4.312	4.274	4.364	3.816	4.210	5.202
28	.0	30.0	9.3	Mean	.414	.104	-.146	-.050	.158	.010
				Max	.946	.240	.377	.082	.378	.110
				Min	.073	.003	-.922	-.160	.023	-.056
				Rms	.126	.032	.201	.028	.053	.017
				GFAC	2.286	2.305	6.320	3.224	2.394	11.002
				PFAC	4.225	4.270	3.859	3.982	4.179	5.715
29	.0	30.0	9.2	Mean	.620	.134	-.470	-.066	.229	.002
				Max	.957	.266	-.067	.049	.391	.080
				Min	.336	.004	-1.008	-.181	.118	-.064
				Rms	.083	.035	.126	.030	.037	.019
				GFAC	1.545	1.988	2.144	2.728	1.706	43.092
				PFAC	4.083	3.735	4.281	3.785	4.389	4.168

DATA FILE: SCT

RUN #	WIND	TILT	VELOCITY	COMP:	FX	FY	FZ	MX	MY	MZ
30	.0	30.0	9.2	Mean	.755	.150	-.733	-.072	.266	.004
				Max	1.128	.334	-.268	.031	.419	.072
				Min	.459	-.019	-1.297	-.219	.121	-056
				Rms	.099	.044	.149	.033	.044	.019
				GFAC	1.494	2.223	1.770	3.048	1.575	19.131
				PFAC	3.773	4.202	3.788	4.432	3.458	3.545
31	.0	30.0	9.2	Mean	1.079	.177	-1.311	-.089	.401	.003
				Max	1.524	.299	-.784	.004	.594	.072
				Min	.748	.068	-1.979	-.184	.227	-.056
				Rms	.120	.032	.184	.026	.054	.017
				GFAC	1.412	1.691	1.509	2.062	1.482	26.478
				PFAC	3.717	3.811	3.624	3.673	3.588	4.008
32	.0	30.0	9.2	Mean	.209	.075	.196	-.034	.094	.010
				Max	.603	.209	.512	.047	.282	.077
				Min	.002	.004	-.440	-.133	-.011	-.042
				Rms	.093	.022	.144	.022	.045	.014
				GFAC	2.885	2.776	2.606	3.908	2.989	7.427
				PFAC	4.241	5.944	2.183	4.421	4.177	4.902
33	.0	30.0	9.2	Mean	.989	.181	-1.229	-.081	.314	-.001
				Max	1.420	.306	-.716	-.004	.483	.049
				Min	.639	.078	-1.902	-.166	.179	-.064
				Rms	.125	.031	.194	.026	.049	.015
				GFAC	1.436	1.693	1.547	2.058	1.541	56.018
				PFAC	3.444	3.985	3.462	3.333	3.492	4.302
34	.0	30.0	9.2	Mean	.079	.055	.362	-.023	.030	.010
				Max	.260	.113	.624	.002	.195	.025

DATA FILE: SCT

RUN #	WIND	TILT	VELOCITY	COMP:	FX	FY	FZ	MX	MY	MZ
				Min	-.085	.019	.034	-.071	-.062	-.007
				Rms	.043	.010	.063	.007	.029	.004
				GFAC	3.305	2.050	1.723	3.128	6.598	2.479
				PFAC	4.201	5.571	4.171	6.598	5.662	3.318
35	.0	30.0	9.3	Mean	1.065	.192	-1.311	-.088	.357	.004
				Max	1.514	.352	-.665	.027	.577	.075
				Min	.628	.045	-1.951	-.194	.147	-.058
				Rms	.126	.038	.192	.031	.060	.017
				GFAC	1.422	1.837	1.488	2.199	1.614	20.645
				PFAC	3.577	4.176	3.339	3.420	3.640	4.097
36	.0	30.0	9.3	Mean	.372	.094	-.113	-.040	.135	.006
				Max	1.065	.251	.397	.112	.373	.105
				Min	.001	-.006	-1.284	-.188	-.008	-.075
				Rms	.142	.033	.225	.032	.056	.018
				GFAC	2.865	2.676	11.373	4.710	2.757	19.070
				PFAC	4.871	4.806	5.214	4.619	4.277	5.393
37	.0	30.0	9.1	Mean	.838	.163	-.876	-.072	.247	.001
				Max	1.408	.349	-.318	.043	.472	.080
				Min	.550	.022	-1.624	-.178	.117	-.059
				Rms	.098	.037	.156	.027	.044	.016
				GFAC	1.680	2.143	1.854	2.466	1.910	114.281
				PFAC	5.841	4.979	4.797	3.913	5.132	5.089
38	.0	30.0	9.3	Mean	.608	.132	-.505	-.061	.197	.006
				Max	1.220	.341	.146	.051	.457	.102
				Min	.205	.013	-1.558	-.206	.029	-.071

DATA FILE: SCT

RUN #	WIND	TILT	VELOCITY	COMP:	FX	FY	FZ	MX	MY	MZ
				Rms	.172	.046	.279	.036	.068	.020
				GFAC	2.006	2.573	3.086	3.366	2.325	17.204
				PFAC	3.556	4.537	3.775	4.011	3.831	4.898
39	.0	30.0	9.1	Mean	.535	.121	-.366	-.057	.176	.005
				Max	1.237	.308	.283	.065	.435	.089
				Min	.110	-.007	-1.509	-.185	.013	-.065
				Rms	.176	.043	.285	.035	.068	.019
				GFAC	2.314	2.535	4.128	3.243	2.467	16.498
				PFAC	3.987	4.333	4.008	3.674	3.802	4.298
40	.0	30.0	9.1	Mean	.618	.130	-.514	-.060	.200	.002
				Max	1.117	.325	-.088	.046	.421	.066
				Min	.317	.023	-1.261	-.207	.064	-.066
				Rms	.107	.038	.173	.032	.047	.019
				GFAC	1.809	2.498	2.450	3.474	2.102	32.335
				PFAC	4.676	5.130	4.304	4.604	4.720	3.412
41	.0	90.0	9.1	Mean	1.220	.071	.462	-.047	.638	.028
				Max	2.722	.169	.621	-.003	1.361	.235
				Min	.449	-.017	.313	-.116	.211	-.122
				Rms	.336	.025	.044	.014	.183	.046
				GFAC	2.231	2.365	1.344	2.452	2.133	8.464
				PFAC	4.472	3.832	3.589	5.011	3.945	4.551
42	.0	90.0	9.2	Mean	1.001	.058	.458	-.040	.519	.027
				Max	2.275	.175	.619	.003	1.189	.175
				Min	.238	-.031	.294	-.095	.144	-.130
				Rms	.285	.024	.044	.012	.156	.039
				GFAC	2.272	3.025	1.351	2.377	2.291	6.424
				PFAC	4.472	4.922	3.692	4.412	4.296	3.735

DATA FILE: SCT

RUN #	WIND	TILT	VELOCITY	COMP:	FX	FY	FZ	MX	MY	MZ
43	.0	90.0	9.2	Mean	1.110	.064	.477	-.046	.572	.027
				Max	2.677	.149	.610	-.004	1.407	.216
				Min	.117	-.033	.292	-.096	.116	-.112
				Rms	.306	.023	.044	.012	.167	.040
				GFAC	2.411	2.332	1.278	2.091	2.459	7.899
				PFAC	5.126	3.747	3.013	4.108	4.992	4.655
44	.0	90.0	9.1	Mean	1.498	.065	.477	-.052	.770	.030
				Max	3.444	.188	.621	-.004	1.703	.211
				Min	.467	-.036	.297	-.126	.238	-.252
				Rms	.385	.028	.047	.016	.207	.048
				GFAC	2.298	2.917	1.301	2.395	2.213	7.024
				PFAC	5.058	4.358	3.054	4.701	4.513	3.752
45	.0	90.0	9.2	Mean	1.364	.059	.456	-.048	.694	.036
				Max	3.040	.160	.630	-.011	1.551	.250
				Min	.500	-.037	.289	-.113	.216	-.153
				Rms	.346	.027	.047	.014	.187	.049
				GFAC	2.229	2.721	1.382	2.336	2.236	6.884
				PFAC	4.848	3.754	3.712	4.637	4.597	4.317
46	.0	90.0	9.0	Mean	1.317	.065	.466	-.049	.675	.034
				Max	2.830	.170	.611	-.001	1.388	.260
				Min	.484	-.040	.309	-.115	.268	-.152
				Rms	.325	.025	.045	.014	.177	.048
				GFAC	2.149	2.601	1.309	2.337	2.058	7.701
				PFAC	4.654	4.172	3.172	4.791	4.029	4.672
47	.0	90.0	8.9	Mean	1.246	.078	.607	-.049	.621	.027
				Max	2.445	.168	.756	-.017	1.230	.240

DATA FILE: SCT

RUN #	WIND	TILT	VELOCITY	COMP:	FX	FY	FZ	MX	MY	MZ
				Min	.548	-.011	.469	-.105	.253	-.148
				Rms	.291	.021	.045	.011	.153	.050
				GFAC	1.962	2.149	1.245	2.126	1.980	9.029
				PFAC	4.115	4.226	3.292	4.853	3.972	4.247
48	.0	90.0	9.2	Mean	1.198	.071	.509	-.047	.599	.030
				Max	2.883	.147	.664	-.016	1.448	.223
				Min	.498	.002	.361	-.094	.232	-.138
				Rms	.290	.019	.044	.011	.155	.044
				GFAC	2.407	2.070	1.303	2.002	2.416	7.526
				PFAC	5.820	3.945	3.517	4.312	5.470	4.432
49	.0	30.0	9.2	Mean	.539	.127	-.308	-.054	.155	.004
				Max	.930	.252	.052	.011	.330	.056
				Min	.323	.053	-1.025	-.163	.079	-.056
				Rms	.086	.027	.142	.022	.032	.013
				GFAC	1.725	1.984	3.323	3.018	2.130	13.972
				PFAC	4.544	4.673	5.051	5.006	5.477	4.129
50	.0	30.0	8.9	Mean	.610	.142	-.433	-.062	.176	.004
				Max	1.254	.305	.188	.058	.396	.092
				Min	.236	-.004	-1.397	-.193	.053	-.070
				Rms	.147	.042	.238	.035	.052	.020
				GFAC	2.057	2.145	3.222	3.088	2.249	22.120
				PFAC	4.394	3.875	4.043	3.729	4.259	4.425
51	.0	30.0	9.0	Mean	.693	.154	-.611	-.069	.217	.004
				Max	1.330	.331	.038	.041	.554	.066
				Min	.296	.045	-1.764	-.196	.065	-.067
				Rms	.155	.041	.254	.033	.065	.019

DATA FILE: SCT

RUN #	WIND	TILT	VELOCITY	COMP:	FX	FY	FZ	MX	MY	MZ
				GFAC	1.919	2.149	2.888	2.831	2.550	15.836
				PFAC	4.101	4.285	4.535	3.798	5.184	3.275
52	.0	30.0	9.3	Mean	.658	.141	-.642	-.060	.196	.003
				Max	.929	.257	-.293	.016	.329	.047
				Min	.426	.039	-1.103	-.159	.109	-.039
				Rms	.073	.027	.118	.020	.032	.012
				GFAC	1.412	1.824	1.719	2.644	1.675	14.051
				PFAC	3.725	4.296	3.901	4.854	4.142	3.739
53	.0	-30.0	9.2	Mean	.612	.046	1.168	-.015	.414	.030
				Max	1.199	.192	1.775	.106	.865	.105
				Min	.173	-.109	.724	-.141	.186	-.024
				Rms	.131	.034	.147	.031	.086	.017
				GFAC	1.959	4.202	1.520	9.187	2.087	3.484
				PFAC	4.482	4.300	4.123	4.005	5.233	4.398
54	.0	-30.0	9.0	Mean	.550	.002	1.094	-.020	.397	.029
				Max	1.169	.185	1.671	.142	.785	.101
				Min	.007	-.187	.521	-.177	.040	-.040
				Rms	.133	.038	.156	.038	.095	.019
				GFAC	2.124	88.330	1.528	8.857	1.976	3.467
				PFAC	4.642	4.821	3.709	4.179	4.077	3.781
55	.0	-30.0	9.0	Mean	.676	.068	1.311	-.016	.475	.042
				Max	1.642	.224	2.330	.191	1.114	.134
				Min	.201	-.155	.777	-.202	.170	-.017
				Rms	.147	.041	.176	.042	.103	.020
				GFAC	2.428	3.302	1.777	12.897	2.343	3.158
				PFAC	6.552	3.789	5.796	4.479	6.174	4.480

DATA FILE: SCT

RUN #	WIND	TILT	VELOCITY	COMP:	FX	FY	FZ	MX	MY	MZ
56	.0	-30.0	9.2	Mean	.628	-.001	1.227	-.014	.461	.035
				Max	1.194	.146	1.884	.189	.858	.104
				Min	.198	-.209	.752	-.146	.180	-.048
				Rms	.131	.038	.149	.038	.092	.019
				GFAC	1.902	168.626	1.536	10.756	1.862	2.972
				PFAC	4.320	5.426	4.408	3.513	4.304	3.713
57	20.0	90.0	9.0	Mean	1.346	.452	.539	-.245	.669	-.068
				Max	2.832	.922	.746	.135	1.426	.100
				Min	.544	-.224	-.032	-.526	.289	-.300
				Rms	.314	.154	.085	.077	.159	.052
				GFAC	2.105	2.039	1.385	2.145	2.131	4.423
				PFAC	4.729	3.059	2.448	3.657	4.763	4.508
58	20.0	90.0	9.1	Mean	1.331	.452	.494	-.230	.646	-.049
				Max	2.689	.840	.652	-.102	1.343	.072
				Min	.558	.216	.317	-.446	.267	-.263
				Rms	.303	.090	.047	.050	.154	.045
				GFAC	2.021	1.859	1.320	1.938	2.073	5.340
				PFAC	4.478	4.289	3.394	4.346	4.534	4.801
59	20.0	90.0	9.0	Mean	1.185	.396	.478	-.208	.589	-.037
				Max	2.370	.746	.622	-.094	1.196	.092
				Min	.495	.182	.327	-.424	.242	-.234
				Rms	.285	.085	.045	.047	.146	.043
				GFAC	2.000	1.886	1.303	2.037	2.032	6.338
				PFAC	4.154	4.121	3.227	4.560	4.158	4.638
60	20.0	90.0	9.2	Mean	1.222	.399	.430	-.212	.617	-.024
				Max	2.576	.816	.594	-.080	1.313	.144

DATA FILE: SCT

RUN #	WIND	TILT	VELOCITY	COMP:	FX	FY	FZ	MX	MY	MZ
				Min	.449	.148	.258	-.437	.209	-.234
				Rms	.315	.096	.045	.053	.164	.041
				GFAC	2.108	2.043	1.380	2.060	2.129	9.613
				PFAC	4.295	4.341	3.614	4.215	4.249	5.153
61	20.0	90.0	9.1	Mean	1.485	.471	.394	-.253	.745	-.034
				Max	3.004	.910	.565	-.064	1.497	.147
				Min	.477	.139	.213	-.502	.201	-.213
				Rms	.373	.112	.047	.063	.195	.046
				GFAC	2.023	1.930	1.434	1.986	2.010	6.317
				PFAC	4.074	3.901	3.611	3.928	3.854	3.924
62	45.0	90.0	9.2	Mean	1.012	1.061	.298	-.576	.492	-.158
				Max	1.977	2.060	.435	-.190	.962	.013
				Min	.369	.361	.147	-1.116	.182	-.397
				Rms	.226	.248	.042	.133	.109	.059
				GFAC	1.954	1.942	1.461	1.937	1.954	2.517
				PFAC	4.270	4.036	3.266	4.063	4.310	4.038
63	45.0	90.0	9.1	Mean	.815	.869	.322	-.467	.395	-.110
				Max	1.685	1.820	.449	-.123	.827	.023
				Min	.198	.215	.144	-.979	.109	-.321
				Rms	.219	.237	.041	.129	.106	.051
				GFAC	2.069	2.095	1.395	2.094	2.095	2.924
				PFAC	3.981	4.016	3.081	3.974	4.058	4.149
64	45.0	90.0	9.0	Mean	.806	.791	.453	-.429	.386	-.107
				Max	1.659	1.698	.589	-.119	.796	.025
				Min	.343	.235	.275	-.922	.158	-.337

DATA FILE: SCT

RUN #	WIND	TILT	VELOCITY	COMP:	FX	FY	FZ	MX	MY	MZ
				Rms	.197	.219	.044	.119	.096	.049
				GFAC	2.057	2.146	1.299	2.146	2.060	3.148
				PFAC	4.334	4.137	3.097	4.133	4.256	4.674
65	45.0	90.0	9.1	Mean	.976	.914	.397	-.498	.462	-.130
				Max	1.770	1.827	.551	-.231	.850	.016
				Min	.508	.386	.266	-.952	.251	-.354
				Rms	.176	.199	.040	.107	.084	.051
				GFAC	1.814	2.000	1.386	1.911	1.838	2.736
				PFAC	4.523	4.590	3.800	4.248	4.608	4.435
66	.0	90.0	9.2	Mean	.798	.064	.560	-.040	.410	.035
				Max	1.802	.143	.699	-.003	.927	.189
				Min	.120	-.007	.407	-.082	.061	-.083
				Rms	.249	.020	.045	.011	.132	.035
				GFAC	2.258	2.258	1.246	2.063	2.263	5.407
				PFAC	4.037	3.964	3.098	3.949	3.921	4.452
67	.0	90.0	9.1	Mean	.666	.073	.529	-.039	.344	.020
				Max	1.684	.140	.691	-.009	.896	.147
				Min	.083	.022	.387	-.079	.056	-.082
				Rms	.220	.016	.044	.009	.119	.030
				GFAC	2.528	1.903	1.306	2.006	2.608	7.300
				PFAC	4.635	4.186	3.666	4.487	4.640	4.267
68	.0	90.0	9.1	Mean	.761	.073	.512	-.044	.397	.019
				Max	1.861	.164	.658	-.004	1.002	.163
				Min	.194	-.007	.333	-.100	.101	-.107
				Rms	.254	.024	.047	.013	.138	.034
				GFAC	2.446	2.252	1.287	2.304	2.526	8.475
				PFAC	4.327	3.792	3.100	4.405	4.378	4.237

Data File: SCT

RUN #	WIND	TILT	VELOCITY	COMP:	FX	FY	FZ	MX	MY	MZ
69	.0	90.0	9.1	Mean	1.045	.071	.471	-.048	.542	.029
				Max	2.677	.189	.635	-.003	1.361	.243
				Min	.145	-.043	.312	-.118	.083	-.130
				Rms	.339	.030	.049	.016	.180	.048
				GFAC	2.563	2.665	1.347	2.446	2.513	8.279
				PFAC	4.815	3.890	3.367	4.320	4.561	4.489
70	.0	-30.0	9.3	Mean	.663	.024	1.135	-.008	.370	.024
				Max	1.214	.155	1.643	.067	.667	.068
				Min	.203	-.090	.623	-.099	.125	-.019
				Rms	.148	.030	.148	.020	.081	.012
				GFAC	1.831	6.499	1.448	11.692	1.799	2.797
				PFAC	3.731	4.375	3.435	4.548	3.669	3.769
71	.0	-30.0	9.1	Mean	.280	.034	.683	-.010	.158	.018
				Max	.709	.178	1.171	.083	.394	.064
				Min	-.013	-.096	.328	-.142	.005	-.026
				Rms	.097	.028	.114	.022	.054	.011
				GFAC	2.528	5.316	1.713	14.092	2.500	3.610
				PFAC	4.435	5.250	4.275	5.944	4.362	4.180
72	.0	-30.0	9.2	Mean	.326	.029	.749	-.008	.182	.014
				Max	.870	.157	1.262	.106	.481	.063
				Min	.021	-.117	.388	-.104	.023	-.032
				Rms	.099	.031	.116	.025	.056	.012
				GFAC	2.668	5.313	1.686	12.831	2.648	4.645
				PFAC	5.516	4.155	4.423	3.818	5.383	4.320
73	.0	-30.0	9.2	Mean	.543	.014	.964	-.008	.317	.021
				Max	1.214	.112	1.567	.073	.687	.066

DATA FILE: SCT

RUN #	WIND	TILT	VELOCITY	COMP:	FX	FY	FZ	MX	MY	MZ
				Min	.172	-.101	.546	-.106	.113	-.021
				Rms	.129	.029	.131	.022	.072	.011
				GFAC	2.236	8.025	1.626	12.566	2.170	3.118
				PFAC	5.200	3.430	4.601	4.524	5.172	4.015
74	.0	30.0	9.2	Mean	.367	.100	-.099	-.042	.120	.010
				Max	.604	.185	.192	.020	.256	.062
				Min	.205	.035	-.461	-.110	.044	-.026
				Rms	.058	.020	.091	.016	.026	.010
				GFAC	1.645	1.839	4.530	2.638	2.128	5.976
				PFAC	4.066	4.220	3.972	4.418	5.299	5.231
75	.0	30.0	9.2	Mean	.462	.111	-.231	-.047	.157	.009
				Max	1.050	.249	.214	.047	.411	.080
				Min	.154	.028	-1.153	-.165	.035	-.048
				Rms	.121	.030	.187	.028	.047	.017
				GFAC	2.272	2.240	4.991	3.510	2.619	8.882
				PFAC	4.844	4.528	4.921	4.283	5.395	4.063
76	.0	30.0	9.2	Mean	.499	.114	-.277	-.047	.186	.010
				Max	1.027	.255	.183	.057	.436	.089
				Min	.174	.016	-1.192	-.188	.058	-.071
				Rms	.128	.030	.199	.028	.054	.018
				GFAC	2.060	2.236	4.300	3.981	2.341	9.001
				PFAC	4.140	4.631	4.592	4.972	4.666	4.319
77	.0	30.0	9.2	Mean	.596	.117	-.512	-.044	.185	.015
				Max	.927	.244	-.158	.031	.295	.070
				Min	.370	.014	-.935	-.133	.086	-.027
				Rms	.074	.029	.117	.021	.032	.013

DATA FILE: SCT

RUN #	WIND	TILT	VELOCITY	COMP:	FX	FY	FZ	MX	MY	MZ
				GFAC	1.557	2.081	1.827	3.023	1.597	4.646
				PFAC	4.483	4.385	3.621	4.229	3.491	4.193
78	.0	90.0	9.1	Mean	1.100	.481	.479	-.266	.559	-.024
				Max	2.753	1.103	.674	-.042	1.332	.115
				Min	.142	.068	.270	-.614	.081	-.273
				Rms	.400	.163	.051	.093	.205	.054
				GFAC	2.503	2.290	1.409	2.309	2.385	11.263
				PFAC	4.133	3.818	3.855	3.744	3.775	4.655
79	20.0	90.0	9.0	Mean	.921	.413	.503	-.224	.464	-.028
				Max	2.235	.908	.669	-.035	1.129	.108
				Min	.162	.089	.326	-.518	.063	-.208
				Rms	.286	.116	.052	.066	.148	.043
				GFAC	2.426	2.199	1.331	2.311	2.430	7.491
				PFAC	4.600	4.283	3.185	4.416	4.495	4.236
80	20.0	90.0	9.2	Mean	.659	.301	.466	-.164	.338	-.014
				Max	1.711	.745	.597	-.025	.897	.096
				Min	.040	.054	.320	-.418	.014	-.169
				Rms	.219	.088	.042	.052	.115	.031
				GFAC	2.595	2.479	1.282	2.543	2.654	12.181
				PFAC	4.806	5.026	3.114	4.868	4.864	5.036
81	20.0	90.0	9.2	Mean	.697	.336	.401	-.182	.358	-.016
				Max	1.998	.851	.535	-.028	1.097	.110
				Min	.014	.061	.219	-.516	.012	-.160
				Rms	.249	.102	.046	.060	.131	.031
				GFAC	2.866	2.536	1.333	2.830	3.064	10.017
				PFAC	5.216	5.070	2.932	5.590	5.650	4.612

DATA FILE: SCT

RUN #	WIND	TILT	VELOCITY	COMP:	FX	FY	FZ	MX	MY	MZ
82	45.0	90.0	9.1	Mean	.458	.509	.408	-.278	.227	-.046
				Max	1.137	1.304	.572	-.070	.594	.049
				Min	.105	.134	.183	-.722	.063	-.212
				Rms	.154	.175	.046	.099	.079	.035
				GFAC	2.484	2.561	1.402	2.598	2.620	4.620
				PFAC	4.404	4.535	3.558	4.488	4.651	4.791
83	45.0	90.0	9.2	Mean	.425	.446	.435	-.247	.213	-.029
				Max	1.108	1.221	.607	-.044	.536	.088
				Min	.081	.086	.277	-.634	.047	-.193
				Rms	.140	.160	.046	.092	.072	.033
				GFAC	2.610	2.739	1.395	2.608	2.515	6.627
				PFAC	4.873	4.830	3.762	.326	4.468	4.927
84	45.0	90.0	9.1	Mean	.591	.514	.399	-.305	.297	-.032
				Max	1.189	1.216	.551	-.054	.615	.108
				Min	.140	.016	.245	-.711	.095	-.229
				Rms	.153	.181	.045	.098	.074	.046
				GFAC	2.013	2.368	1.380	2.330	2.070	7.187
				PFAC	3.906	3.871	3.354	4.138	4.282	4.253
85	45.0	90.0	9.2	Mean	.720	.697	.315	-.406	.361	-.086
				Max	1.587	1.890	.484	-.081	.778	.067
				Min	.197	.088	.159	-.946	.096	-.408
				Rms	.195	.232	.044	.125	.095	.056
				GFAC	2.204	2.713	1.537	2.332	2.151	4.747
				PFAC	4.444	5.151	3.863	4.335	4.367	5.742
86	.0	-30.0	9.3	Mean	.551	.001	1.120	-.021	.429	.023
				Max	1.174	.142	1.752	.119	.817	.085

DATA FILE: SCT

RUN #	WIND	TILT	VELOCITY	COMP:	FX	FY	FZ	MX	MY	MZ
				Min	.043	-.138	.657	-.173	.112	-.040
				Rms	.143	.039	.147	.033	.089	.016
				GFAC	2.133	120.342	1.564	8.442	1.905	3.727
				PFAC	4.350	3.649	4.293	4.602	4.387	3.815
87	.0	-30.0	9.3	Mean	.203	.031	.640	-.026	.155	.023
				Max	.610	.147	1.039	.042	.409	.085
				Min	-.065	-.065	.349	-.156	-.015	-.008
				Rms	.088	.021	.106	.021	.059	.011
				GFAC	3.014	4.741	1.623	5.949	2.636	3.655
				PFAC	4.650	5.464	3.749	6.157	4.272	5.622
88	.0	-30.0	9.3	Mean	.193	.041	.659	-.028	.144	.020
				Max	.672	.120	1.060	.046	.431	.070
				Min	-.109	-.042	.346	-.113	-.020	-.015
				Rms	.083	.020	.105	.019	.056	.010
				GFAC	3.482	2.939	1.608	4.078	2.991	3.494
				PFAC	5.745	3.990	3.810	4.459	5.131	5.160
89	.0	-30.0	9.2	Mean	.448	.018	.975	-.021	.324	.028
				Max	1.221	.136	1.563	.055	.733	.071
				Min	.005	-.080	.570	-.105	.100	-.017
				Rms	.129	.028	.122	.021	.080	.013
				GFAC	2.724	7.430	1.603	4.954	2.266	2.563
				PFAC	5.968	4.157	4.809	3.935	5.124	3.446
90	.0	-30.0	9.2	Mean	.727	.000	1.363	-.015	.453	.034
				Max	1.098	.146	1.851	.103	.677	.078
				Min	.369	-.167	.928	-.120	.256	-.018
				Rms	.108	.032	.133	.025	.062	.012
				GFAC	1.509	510.520	1.358	8.071	1.493	2.272
				PFAC	3.421	4.596	3.663	4.203	3.587	3.783

DATA FILE: SCT

RUN #	WIND	TILT	VELOCITY	COMP:	FX	FY	FZ	MX	MY	MZ
91	.0	-30.0	9.2	Mean	.136	.044	.600	-.022	.098	.019
				Max	.531	.137	.960	.064	.331	.056
				Min	-.217	-.035	.301	-.105	-.093	-.023
				Rms	.074	.018	.090	.015	.049	.009
				GFAC	3.916	3.139	1.600	4.837	3.369	3.021
				PFAC	5.336	5.261	4.014	5.397	4.778	4.364
92	.0	-30.0	9.1	Mean	.102	.061	.584	-.023	.064	.017
				Max	.496	.112	.918	.008	.266	.041
				Min	-.310	.012	.270	-.063	-.136	-.008
				Rms	.078	.014	.077	.009	.041	.007
				GFAC	4.869	1.818	1.574	2.759	4.192	2.408
				PFAC	5.035	3.724	4.362	4.691	4.891	3.504
93	.0	-30.0	9.3	Mean	.889	-.009	1.554	-.028	.648	.037
				Max	1.264	.094	2.037	.076	.898	.086
				Min	.560	-.106	1.168	-.123	.442	-.008
				Rms	.101	.028	.129	.027	.069	.012
				GFAC	1.422	12.237	1.311	4.404	1.386	2.308
				PFAC	3.717	3.514	3.742	3.492	3.610	3.944
94	.0	-30.0	9.2	Mean	.631	.024	1.216	-.040	.405	.036
				Max	1.080	.170	1.669	.121	.668	.096
				Min	.034	-.187	.645	-.157	.152	-.024
				Rms	.114	.046	.135	.039	.067	.016
				GFAC	1.712	6.932	1.373	3.888	1.649	2.709
				PFAC	3.941	3.176	3.358	3.001	3.948	3.791
95	.0	-30.0	9.3	Mean	.257	.032	.732	-.026	.191	.020
				Max	.719	.143	1.182	.080	.482	.071

DATA FILE: SCT

RUN #	WIND	TILT	VELOCITY	COMP:	FX	FY	FZ	MX	MY	MZ
				Min	-.008	-.121	.402	-.145	.008	-.023
				Rms	.091	.027	.112	.026	.063	.012
				GFAC	2.803	4.463	1.614	5.603	2.516	3.622
				PFAC	5.059	4.077	4.025	4.581	4.596	4.319
96	.0	-30.0	9.3	Mean	.407	.016	.899	-.021	.302	.021
				Max	.949	.136	1.412	.135	.682	.086
				Min	.061	-.119	.457	-.164	.078	-.047
				Rms	.117	.033	.144	.035	.083	.015
				GFAC	2.331	8.271	1.571	7.886	2.257	4.033
				PFAC	4.619	3.575	3.572	4.068	4.589	4.201
97	.0	-30.0	9.3	Mean	.831	-.005	1.461	-.032	.627	.034
				Max	1.451	.125	2.062	.101	1.042	.101
				Min	.339	-.144	.921	-.139	.307	-.039
				Rms	.167	.033	.196	.029	.109	.016
				GFAC	1.747	30.433	1.412	4.296	1.663	3.005
				PFAC	3.716	4.196	3.061	3.719	3.802	4.260
98	.0	-30.0	9.2	Mean	.611	-.022	1.258	.015	.485	.024
				Max	1.272	.132	1.919	.159	.934	.102
				Min	.088	-.163	.784	-.133	.148	-.034
				Rms	.160	.039	.161	.036	.100	.019
				GFAC	2.082	7.512	1.525	10.913	1.927	4.313
				PFAC	4.133	3.637	4.093	4.053	4.475	4.137
99	.0	-30.0	9.2	Mean	.528	.007	1.085	-.024	.401	.028
				Max	1.413	.156	1.772	.138	.885	.143
				Min	.031	-.202	.549	-.190	.121	-.032
				Rms	.146	.041	.154	.040	.097	.019
				GFAC	2.674	23.256	1.634	7.840	2.205	5.067
				PFAC	6.071	3.612	4.468	4.142	5.006	5.888

DATA FILE: SCT

RUN #	WIND	TILT	VELOCITY	COMP:	FX	FY	FZ	MX	MY	MZ
100	.0	-30.0	9.2	Mean	.588	.001	1.172	-.021	.437	.021
				Max	1.235	.168	1.821	.152	.870	.104
				Min	.105	-.206	.675	-.174	.160	-.049
				Rms	.152	.049	.159	.046	.095	.022
				GFAC	2.101	137.856	1.554	8.189	1.991	5.025
				PFAC	4.262	3.408	4.093	3.309	4.565	3.832
101	.0	-30.0	9.2	Mean	.630	-.057	1.256	.034	.508	.013
				Max	1.279	.137	1.922	.178	.968	.079
				Min	.058	-.237	.762	-.123	.207	-.049
				Rms	.157	.047	.173	.043	.102	.018
				GFAC	2.031	4.173	1.530	5.207	1.903	6.302
				PFAC	4.137	3.841	3.857	3.376	4.493	3.668
102	.0	30.0	9.2	Mean	.464	.112	-.349	-.044	.128	.010
				Max	.901	.275	.102	.115	.337	.119
				Min	.204	-.024	-1.150	-.202	.020	-.079
				Rms	.100	.041	.170	.039	.045	.022
				GFAC	1.941	2.448	3.295	4.554	2.640	11.659
				PFAC	4.363	3.937	4.720	4.029	4.671	4.866
103	.0	30.0	9.2	Mean	.395	.118	-.149	-.066	.104	-.003
				Max	.797	.296	.292	.054	.266	.073
				Min	.129	-.015	-.778	-.218	-.005	-.081
				Rms	.095	.038	.157	.036	.041	.020
				GFAC	2.015	2.501	5.222	3.286	2.556	27.122
				PFAC	4.209	4.615	4.007	4.219	3.950	3.918
104	.0	30.0	9.3	Mean	.305	.104	-.063	-.067	.081	-.004
				Max	.584	.238	.234	.015	.232	.039

DATA FILE: SCT

RUN #	WIND	TILT	VELOCITY	COMP:	FX	FY	FZ	MX	MY	MZ
				Min	.111	.001	-.479	-.178	.001	-.063
				Rms	.064	.029	.104	.025	.026	.013
				GFAC	1.918	2.300	7.549	2.673	2.867	15.120
				PFAC	4.395	4.716	3.975	4.405	5.754	4.660
105	.0	30.0	9.2	Mean	.403	.104	-.283	-.031	.109	.005
				Max	.756	.224	.127	.065	.298	.063
				Min	.177	-.020	-.924	-.147	.019	-.048
				Rms	.083	.026	.149	.023	.035	.014
				GFAC	1.874	2.158	3.270	4.767	2.749	11.651
				PFAC	4.250	4.552	4.312	5.124	5.372	4.130
106	.0	90.0	9.2	Mean	1.000	.045	.459	-.034	.530	.060
				Max	2.770	.175	.670	.008	1.451	.295
				Min	.184	-.048	.288	-.101	.084	-.098
				Rms	.348	.027	.051	.013	.184	.050
				GFAC	2.769	3.876	1.459	2.991	2.737	4.920
				PFAC	5.086	4.721	4.141	5.121	4.996	4.729
107	.0	90.0	9.2	Mean	.884	.042	.498	-.028	.462	.055
				Max	2.393	.115	.653	.010	1.230	.296
				Min	.108	-.043	.310	-.071	.068	-.084
				Rms	.307	.022	.048	.011	.160	.046
				GFAC	2.707	2.725	1.310	2.498	2.660	5.396
				PFAC	4.912	3.342	3.246	3.951	4.787	5.222
108	.0	90.0	9.0	Mean	1.035	.052	.475	-.034	.527	.031
				Max	2.359	.144	.652	-.001	1.305	.199
				Min	.238	-.021	.311	-.086	.127	-.149
				Rms	.299	.022	.048	.011	.156	.044

DATA FILE: SCT

RUN #	WIND	TILT	VELOCITY	COMP:	FX	FY	FZ	MX	MY	MZ
				GFAC	2.280	2.755	1.373	2.496	2.476	6.495
				PFAC	4.431	4.137	3.668	4.728	4.989	3.820
109	.0	90.0	9.2	Mean	1.002	.042	.466	-.034	.515	.030
				Max	1.960	.161	.645	.004	1.048	.232
				Min	.170	-.055	.273	-.106	.103	-.170
				Rms	.288	.027	.050	.013	.153	.047
				GFAC	1.957	3.796	1.384	3.117	2.036	7.791
				PFAC	3.329	4.416	3.555	5.505	3.491	4.275
110	20.0	90.0	9.1	Mean	1.022	.464	.385	-.246	.511	-.044
				Max	2.416	.955	.544	-.081	1.218	.130
				Min	.256	.147	.226	-.534	.130	-.210
				Rms	.301	.127	.048	.071	.152	.045
				GFAC	2.364	2.059	1.412	2.173	2.385	4.773
				PFAC	4.624	3.869	3.281	4.083	4.643	2.704
111	20.0	90.0	9.0	Mean	1.087	.477	.473	-.255	.547	-.052
				Max	2.337	.964	.623	-.077	1.182	.091
				Min	.270	.149	.308	-.528	.155	-.225
				Rms	.304	.124	.047	.071	.155	.048
				GFAC	2.151	2.021	1.315	2.068	2.162	4.350
				PFAC	4.114	3.912	3.148	3.845	4.111	3.583
112	20.0	90.0	9.1	Mean	1.209	.521	.444	-.280	.601	-.066
				Max	2.364	1.001	.639	-.084	1.184	.078
				Min	.319	.146	.263	-.566	.154	-.284
				Rms	.302	.122	.049	.070	.154	.047
				GFAC	1.954	1.922	1.439	2.020	1.972	4.298
				PFAC	3.820	3.924	3.989	4.063	3.786	4.640

DATA FILE: SCT

RUN #	WIND	TILT	VELOCITY	COMP:	FX	FY	FZ	MX	MY	MZ
113	20.0	90.0	9.0	Mean	1.155	.515	.452	-.274	.577	-.066
				Max	2.384	1.056	.621	-.081	1.188	.075
				Min	.297	.141	.279	-.566	.149	-.258
				Rms	.312	.130	.050	.073	.158	.048
				GFAC	2.065	2.051	1.374	2.069	2.059	3.925
				PFAC	3.937	4.157	3.378	3.996	3.873	3.991
114	20.0	90.0	9.1	Mean	1.162	.527	.406	-.278	.579	-.069
				Max	2.516	1.093	.572	-.085	1.278	.084
				Min	.316	.126	.220	-.618	.175	-.323
				Rms	.313	.132	.051	.074	.158	.049
				GFAC	2.165	2.076	1.409	2.227	2.209	4.670
				PFAC	4.327	4.298	3.282	4.632	4.438	5.134
115	45.0	90.0	9.1	Mean	1.016	.930	.327	-.511	.476	-.172
				Max	2.051	2.013	.498	-.047	.975	.022
				Min	.213	.123	.154	-1.091	.097	-.489
				Rms	.261	.278	.047	.146	.124	.071
				GFAC	2.020	2.165	1.524	2.135	2.048	2.835
				PFAC	3.970	3.892	3.634	3.962	4.027	4.448
116	45.0	90.0	9.1	Mean	.910	.778	.366	-.445	.435	-.145
				Max	1.632	1.609	.565	-.095	.784	.042
				Min	.281	.107	.188	-.871	.141	-.362
				Rms	.211	.222	.048	.118	.099	.058
				GFAC	1.793	2.068	1.545	1.959	1.801	2.504
				PFAC	3.426	3.735	4.172	3.614	3.533	3.733
117	45.0	90.0	9.1	Mean	.849	.734	.340	-.423	.412	-.131
				Max	1.828	1.751	.498	-.088	.843	.024

DATA FILE: SCT

RUN #	WIND	TILT	VELOCITY	COMP:	FX	FY	FZ	MX	MY	MZ
				Min	.225	.090	.159	-.920	.140	-.365
				Rms	.220	.229	.045	.122	.103	.059
				GFAC	2.154	2.387	1.465	2.174	2.048	2.794
				PFAC	4.458	4.440	3.493	4.060	4.209	3.983
118	45.0	90.0	9.3	Mean	.892	.812	.314	-.454	.426	-.148
				Max	1.966	1.896	.460	-.070	.939	.027
				Min	.188	.074	.108	-1.011	.133	-.451
				Rms	.257	.271	.046	.145	.122	.066
				GFAC	2.204	2.335	1.467	2.230	2.206	3.035
				PFAC	4.182	4.005	3.202	3.854	4.219	4.585
119	.0	90.0	9.2	Mean	.497	.079	.615	-.027	.245	.028
				Max	2.041	.141	.773	.009	1.107	.191
				Min	-.006	.003	.395	-.061	-.036	-.103
				Rms	.228	.018	.045	.009	.125	.033
				GFAC	4.107	1.794	1.258	2.280	4.516	6.735
				PFAC	6.762	3.402	3.521	4.022	6.898	4.985
120	.0	90.0	9.1	Mean	.369	.060	.557	-.029	.192	.026
				Max	1.447	.115	.710	-.006	.796	.171
				Min	-.117	.000	.392	-.059	-.053	-.081
				Rms	.182	.016	.044	.008	.100	.027
				GFAC	3.925	1.926	1.275	2.020	4.139	6.543
				PFAC	5.922	3.489	3.500	3.923	6.052	5.366
121	.0	90.0	9.2	Mean	.427	.057	.512	-.030	.229	.022
				Max	1.462	.156	.662	.006	.777	.154
				Min	-.126	-.033	.298	-.080	-.057	-.089
				Rms	.214	.021	.048	.010	.116	.031

DATA FILE: SCT

RUN #	WIND	TILT	VELOCITY	COMP:	FX	FY	FZ	MX	MY	MZ
				GFAC	3.421	2.730	1.293	2.674	3.394	6.983
				PFAC	4.834	4.734	3.130	4.846	4.707	4.267
122	.0	90.0	9.3	Mean	.550	.050	.505	-.030	.299	.029
				Max	1.896	.134	.674	.014	.960	.238
				Min	-.131	-.038	.338	-.077	-.061	-.095
				Rms	.266	.024	.046	.011	.144	.037
				GFAC	3.447	2.693	1.333	2.552	3.209	8.306
				PFAC	5.064	3.574	3.631	4.117	4.574	5.575
123	.0	80.0	9.1	Mean	.527	.063	.508	-.034	.285	.025
				Max	2.023	.136	.700	.015	1.104	.138
				Min	-.081	-.028	.201	-.089	-.038	-.130
				Rms	.244	.022	.061	.013	.135	.033
				GFAC	3.841	2.168	1.378	2.618	3.874	5.609
				PFAC	6.127	3.378	3.119	4.183	6.057	3.494
124	.0	80.0	9.2	Mean	.421	.058	.562	-.030	.223	.029
				Max	1.519	.112	.732	.007	.786	.174
				Min	-.100	-.007	.369	-.080	-.065	-.088
				Rms	.206	.017	.053	.010	.114	.032
				GFAC	3.608	1.938	1.302	2.664	3.523	6.135
				PFAC	5.342	3.227	3.201	5.007	4.920	4.572
125	.0	80.0	9.1	Mean	.377	.060	.517	-.028	.199	.028
				Max	1.266	.108	.685	.003	.729	.139
				Min	-.056	.002	.295	-.077	-.052	-.082
				Rms	.181	.015	.055	.009	.100	.027
				GFAC	3.357	1.799	1.326	2.703	3.664	5.037
				PFAC	4.903	3.176	3.074	5.371	5.307	4.109

DATA FILE: SCT

RUN #	WIND	TILT	VELOCITY	COMP:	FX	FY	FZ	MX	MY	MZ
126	.0	80.0	9.1	Mean	.444	.045	.462	-.027	.233	.020
				Max	1.444	.125	.650	.024	.785	.178
				Min	-.108	-.032	.237	-.083	-.062	-.106
				Rms	.216	.020	.060	.012	.119	.031
				GFAC	3.250	2.763	1.408	3.034	3.362	8.759
				PFAC	4.620	4.052	3.123	4.588	4.621	5.161

Data File: SCT1

For Single Square Model

In the file labelled "SCT" the coefficient denoted by "MX" and "MY" are the base moment coefficients. However, in the files labelled "SCT1" and "SCT2" the coefficient of "MX" and "MY" are the hinge moment coefficients about the y-axis at the motor drive level.

Comments: 1. Because of system lift force, $F_{z\ actual} = F_z - 0.160$

(e.g. $F_z = 0.353$ (Run # 254), $F_{z\ actual} = 0.353 - 0.160 = 0.193$)

2. MY is the hinge moment coefficient, C_{MHy} in data file: SCT1

DATA FILE: SCT1

RUN #	WIND	TILT	VELOCITY	COMP:	FX	FY	FZ	MX	MY	MZ
254	.0	90.0	9.3	Mean	1.988	.124	.353	.023	.017	.064
				Max	4.318	.338	.565	.048	.388	.352
				Min	.697	-.003	.120	.000	-.178	-.221
				Rms	.504	.036	.072	.006	.051	.075
				GFAC	2.172	2.727	1.598	2.089	22.448	5.489
				PFAC	4.626	5.891	2.926	4.240	7.303	3.824
255	.0	75.0	9.5	Mean	1.895	.146	-.101	.024	-.019	.053
				Max	3.986	.346	.344	.108	.204	.331
				Min	.640	.015	-.642	-.033	-.201	.202
				Rms	.489	.039	.143	.017	.046	.068
				GFAC	2.103	2.369	6.368	4.591	10.756	6.198
				PFAC	4.274	5.145	3.793	5.091	3.928	4.099
256	.0	60.0	9.6	Mean	1.681	.165	-.499	.025	-.066	.039
				Max	3.481	.345	.149	.130	.148	.272
				Min	.528	.045	-1.360	-.073	-.286	-.143
				Rms	.455	.041	.241	.027	.047	.055
				GFAC	2.071	2.094	2.724	5.169	4.299	6.990
				PFAC	3.956	4.446	3.573	3.874	4.676	4.235
257	.0	45.0	9.4	Mean	1.306	.170	-.829	.026	-.107	.025
				Max	2.798	.383	.008	.169	.060	.181
				Min	.423	.058	-2.086	-.104	-.300	-.123
				Rms	.369	.043	.347	.035	.044	.040
				GFAC	2.142	2.252	2.516	6.506	2.792	7.259
				PFAC	4.048	4.943	3.623	4.081	4.398	3.918
258	.0	30.0	9.6	Mean	.998	.181	-1.073	.025	-.195	.011
				Max	1.971	.403	-.097	.202	-.050	.152

DATA FILE: SCT1

RUN #	WIND	TILT	VELOCITY	COMP:	FX	FY	FZ	MX	MY	MZ
				Min	.326	.043	-2.507	-.142	-.431	-.119
				Rms	.296	.053	.449	.045	.059	.033
				GFAC	1.975	2.223	2.337	8.219	2.212	14.417
				PFAC	3.290	4.204	3.197	3.900	3.972	4.317
259	.0	20.0	9.4	Mean	.613	.157	-.871	.020	-.226	.002
				Max	1.343	.428	.384	.266	-.013	.114
				Min	.083	-.060	-2.451	-.214	-.590	-.090
				Rms	.206	.062	.463	.062	.083	.030
				GFAC	2.190	2.731	2.815	13.612	2.610	53.299
				PFAC	3.539	4.355	3.411	3.968	4.371	3.786
260	.0	10.0	9.4	Mean	.220	.111	-.239	.014	-.134	.003
				Max	.828	.328	.565	.221	.054	.041
				Min	-.139	-.159	-1.635	-.195	-.546	-.050
				Rms	.105	.051	.343	.045	.087	.013
				GFAC	3.763	2.952	6.834	15.277	4.080	13.281
				PFAC	5.810	4.256	4.071	4.584	4.753	2.941
261	.0	.0	9.5	Mean	.111	.086	.177	.010	-.027	.003
				Max	.634	.276	.873	.134	.178	.033
				Min	-.219	-.070	-.841	-.121	-.331	-.033
				Rms	.086	.043	.236	.027	.072	.009
				GFAC	5.712	3.194	4.946	13.119	12.394	10.901
				PFAC	6.101	4.419	2.955	4.586	4.239	3.370
262	.0	-10.0	9.1	Mean	.146	.072	.710	.013	.122	.008
				Max	.798	.278	1.897	.153	.455	.044
				Min	-.371	-.124	-.134	-.152	-.205	-.026
				Rms	.115	.043	.222	.034	.077	.009

DATA FILE: SCT1

RUN #	WIND	TILT	VELOCITY	COMP:	FX	FY	FZ	MX	MY	MZ
				GFAC	5.450	3.865	2.672	11.531	3.725	5.755
				PFAC	5.665	4.743	5.337	4.158	4.342	4.097
263	.0	-20.0	9.4	Mean	.304	.081	1.074	.015	.201	.012
				Max	.956	.358	2.138	.235	.551	.107
				Min	-.418	-.117	.293	-.231	-.072	-.042
				Rms	.141	.045	.240	.049	.080	.014
				GFAC	3.147	4.414	1.991	15.268	2.744	9.012
				PFAC	4.627	6.211	4.425	4.496	4.356	6.989
264	.0	-30.0	9.3	Mean	.634	.091	1.481	.015	.261	.022
				Max	1.577	.362	2.659	.263	.663	.145
				Min	-.178	-.174	.619	-.218	-.050	-.102
				Rms	.205	.049	.294	.059	.092	.027
				GFAC	2.487	3.988	1.795	17.487	2.538	6.693
				PFAC	4.602	5.509	4.011	4.201	4.344	4.495
265	.0	-45.0	9.4	Mean	1.212	.099	1.523	.018	.163	.037
				Max	2.325	.343	2.498	.223	.486	.181
				Min	.388	-.133	.816	-.133	-.037	-.124
				Rms	.305	.059	.261	.046	.066	.040
				GFAC	1.919	3.459	1.640	12.563	2.984	4.898
				PFAC	3.649	4.122	3.740	4.486	4.866	3.583
266	.0	-60.0	9.3	Mean	1.513	.114	1.276	.022	.116	.031
				Max	2.867	.402	2.030	.201	.428	.228
				Min	.466	-.182	.629	-.099	-.088	-.203
				Rms	.385	.062	.213	.039	.061	.057
				GFAC	1.895	3.524	1.591	9.029	3.686	7.343
				PFAC	3.514	4.657	3.532	4.651	5.091	3.456

DATA FILE: SCT1

RUN #	WIND	TILT	VELOCITY	COMP:	FX	FY	FZ	MX	MY	MZ
267	.0	-75.0	9.4	Mean	1.817	.133	.972	.024	.059	.037
				Max	3.744	.405	1.594	.156	.390	.378
				Min	.520	-.131	.593	-.098	-.167	-.270
				Rms	.478	.067	.155	.030	.058	.080
				GFAC	2.061	3.045	1.639	6.628	6.637	10.197
				PFAC	4.030	4.062	4.001	4.402	5.697	4.263
268	.0	-90.0	9.4	Mean	1.857	.144	.447	.016	.027	.036
				Max	3.852	.451	.697	.062	.274	.361
				Min	.525	-.096	.240	-.012	-.191	-.312
				Rms	.501	.069	.070	.008	.049	.088
				GFAC	2.074	3.136	1.561	3.850	10.036	9.937
				PFAC	3.978	4.438	3.556	5.466	5.030	3.712

Data File: SCT1

For Single Round Model

In the file labelled "SCT" the coefficient denoted by "MX" and "MY" are the base moment coefficients. However, in the files labelled "SCT1" and "SCT2" the coefficient of "MX" and "MY" are the hinge moment coefficients about the y-axis at the motor drive level.

Comments: 1. Because of system lift force, $F_{z\ actual} = F_z - 0.200$

(e.g. $F_z = 0.411$ (Run # 270), $F_{z\ actual} = 0.411 - 0.200 = 0.211$)

2. MY is the hinge moment coefficient, C_{MHy} in data file: SCT1

DATA FILE: SCT1

RUN #	WIND	TILT	VELOCITY	COMP:	FX	FY	FZ	MX	MY	MZ
270	.0	90.0	9.4	Mean	1.938	.192	.411	.021	.016	.039
				Max	4.018	.316	.695	.039	.267	.283
				Min	.442	.100	.141	.009	-.153	-.147
				Rms	.525	.032	.091	.004	.046	.056
				GFAC	2.073	1.640	1.693	1.825	16.280	7.181
				PFAC	3.960	3.891	3.125	4.286	5.442	4.384
271	.0	75.0	9.5	Mean	1.943	.215	-.106	.020	-.039	.030
				Max	4.300	.400	.391	.089	.160	.311
				Min	.749	.106	-.803	-.032	-.196	-.155
				Rms	.541	.039	.178	.013	.044	.052
				GFAC	2.214	1.864	7.567	4.362	5.042	10.366
				PFAC	4.357	4.772	3.915	5.116	3.570	5.429
272	.0	60.0	9.4	Mean	1.790	.212	-.417	.017	-.073	.024
				Max	4.168	.404	.259	.141	.144	.296
				Min	.384	.080	-1.485	-.063	-.249	-.148
				Rms	.515	.043	.266	.021	.043	.047
				GFAC	2.328	1.906	3.556	8.233	3.416	12.238
				PFAC	4.613	4.476	4.009	5.879	4.111	5.810
273	.0	45.0	9.5	Mean	1.413	.197	-.803	.016	-.103	.020
				Max	3.025	.342	.096	.121	.034	.133
				Min	.595	.060	-2.083	-.093	-.270	-.097
				Rms	.393	.040	.359	.028	.039	.033
				GFAC	2.140	1.740	2.595	7.588	2.621	6.686
				PFAC	4.099	3.648	3.564	3.796	4.311	3.464
274	.0	30.0	9.6	Mean	1.071	.185	-1.084	.012	-.176	.009
				Max	2.068	.418	-.020	.169	-.039	.120

DATA FILE: SCT1

RUN #	WIND	TILT	VELOCITY	COMP:	FX	FY	FZ	MX	MY	MZ
				Min	.363	.039	-2.634	-.142	-.365	-.104
				Rms	.305	.047	.461	.039	.050	.027
				GFAC	1.932	2.262	2.428	14.005	2.069	13.035
				PFAC	3.267	4.951	3.359	4.022	3.795	4.118
275	.0	20.0	9.7	Mean	.644	.156	-.824	.016	-.207	.003
				Max	1.475	.417	.329	.212	-.030	.091
				Min	.140	-.012	-2.558	-.180	-.489	-.098
				Rms	.217	.045	.479	.045	.073	.021
				GFAC	2.289	2.674	3.104	13.391	2.368	28.139
				PFAC	3.834	5.828	3.619	4.314	3.862	4.230
276	.0	10.0	9.6	Mean	.286	.113	-.255	.011	-.143	.005
				Max	.931	.283	.582	.172	.045	.040
				Min	-.016	-.034	-1.717	-.171	-.504	-.041
				Rms	.111	.039	.365	.038	.079	.011
				GFAC	3.253	2.510	6.743	16.238	3.522	7.925
				PFAC	5.783	4.401	4.010	4.206	4.545	3.299
277	.0	.0	9.3	Mean	.138	.093	.393	.014	.017	.012
				Max	.724	.270	1.100	.134	.344	.023
				Min	-.342	-.053	-.600	-.133	-.302	.001
				Rms	.089	.036	.255	.027	.071	.004
				GFAC	5.248	2.889	2.797	9.465	20.169	1.861
				PFAC	6.552	4.936	2.769	4.459	4.625	2.376
278	.0	-10.0	9.6	Mean	.153	.096	.660	.017	.092	.017
				Max	.966	.240	1.484	.121	.419	.041
				Min	-.228	-.068	-.255	-.089	-.165	.000
				Rms	.091	.033	.222	.026	.063	.006

DATA FILE: SCT1

RUN #	WIND	TILT	VELOCITY	COMP:	FX	FY	FZ	MX	MY	MZ
				GFAC	6.326	2.489	2.247	7.172	4.576	2.333
				PFAC	8.940	4.394	3.716	4.057	5.161	3.698
279	.0	-20.0	9.3	Mean	.377	.091	1.204	.011	.199	.027
				Max	1.165	.237	2.374	.152	.533	.105
				Min	-.139	-.051	.275	-.184	-.055	-.024
				Rms	.143	.034	.268	.037	.079	.015
				GFAC	3.088	2.600	1.971	14.200	2.679	3.892
				PFAC	5.508	4.253	4.364	3.777	4.233	5.330
280	.0	-30.0	9.6	Mean	.688	.097	1.500	.006	.207	.037
				Max	1.680	.237	2.555	.132	.532	.152
				Min	-.158	-.007	.694	-.148	-.058	-.030
				Rms	.201	.029	.271	.037	.075	.022
				GFAC	2.442	2.432	1.704	21.524	2.563	4.119
				PFAC	4.934	4.759	3.891	3.455	4.348	5.136
281	.0	-45.0	9.4	Mean	1.236	.142	1.518	.008	.127	.058
				Max	2.561	.272	2.739	.150	.409	.209
				Min	.136	.047	.785	-.117	-.134	-.095
				Rms	.314	.028	.258	.028	.060	.032
				GFAC	2.073	1.918	1.804	19.593	3.227	3.626
				PFAC	4.217	4.629	4.733	5.105	4.712	4.661
282	.0	-60.0	9.5	Mean	1.550	.179	1.291	.008	.087	.052
				Max	3.206	.310	2.044	.085	.361	.240
				Min	.527	.074	.670	-.101	-.097	-.094
				Rms	.397	.033	.215	.021	.054	.041
				GFAC	2.069	1.737	1.583	10.306	4.153	4.648
				PFAC	4.176	3.986	3.503	3.616	5.117	4.640

DATA FILE: SCT1

RUN #	WIND	TILT	VELOCITY	COMP:	FX	FY	FZ	MX	MY	MZ
283	.0	-75.0	9.6	Mean	1.819	.207	.889	.014	.040	.052
				Max	3.742	.372	1.429	.068	.270	.310
				Min	.664	.101	.474	-.041	-.144	-.090
				Rms	.476	.040	.134	.012	.050	.050
				GFAC	2.057	1.796	1.608	4.862	6.798	5.977
				PFAC	4.040	4.157	4.026	4.432	4.643	5.207
270	.0	-90.0	9.5	Mean	1.918	.223	.508	.016	.023	.055
				Max	3.843	.398	.775	.036	.259	.250
				Min	.718	.099	.264	.002	-.126	-.153
				Rms	.499	.043	.085	.005	.046	.055
				GFAC	2.004	1.784	1.524	2.217	11.317	4.539
				PFAC	3.859	4.021	3.123	4.124	5.183	3.554

Data File: SCT1

For Single Edge-porous Model

In the file labelled "SCT" the coefficient denoted by "MX" and "MY" are the base moment coefficients. However, in the files labelled "SCT1" and "SCT2" the coefficient of "MX" and "MY" are the hinge moment coefficients about the y-axis at the motor drive level.

Comments: 1. Because of system lift force, $F_{z\ actual} = F_z - 0.160$

(e.g. $F_z = 0.332$ (Run # 271), $F_{z\ actual} = 0.332 - 0.160 = 0.172$)

2. MY is the hinge moment coefficient, C_{MHy} in data file: SCT1

DATA FILE: SCT1

RUN #	WIND	TILT	VELOCITY	COMP:	FX	FY	FZ	MX	MY	MZ
271	.0	90.0	9.6	Mean	1.716	.160	.332	.020	.008	.031
				Max	3.458	.294	.567	.038	.213	.297
				Min	.650	.060	.097	.006	-.146	-.157
				Rms	.449	.033	.073	.005	.044	.051
				GFAC	2.015	1.842	1.709	1.884	27.142	9.686
				PFAC	3.881	4.134	3.221	3.829	4.640	5.180
272	.0	75.0	9.5	Mean	1.690	.160	-.104	.019	-.023	.037
				Max	4.060	.335	.347	.065	.237	.250
				Min	.556	.065	-.688	-.026	-.182	-.155
				Rms	.459	.036	.142	.013	.042	.051
				GFAC	2.403	2.090	6.597	3.475	7.735	6.746
				PFAC	5.161	4.840	4.118	3.680	3.774	4.167
273	.0	60.0	9.6	Mean	1.494	.174	-.355	.018	-.043	.026
				Max	2.914	.301	.211	.088	.116	.183
				Min	.487	.056	-1.072	-.079	-.199	-.191
				Rms	.413	.036	.203	.019	.037	.046
				GFAC	1.950	1.736	3.021	4.822	4.654	7.079
				PFAC	3.436	3.513	3.531	3.689	4.164	3.398
274	.0	45.0	9.4	Mean	1.098	.176	-.578	.016	-.068	.012
				Max	2.357	.370	.163	.125	.048	.150
				Min	.376	.059	-1.577	-.082	-.218	-.106
				Rms	.313	.040	.284	.027	.035	.036
				GFAC	2.147	2.100	2.727	7.873	3.189	12.482
				PFAC	4.019	4.806	3.516	3.978	4.235	3.863
275	.0	30.0	9.5	Mean	.756	.156	-.627	.013	-.107	.006
				Max	1.608	.352	.279	.156	-.007	.113

DATA FILE: SCT1

RUN #	WIND	TILT	VELOCITY	COMP:	FX	FY	FZ	MX	MY	MZ
				Min	.171	.027	-1.726	-.119	-.326	-.089
				Rms	.229	.043	.328	.030	.036	.025
				GFAC	2.128	2.257	2.751	11.713	3.055	17.553
				PFAC	3.714	4.617	3.345	4.745	6.111	4.344
276	.0	20.0	9.2	Mean	.507	.147	-.524	.013	-.116	.003
				Max	1.042	.395	.232	.160	.007	.087
				Min	.122	.001	-1.751	-.143	-.336	-.094
				Rms	.168	.046	.355	.036	.048	.021
				GFAC	2.054	2.681	3.344	11.982	2.904	31.954
				PFAC	3.176	5.402	3.458	4.095	4.623	3.976
277	.0	10.0	9.5	Mean	.249	.107	-.189	.011	-.078	.006
				Max	.691	.311	.487	.180	.043	.056
				Min	.029	-.010	-1.562	-.130	-.371	-.041
				Rms	.091	.039	.283	.031	.051	.013
				GFAC	2.779	2.905	8.244	15.661	4.788	9.635
				PFAC	4.846	5.204	4.856	5.465	5.789	3.871
278	.0	.0	9.6	Mean	.135	.070	.222	.010	.002	.010
				Max	.457	.242	.980	.100	.201	.035
				Min	-.130	-.114	-.647	-.084	-.181	-.028
				Rms	.065	.037	.204	.021	.047	.007
				GFAC	3.394	3.432	4.414	9.652	100.009	3.594
				PFAC	4.933	4.571	3.717	4.320	4.190	3.452
279	.0	-10.0	9.3	Mean	.173	.079	.587	.011	.081	.009
				Max	.617	.297	1.178	.106	.304	.051
				Min	-.145	-.112	-.075	-.121	-.083	-.016
				Rms	.088	.039	.188	.024	.050	.008

DATA FILE: SCT1

RUN #	WIND	TILT	VELOCITY	COMP:	FX	FY	FZ	MX	MY	MZ
				GFAC	3.578	3.752	2.006	9.950	3.741	5.433
				PFAC	5.061	5.592	3.140	3.887	4.428	5.216
280	.0	-20.0	9.8	Mean	.301	.070	.832	.005	.119	.018
				Max	.834	.270	1.533	.134	.366	.071
				Min	-.031	-.120	.172	-.123	-.034	-.021
				Rms	.114	.039	.183	.029	.052	.011
				GFAC	2.772	3.880	1.843	24.983	3.084	3.935
				PFAC	4.690	5.100	3.821	4.484	4.752	4.776
281	.0	-30.0	9.2	Mean	.599	.083	1.154	.006	.138	.034
				Max	1.452	.288	1.938	.134	.403	.128
				Min	.102	-.084	.501	-.166	-.016	-.034
				Rms	.179	.047	.218	.035	.056	.022
				GFAC	2.423	3.486	1.679	21.605	2.916	3.746
				PFAC	4.762	4.405	3.596	3.667	4.705	4.325
282	.0	-45.0	9.5	Mean	.883	.088	1.119	.008	.100	.045
				Max	1.896	.295	1.899	.117	.359	.163
				Min	.218	-.087	.564	-.106	-.049	-.046
				Rms	.223	.050	.188	.031	.048	.030
				GFAC	2.146	3.350	1.697	15.147	3.582	3.653
				PFAC	4.537	4.106	4.150	3.490	5.448	3.932
283	.0	-60.0	9.4	Mean	1.296	.100	1.070	.008	.087	.047
				Max	2.497	.333	1.686	.123	.380	.224
				Min	.453	-.097	.601	-.089	-.094	-.099
				Rms	.326	.057	.170	.029	.051	.047
				GFAC	1.926	3.340	1.576	14.629	4.360	4.741
				PFAC	3.682	4.106	3.616	3.879	5.692	3.757

DATA FILE: SCT1

RUN #	WIND	TILT	VELOCITY	COMP:	FX	FY	FZ	MX	MY	MZ
284	.0	-75.0	9.4	Mean	1.520	.113	.826	.012	.058	.050
				Max	3.221	.394	1.313	.100	.358	.285
				Min	.567	-.099	.517	-.056	-.083	-.149
				Rms	.391	.063	.121	.023	.049	.064
				GFAC	2.119	3.492	1.589	8.673	6.192	5.713
				PFAC	4.355	4.483	4.029	3.914	6.170	3.673
285	.0	-90.0	9.5	Mean	1.617	.127	.453	.014	.014	.046
				Max	3.037	.371	.674	.043	.223	.298
				Min	.669	-.060	.267	-.015	-.151	-.218
				Rms	.408	.066	.072	.008	.044	.069
				GFAC	1.878	2.929	1.489	3.103	16.114	6.505
				PFAC	3.479	3.688	3.077	3.817	4.799	3.637

Data File: SCT1

For Field Study

In the file labelled "SCT" the coefficient denoted by "MX" and "MY" are the base moment coefficients. However, in the files labelled "SCT1" and "SCT2" the coefficient of "MX" and "MY" are the hinge moment coefficients about the y-axis at the motor drive level.

Comments: 1. Because of system lift force, $F_{z\ actual} = F_z - 0.160$

(e.g. $F_z = -0.630$ (Run # 197), $F_{z\ actual} = -0.630 - 0.160$

$= -0.790$)

2. MY is the hinge moment coefficient, C_{MHy} in data file: SCT1

DATA FILE: SCT1

RUN #	WIND	TILT	VELOCITY	COMP:	FX	FY	FZ	MX	MY	MZ
197	.0	30.0	10.1	Mean	.629	.147	-.630	.026	-.133	.019
				Max	.940	.239	-.179	.093	-.068	.071
				Min	.384	.046	-1.140	-.034	-.217	-.030
				Rms	.070	.025	.124	.016	.021	.012
				GFAC	1.495	1.630	1.811	3.591	1.627	3.739
				PFAC	4.415	3.698	4.119	4.153	3.891	4.414
198	.0	30.0	9.7	Mean	.669	.179	-.694	.030	-.126	.021
				Max	1.293	.363	-.033	.160	-.005	.100
				Min	.292	.063	-1.668	-.098	-.299	-.072
				Rms	.149	.036	.243	.028	.036	.020
				GFAC	1.933	2.028	2.404	5.328	2.365	4.732
				PFAC	4.194	5.078	4.014	4.586	4.740	3.931
199	.0	30.0	9.7	Mean	.569	.164	-.442	.025	-.126	.014
				Max	1.123	.332	.144	.142	-.019	.090
				Min	.223	.047	-1.324	-.085	-.333	-.057
				Rms	.140	.035	.224	.028	.038	.019
				GFAC	1.974	2.032	2.994	5.601	2.649	6.427
				PFAC	3.972	4.841	3.938	4.143	5.406	3.950
200	.0	30.0	9.9	Mean	.510	.127	-.393	.021	-.115	.008
				Max	.900	.266	-.046	.094	-.043	.054
				Min	.295	.059	-1.043	-.065	-.256	-.058
				Rms	.078	.024	.135	.019	.023	.014
				GFAC	1.765	2.103	2.651	4.453	2.221	6.643
				PFAC	5.008	5.850	4.812	3.756	6.063	3.383
201	.0	-30.0	9.9	Mean	.512	.079	1.154	.024	.165	.020
				Max	1.033	.193	1.793	.177	.362	.090

DATA FILE: SCT1

RUN #	WIND	TILT	VELOCITY	COMP:	FX	FY	FZ	MX	MY	MZ
				Min	.110	-.046	.600	-.093	.003	-.067
				Rms	.117	.031	.157	.031	.054	.017
				GFAC	2.017	2.430	1.554	7.338	2.198	4.518
				PFAC	4.439	3.707	4.081	4.940	3.656	4.144
202	.0	-30.0	9.8	Mean	.512	.089	1.116	.022	.162	.024
				Max	1.079	.229	1.747	.204	.478	.107
				Min	.069	-.057	.619	-.127	-.020	-.061
				Rms	.123	.033	.168	.036	.053	.019
				GFAC	2.109	2.564	1.565	9.155	2.946	4.517
				PFAC	4.603	4.260	3.757	5.033	5.920	4.282
203	.0	-30.0	9.7	Mean	.469	.076	1.040	.015	.147	.023
				Max	1.014	.209	1.735	.178	.376	.109
				Min	.026	-.081	.531	-.123	-.003	-.039
				Rms	.125	.033	.168	.034	.054	.019
				GFAC	2.164	2.739	1.668	11.559	2.566	4.810
				PFAC	4.370	4.088	4.146	4.771	4.235	4.580
204	.0	-30.0	10.0	Mean	.508	.075	1.074	.013	.134	.026
				Max	.988	.203	1.626	.102	.407	.081
				Min	.066	-.032	.542	-.095	-.009	-.015
				Rms	.119	.030	.152	.023	.052	.014
				GFAC	1.945	2.717	1.514	7.840	3.025	3.121
				PFAC	4.042	4.358	3.624	3.793	5.218	3.917
205	.0	-30.0	10.0	Mean	.665	.080	1.322	.010	.235	.034
				Max	1.196	.200	1.965	.154	.498	.087
				Min	.195	-.032	.791	-.080	.054	-.044
				Rms	.142	.032	.176	.026	.057	.016

DATA FILE: SCT1

RUN #	WIND	TILT	VELOCITY	COMP:	FX	FY	FZ	MX	MY	MZ
				GFAC	1.797	2.506	1.486	14.963	2.115	2.591
				PFAC	3.736	3.796	3.644	5.539	4.607	3.383
206	.0	-30.0	10.0	Mean	.311	.073	.756	.010	.094	.021
				Max	.900	.181	1.399	.175	.300	.101
				Min	-.044	-.064	.302	-.102	-.041	.037
				Rms	.098	.027	.136	.029	.041	.016
				GFAC	2.891	2.475	1.850	17.014	3.202	4.689
				PFAC	6.029	3.941	4.728	5.712	5.066	4.956
207	.0	-30.0	10.0	Mean	.352	.085	.874	.018	.102	.021
				Max	.903	.270	1.565	.173	.347	.117
				Min	-.015	-.049	.377	-.130	-.002	-.059
				Rms	.097	.031	.142	.033	.039	.018
				GFAC	2.563	3.189	1.790	9.579	3.385	5.543
				PFAC	5.678	6.058	4.868	4.729	6.259	5.265
208	.0	-30.0	10.0	Mean	.487	.090	1.072	.005	.172	.029
				Max	1.202	.206	1.750	.139	.451	.100
				Min	-.037	-.038	.543	-.100	-.021	-.032
				Rms	.135	.033	.161	.029	.058	.018
				GFAC	2.466	2.287	1.632	27.109	2.619	3.495
				PFAC	5.296	3.485	4.206	4.567	4.776	3.950
209	.0	30.0	9.9	Mean	.595	.154	-.413	.019	-.131	.004
				Max	1.008	.319	.068	.126	-.030	.082
				Min	.335	.026	-1.015	-.088	-.272	-.074
				Rms	.094	.035	.149	.027	.033	.019
				GFAC	1.694	2.074	2.455	6.451	2.079	19.804
				PFAC	4.406	4.772	4.028	3.971	4.249	4.029

Data File: SCT1

RUN #	WIND	TILT	VELOCITY	COMP:	FX	FY	FZ	MX	MY	MZ
210	.0	30.0	9.9	Mean	.484	.144	-.302	.018	-.093	.010
				Max	1.074	.332	.256	.146	.027	.102
				Min	.111	.043	-1.284	-.095	-.283	-.068
				Rms	.147	.037	.228	.029	.038	.021
				GFAC	2.219	2.312	4.252	8.276	3.030	10.464
				PFAC	4.015	5.118	4.307	4.358	4.984	4.345
211	.0	30.0	10.0	Mean	.609	.150	-.535	.018	-.107	.007
				Max	1.256	.346	.192	.158	.010	.109
				Min	.191	.042	-1.640	-.098	-.321	-.086
				Rms	.163	.040	.251	.030	.038	.023
				GFAC	2.062	2.303	3.065	8.756	2.991	14.929
				PFAC	3.975	4.863	4.409	4.606	5.607	4.520
212	.0	30.0	10.0	Mean	.832	.172	-.898	.025	-.163	.011
				Max	1.250	.306	-.397	.096	-.068	.069
				Min	.532	.058	-1.709	-.054	-.286	-.049
				Rms	.089	.033	.144	.021	.030	.017
				GFAC	1.503	1.777	1.903	3.809	1.757	6.507
				PFAC	4.691	4.116	5.639	3.375	4.057	3.533
213	.0	30.0	10.0	Mean	1.074	.206	-1.267	.029	-.173	.013
				Max	1.442	.330	-.689	.112	-.081	.088
				Min	.652	.094	-1.823	-.057	-.318	-.049
				Rms	.120	.035	.183	.025	.031	.020
				GFAC	1.343	1.604	1.439	3.786	1.836	6.817
				PFAC	3.062	3.584	3.032	3.280	4.691	3.756
214	.0	-30.0	10.0	Mean	.578	.061	1.080	.003	.077	.037
				Max	1.038	.204	1.633	.113	.247	.107

DATA FILE: SCT1

RUN #	WIND	TILT	VELOCITY	COMP:	FX	FY	FZ	MX	MY	MZ
				Min	.038	-.087	.623	-.094	-.053	-.031
				Rms	.119	.039	.135	.029	.040	.021
				GFAC	1.794	3.335	1.512	32.406	3.193	2.873
				PFAC	3.854	3.659	4.100	3.824	4.271	3.370
215	.0	-30.0	10.1	Mean	.901	.044	1.461	.011	.186	.045
				Max	1.296	.140	1.894	.087	.322	.107
				Min	.484	-.046	1.066	-.079	.068	-.007
				Rms	.114	.025	.145	.021	.033	.015
				GFAC	1.439	3.201	1.296	7.997	1.729	2.389
				PFAC	3.466	3.798	2.992	3.594	4.094	4.047
216	.0	30.0	10.0	Mean	.990	.186	-1.114	.028	-.183	.014
				Max	1.390	.298	-.562	.100	-.096	.072
				Min	.641	.085	-1.762	-.042	-.289	-.037
				Rms	.124	.029	.188	.021	.026	.016
				GFAC	1.403	1.604	1.582	3.578	1.580	5.206
				PFAC	3.212	3.818	3.451	3.416	4.023	3.562
217	.0	90.0	9.9	Mean	2.132	.164	.405	.023	.016	.081
				Max	3.083	.241	.581	.035	.130	.206
				Min	1.513	.103	.220	.008	-.077	-.023
				Rms	.249	.019	.059	.003	.029	.037
				GFAC	1.446	1.471	1.435	1.531	7.938	2.543
				PFAC	3.828	4.122	2.978	3.463	3.964	3.346
218	.0	30.0	10.0	Mean	.904	.199	-1.242	.031	-.174	.005
				Max	1.312	.327	-.642	.123	-.066	.074
				Min	.609	.097	-2.038	-.052	-.307	-.058
				Rms	.103	.033	.190	.023	.032	.019

DATA FILE: SCT1

RUN #	WIND	TILT	VELOCITY	COMP:	FX	FY	FZ	MX	MY	MZ
				GFAC	1.452	1.642	1.641	4.022	1.761	13.786
				PFAC	3.975	3.875	4.184	3.953	4.138	3.707
219	.0	-30.0	10.1	Mean	.562	.082	1.203	.018	.096	.022
				Max	.915	.213	1.672	.087	.288	.073
				Min	.228	-.038	.811	-.077	-.023	-.020
				Rms	.093	.030	.127	.020	.033	.012
				GFAC	1.627	2.595	1.390	4.751	2.987	3.227
				PFAC	3.812	4.381	3.705	3.439	5.749	4.045
220	.0	30.0	10.0	Mean	.609	.156	-.677	.023	-.136	.010
				Max	.880	.285	-.211	.124	-.012	.075
				Min	.380	.020	-1.237	-.067	-.270	-.049
				Rms	.079	.037	.149	.026	.035	.017
				GFAC	1.444	1.822	1.828	5.511	1.984	7.533
				PFAC	3.432	3.445	3.772	3.966	3.852	3.781
221	.0	30.0	9.9	Mean	.337	.126	-.181	.016	-.055	.011
				Max	.800	.270	.279	.120	.035	.074
				Min	.061	.028	-1.129	-.082	-.204	-.052
				Rms	.098	.030	.187	.126	.029	.017
				GFAC	2.372	2.145	6.240	7.514	3.704	6.411
				PFAC	4.701	4.752	5.069	3.955	5.211	3.668
222	.0	30.0	10.0	Mean	.294	.122	-.097	.014	-.043	.009
				Max	.675	.239	.385	.127	.051	.087
				Min	.056	.031	-.827	-.097	-.169	.051
				Rms	.095	.028	.180	.024	.026	.016
				GFAC	2.293	1.966	8.556	9.356	3.964	9.555
				PFAC	4.000	4.129	4.049	4.699	4.820	5.024

DATA FILE: SCT1

RUN #	WIND	TILT	VELOCITY	COMP:	FX	FY	FZ	MX	MY	MZ
223	.0	30.0	10.0	Mean	.464	.141	-.411	.017	-.085	.009
				Max	.710	.277	-.016	.107	.011	.073
				Min	.267	.032	-.908	-.071	-.197	-.051
				Rms	.066	.031	.124	.025	.027	.017
				GFAC	1.529	1.960	2.209	6.125	2.314	8.104
				PFAC	3.718	4.414	4.020	3.620	4.202	3.773
224	.0	90.0	10.0	Mean	.707	.124	.461	.019	.022	.028
				Max	1.902	.222	.634	.039	.245	.224
				Min	.047	.030	.280	.002	-.127	-.138
				Rms	.284	.025	.061	.005	.042	.044
				GFAC	2.691	1.789	1.376	2.057	11.209	7.892
				PFAC	4.208	3.903	2.851	4.100	5.327	4.419
225	.0	90.0	9.9	Mean	.373	.101	.427	.015	.009	.016
				Max	1.150	.178	.614	.029	.156	.147
				Min	.004	.033	.253	.004	-.066	-.081
				Rms	.152	.018	.061	.003	.025	.027
				GFAC	3.084	1.772	1.438	1.854	16.525	9.232
				PFAC	5.123	4.325	3.075	3.897	5.945	4.877
226	.0	90.0	9.9	Mean	.494	.102	.412	.016	.011	.021
				Max	1.542	.176	.589	.028	.125	.170
				Min	-.004	.026	.220	.003	-.070	-.103
				Rms	.169	.019	.059	.003	.024	.030
				GFAC	3.123	1.719	1.429	1.710	11.677	7.934
				PFAC	6.213	3.824	3.016	3.541	4.683	4.923
227	.0	90.0	9.9	Mean	.962	.112	.407	.018	.028	.042
				Max	2.480	.244	.595	.036	.227	.292

Data File: SCT1

RUN #	WIND	TILT	VELOCITY	COMP:	FX	FY	FZ	MX	MY	MZ
				Min	.144	.015	.217	-.003	-.125	-.224
				Rms	.312	.029	.062	.005	.044	.052
				GFAC	2.576	2.175	1.461	1.977	8.060	6.947
				PFAC	4.869	4.534	3.049	3.500	4.467	4.784
228	.0	90.0	10.1	Mean	.608	.107	.441	.017	.009	.028
				Max	1.843	.184	.612	.031	.159	.178
				Min	.115	.019	.258	.004	-.086	-.155
				Rms	.209	.021	.059	.004	.027	.035
				GFAC	3.029	1.723	1.388	1.847	18.327	6.332
				PFAC	5.893	3.649	2.885	3.886	5.547	4.293
229	.0	90.0	9.9	Mean	.566	.116	.470	.017	.010	.017
				Max	1.596	.184	.647	.028	.154	.160
				Min	.056	.058	.279	.005	-.075	-.093
				Rms	.198	.017	.065	.003	.026	.032
				GFAC	2.819	1.588	1.377	1.660	15.010	9.210
				PFAC	5.202	4.011	2.716	3.369	5.477	4.495
230	.0	90.0	10.0	Mean	.742	.113	.424	.017	.004	.021
				Max	1.740	.198	.619	.032	.158	.192
				Min	.143	.047	.178	.005	-.093	-.101
				Rms	.229	.020	.064	.004	.031	.034
				GFAC	2.344	1.752	1.458	1.903	36.238	8.989
				PFAC	4.348	4.220	3.014	4.197	4.984	4.963
231	.0	90.0	10.0	Mean	.938	.117	.428	.018	.017	.038
				Max	2.231	.237	.625	.041	.246	.228
				Min	.041	-.005	.228	.001	-.108	-.140
				Rms	.303	.029	.063	.005	.040	.050

DATA FILE: SCT1

RUN #	WIND	TILT	VELOCITY	COMP:	FX	FY	FZ	MX	MY	MZ
				GFAC	2.379	2.031	1.460	2.273	14.485	5.938
				PFAC	4.268	4.176	3.134	4.841	5.723	3.824
232	.0	30.0	10.0	Mean	.546	.133	-.429	.022	-.114	.011
				Max	.794	.235	-.067	.086	-.037	.063
				Min	.325	.037	-.863	-.047	-.198	-.032
				Rms	.066	.026	.115	.018	.023	.013
				GFAC	1.456	1.767	2.009	3.936	1.736	5.583
				PFAC	3.787	3.919	3.769	3.582	3.601	3.931
233	.0	30.0	10.1	Mean	.433	.122	-.268	.020	-.058	.012
				Max	.992	.266	.209	.131	.037	.093
				Min	.090	.026	-1.299	-.088	-.219	-.065
				Rms	.115	.029	.186	.026	.026	.018
				GFAC	2.292	2.175	4.839	6.649	3.748	7.731
				PFAC	4.874	5.026	5.533	4.360	6.065	4.410
234	.0	30.0	10.0	Mean	.413	.125	-.187	.018	-.071	.004
				Max	.926	.256	.309	.111	.015	.081
				Min	.138	.025	-.986	-.087	-.225	-.073
				Rms	.113	.027	.182	.025	.028	.017
				GFAC	2.243	2.047	5.275	6.296	3.162	21.566
				PFAC	4.548	4.864	4.385	3.810	5.512	4.550
235	0	30.0	10.2	Mean	.343	.108	-.113	.018	-.065	.008
				Max	.596	.179	.164	.083	-.010	.056
				Min	.188	.044	-.537	-.034	-.139	-.028
				Rms	.054	.018	.098	.013	.015	.009
				GFAC	1.737	1.661	4.753	4.648	2.141	6.850
				PFAC	4.702	3.998	4.310	4.936	4.833	5.213

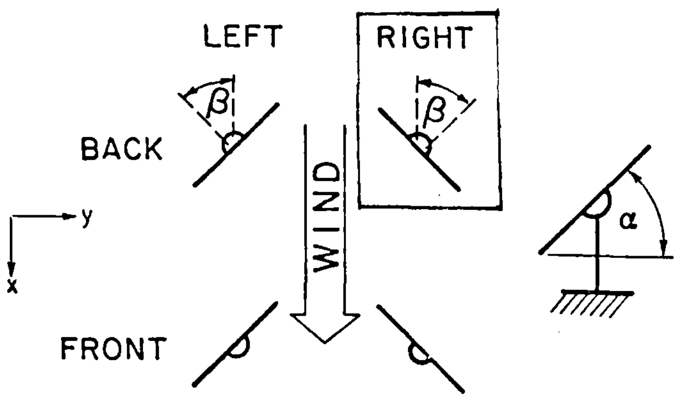

Single Heliostat

Data File: SCT1

RUN #	WIND	TILT	VELOCITY	COMP:	FX	FY	FZ	MX	MY	MZ
237	.0	-80.0	10.0	Mean	.815	.131	.574	.012	.027	.071
				Max	1.822	.313	.793	.065	.286	.321
				Min	.097	-.040	.353	-.039	-.108	-.109
				Rms	.257	.043	.071	.013	.043	.057
				GFAC	2.236	2.388	1.380	5.290	10.591	4.517
				PFAC	3.926	4.222	3.052	4.129	6.026	4.410
238	.0	-80.0	9.9	Mean	.894	.109	.597	.023	.020	.025
				Max	1.879	.277	.823	.088	.244	.268
				Min	.195	-.095	.364	-.031	-.132	-.161
				Rms	.233	.044	.075	.014	.045	.052
				GFAC	2.101	2.548	1.380	3.852	12.206	10.699
				PFAC	4.227	3.824	3.016	4.729	5.008	4.706
239	.0	-80.0	10.0	Mean	.898	.086	.572	.020	.010	.013
				Max	1.973	.260	.838	.084	.229	.239
				Min	.166	-.111	.348	-.029	-.139	-.225
				Rms	.237	.044	.075	.013	.045	.053
				GFAC	2.197	3.025	1.465	4.230	23.244	19.054
				PFAC	4.530	3.975	3.560	4.927	4.839	4.285
240	.0	-80.0	10.0	Mean	.941	.121	.520	.012	.021	.069
				Max	2.271	.367	.783	.078	.235	.335
				Min	.127	-.072	.266	-.052	-.135	-.153
				Rms	.288	.047	.078	.013	.047	.061
				GFAC	2.415	3.025	1.507	6.450	10.960	4.832
				PFAC	4.624	5.200	3.373	4.919	4.521	4.376
241	.0	-30.0	10.1	Mean	.575	.072	1.072	.012	.133	.029
				Max	1.191	.214	1.751	.138	.401	.123

DATA FILE: SCT1

RUN #	WIND	TILT	VELOCITY	COMP:	FX	FY	FZ	MX	MY	MZ
				Min	.060	-.104	.610	-.100	-.052	-.036
				Rms	.152	.040	.155	.032	.058	.023
				GFAC	2.070	2.950	1.634	11.156	3.028	4.249
				PFAC	4.050	3.501	4.398	3.888	4.653	4.030
242	0	-30.0	10.0	Mean	.607	.042	1.117	.045	.182	.014
				Max	1.181	.206	1.710	.147	.423	.106
				Min	.042	-.093	.629	-.097	-.015	-.046
				Rms	.160	.039	.162	.030	.065	.021
				GFAC	1.946	4.870	1.530	3.264	2.319	7.829
				PFAC	3.585	4.223	3.669	3.408	3.703	4.314
243	0	-30.0	9.9	Mean	.596	.049	1.128	.035	.157	.019
				Max	1.239	.198	1.726	.145	.422	.111
				Min	.104	-.110	.620	-.068	-.043	-.052
				Rms	.163	.035	.158	.028	.063	.023
				GFAC	2.081	4.061	1.530	4.102	2.693	5.716
				PFAC	3.952	4.281	3.778	3.893	4.185	4.058
244	.0	-30.0	10.0	Mean	.510	.064	.964	.012	.129	.026
				Max	1.115	.190	1.489	.133	.418	.132
				Min	-.128	-.183	.489	-.129	-.076	-.044
				Rms	.148	.033	.151	.028	.058	.021
				GFAC	2.188	2.957	1.545	10.711	3.247	5.025
				PFAC	4.082	3.770	3.472	4.281	5.007	5.050
245	.0	30.0	10.1	Mean	.472	.129	-.283	.025	-.104	.015
				Max	.855	.243	.106	.135	-.016	.097
				Min	.227	.048	-.903	-.059	-.211	-.040
				Rms	.078	.026	.136	.021	.027	.015

DATA FILE: SCT1

RUN #	WIND	TILT	VELOCITY	COMP:	FX	FY	FZ	MX	MY	MZ
				GFAC	1.813	1.887	3.191	5.349	2.041	6.308
				PFAC	4.945	4.481	4.559	5.233	3.987	5.312
246	.0	30.0	10.0	Mean	.519	.137	-.378	.016	-.103	.012
				Max	1.091	.307	.068	.120	.014	.099
				Min	.227	.022	-1.381	-.131	-.275	-.091
				Rms	.113	.039	.180	.033	.033	.024
				GFAC	2.101	2.239	3.651	7.431	2.676	8.283
				PFAC	5.042	4.333	5.563	3.125	5.252	3.585
247	.0	30.0	10.0	Mean	.450	.144	-.179	-.013	-.104	-.013
				Max	.883	.315	.288	.105	-.004	.078
				Min	.156	.005	-.841	-.145	-.228	-.099
				Rms	.101	.035	.165	.031	.030	.022
				GFAC	1.964	2.185	4.706	11.113	2.187	7.626
				PFAC	4.283	4.834	4.018	4.313	4.190	3.986
248	.0	30.0	10.0	Mean	.330	.118	-.067	-.001	-.078	.001
				Max	.558	.211	.231	.081	-.025	.058
				Min	.152	.047	-.442	-.068	-.144	-.044
				Rms	.054	.019	.100	.016	.017	.012
				GFAC	1.690	1.794	6.574	89.235	1.843	52.407
				PFAC	4.243	4.841	3.756	4.065	3.801	4.859
250	20.0	90.0	10.0	Mean	.996	.427	.364	.013	.017	-.028
				Max	2.172	.896	.564	.060	.192	.154
				Min	.130	.136	.161	-.035	-.126	-.219
				Rms	.206	.103	.071	.012	.043	.051
				GFAC	2.179	2.096	1.547	4.638	11.113	7.848
				PFAC	4.116	4.557	2.803	3.865	4.069	3.746

DATA FILE: SCT1

RUN #	WIND	TILT	VELOCITY	COMP:	FX	FY	FZ	MX	MY	MZ
251	20.0	90.0	10.0	Mean	1.130	.466	.331	.014	.014	-.054
				Max	2.226	.886	.527	.058	.202	.137
				Min	.322	.191	.120	-.039	-.135	-.251
				Rms	.274	.099	.072	.012	.043	.049
				GFAC	1.971	1.902	1.594	4.269	14.472	4.660
				PFAC	3.995	4.240	2.746	3.583	4.391	4.010
252	20.0	90.0	9.9	Mean	1.184	.509	.379	.016	.018	-.065
				Max	2.311	.874	.571	.058	.213	.111
				Min	.303	.195	.188	-.034	-.123	-.259
				Rms	.265	.091	.071	.011	.040	.050
				GFAC	1.952	1.719	1.507	3.643	12.051	3.971
				PFAC	4.254	4.022	2.709	3.675	4.887	3.901
253	20.0	90.0	9.9	Mean	1.049	.434	.359	.009	.021	-.035
				Max	2.166	.819	.576	.048	.240	.140
				Min	.190	.166	.136	-.049	-.139	-.247
				Rms	.285	.098	.073	.012	.042	.052
				GFAC	2.065	1.887	1.604	5.409	11.296	7.096
				PFAC	3.914	3.921	2.973	3.266	5.170	4.072

Data File: SCT2

For Single Square Model

In the file labelled "SCT" the coefficient denoted by "MX" and "MY" are the base moment coefficients. However, in the files labelled "SCT1" and "SCT2" the coefficient of "MX" and "MY" are the hinge moment coefficients about the y-axis at the motor drive level.

Comment: MY is the hinge moment coefficient, C_{MHy} in data file: SCT2

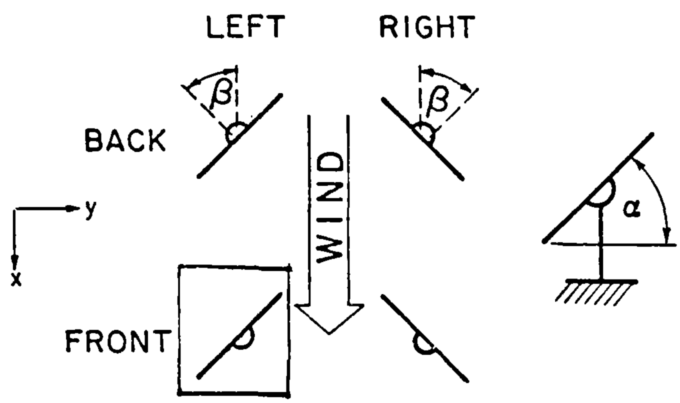

Single Heliostat

DATA FILE: SCT2

RUN #	WIND	TILT	VELOCITY	COMP:	FX	FY	FZ	MX	MY	MZ
8	.0	90.0	9.6	Mean	2.093	.084	-.062	.013	.013	.062
				Max	4.986	.315	.049	.046	.318	.352
				Min	.849	-.064	-.199	-.012	-.163	-.314
				Rms	.575	.041	.035	.007	.053	.072
				GFAC	2.382	3.734	3.191	3.453	24.694	5.705
				PFAC	5.026	5.651	3.883	4.647	5.735	4.004
9	10.0	90.0	9.6	Mean	2.000	.516	-.137	.013	.015	-.002
				Max	4.349	1.056	.005	.053	.274	.275
				Min	.505	.154	-.303	-.042	-.164	-.259
				Rms	.550	.138	.045	.011	.053	.067
				GFAC	2.174	2.045	2.214	3.906	18.176	170.623
				PFAC	4.268	3.906	3.725	3.532	4.878	3.851
10	20.0	90.0	9.9	Mean	1.756	.822	-.130	.005	.014	-.044
				Max	4.041	1.812	.001	.101	.204	.185
				Min	.543	.256	-.297	-.063	-.220	-.264
				Rms	.516	.238	.046	.017	.043	.059
				GFAC	2.302	2.204	2.284	18.920	14.416	6.004
				PFAC	4.431	4.167	3.592	5.678	4.404	3.743
11	30.0	90.0	9.5	Mean	1.562	1.049	-.149	.001	.012	-.079
				Max	3.433	2.217	-.009	.086	.213	.102
				Min	.401	.270	-.319	-.111	-.150	-.304
				Rms	.426	.282	.045	.024	.041	.053
				GFAC	2.198	2.113	2.137	80.918	17.198	3.828
				PFAC	4.388	4.141	3.731	3.615	4.835	4.244
12	40.0	90.0	9.7	Mean	1.303	1.218	-.127	-.003	.013	-.103
				Max	2.946	2.731	.029	.108	.192	.067

DATA FILE: SCT2

RUN #	WIND	TILT	VELOCITY	COMP:	FX	FY	FZ	MX	MY	MZ
				Min	.261	.262	-.326	-.147	-.131	-.381
				Rms	.406	.374	.051	.027	.034	.058
				GFAC	2.261	2.242	2.557	43.600	14.367	3.699
				PFAC	4.043	4.044	3.924	5.242	5.205	4.786
13	50.0	90.0	9.8	Mean	.936	1.323	-.129	-.006	.013	-.148
				Max	2.253	3.197	.022	.128	.141	.029
				Min	.185	.216	-.315	-.172	-.093	-.475
				Rms	.299	.418	.047	.033	.027	.070
				GFAC	2.408	2.416	2.441	28.378	11.099	3.203
				PFAC	4.405	4.480	3.975	5.059	4.691	4.640
8	55.0	90.0	9.9	Mean	.822	1.326	-.124	-.012	.013	-.160
				Max	2.307	3.705	.006	.146	.119	.008
				Min	.172	.264	-.344	-.169	-.099	.750
				Rms	.282	.452	.049	.035	.025	.077
				GFAC	2.808	2.795	2.774	14.607	8.904	4.680
				PFAC	5.275	5.264	4.465	4.546	4.261	7.702
14	60.0	90.0	9.7	Mean	.701	1.378	-.123	-.017	.013	-.193
				Max	1.696	3.456	.023	.145	.125	.022
				Min	.136	.144	-.375	-.231	-.071	-.613
				Rms	.252	.511	.056	.041	.024	.093
				GFAC	2.420	2.508	3.064	13.945	9.704	3.169
				PFAC	3.954	4.066	4.478	5.247	4.686	4.529
9	65.0	90.0	9.8	Mean	.576	1.312	-.117	-.021	.012	-.202
				Max	1.542	3.838	.019	.133	.104	.064
				Min	.077	.014	-.355	-.242	-.061	-.737
				Rms	.210	.530	.054	.044	.021	.093

DATA FILE: SCT2

RUN #	WIND	TILT	VELOCITY	COMP:	FX	FY	FZ	MX	MY	MZ
				GFAC	2.678	2.926	3.030	11.462	8.649	3.647
				PFAC	4.593	4.764	4.403	4.983	4.273	5.767
15	70.0	90.0	9.7	Mean	.436	1.172	-.112	-.019	.012	-.193
				Max	1.142	3.375	.024	.144	.093	.112
				Min	.103	-.126	-.338	-.209	-.056	-.622
				Rms	.154	.521	.057	.044	.018	.101
				GFAC	2.618	2.879	3.020	11.243	7.663	3.224
				PFAC	4.589	4.231	3.962	4.296	4.385	4.241
54	75.0	90.0	9.9	Mean	.268	.830	-.084	-.004	.010	-.131
				Max	.676	3.006	.067	.174	.070	.288
				Min	.027	-.497	-.284	-.173	-.035	-.621
				Rms	.083	.463	.049	.042	.015	.114
				GFAC	2.517	3.623	3.397	39.049	7.326	4.721
				PFAC	4.880	4.705	4.061	4.001	3.941	4.310
3	80.0	90.0	9.9	Mean	.204	.632	-.035	.000	.007	-.064
				Max	.478	2.460	.091	.169	.069	.338
				Min	.049	-.658	-.186	-.184	-.041	-.482
				Rms	.062	.429	.042	.043	.013	.113
				GFAC	2.346	3.892	5.334	591.431	9.657	7.539
				PFAC	4.434	4.256	3.583	3.963	4.643	3.703
5	85.0	90.0	10.0	Mean	.161	.363	-.034	.004	.002	.013
				Max	.395	2.030	.098	.162	.060	.389
				Min	-.002	-.906	-.197	-.161	-.051	-.451
				Rms	.057	.366	.038	.039	.012	.109
				GFAC	2.447	5.595	5.702	40.058	30.430	29.177
				PFAC	4.122	4.554	4.217	4.010	4.702	3.446

DATA FILE: SCT2

RUN #	WIND	TILT	VELOCITY	COMP:	FX	FY	FZ	MX	MY	MZ
4	90.0	90.0	9.6	Mean	.151	.165	.013	.008	.003	.074
				Max	.404	2.376	.141	.191	.074	.476
				Min	-.056	-1.122	-.184	-.188	-.049	-.476
				Rms	.067	.407	.040	.044	.013	.122
				GFAC	2.670	14.439	10.973	25.275	23.252	6.446
				PFAC	3.776	5.430	3.189	4.174	5.325	3.293

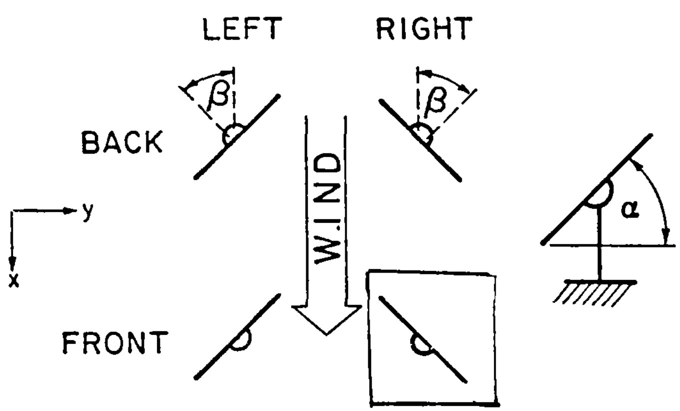

Single Heliostat

DATA FILE: SCT2

RUN #	WIND	TILT	VELOCITY	COMP:	FX	FY	FZ	MX	MY	MZ
10	.0	90.0	9.7	Mean	2.045	.087	-.074	.014	.008	.053
				Max	4.107	.315	.033	.038	.214	.354
				Min	.495	-.059	-.199	-.006	-.158	-.280
				Rms	.584	.040	.033	.007	.051	.069
				GFAC	2.008	3.629	2.683	2.695	28.572	6.656
				PFAC	3.528	5.764	3.725	3.610	4.040	4.335
11	10.0	90.0	9.7	Mean	1.978	-.287	-.065	.018	.005	.106
				Max	4.080	-.058	.043	.072	.247	.348
				Min	.732	-.622	-.171	-.020	-.186	-.102
				Rms	.531	.091	.030	.012	.050	.065
				GFAC	2.063	2.166	2.606	3.964	45.195	3.270
				PFAC	3.957	3.682	3.460	4.420	4.866	3.707
12	25.0	90.0	9.8	Mean	1.734	-.759	.026	.020	.006	.167
				Max	3.737	-.154	.152	.143	.231	.457
				Min	.432	-1.661	-.096	-.056	-.150	.012
				Rms	.495	.225	.034	.023	.045	.065
				GFAC	2.155	2.189	5.926	7.240	38.668	2.728
				PFAC	4.051	4.011	3.684	5.405	5.006	4.479
13	45.0	90.0	9.7	Mean	1.267	-1.184	.067	.023	.001	.207
				Max	3.094	-.212	.232	.193	.174	.568
				Min	.296	-2.962	-.052	-.094	-.134	.022
				Rms	.404	.392	.041	.035	.036	.072
				GFAC	2.442	2.501	3.483	8.322	174.442	2.739
				PFAC	4.524	4.534	4.078	4.850	4.813	4.977
14	50.0	90.0	9.7	Mean	1.078	-1.258	.091	.0~~1~~6 2	.003	.216
				Max	2.873	.039	.298	.246	.164	.700

DATA FILE: SCT2

RUN #	WIND	TILT	VELOCITY	COMP:	FX	FY	FZ	MX	MY	MZ
				Min	.045	-3.373	-.052	-.115	-.105	.015
				Rms	.385	.469	.051	.039	.032	.086
				GFAC	2.665	2.681	3.287	9.423	48.029	3.232
				PFAC	4.657	4.510	4.054	5.694	5.028	5.614
15	55.0	90.0	9.7	Mean	.952	-1.270	.112	.030	.004	.229
				Max	2.363	-.008	.342	.233	.113	.755
				Min	.096	-3.291	-.053	-.124	-.109	-.001
				Rms	.346	.488	.053	.040	.029	.091
				GFAC	2.482	2.592	3.041	7.700	26.773	3.292
				PFAC	4.072	4.138	4.332	5.027	3.765	5.803
16	60.0	90.0	10.1	Mean	.685	-1.189	.088	.030	.009	.232
				Max	1.732	-.011	.284	.194	.092	.657
				Min	.098	-3.122	-.046	-.097	-.072	-.001
				Rms	.248	.482	.049	.040	.022	.095
				GFAC	2.531	2.626	3.226	6.368	10.310	2.832
				PFAC	4.221	4.014	3.960	4.051	3.841	4.478
17	65.0	90.0	9.9	Mean	.569	-1.107	.084	.028	.003	.224
				Max	1.530	.126	.313	.240	.079	.656
				Min	.099	-3.363	-.055	-.125	-.077	-.119
				Rms	.202	.495	.049	.044	.020	.102
				GFAC	2.687	3.037	3.708	8.661	22.732	2.929
				PFAC	4.757	4.555	4.628	4.780	3.849	4.221
18	70.0	90.0	9.4	Mean	.446	-.994	.066	.022	.004	.202
				Max	1.117	.381	.291	.262	.066	.628
				Min	.041	-3.141	-.062	-.147	-.071	-.236
				Rms	.164	.539	.049	.049	.018	.120

DATA FILE: SCT2

RUN #	WIND	TILT	VELOCITY	COMP:	FX	FY	FZ	MX	MY	MZ
				GFAC	2.507	3.158	4.393	11.798	16.767	3.117
				PFAC	4.094	3.985	4.615	4.850	3.485	3.568
19	80.0	90.0	9.9	Mean	.191	-.357	.029	.004	.007	.029
				Max	.465	1.019	.228	.156	.060	.565
				Min	-.007	-2.403	-.109	-.136	-.044	-.408
				Rms	.064	.390	.039	.042	.012	.109
				GFAC	2.439	6.728	7.957	36.400	8.755	19.235
				PFAC	4.318	5.239	5.086	3.629	4.557	4.917
20	90.0	90.0	9.8	Mean	.143	.028	.014	-.002	.008	-.079
				Max	.343	1.961	.197	.154	.052	.349
				Min	.008	-1.564	-.140	-.213	-.046	-.532
				Rms	.050	.392	.040	.043	.011	.105
				GFAC	2.409	69.954	14.010	115.097	6.407	6.717
				PFAC	4.019	4.926	4.528	4.923	3.826	4.297

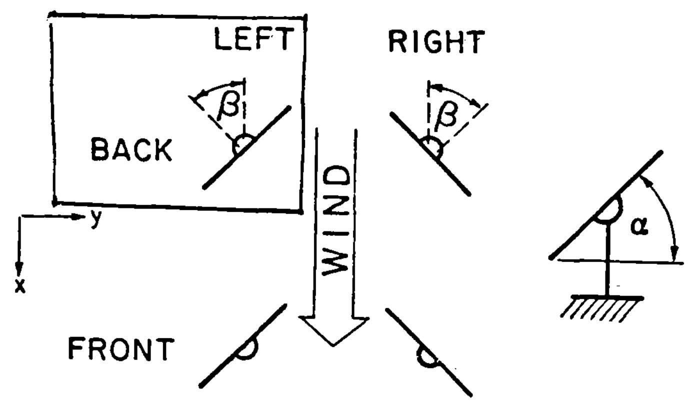

Single Heliostat

DATA FILE: SCT2

RUN #	WIND	TILT	VELOCITY	COMP:	FX	FY	FZ	MX	MY	MZ
26	.0	90.0	9.8	Mean	1.983	.086	-.085	.016	.016	.054
				Max	4.176	.384	.027	.052	.315	.407
				Min	.563	-.144	-.253	-.016	-.203	-.247
				Rms	.543	.070	.038	.009	.055	.090
				GFAC	2.106	4.450	2.968	3.293	19.069	7.590
				PFAC	4.038	4.238	4.395	4.265	5.405	3.944
27	20.0	90.0	9.5	Mean	1.782	.556	-.129	.010	.015	-.076
				Max	3.919	1.231	.032	.060	.293	.189
				Min	.592	.125	-.334	-.070	-.159	-.367
				Rms	.501	.166	.049	.015	.048	.088
				GFAC	2.199	2.215	2.589	6.321	20.077	4.846
				PFAC	4.262	4.062	4.154	3.439	5.808	3.298
28	45.0	90.0	9.8	Mean	1.058	.880	-.105	.003	.019	-.176
				Max	2.488	2.255	.040	.122	.184	.000
				Min	.278	.140	-.334	-.151	-.144	-.473
				Rms	.327	.296	.048	.028	.033	.067
				GFAC	2.351	2.563	3.169	36.373	9.898	2.698
				PFAC	4.371	4.646	4.726	4.234	4.995	4.470
50	60.0	90.0	9.7	Mean	.775	1.005	-.141	-.002	.017	-.188
				Max	2.004	2.813	.065	.193	.143	.037
				Min	.075	-.087	-.397	-.164	-.109	-.544
				Rms	.281	.425	.063	.036	.025	.076
				GFAC	2.586	2.799	2.811	94.133	8.483	2.891
				PFAC	4.380	4.258	4.047	4.481	5.005	4.666
22	65.0	90.0	10.1	Mean	.531	.938	-.100	-.017	.020	-.219
				Max	1.309	2.691	.077	.106	.111	.028

DATA FILE: SCT2

RUN #	WIND	TILT	VELOCITY	COMP:	FX	FY	FZ	MX	MY	MZ
				Min	-.017	-.310	-.308	-.194	-.041	-.667
				Rms	.192	.426	.055	.039	.020	.092
				GFAC	2.466	2.868	3.072	11.236	5.543	3.046
				PFAC	4.048	4.116	3.774	4.569	4.658	4.893
51	70.0	90.0	10.0	Mean	.544	.966	-.115	-.017	.018	-.222
				Max	1.421	2.931	.067	.130	.136	.056
				Min	-.042	-.448	-.344	-.253	-.065	-.606
				Rms	.201	.450	.061	.041	.020	.091
				GFAC	2.613	3.033	2.993	15.163	7.673	2.723
				PFAC	4.365	4.368	3.778	5.711	5.940	4.205
29	80.0	90.0	9.8	Mean	.248	.591	-.028	-.008	.015	-.206
				Max	.775	2.701	.117	.140	.089	.051
				Min	.004	-.561	-.271	-.221	-.030	-.604
				Rms	.104	.436	.050	.044	.015	.098
				GFAC	3.120	4.566	9.583	26.632	5.812	2.925
				PFAC	5.057	4.836	4.823	4.855	4.886	4.043

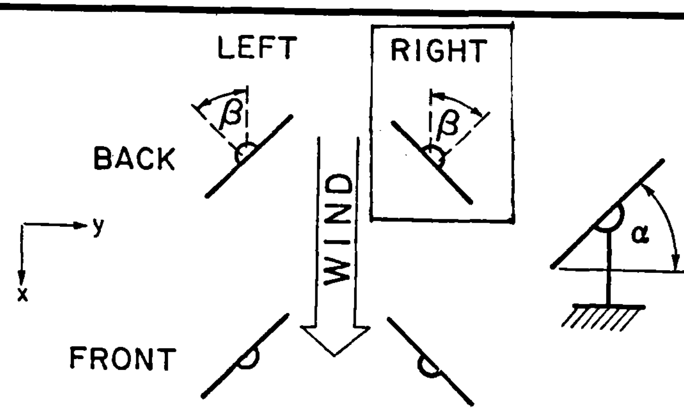

Single Heliostat

DATA FILE: SCT2

RUN #	WIND	TILT	VELOCITY	COMP:	FX	FY	FZ	MX	MY	MZ
30	20.0	90.0	9.6	Mean	1.772	-.416	-.013	.022	.020	.174
				Max	4.003	-.050	.095	.117	.309	.531
				Min	.485	-1.121	-.121	-.041	-.173	-.097
				Rms	.519	.159	.031	.019	.051	.085
				GFAC	2.259	2.695	9.208	5.225	15.728	3.056
				PFAC	4.300	4.443	3.473	5.082	5.701	4.184
31	40.0	90.0	10.0	Mean	1.253	-.691	.014	.023	.011	.227
				Max	2.666	.030	.113	.146	.194	.531
				Min	.267	-1.710	-.070	-.083	-.159	-.018
				Rms	.386	.251	.026	.027	.038	.079
				GFAC	2.128	2.474	7.836	6.300	17.267	2.341
				PFAC	3.658	4.060	3.723	4.496	4.828	3.853
49	55.0	90.0	9.7	Mean	.927	-.802	-.030	.029	-.003	.240
				Max	2.333	.128	.123	.233	.122	.819
				Min	.137	-2.585	-.147	-.105	-.134	.022
				Rms	.326	.380	.038	.037	.029	.092
				GFAC	2.516	3.222	4.914	8.040	52.035	3.412
				PFAC	4.318	4.687	3.062	5.570	4.543	6.272
25	60.0	90.0	9.7	Mean	.828	-.889	.085	.026	.013	.256
				Max	2.231	.243	.232	.180	.116	.787
				Min	.081	-2.739	-.046	-.118	-.122	.041
				Rms	.324	.432	.038	.038	.026	.100
				GFAC	2.694	3.083	2.734	7.045	8.705	3.080
				PFAC	4.336	4.283	3.919	4.021	3.917	5.342
24	65.0	90.0	9.8	Mean	.651	-.843	.098	.027	.005	.247
				Max	1.687	.304	.223	.254	.138	.793

DATA FILE: SCT2

RUN #	WIND	TILT	VELOCITY	COMP:	FX	FY	FZ	MX	MY	MZ
				Min	-.025	-2.646	-.013	-.103	-.078	-.007
				Rms	.268	.446	.039	.041	.023	.104
				GFAC	2.592	3.140	2.287	9.259	27.561	3.208
				PFAC	3.870	4.042	3.253	5.467	5.780	5.271
32	80.0	90.0	9.6	Mean	.245	-.341	.038	.016	.000	.198
				Max	.744	1.141	.186	.212	.072	.572
				Min	-.167	-1.835	-.103	-.157	-.051	-.244
				Rms	.116	.427	.045	.046	.015	.113
				GFAC	3.037	5.385	4.913	13.230	158.377	2.888
				PFAC	4.308	3.498	3.318	4.236	3.366	3.315

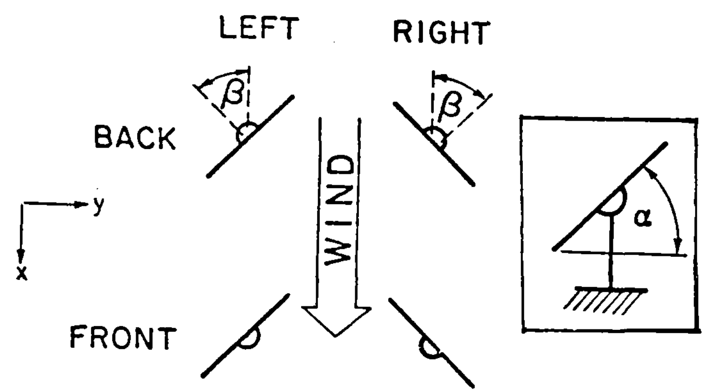

Single Heliostat

DATA FILE: SCT2

RUN #	WIND	TILT	VELOCITY	COMP:	FX	FY	FZ	MX	MY	MZ
33	60.0	80.0	9.7	Mean	.768	-1.185	-.155	.036	-.035	.222
				Max	1.853	.191	-.007	.239	.066	.702
				Min	.072	-3.122	-.348	-.136	-.134	-.079
				Rms	.272	.479	.049	.043	.023	.093
				GFAC	2.412	2.634	2.239	6.559	3.828	3.167
				PFAC	3.984	4.041	3.969	4.654	4.300	5.191
34	60.0	60.0	9.4	Mean	.714	-.973	-.639	.045	-.116	.212
				Max	1.609	-.030	-.103	.313	.026	.547
				Min	.164	-2.504	-1.529	-.109	-.320	-.001
				Rms	.238	.409	.225	.053	.046	.083
				GFAC	2.254	2.573	2.392	6.895	2.747	2.579
				PFAC	3.756	3.742	3.949	5.074	4.424	4.032
35	65.0	45.0	9.7	Mean	.555	-.622	-.731	.032	-.144	.142
				Max	1.353	.164	.038	.263	.041	.413
				Min	.089	-1.924	-1.908	-.137	-.409	-.060
				Rms	.187	.297	.298	.055	.063	.063
				GFAC	2.437	3.094	2.609	8.203	2.848	2.920
				PFAC	4.268	4.389	3.946	4.223	4.218	4.296
36	65.0	30.0	9.8	Mean	.377	-.259	-.694	.014	-.128	.059
				Max	1.029	.338	.158	.239	.143	.254
				Min	.036	-1.062	-2.104	-.160	-.519	-.102
				Rms	.127	.176	.325	.051	.075	.038
				GFAC	2.731	4.101	3.030	16.580	4.060	4.329
				PFAC	5.127	4.558	4.343	4.446	5.246	5.169
37	65.0	15.0	9.6	Mean	.240	-.012	-.454	-.004	-.064	.002
				Max	.727	.396	.210	.192	.122	.075

Data File: SCT2

RUN #	WIND	TILT	VELOCITY	COMP:	FX	FY	FZ	MX	MY	MZ
				Min	-.086	-.437	-1.572	-.174	-.396	-.045
				Rms	.097	.079	.300	.044	.071	.017
				GFAC	3.026	35.533	3.461	41.584	6.150	31.761
				PFAC	5.021	5.392	3.731	3.848	4.661	4.372
38	65.0	0.0	9.9	Mean	.182	.086	-.071	-.012	.025	-.009
				Max	.585	.323	.815	.156	.285	.024
				Min	-.210	-.141	-1.234	-.201	-.269	-.047
				Rms	.089	.050	.247	.035	.062	.010
				GFAC	3.214	3.757	17.324	17.227	11.545	5.442
				PFAC	4.517	4.772	4.710	5.386	4.185	3.974
39	65.0	15.0	9.9	Mean	.243	.001	.464	-.011	.158	.031
				Max	.957	.253	1.611	.182	.579	.135
				Min	-.134	-.350	-.329	-.183	-.124	-.043
				Rms	.114	.072	.229	.037	.069	.018
				GFAC	3.942	297.950	3.475	16.958	3.663	4.350
				PFAC	6.271	3.507	5.012	4.691	6.078	5.672
40	65.0	30.0	9.7	Mean	.417	-.261	.767	.010	.210	.112
				Max	1.368	.164	2.368	.249	.649	.292
				Min	-.040	-1.140	-.017	-.203	-.001	.000
				Rms	.166	.156	.301	.049	.083	.039
				GFAC	3.281	4.366	3.087	23.985	3.085	2.593
				PFAC	5.727	5.647	5.317	4.877	5.264	4.579
41	65.0	45.0	9.5	Mean	.623	-.596	.886	.015	.213	.205
				Max	1.617	.147	2.178	.277	.558	.435
				Min	-.045	-1.677	.094	-.173	-.011	.014
				Rms	.232	.254	.311	.052	.083	.062

DATA FILE: SCT2

RUN #	WIND	TILT	VELOCITY	COMP:	FX	FY	FZ	MX	MY	MZ
				GFAC	2.594	2.813	2.459	18.509	2.627	2.128
				PFAC	4.290	4.257	4.154	5.082	4.178	3.714
45	65.0	55.0	9.7	Mean	.739	-.770	.792	.011	.171	.243
				Max	1.778	.044	1.721	.269	.443	.545
				Min	-.007	-1.860	.033	-.177	-.053	.030
				Rms	.254	.296	.258	.047	.068	.073
				GFAC	2.405	2.417	2.173	24.177	2.591	2.243
				PFAC	4.082	3.680	3.597	5.484	4.006	4.125
42	65.0	60.0	9.5	Mean	.843	-.883	.757	.011	.152	.275
				Max	2.159	.004	1.768	.237	.403	.607
				Min	.155	-2.292	.134	-.187	-.021	.090
				Rms	.289	.347	.253	.048	.064	.082
				GFAC	2.562	2.596	2.335	20.676	2.641	2.202
				PFAC	4.547	4.057	3.999	4.721	3.909	4.058
47	65.0	65.0	9.7	Mean	.816	-.893	.616	.010	.123	.267
				Max	2.084	.254	1.496	.227	.381	.674
				Min	.086	-2.432	.065	-.166	-.063	.058
				Rms	.278	.341	.200	.042	.052	.081
				GFAC	2.554	2.725	2.426	22.390	3.091	2.523
				PFAC	4.565	4.520	4.400	5.213	4.979	5.024
48	65.0	70.0	10.0	Mean	.835	-.893	.498	.010	.090	.255
				Max	2.106	.153	1.285	.186	.275	.657
				Min	.054	-2.490	.039	-.140	-.042	.049
				Rms	.281	.348	.166	.040	.045	.080
				GFAC	2.522	2.788	2.583	19.249	3.052	2.572
				PFAC	4.526	4.595	4.743	4.397	4.116	5.030

DATA FILE: SCT2

RUN #	WIND	TILT	VELOCITY	COMP:	FX	FY	FZ	MX	MY	MZ
43	65.0	80.0	10.0	Mean	.823	-.853	.265	.011	.043	.255
				Max	2.088	.104	.652	.167	.193	.708
				Min	.087	-2.295	-.003	-.161	-.086	.021
				Rms	.287	.362	.096	.037	.034	.087
				GFAC	2.536	2.689	2.461	15.159	4.523	2.782
				PFAC	4.413	3.984	4.024	4.162	4.421	5.236

Data File: SCT2

For Single Round Model

In the file labelled "SCT" the coefficient denoted by "MX" and "MY" are the base moment coefficients. However, in the files labelled "SCT1" and "SCT2" the coefficient of "MX" and "MY" are the hinge moment coefficients about the y-axis at the motor drive level.

Comment: MY is the hinge moment coefficient, C_{MHy} in data file: SCT2

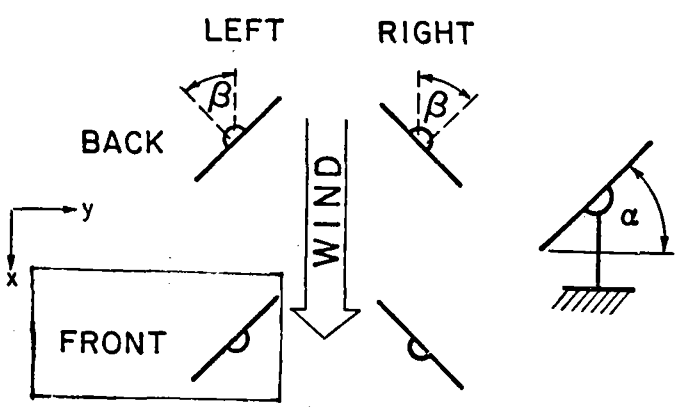

Single Heliostat

DATA FILE: SCT2

RUN #	WIND	TILT	VELOCITY	COMP:	FX	FY	FZ	MX	MY	MZ
57	.0	90.0	9.9	Mean	2.059	.043	.019	.017	.007	.047
				Max	4.507	.130	.193	.046	.232	.255
				Min	.609	-.043	-.111	-.004	-.231	-.154
				Rms	.584	.024	.047	.006	.048	.055
				GFAC	2.189	3.033	10.298	2.677	34.765	5.413
				PFAC	4.194	3.609	3.664	4.587	4.665	3.758
58	15.0	90.0	9.8	Mean	1.972	.621	-.032	.012	.009	-.016
				Max	4.230	1.276	.153	.059	.268	.180
				Min	.584	.206	-.189	-.049	-.181	-.261
				Rms	.553	.168	.049	.012	.046	.052
				GFAC	2.145	2.054	5.839	4.874	30.939	16.476
				PFAC	4.084	3.894	3.233	3.925	5.669	4.674
59	30.0	90.0	9.9	Mean	1.576	.959	-.015	.006	.015	-.061
				Max	3.381	2.024	.181	.067	.184	.144
				Min	.429	.275	-.155	-.088	-.106	-.235
				Rms	.467	.277	.045	.018	.036	.045
				GFAC	2.145	2.109	10.668	11.275	12.445	3.869
				PFAC	3.864	3.838	3.101	3.421	4.691	3.855
60	45.0	90.0	9.8	Mean	1.221	1.276	-.073	.008	.004	-.098
				Max	3.153	3.255	.093	.120	.153	.046
				Min	.326	.348	-.212	-.106	-.134	-.357
				Rms	.405	.416	.047	.026	.030	.050
				GFAC	2.582	2.551	2.891	16.006	43.289	3.636
				PFAC	4.767	4.761	2.975	4.274	4.950	5.131
61	55.0	90.0	10.0	Mean	.972	1.396	-.080	.002	.009	-.138
				Max	2.224	3.073	.069	.124	.122	.012

DATA FILE: SCT2

RUN #	WIND	TILT	VELOCITY	COMP:	FX	FY	FZ	MX	MY	MZ
				Min	.250	.358	-.310	-.132	-.103	-.470
				Rms	.322	.454	.047	.031	.026	.061
				GFAC	2.288	2.202	3.884	62.289	12.993	3.400
				PFAC	3.888	3.694	4.942	3.988	4.379	5.449
62	60.0	90.0	9.9	Mean	.820	1.438	-.072	-.004	.013	-.159
				Max	1.975	3.400	.091	.120	.127	.027
				Min	.069	.094	-.300	-.164	-.065	-.537
				Rms	.283	.492	.050	.034	.024	.072
				GFAC	2.408	2.364	4.162	44.472	9.800	3.387
				PFAC	4.083	3.988	4.593	4.656	4.700	5.267
63	70.0	90.0	10.0	Mean	.523	1.301	-.106	-.009	.011	-.191
				Max	1.361	3.518	.058	.152	.095	.009
				Min	.073	.033	-.265	-.199	-.071	-.565
				Rms	.193	.511	.052	.040	.019	.078
				GFAC	2.603	2.704	2.507	22.322	8.350	2.953
				PFAC	4.346	4.335	3.036	4.720	4.422	4.781
64	65.0	90.0	9.7	Mean	.646	1.418	-.036	-.011	.021	-.186
				Max	1.670	3.699	.121	.142	.153	.029
				Min	.059	.062	-.214	-.256	-.066	-.673
				Rms	.248	.559	.048	.041	.023	.086
				GFAC	2.586	2.609	5.892	23.530	7.142	3.613
				PFAC	4.136	4.083	3.725	6.018	5.611	5.641
65	75.0	90.0	10.0	Mean	.295	1.009	-.040	-.011	.009	-.165
				Max	.855	3.250	.117	.151	.079	.133
				Min	-.007	-.397	-.216	-.265	-.038	-.485
				Rms	.124	.522	.051	.045	.014	.089

DATA FILE: SCT2

RUN #	WIND	TILT	VELOCITY	COMP:	FX	FY	FZ	MX	MY	MZ
				GFAC	2.898	3.221	5.348	23.927	8.843	2.932
				PFAC	4.511	4.297	3.461	5.646	4.942	3.583
66	80.0	90.0	9.6	Mean	.171	.704	-.021	-.011	.005	-.120
				Max	.467	2.824	.161	.175	.056	.284
				Min	-.094	-.987	-.206	-.256	-.038	-.490
				Rms	.073	.511	.053	.049	.011	.102
				GFAC	2.726	4.011	9.789	23.667	12.473	4.086
				PFAC	4.037	4.151	3.490	4.968	4.746	3.640
67	90.0	90.0	10.2	Mean	.070	.140	.033	.002	-.003	.003
				Max	.166	2.186	.204	.194	.017	.292
				Min	-.023	-1.044	-.160	-.165	-.021	-.429
				Rms	.025	.411	.042	.044	.006	.102
				GFAC	2.376	15.616	6.211	120.417	7.619	101.983
				PFAC	3.788	4.974	4.033	4.385	3.236	2.848

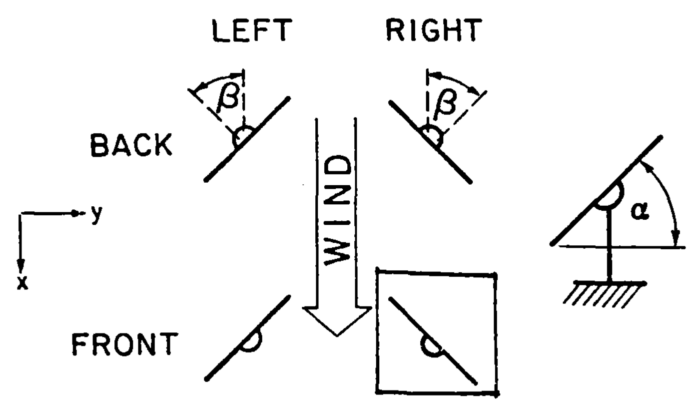

Single Heliostat

DATA FILE: SCT2

RUN #	WIND	TILT	VELOCITY	COMP:	FX	FY	FZ	MX	MY	MZ
68	15.0	90.0	9.7	Mean	1.952	-.401	.056	.022	.007	.095
				Max	4.423	-.075	.256	.097	.230	.319
				Min	.492	-.947	-.093	-.021	-.205	-.066
				Rms	.567	.131	.052	.014	.046	.054
				GFAC	2.266	2.359	4.599	4.324	31.901	3.353
				PFAC	4.358	4.168	3.859	5.448	4.870	4.178
69	30.0	90.0	9.9	Mean	1.612	-.782	.066	.017	.001	.133
				Max	4.063	-.178	.299	.118	.203	.413
				Min	.419	-2.066	-.100	-.055	-.148	-.036
				Rms	.476	.240	.052	.021	.039	.052
				GFAC	2.520	2.642	4.495	6.846	285.931	3.102
				PFAC	5.150	5.358	4.480	4.806	5.213	5.357
70	45.0	90.0	10.0	Mean	1.242	-1.125	.122	.020	.000	.159
				Max	2.711	.009	.332	.159	.153	.454
				Min	.020	-2.563	-.070	-.083	-.117	-.002
				Rms	.415	.391	.063	.030	.033	.058
				GFAC	2.184	2.278	2.726	8.082	2316.482	2.848
				PFAC	3.540	3.682	3.324	4.654	3.567	5.115
71	55.0	90.0	9.9	Mean	.978	-1.299	.158	.022	.011	.191
				Max	2.616	-.165	.446	.202	.141	.625
				Min	.140	-3.446	-.067	-.103	-.086	.000
				Rms	.353	.484	.071	.035	.027	.076
				GFAC	2.673	2.653	2.824	9.265	12.391	3.270
				PFAC	4.645	4.431	4.040	5.084	4.784	5.710
72	60.0	90.0	9.8	Mean	.808	-1.314	.210	.023	.016	.203
				Max	2.217	-.044	.511	.196	.124	.727

DATA FILE: SCT2

RUN #	WIND	TILT	VELOCITY	COMP:	FX	FY	FZ	MX	MY	MZ
				Min	.048	-3.733	-.027	-.140	-.085	-.009
				Rms	.306	.525	.080	.041	.026	.082
				GFAC	2.744	2.841	2.439	8.482	7.773	3.585
				PFAC	4.607	4.610	3.755	4.178	4.217	6.375
73	65.0	90.0	9.8	Mean	.694	-1.263	.180	.029	.005	.212
				Max	1.969	.303	.514	.231	.102	.629
				Min	-.128	-3.823	-.068	-.132	-.090	-.074
				Rms	.272	.547	.084	.044	.024	.088
				GFAC	2.839	3.028	2.854	8.027	18.608	2.961
				PFAC	4.690	4.681	3.987	4.605	4.116	4.720
75	70.0	90.0	9.8	Mean	.435	-.998	.177	.028	.000	.189
				Max	1.199	.466	.489	.234	.083	.576
				Min	-.095	-3.093	-.023	-.114	-.054	-.120
				Rms	.200	.571	.082	.048	.018	.097
				GFAC	2.757	3.099	2.756	8.361	357.589	3.049
				PFAC	3.812	3.667	3.815	4.300	4.642	3.975
76	80.0	90.0	9.7	Mean	.171	-.525	.079	.016	-.001	.107
				Max	.602	1.024	.423	.279	.051	.523
				Min	-.086	-2.715	-.183	-.180	-.035	-.299
				Rms	.092	.499	.076	.048	.010	.107
				GFAC	3.518	5.168	5.356	17.690	54.804	4.873
				PFAC	4.670	4.389	4.526	5.497	3.558	3.875
77	90.0	90.0	9.9	Mean	.069	.111	.009	.007	-.002	-.040
				Max	.164	1.793	.255	.175	.013	.366
				Min	-.003	-1.729	-.214	-.164	-.018	-.427
				Rms	.024	.409	.060	.044	.004	.098

Data File: SCT2

RUN #	WIND	TILT	VELOCITY	COMP:	FX	FY	FZ	MX	MY	MZ
				GFAC	2.388	16.100	29.071	26.156	11.428	10.610
				PFAC	3.900	4.109	4.089	3.858	4.679	3.966

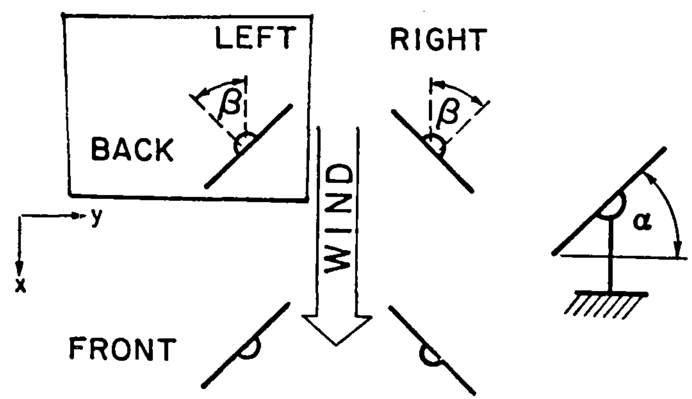

Single Heliostat

DATA FILE: SCT2

RUN #	WIND	TILT	VELOCITY	COMP:	FX	FY	FZ	MX	MY	MZ
78	.0	90.0	9.7	Mean	2.078	.105	-.058	.018	-.001	.062
				Max	4.836	.236	.139	.040	.194	.302
				Min	.645	-.002	-.291	-.002	-.175	-.132
				Rms	.593	.033	.064	.006	.046	.057
				GFAC	2.327	2.244	5.046	2.246	134.227	4.896
				PFAC	4.649	3.944	3.619	3.626	3.757	4.185
79	20.0	90.0	9.9	Mean	1.835	.771	-.198	.012	.000	-.032
				Max	3.873	1.594	.106	.083	.218	.163
				Min	.564	.234	-.513	-.054	-.191	-.227
				Rms	.511	.203	.086	.015	.041	.049
				GFAC	2.111	2.068	2.584	6.822	475.230	7.154
				PFAC	3.990	4.061	3.654	4.824	4.632	3.963
80	40.0	90.0	9.9	Mean	1.849	.744	-.121	.010	.002	-.019
				Max	3.618	1.455	.078	.067	.239	.193
				Min	.598	.296	-.379	-.056	-.155	-.200
				Rms	.492	.192	.071	.014	.043	.049
				GFAC	1.957	1.957	3.127	6.951	120.025	10.312
				PFAC	3.596	3.710	3.627	3.981	5.555	3.690
81	55.0	90.0	9.9	Mean	.936	1.338	-.169	-.006	.004	-.125
				Max	2.197	3.128	.057	.107	.128	.018
				Min	.093	.085	-.466	-.175	-.080	-.516
				Rms	.331	.476	.078	.033	.025	.065
				GFAC	2.348	2.338	2.751	31.589	31.393	4.111
				PFAC	3.807	3.759	3.792	5.078	5.007	5.974
82	60.0	90.0	9.8	Mean	.815	1.387	-.159	-.006	.008	-.164
				Max	2.066	3.521	.130	.135	.114	.041

Data File: SCT2

RUN #	WIND	TILT	VELOCITY	COMP:	FX	FY	FZ	MX	MY	MZ
				Min	.063	.044	-.470	-.180	-.090	-.508
				Rms	.288	.499	.076	.037	.023	.076
				GFAC	2.537	2.538	2.957	30.123	14.813	3.096
				PFAC	4.340	4.280	4.090	4.737	4.584	4.541
83	65.0	90.0	9.8	Mean	.700	1.316	-.154	-.013	.008	-.167
				Max	1.895	3.597	.089	.119	.117	.009
				Min	.059	.040	-.446	-.234	-.072	-.679
				Rms	.264	.510	.079	.038	.021	.082
				GFAC	2.705	2.733	2.892	18.388	14.160	4.058
				PFAC	4.527	4.472	3.714	5.764	5.134	6.216
84	70.0	90.0	10.1	Mean	.428	1.124	-.101	-.016	.009	-.184
				Max	1.249	3.382	.130	.120	.094	.032
				Min	-.011	-.173	-.488	-.230	-.050	-.660
				Rms	.177	.496	.072	.042	.016	.084
				GFAC	2.920	3.008	4.834	14.851	10.322	3.596
				PFAC	4.654	4.552	5.371	5.063	5.174	5.677
85	75.0	90.0	9.9	Mean	.348	1.020	-.106	-.016	.001	-.186
				Max	1.054	3.170	.108	.160	.064	.072
				Min	-.056	-.431	-.443	-.204	-.062	-.578
				Rms	.148	.495	.082	.045	.014	.086
				GFAC	3.033	3.107	4.175	12.429	65.432	3.099
				PFAC	4.762	4.344	4.122	4.140	4.463	4.546
86	80.0	90.0	9.9	Mean	.161	.687	-.051	-.010	.002	-.159
				Max	.476	2.488	.200	.155	.034	.172
				Min	-.043	-.812	-.307	-.213	-.031	-.508
				Rms	.080	.498	.072	.047	.009	.094

DATA FILE: SCT2

RUN #	WIND	TILT	VELOCITY	COMP:	FX	FY	FZ	MX	MY	MZ
				GFAC	2.951	3.621	5.970	22.211	19.867	3.203
				PFAC	3.937	3.619	3.566	4.287	3.662	3.738
88	85.0	90.0	9.6	Mean	.156	.621	-.046	-.004	.000	-.148
				Max	.470	2.825	.181	.167	.040	.164
				Min	-.018	-.918	-.322	-.240	-.027	-.590
				Rms	.067	.495	.070	.048	.008	.099
				GFAC	3.020	4.552	7.001	54.597	175.137	3.982
				PFAC	4.704	4.451	3.932	4.877	3.304	4.467
87	90.0	90.0	9.8	Mean	.067	.054	.025	.006	-.001	-.032
				Max	.207	1.811	.285	.200	.014	.361
				Min	-.034	-1.792	-.244	-.173	-.014	-.398
				Rms	.029	.455	.063	.046	.004	.107
				GFAC	3.096	33.482	11.618	33.431	14.916	12.644
				PFAC	4.826	3.863	4.151	4.216	3.341	3.436

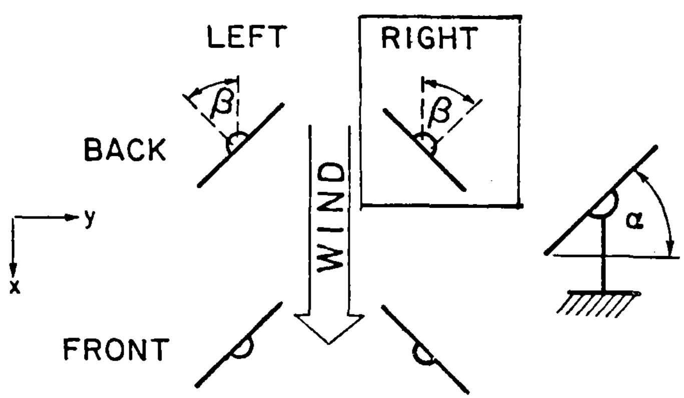

Single Heliostat

DATA FILE: SCT2

RUN #	WIND	TILT	VELOCITY	COMP:	FX	FY	FZ	MX	MY	MZ
89	20.0	90.0	9.8	Mean	1.832	-.547	-.049	.023	-.005	.125
				Max	3.632	-.046	.143	.094	.175	.371
				Min	.390	-1.206	-.249	-.034	-.147	-.054
				Rms	.526	.170	.056	.018	.044	.059
				GFAC	1.982	2.204	5.067	4.051	29.035	2.977
				PFAC	3.419	3.868	3.550	3.995	3.263	4.148
90	40.0	90.0	10.1	Mean	1.330	-.953	.049	.026	.000	.166
				Max	2.822	-.187	.179	.162	.162	.451
				Min	.302	-2.123	-.079	-.081	-.149	.032
				Rms	.424	.321	.040	.027	.033	.060
				GFAC	2.121	2.228	3.641	6.227	484.282	2.709
				PFAC	3.518	3.644	3.240	4.977	4.842	4.775
91	55.0	90.0	9.9	Mean	.916	-1.143	.110	.032	.001	.190
				Max	2.320	-.073	.283	.179	.101	.560
				Min	.130	-2.996	-.059	-.086	-.086	.000
				Rms	.326	.436	.044	.035	.024	.076
				GFAC	2.534	2.620	2.564	5.553	73.905	2.955
				PFAC	4.304	4.247	3.909	4.236	4.095	4.889
92	60.0	90.0	9.6	Mean	.865	-1.218	.094	.037	-.006	.217
				Max	2.305	.292	.295	.251	.141	.702
				Min	-.118	-3.478	-.065	-.110	-.093	-.044
				Rms	.330	.512	.050	.044	.026	.093
				GFAC	2.665	2.857	3.147	6.724	15.313	3.230
				PFAC	4.363	4.418	4.024	4.885	3.337	5.194
93	65.0	90.0	10.0	Mean	.639	-1.088	.118	.034	-.003	.222
				Max	1.704	.256	.371	.265	.111	.597

DATA FILE: SCT2

RUN #	WIND	TILT	VELOCITY	COMP:	FX	FY	FZ	MX	MY	MZ
				Min	-.057	-3.204	-.034	-.120	-.082	-.044
				Rms	.256	.495	.052	.043	.021	.090
				GFAC	2.664	2.944	3.150	7.894	31.030	2.693
				PFAC	4.162	4.275	4.830	5.406	3.775	4.159
94	70.0	90.0	9.8	Mean	.518	-1.033	.119	.029	-.004	.221
				Max	1.290	.297	.314	.215	.066	.618
				Min	-.038	-2.835	-.042	-.104	-.068	-.037
				Rms	.217	.503	.052	.045	.018	.095
				GFAC	2.490	2.744	2.636	7.397	15.176	2.797
				PFAC	3.554	3.583	3.759	4.172	3.495	4.179
95	75.0	90.0	9.7	Mean	.361	-.836	.102	.026	-.011	.213
				Max	1.093	.487	.303	.252	.054	.704
				Min	-.064	-2.975	-.073	-.107	-.058	-.099
				Rms	.166	.505	.054	.048	.015	.104
				GFAC	3.032	3.557	2.968	9.738	5.205	3.309
				PFAC	4.403	4.234	3.738	4.713	3.165	4.713
96	80.0	90.0	9.7	Mean	.191	-.534	.079	.016	-.008	.160
				Max	.715	.807	.315	.208	.034	.631
				Min	-.159	-2.909	-.073	-.167	-.048	-.179
				Rms	.110	.485	.051	.049	.011	.111
				GFAC	3.741	5.445	3.971	13.395	5.926	3.948
				PFAC	4.764	4.891	4.637	3.950	3.711	4.229
97	85.0	90.0	9.5	Mean	.120	-.272	.069	.015	-.009	.102
				Max	.476	1.169	.275	.236	.030	.585
				Min	-.117	-2.573	-.063	-.150	-.046	-.245
				Rms	.070	.448	.044	.049	.010	.109

DATA FILE: SCT2

RUN #	WIND	TILT	VELOCITY	COMP:	FX	FY	FZ	MX	MY	MZ
				GFAC	3.963	9.466	3.977	15.443	5.256	5.724
				PFAC	5.123	5.138	4.671	4.546	3.807	4.425

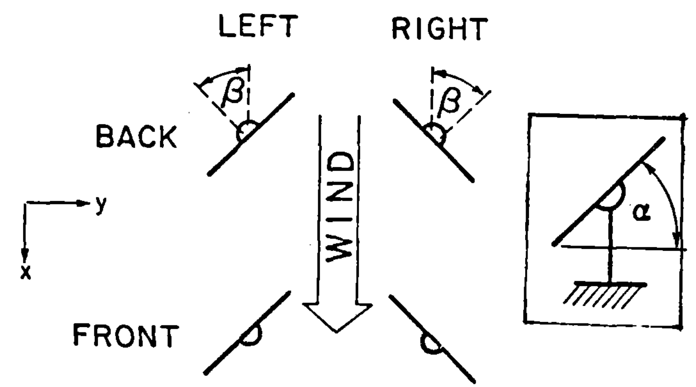

Single Heliostat

DATA FILE: SCT2

RUN #	WIND	TILT	VELOCITY	COMP:	FX	FY	FZ	MX	MY	MZ
98	65.0	75.0	9.6	Mean	.682	-1.210	-.198	.035	-.045	.205
				Max	1.764	.173	.052	.287	.037	.564
				Min	.000	-3.542	-.537	-.133	-.140	-.038
				Rms	.256	.531	.090	.049	.023	.087
				GFAC	2.584	2.926	2.719	8.157	3.128	2.751
				PFAC	4.225	4.394	3.778	5.118	4.075	4.111
99	65.0	60.0	9.8	Mean	.576	-.968	-.543	.028	-.095	.181
				Max	1.369	.385	.064	.286	.064	.510
				Min	-.015	-2.646	-1.409	-.165	-.249	-.077
				Rms	.213	.447	.226	.048	.039	.077
				GFAC	2.379	2.732	2.594	10.135	2.634	2.823
				PFAC	3.727	3.752	3.836	5.323	3.968	4.263
100	65.0	45.0	9.8	Mean	.422	-.626	-.648	.022	-.127	.139
				Max	1.043	.310	.260	.278	.055	.416
				Min	-.057	-1.974	-1.987	-.144	-.380	-.083
				Rms	.167	.339	.327	.052	.060	.066
				GFAC	2.474	3.151	3.068	12.871	2.994	2.990
				PFAC	3.717	3.980	4.091	4.930	4.190	4.173
101	65.0	30.0	9.7	Mean	.261	-.294	-.599	.015	-.117	.072
				Max	.750	.348	.287	.213	.085	.245
				Min	-.088	-1.127	-2.003	-.155	-.417	-.066
				Rms	.115	.202	.353	.047	.074	.045
				GFAC	2.869	3.835	3.342	14.285	3.562	3.404
				PFAC	4.246	4.114	3.980	4.219	4.080	3.860
102	65.0	15.0	9.6	Mean	.153	-.073	-.392	.010	-.075	.027
				Max	.513	.368	.553	.169	.188	.106

DATA FILE: SCT2

RUN #	WIND	TILT	VELOCITY	COMP:	FX	FY	FZ	MX	MY	MZ
				Min	-.079	-.468	-1.554	-.160	-.367	-.067
				Rms	.081	.097	.319	.040	.072	.022
				GFAC	3.351	6.422	3.961	17.599	4.921	3.963
				PFAC	4.424	4.051	3.643	3.957	4.040	3.520
103	65.0	.0	9.6	Mean	.096	.025	-.019	.002	.008	.010
				Max	.516	.218	.704	.155	.212	.029
				Min	-.300	-.221	-1.238	-.149	-.281	-.010
				Rms	.081	.042	.268	.028	.067	.006
				GFAC	5.360	8.874	63.917	91.723	27.376	2.970
				PFAC	5.200	4.555	4.545	5.404	3.045	3.286
104	65.0	15.0	9.6	Mean	.140	-.076	.405	.005	.104	.049
				Max	.851	.355	1.762	.187	.477	.171
				Min	-.254	-.696	-.767	-.161	-.242	-.069
				Rms	.105	.099	.264	.031	.074	.026
				GFAC	6.098	9.160	4.353	35.130	4.589	3.510
				PFAC	6.747	6.280	5.132	5.784	5.075	4.708
105	65.0	30.0	9.4	Mean	.247	-.297	.628	.010	.146	.107
				Max	1.187	.235	2.328	.212	.492	.301
				Min	-.253	-1.394	-.247	-.152	-.084	-.050
				Rms	.141	.193	.317	.040	.077	.048
				GFAC	4.801	4.693	3.708	22.059	3.364	2.811
				PFAC	6.654	5.669	5.365	5.076	4.488	4.073
106	65.0	45.0	9.7	Mean	.400	-.607	.757	.012	.147	.177
				Max	1.188	.182	2.135	.192	.424	.412
				Min	-.123	-1.876	.009	-.126	-.059	-.004
				Rms	.178	.279	.302	.040	.067	.063

DATA FILE: SCT2

RUN #	WIND	TILT	VELOCITY	COMP:	FX	FY	FZ	MX	MY	MZ
				GFAC	2.974	3.089	2.821	15.761	2.875	2.320
				PFAC	4.443	4.551	4.564	4.459	4.132	3.700
107	65.0	55.0	9.8	Mean	.528	-.844	.789	.020	.125	.220
				Max	1.561	.188	2.076	.270	.407	.534
				Min	-.075	-2.426	.020	-.137	-.094	-.021
				Rms	.220	.366	.291	.042	.059	.074
				GFAC	2.957	2.876	2.630	13.410	3.247	2.433
				PFAC	4.691	4.318	4.427	5.966	4.748	4.251
108	65.0	60.0	9.9	Mean	.573	-.946	.736	.020	.112	.222
				Max	1.714	.019	2.007	.247	.356	.567
				Min	-.039	-2.856	.117	-.192	-.093	.009
				Rms	.235	.403	.278	.042	.054	.077
				GFAC	2.991	3.018	2.727	12.650	3.184	2.549
				PFAC	4.863	4.737	4.572	5.400	4.525	4.477
109	65.0	65.0	9.5	Mean	.654	-1.087	.717	.019	.097	.246
				Max	1.834	.028	1.784	.218	.358	.607
				Min	-.008	-3.069	.064	-.156	-.080	.004
				Rms	.234	.438	.251	.046	.052	.085
				GFAC	2.804	2.824	2.490	11.660	3.687	2.464
				PFAC	4.640	4.525	4.262	4.361	4.963	4.217
110	65.0	70.0	9.6	Mean	.680	-1.143	.605	.024	.076	.249
				Max	1.725	-.017	1.495	.260	.321	.712
				Min	-.014	-2.947	.018	-.132	-.066	.010
				Rms	.268	.478	.220	.045	.045	.090
				GFAC	2.538	2.579	2.471	11.068	4.240	2.860
				PFAC	3.896	3.776	4.042	5.311	5.461	5.168

DATA FILE: SCT2

RUN #	WIND	TILT	VELOCITY	COMP:	FX	FY	FZ	MX	MY	MZ
111	65.0	75.0	10.0	Mean	.678	-1.146	.482	.023	.056	.235
				Max	1.761	.070	1.153	.290	.266	.608
				Min	-.021	-2.962	.017	-.148	-.086	.000
				Rms	.265	.471	.175	.042	.039	.089
				GFAC	2.599	2.584	2.393	12.876	4.746	2.583
				PFAC	4.096	3.858	3.839	6.418	5.424	4.168
112	65.0	80.0	9.6	Mean	.758	-1.264	.395	.027	.037	.252
				Max	1.874	.419	.941	.288	.221	.664
				Min	-.128	-3.120	.004	-.138	-.074	-.080
				Rms	.308	.549	.149	.048	.037	.102
				GFAC	2.473	2.467	2.386	10.622	5.993	2.634
				PFAC	3.619	3.380	3.672	5.488	4.999	4.045
113	65.0	85.0	9.8	Mean	.720	-1.202	.271	.028	.020	.238
				Max	1.939	.056	.688	.235	.150	.613
				Min	.013	-3.422	.012	-.141	-.084	-.039
				Rms	.285	.511	.097	.044	.029	.092
				GFAC	2.694	2.847	2.538	8.357	7.576	2.579
				PFAC	4.282	4.344	4.312	4.704	4.564	4.076
114	65.0	90.0	9.5	Mean	.723	-1.203	.154	.033	.004	.234
				Max	1.747	.249	.382	.255	.126	.780
				Min	-.056	-3.170	-.051	-.119	-.094	-.039
				Rms	.296	.539	.063	.046	.024	.098
				GFAC	2.417	2.635	2.484	7.625	29.998	3.340
				PFAC	3.458	3.647	3.630	4.869	5.018	5.595

Data File: SCT2

For Field Study

In the file labelled "SCT" the coefficient denoted by "MX" and "MY" are the base moment coefficients. However, in the files labelled "SCT1" and "SCT2" the coefficient of "MX" and "MY" are the hinge moment coefficients about the y-axis at the motor drive level.

Comment: MY is the hinge moment coefficient, C_{MHy} in data file: SCT2

DATA FILE: SCT2

RUN #	WIND	TILT	VELOCITY	COMP:	FX	FY	FZ	MX	MY	MZ
129	60.0	60.0	10.3	Mean	.664	-.737	.582	.008	.109	.224
				Max	1.131	-.384	.963	.089	.210	.340
				Min	.377	-1.286	.334	-.077	.032	.122
				Rms	.107	.131	.090	.021	.024	.032
				GFAC	1.703	1.746	1.655	11.488	1.931	1.519
				PFAC	4.353	4.181	4.257	3.799	4.210	3.621
130	60.0	60.0	9.9	Mean	.046	-.004	.067	.012	.009	.023
				Max	.239	.269	.231	.119	.079	.077
				Min	-.167	-.283	-.112	-.052	-.042	-.028
				Rms	.048	.065	.042	.017	.015	.012
				GFAC	5.143	69.114	3.453	9.646	8.460	3.379
				PFAC	4.005	4.305	3.914	6.314	4.829	4.377
131	60.0	60.0	9.8	Mean	.534	-.561	.469	.002	.108	.219
				Max	.948	-.224	.815	.074	.211	.348
				Min	.219	-1.065	.276	-.071	.025	.100
				Rms	.092	.108	.071	.020	.024	.033
				GFAC	1.776	1.900	1.740	47.763	1.956	1.593
				PFAC	4.482	4.667	4.899	3.598	4.338	3.975
132	60.0	60.0	9.6	Mean	.089	-.063	.124	.016	.017	.031
				Max	.488	.229	.371	.157	.157	.113
				Min	-.098	-.505	-.034	-.065	-.039	-.022
				Rms	.060	.083	.054	.020	.018	.017
				GFAC	5.501	7.981	3.001	9.601	9.094	3.602
				PFAC	6.650	5.329	4.582	6.984	7.596	4.797
133	60.0	60.0	9.7	Mean	.377	-.349	.332	.003	.097	.168
				Max	.804	-.018	.654	.136	.244	.323

DATA FILE: SCT2

RUN #	WIND	TILT	VELOCITY	COMP:	FX	FY	FZ	MX	MY	MZ
				Min	.088	-.830	.136	-.085	-.003	.051
				Rms	.102	.111	.074	.027	.033	.038
				GFAC	2.131	2.380	1.967	51.076	2.525	1.924
				PFAC	4.166	4.340	4.354	4.918	4.537	4.101
134	60.0	60.0	9.7	Mean	.138	-.121	.166	.016	.035	.052
				Max	.464	.162	.412	.135	.163	.176
				Min	-.075	-.542	-.012	-.052	-.028	-.007
				Rms	.074	.097	.065	.022	.024	.026
				GFAC	3.351	4.470	2.491	8.626	4.698	3.367
				PFAC	4.376	4.334	3.813	5.307	5.433	4.788
135	60.0	60.0	9.7	Mean	.122	-.102	.155	.015	.032	.046
				Max	.472	.166	.461	.133	.151	.189
				Min	-.079	-.573	-.039	-.084	-.025	-.019
				Rms	.072	.096	.064	.022	.023	.024
				GFAC	3.874	5.612	2.979	8.647	4.691	4.121
				PFAC	4.847	4.924	4.811	5.273	5.221	5.962
136	60.0	60.0	9.8	Mean	.296	-.227	.243	.006	.075	.124
				Max	.719	.142	.534	.116	.214	.275
				Min	.013	-.757	.035	-.078	-.021	.006
				Rms	.102	.108	.072	.025	.032	.038
				GFAC	2.427	3.331	2.195	20.570	2.865	2.212
				PFAC	4.152	4.895	4.059	4.494	4.378	4.008
137	60.0	60.0	9.5	Mean	.291	-.171	.181	-.001	.069	.133
				Max	.703	.148	.457	.144	.218	.283
				Min	.048	-.632	.006	-.100	-.021	.016
				Rms	.090	.103	.064	.027	.030	.035

DATA FILE: SCT2

RUN #	WIND	TILT	VELOCITY	COMP:	FX	FY	FZ	MX	MY	MZ
				GFAC	2.417	3.705	2.519	111.601	3.172	2.129
				PFAC	4.580	4.485	4.333	3.628	4.974	4.275
138	60.0	60.0	9.8	Mean	.196	-.193	.184	.013	.045	.079
				Max	.692	.129	.534	.146	.207	.232
				Min	-.044	-.749	-.045	-.060	-.022	-.009
				Rms	.088	.116	.078	.024	.026	.031
				GFAC	3.529	3.881	2.906	11.529	4.651	2.919
				PFAC	5.612	4.802	4.514	5.535	6.189	4.907
139	60.0	60.0	9.7	Mean	.225	-.207	.164	.019	.046	.076
				Max	.674	.083	.441	.159	.172	.216
				Min	-.005	-.724	-.043	-.070	-.024	-.007
				Rms	.092	.118	.079	.026	.028	.032
				GFAC	3.001	3.492	2.694	8.549	3.757	2.832
				PFAC	4.883	4.387	3.533	5.476	4.475	4.357
140	60.0	60.0	9.7	Mean	.252	-.134	.123	-.001	.052	.103
				Max	.525	.101	.329	.126	.169	.223
				Min	.040	-.493	-.014	-.071	-.025	.022
				Rms	.072	.084	.049	.023	.024	.027
				GFAC	2.085	3.691	2.686	110.462	3.264	2.166
				PFAC	3.786	4.267	4.184	3.036	4.854	4.446
141	60.0	60.0	9.7	Mean	.515	-.544	.442	.004	.100	.194
				Max	.878	-.190	.791	.084	.207	.295
				Min	.250	-1.046	.217	-.068	.022	.096
				Rms	.088	.110	.072	.020	.022	.028
				GFAC	1.705	1.922	1.789	19.256	2.074	1.520
				PFAC	4.128	4.553	4.854	4.065	4.875	3.673

DATA FILE: SCT2

RUN #	WIND	TILT	VELOCITY	COMP:	FX	FY	FZ	MX	MY	MZ
142	60.0	60.0	9.8	Mean	.156	-.162	.176	.015	.039	.059
				Max	.574	.218	.515	.132	.162	.197
				Min	-.064	-.711	-.034	-.084	-.034	-.022
				Rms	.085	.114	.075	.025	.026	.027
				GFAC	3.665	4.399	2.919	8.606	4.166	3.366
				PFAC	4.914	4.829	4.530	4.676	4.816	5.076
143	60.0	60.0	9.7	Mean	.403	-.440	.373	.004	.082	.158
				Max	.962	-.012	.796	.120	.220	.330
				Min	.098	-1.130	.105	-.082	-.024	.046
				Rms	.111	.136	.092	.026	.030	.037
				GFAC	2.386	2.571	2.136	29.823	2.692	2.087
				PFAC	5.019	5.083	4.610	4.420	4.569	4.617
144	60.0	60.0	9.7	Mean	.266	-.292	.268	.012	.058	.105
				Max	.732	.090	.619	.124	.209	.296
				Min	-.020	-.845	.019	-.063	-.020	-.015
				Rms	.104	.134	.089	.025	.029	.036
				GFAC	2.749	2.894	2.309	10.627	3.601	2.819
				PFAC	4.478	4.124	3.929	4.586	5.216	5.364
145	60.0	60.0	9.6	Mean	.243	-.266	.245	.013	.054	.093
				Max	.737	.095	.582	.176	.195	.226
				Min	-.011	-.782	.027	-.068	-.019	.008
				Rms	.102	.131	.087	.026	.029	.034
				GFAC	3.029	2.936	2.379	13.589	3.620	2.429
				PFAC	4.855	3.933	3.879	6.387	4.916	3.907
146	60.0	60.0	9.8	Mean	.347	-.370	.320	.010	.081	.136
				Max	.924	.066	.724	.113	.225	.322
				Min	.010	-1.020	.052	-.081	-.022	.015
				Rms	.126	.146	.097	.027	.033	.042

Data File: SCT2

RUN #	WIND	TILT	VELOCITY	COMP:	FX	FY	FZ	MX	MY	MZ
				GFAC	2.666	2.759	2.258	11.334	2.772	2.373
				PFAC	4.601	4.457	4.145	3.776	4.403	4.442
147	60.0	60.0	9.6	Mean	.392	-.388	.343	.007	.087	.169
				Max	.831	-.013	.688	.113	.217	.313
				Min	.110	-.919	.101	-.085	-.006	.058
				Rms	.097	.121	.078	.024	.027	.034
				GFAC	2.118	2.369	2.009	15.947	2.505	1.850
				PFAC	4.507	4.391	4.428	4.477	4.865	4.220
148	60.0	60.0	9.5	Mean	.389	-.420	.366	.009	.081	.154
				Max	.843	.028	.754	.125	.209	.315
				Min	.084	-1.000	.098	-.103	.000	.046
				Rms	.124	.155	.105	.026	.032	.043
				GFAC	2.167	2.379	2.058	13.711	2.587	2.043
				PFAC	3.670	3.731	3.677	4.403	3.966	3.767
149	60.0	60.0	9.5	Mean	.370	-.368	.296	.010	.072	.139
				Max	1.045	.035	.876	.152	.229	.391
				Min	.045	-1.176	.049	-.083	-.014	.029
				Rms	.113	.145	.097	.024	.031	.042
				GFAC	2.822	3.192	2.957	15.500	3.180	2.823
				PFAC	5.993	5.551	5.956	5.929	5.110	6.085
137	60.0	60.0	9.7	Mean	.366	-.297	.255	.015	.085	.145
				Max	.859	.017	.654	.111	.190	.298
				Min	.123	-.929	.067	-.059	.006	.038
				Rms	.088	.111	.070	.022	.026	.033
				GFAC	2.347	3.133	2.562	7.405	2.240	2.057
				PFAC	5.582	5.704	5.730	4.289	4.007	4.604

DATA FILE: SCT2

RUN #	WIND	TILT	VELOCITY	COMP:	FX	FY	FZ	MX	MY	MZ
138	60.0	90.0	9.7	Mean	.384	-.352	.053	.031	.017	.157
				Max	1.015	.034	.134	.140	.110	.384
				Min	.100	-1.203	-.003	-.051	-.038	.037
				Rms	.099	.138	.017	.022	.017	.042
				GFAC	2.641	3.418	2.520	4.466	6.448	2.447
				PFAC	6.378	6.157	4.640	4.938	5.404	5.414
139	60.0	90.0	9.5	Mean	.417	-.436	.060	.028	.017	.168
				Max	1.090	.031	.150	.142	.104	.421
				Min	.071	-1.301	.000	-.066	-.062	.025
				Rms	.154	.199	.022	.024	.018	.062
				GFAC	2.617	2.981	2.512	4.977	6.014	2.501
				PFAC	4.365	4.345	4.128	4.678	4.733	4.057
140	60.0	90.0	9.4	Mean	.434	-.483	.077	.023	.021	.180
				Max	1.200	.010	.207	.135	.104	.442
				Min	.080	-1.471	.011	-.063	-.047	.020
				Rms	.153	.197	.024	.024	.018	.058
				GFAC	2.764	3.044	2.680	5.986	4.922	2.454
				PFAC	5.019	5.010	5.317	4.748	4.639	4.535
141	60.0	90.0	9.7	Mean	.461	-.505	.080	.025	.017	.207
				Max	1.063	.091	.167	.111	.081	.441
				Min	.064	-1.187	.005	-.065	-.054	.039
				Rms	.126	.170	.022	.023	.018	.049
				GFAC	2.305	2.350	2.094	4.338	4.844	2.127
				PFAC	4.784	4.016	3.986	3.694	3.538	4.750
142	60.0	90.0	9.7	Mean	.408	-.510	.064	.034	-.001	.109
				Max	.816	-.052	.144	.126	.054	.344

DATA FILE: SCT2

RUN #	WIND	TILT	VELOCITY	COMP:	FX	FY	FZ	MX	MY	MZ
				Min	.175	-1.314	.000	-.049	-.060	-.022
				Rms	.088	.173	.020	.024	.014	.047
				GFAC	1.998	2.574	2.256	3.676	47.446	3.165
				PFAC	4.627	4.632	3.938	3.840	4.316	4.959
143	60.0	90.0	9.4	Mean	.401	-.574	.077	.028	.003	.138
				Max	1.052	-.002	.178	.161	.085	.401
				Min	.068	-1.701	.006	-.063	-.051	-.008
				Rms	.127	.237	.025	.026	.015	.058
				GFAC	2.626	2.961	2.294	5.666	25.392	2.911
				PFAC	5.116	4.743	3.963	5.045	5.435	4.562
144	60.0	90.0	9.2	Mean	.379	-.468	.034	.028	.000	.089
				Max	.904	.058	.120	.151	.054	.359
				Min	.126	-1.469	-.043	-.056	-.057	-.082
				Rms	.116	.221	.023	.027	.014	.057
				GFAC	2.383	3.140	3.558	5.394	114.446	4.013
				PFAC	4.514	4.538	3.694	4.593	3.777	4.696
145	60.0	90.0	9.6	Mean	.349	-.298	.015	.045	.008	.032
				Max	.641	.112	.073	.119	.055	.232
				Min	.118	-.976	-.043	-.050	-.042	-.090
				Rms	.075	.142	.018	.023	.013	.042
				GFAC	1.840	3.273	5.014	2.629	6.756	7.283
				PFAC	3.905	4.788	3.306	3.269	3.572	4.810
146	65.0	90.0	9.6	Mean	.208	-.114	-.001	.018	.005	-.017
				Max	.576	.199	.066	.129	.059	.166
				Min	.031	-.733	-.065	-.069	-.039	-.122
				Rms	.061	.112	.018	.022	.012	.033

DATA FILE: SCT2

RUN #	WIND	TILT	VELOCITY	COMP:	FX	FY	FZ	MX	MY	MZ
				GFAC	2.767	6.441	120.313	7.257	10.910	7.080
				PFAC	6.071	5.547	3.593	5.175	4.281	3.184
147	65.0	90.0	9.6	Mean	.209	-.283	.037	.026	.004	.058
				Max	.670	.207	.145	.186	.091	.271
				Min	-.002	-1.269	-.045	-.084	-.052	-.047
				Rms	.090	.168	.023	.026	.013	.038
				GFAC	3.199	4.487	3.941	7.188	21.193	4.698
				PFAC	5.768	5.886	4.645	6.105	6.909	5.629
148	65.0	90.0	9.7	Mean	.193	-.283	.064	.025	.006	.063
				Max	.581	.179	.170	.178	.069	.265
				Min	-.005	-1.022	-.019	-.086	-.042	-.037
				Rms	.083	.178	.025	.027	.013	.040
				GFAC	3.011	3.608	2.659	7.229	11.155	4.210
				PFAC	4.681	4.141	4.247	5.596	4.780	5.040
149	65.0	90.0	9.7	Mean	.223	-.173	.051	.016	.007	.006
				Max	.467	.183	.129	.115	.059	.186
				Min	.032	-.796	-.015	-.068	-.039	-.119
				Rms	.063	.120	.018	.024	.014	.035
				GFAC	2.089	4.601	2.526	7.272	7.989	32.737
				PFAC	3.840	5.215	4.218	4.162	3.610	5.162
150	65.0	90.0	9.8	Mean	.335	-.417	.065	.013	.005	.103
				Max	.670	-.013	.143	.133	.070	.268
				Min	.091	-1.029	.003	-.069	-.053	-.022
				Rms	.076	.147	.020	.026	.017	.045
				GFAC	1.999	2.465	2.184	9.942	13.853	2.606
				PFAC	4.421	4.155	3.947	4.601	3.750	3.654

DATA FILE: SCT2

RUN #	WIND	TILT	VELOCITY	COMP:	FX	FY	FZ	MX	MY	MZ
151	65.0	90.0	9.7	Mean	.150	-.212	.066	.026	.007	.053
				Max	.516	.200	.156	.170	.070	.228
				Min	-.065	-.883	-.024	-.058	-.034	-.030
				Rms	.069	.144	.024	.025	.012	.031
				GFAC	3.431	4.172	2.370	6.487	9.784	4.339
				PFAC	5.278	4.667	3.701	5.667	5.100	5.687
152	65.0	90.0	9.6	Mean	.147	-.210	.075	.025	.006	.051
				Max	.484	.176	.175	.141	.061	.247
				Min	-.027	-.938	.007	-.064	-.049	-.031
				Rms	.069	.142	.023	.026	.013	.031
				GFAC	3.282	4.469	2.323	5.753	11.020	4.838
				PFAC	4.862	5.125	4.290	4.545	4.450	6.243
153	65.0	90.0	9.6	Mean	.254	-.292	.069	.013	.009	.070
				Max	.625	.095	.173	.126	.077	.247
				Min	.055	-.912	-.005	-.064	-.042	-.067
				Rms	.070	.138	.020	.023	.015	.042
				GFAC	2.466	3.124	2.493	9.882	8.549	3.545
				PFAC	5.325	4.490	5.127	4.822	4.601	4.239
154	65.0	90.0	9.6	Mean	.276	.364	-.078	-.001	.002	-.030
				Max	.546	1.030	.000	.090	.061	.068
				Min	.103	-.020	-.164	-.132	-.043	-.203
				Rms	.057	.127	.024	.024	.014	.035
				GFAC	1.979	2.831	2.009	143.352	30.773	6.799
				PFAC	4.719	5.230	3.584	5.351	4.301	4.942
155	65.0	90.0	9.6	Mean	.202	.410	-.007	-.016	.009	-.058
				Max	.598	1.326	.073	.082	.069	.061

DATA FILE: SCT2

RUN #	WIND	TILT	VELOCITY	COMP:	FX	FY	FZ	MX	MY	MZ
				Min	-.004	-.106	-.126	-.159	-.031	-.295
				Rms	.076	.182	.028	.026	.013	.039
				GFAC	2.962	3.231	17.674	9.856	7.265	5.089
				PFAC	5.235	5.036	4.210	5.462	4.707	6.043
156	65.0	90.0	9.7	Mean	.181	.394	-.024	-.015	.011	-.056
				Max	.507	1.152	.072	.070	.074	.059
				Min	-.005	-.063	-.148	-.128	-.030	-.245
				Rms	.073	.176	.028	.025	.012	.037
				GFAC	2.802	2.923	6.235	8.695	6.943	4.400
				PFAC	4.477	4.319	4.384	4.555	5.139	5.074
157	65.0	90.0	9.7	Mean	.285	.411	-.013	-.010	.005	-.049
				Max	.577	1.018	.061	.066	.075	.066
				Min	.071	.044	-.104	-.126	-.056	-.242
				Rms	.061	.138	.022	.026	.015	.038
				GFAC	2.020	2.478	7.906	12.825	15.157	4.947
				PFAC	4.780	4.404	4.174	4.415	4.569	5.030
158	60.0	60.0	9.7	Mean	.491	-.356	.343	.015	.124	.194
				Max	1.032	.007	.701	.132	.262	.376
				Min	.118	-.855	.071	-.069	-.002	.030
				Rms	.124	.128	.091	.028	.037	.043
				GFAC	2.104	2.404	2.042	8.858	2.111	1.943
				PFAC	4.383	3.907	3.933	4.229	3.701	4.234
159	60.0	60.0	9.7	Mean	.396	-.352	.325	.012	.085	.133
				Max	.986	.036	.730	.132	.247	.306
				Min	.026	-1.042	.057	-.079	.001	.023
				Rms	.121	.130	.090	.027	.033	.039

DATA FILE: SCT2

RUN #	WIND	TILT	VELOCITY	COMP:	FX	FY	FZ	MX	MY	MZ
				GFAC	2.488	2.960	2.249	10.959	2.895	2.291
				PFAC	4.857	5.314	4.482	4.406	4.836	4.425
160	60.0	60.0	9.6	Mean	.398	-.358	.345	.007	.075	.137
				Max	.961	-.001	.695	.144	.243	.279
				Min	.053	-.950	.100	-.077	-.015	.023
				Rms	.117	.128	.087	.027	.031	.036
				GFAC	2.417	2.655	2.017	21.800	3.217	2.037
				PFAC	4.828	4.641	4.025	5.034	5.339	3.963
161	60.0	60.0	9.7	Mean	.453	-.356	.360	.005	.102	.181
				Max	.965	.008	.698	.112	.247	.352
				Min	.125	-.916	.113	-.106	.011	.051
				Rms	.128	.127	.089	.027	.035	.045
				GFAC	2.131	2.574	1.941	21.113	2.416	1.939
				PFAC	4.014	4.403	3.784	4.010	4.101	3.828
162	60.0	90.0	9.7	Mean	.527	-.442	.085	.032	.015	.241
				Max	1.112	.132	.158	.166	.117	.477
				Min	.053	-1.154	.014	-.076	-.071	.067
				Rms	.140	.169	.022	.031	.024	.056
				GFAC	2.111	2.610	1.863	5.128	7.956	1.977
				PFAC	4.190	4.218	3.350	4.332	4.333	4.197
163	60.0	90.0	9.7	Mean	.532	-.476	.044	.038	.024	.170
				Max	1.203	.008	.132	.170	.107	.380
				Min	.141	-1.224	-.025	-.044	-.062	.031
				Rms	.147	.174	.024	.028	.022	.049
				GFAC	2.263	2.571	3.014	4.435	4.454	2.231
				PFAC	4.574	4.303	3.710	4.666	3.709	4.271

DATA FILE: SCT2

RUN #	WIND	TILT	VELOCITY	COMP:	FX	FY	FZ	MX	MY	MZ
164	60.0	90.0	9.5	Mean	.546	-.515	.073	.042	.032	.194
				Max	1.278	.084	.173	.178	.159	.399
				Min	.076	-1.422	-.005	-.057	-.053	.008
				Rms	.167	.200	.025	.031	.025	.058
				GFAC	2.341	2.760	2.355	4.204	4.901	2.056
				PFAC	4.381	4.536	4.020	4.435	5.111	3.551
165	60.0	90.0	9.6	Mean	.583	-.496	.075	.050	.039	.272
				Max	1.219	.087	.185	.212	.154	.500
				Min	.099	-1.179	-.005	-.057	-.062	.076
				Rms	.166	.198	.024	.035	.028	.066
				GFAC	2.093	2.378	2.475	4.240	3.975	1.837
				PFAC	3.843	3.456	4.534	4.586	4.184	3.437
166	60.0	90.0	9.8	Mean	.597	-.555	.079	.041	.028	.259
				Max	1.156	-.080	.153	.179	.139	.469
				Min	.189	-1.188	.022	-.057	-.064	.110
				Rms	.131	.158	.020	.033	.026	.048
				GFAC	1.938	2.140	1.933	4.383	5.019	1.808
				PFAC	4.258	4.008	3.666	4.226	4.297	4.343
167	60.0	90.0	9.7	Mean	.467	-.424	.063	.025	.019	.203
				Max	.946	-.021	.130	.132	.112	.356
				Min	.111	-1.109	.007	-.058	-.057	.015
				Rms	.107	.133	.019	.027	.022	.043
				GFAC	2.026	2.618	2.057	5.355	5.888	1.751
				PFAC	4.466	5.152	3.485	3.971	4.195	3.560
168	60.0	90.0	9.7	Mean	.442	-.386	.058	.023	.018	.120
				Max	1.086	.062	.147	.148	.145	.276

DATA FILE: SCT2

RUN #	WIND	TILT	VELOCITY	COMP:	FX	FY	FZ	MX	MY	MZ
				Min	.117	-1.202	-.015	-.068	-.050	.022
				Rms	.130	.150	.022	.028	.022	.039
				GFAC	2.455	3.112	2.558	6.497	8.037	2.309
				PFAC	4.946	5.445	3.994	4.460	5.682	4.015
169	60.0	90.0	9.6	Mean	.482	-.433	.051	.024	.019	.137
				Max	1.153	.158	.136	.142	.123	.333
				Min	.070	-1.273	-.020	-.092	-.085	.007
				Rms	.144	.169	.023	.029	.023	.045
				GFAC	2.394	2.941	2.666	5.845	6.504	2.426
				PFAC	4.666	4.980	3.686	4.022	4.563	4.362
170	60.0	90.0	9.7	Mean	.682	-.621	.071	.029	.022	.227
				Max	1.123	-.138	.138	.135	.087	.391
				Min	.240	-1.199	.009	-.044	-.039	.080
				Rms	.119	.141	.020	.021	.017	.042
				GFAC	1.647	1.930	1.931	4.655	3.952	1.718
				PFAC	3.714	4.099	3.329	5.047	3.927	3.870
171	60.0	90.0	9.6	Mean	.377	-.317	.047	.015	.014	.097
				Max	.951	.158	.126	.119	.097	.278
				Min	.041	-1.034	-.019	-.075	-.061	.015
				Rms	.115	.141	.021	.025	.020	.033
				GFAC	2.519	3.265	2.650	7.945	6.891	2.855
				PFAC	5.000	5.081	3.664	4.128	4.173	5.406
172	60.0	90.0	9.8	Mean	.653	-.571	.069	.017	.012	.177
				Max	1.070	-.193	.132	.080	.064	.290
				Min	.358	-1.075	.010	-.046	-.029	.086
				Rms	.115	.132	.018	.017	.013	.031

DATA FILE: SCT2

RUN #	WIND	TILT	VELOCITY	COMP:	FX	FY	FZ	MX	MY	MZ
				GFAC	1.639	1.881	1.905	4.723	5.239	1.635
				PFAC	3.640	3.816	3.412	3.745	3.890	3.665
173	65.0	90.0	9.8	Mean	.457	1.108	-.094	-.016	.013	-.192
				Max	.769	1.807	-.033	.060	.056	-.071
				Min	.217	.519	-.165	-.096	-.025	-.319
				Rms	.079	.187	.022	.019	.012	.039
				GFAC	1.684	1.631	1.743	5.905	4.300	1.663
				PFAC	3.948	3.734	3.197	4.245	3.602	3.230
174	65.0	90.0	9.6	Mean	.299	.457	-.027	.007	-.002	-.052
				Max	.501	.978	.034	.090	.059	.068
				Min	.141	.107	-.097	-.097	-.047	-.180
				Rms	.053	.125	.019	.024	.014	.035
				GFAC	1.676	2.138	3.555	13.274	25.080	3.487
				PFAC	3.777	4.152	3.669	3.422	3.327	3.699
175	65.0	90.0	9.6	Mean	.254	.306	-.018	-.014	-.001	.008
				Max	.480	.841	.044	.061	.048	.137
				Min	.038	-.175	-.102	-.126	-.041	-.145
				Rms	.052	.126	.020	.024	.013	.034
				GFAC	1.887	2.752	5.597	9.151	29.068	16.188
				PFAC	4.303	4.265	4.173	4.732	3.058	3.725
176	65.0	90.0	9.6	Mean	.262	.293	-.019	-.030	.004	.003
				Max	.520	.919	.054	.071	.056	.159
				Min	.083	-.181	-.102	-.156	-.033	-.181
				Rms	.061	.174	.023	.028	.013	.050
				GFAC	1.987	3.137	5.312	5.141	13.551	45.852
				PFAC	4.266	3.596	3.519	4.564	4.064	3.095

Data File: SCT2

RUN #	WIND	TILT	VELOCITY	COMP:	FX	FY	FZ	MX	MY	MZ
177	60.0	90.0	9.7	Mean	.325	-.313	.046	.027	.015	.073
				Max	.699	.250	.138	.163	.084	.306
				Min	-.005	-1.052	-.029	-.085	-.040	-.080
				Rms	.104	.197	.025	.032	.016	.059
				GFAC	2.152	3.366	2.972	6.032	5.609	4.165
				PFAC	3.599	3.748	3.726	4.292	4.220	3.954
178	60.0	90.0	9.6	Mean	.393	-.452	.062	.033	.008	.099
				Max	.863	.125	.163	.169	.071	.308
				Min	.143	-1.352	-.010	-.065	-.057	-.066
				Rms	.086	.172	.024	.032	.016	.048
				GFAC	2.196	2.988	2.628	5.092	8.552	3.122
				PFAC	5.497	5.236	4.159	4.316	3.842	4.384
179	60.0	90.0	9.7	Mean	.493	-.726	.084	.033	.014	.187
				Max	.901	-.170	.184	.138	.072	.374
				Min	.230	-1.512	.009	-.051	-.046	.037
				Rms	.095	.183	.024	.023	.013	.046
				GFAC	1.829	2.082	2.179	4.225	5.093	2.005
				PFAC	4.308	4.281	4.087	4.514	4.338	4.113
180	60.0	90.0	9.8	Mean	.563	-.952	.118	.025	.003	.176
				Max	.978	-.417	.200	.099	.048	.359
				Min	.293	-1.650	.031	-.056	-.045	.073
				Rms	.098	.178	.024	.018	.011	.038
				GFAC	1.736	1.734	1.701	3.955	16.559	2.042
				PFAC	4.226	3.914	3.504	4.094	4.095	4.771
181	60.0	90.0	9.7	Mean	.652	-.613	.076	.014	.008	.179
				Max	1.074	-.203	.128	.087	.058	.304

DATA FILE: SCT2

RUN #	WIND	TILT	VELOCITY	COMP:	FX	FY	FZ	MX	MY	MZ
				Min	.336	-1.146	.018	-.039	-.033	.082
				Rms	.113	.138	.017	.016	.012	.032
				GFAC	1.649	1.869	1.692	6.088	6.956	1.704
				PFAC	3.731	3.848	3.126	4.516	4.208	3.931
182	60.0	90.0	9.7	Mean	.652	-.639	.072	.028	.018	.230
				Max	1.065	-.181	.148	.116	.082	.403
				Min	.226	-1.146	.009	-.033	-.032	.075
				Rms	.114	.142	.019	.019	.014	.045
				GFAC	1.634	1.792	2.071	4.115	4.618	1.752
				PFAC	3.638	3.575	4.040	4.701	4.623	3.865
183	60.0	90.0	9.6	Mean	.561	-.523	.065	.046	.025	.253
				Max	1.090	-.013	-.128	.171	.107	.452
				Min	.147	-1.199	.002	-.060	-.065	.060
				Rms	.119	.152	.020	.030	.022	.051
				GFAC	1.943	2.294	1.966	3.755	4.335	1.788
				PFAC	4.439	4.445	3.072	4.140	3.747	3.906
184	60.0	90.0	9.6	Mean	.512	-.430	.060	.048	.028	.248
				Max	1.181	.038	.152	.172	.110	.471
				Min	.092	-1.330	-.008	-.057	-.043	.072
				Rms	.146	.186	.022	.033	.023	.064
				GFAC	2.306	3.094	2.548	3.539	3.894	1.901
				PFAC	4.583	4.831	4.219	3.731	3.567	3.468
185	65.0	90.0	9.7	Mean	.376	.501	-.038	-.033	.033	-.180
				Max	.773	1.087	.038	.053	.113	-.063
				Min	.127	.049	-.119	-.161	-.019	-.367
				Rms	.093	.165	.025	.030	.019	.044

DATA FILE: SCT2

RUN #	WIND	TILT	VELOCITY	COMP:	FX	FY	FZ	MX	MY	MZ
				GFAC	2.056	2.171	3.170	4.864	3.407	2.044
				PFAC	4.246	3.560	3.290	4.313	4.236	4.257
186	65.0	90.0	9.6	Mean	.371	.514	-.029	-.014	.018	-.159
				Max	.702	1.036	.035	.063	.085	-.046
				Min	.137	.074	-.112	-.124	-.026	-.312
				Rms	.070	.124	.022	.021	.014	.032
				GFAC	1.892	2.013	3.835	8.871	4.791	1.963
				PFAC	4.747	4.205	3.820	5.156	4.863	4.744
187	65.0	90.0	9.8	Mean	.449	.621	-.042	-.004	.017	-.164
				Max	.799	1.256	.019	.070	.077	-.053
				Min	.244	.228	-.116	-.112	-.037	-.299
				Rms	.072	.124	.020	.022	.014	.034
				GFAC	1.777	2.022	2.733	25.021	4.526	1.817
				PFAC	4.826	5.125	3.685	4.853	4.415	3.926

SELECTED DISTRIBUTION LIST

ARCO Solar, Inc.
9315 Deering
Chatsworth, CA 91311
Mr. Jim Caldwell

Acurex Solar Corporation
485 Clyde Ave.
Mt. View, CA 94042
Mr. Don Duffy

Advanco Corporation
40701 Monterey Ave.
Palm Desert, CA 92260
Mr. Byron Washom

Arizona Public Service Company
P.O. Box 21666
Phoenix, AZ 85036
Mr. Eric Weber

Babcock and Wilcox
91 Stirling Ave.
Barberton, OH 44203
Mr. Paul Elsbree

Battelle Pacific NW Laboratory
P.O. Box 999
Richland, WA 99352
Dr. Ben Johnson
Dr. Kevin Drost
Mr. Tom A. Williams

Bechtel Corporation
P.O. Box 3965
San Francisco, CA 94119
Mr. Pascal deLaquil

Black and Veatch Consulting Engineers
1500 Meadow Lake Parkway
Kansas City, MO 64114
Dr. Charles Grosskreutz

Brumleve, Mr. Tom
Consultant
1512 N. Gate Road
Walnut Creek, CA 94598

Dan-Ka Products, Inc.
3862 South Kalamath
Englewood, CO 80110
Mr. Daniel Sallis

Department of Energy/ALO
P.O. Box 1500
Albuquerque, NM 87115
Mr. Dean Graves
Mr. Joe Weisiger
Mr. Nyles Lackey

Department of Energy/HQ
Forrestal Building
1000 Independence Ave., SW
Washington, DC 20585
Dr. H. Coleman
Mr. S. Gronich
Mr. C. Mangold
Mr. M. Scheve
Mr. Frank Wilkins

Department of Energy/SAO
1617 Cole Blvd.
Golden, CO 80401
Mr. Paul K. Kearns

El Paso Electric
P.O. Box 982
El Paso, TX 79960
Mr. James E. Brown

Electric Power Research Institute
P.O. Box 10412
Palo Alto, CA 94303
Mr. Donald Augenstein

Entech, Incorporated
P.O. Box 612246
DFW Airport, TX 75261
Mr. Walter Hesse

Foster Wheeler Solar Development Corp.
12 Peach Tree Hill Road
Livingston, NJ 07070
Mr. Robert J. Zoschak

Georgia Tech Research Institute
Energy and Materials Sciences Lab
Atlanta, GA 30332
Dr. Daniel O'Neil

LaJet Energy Company
P.O. Box 3599
Abilene, TX 79604
Mr. Monte McGlaun

Luz Engineering Corp.
15720 Ventura Blvd.
Suite 504
Encino, CA 91436
Dr. David Kearney

Martin Marietta
P.O. Box 179
Denver, CO 80201
Mr. Tom Tracey

McDonnell Douglas Astronautics
Company
5301 Bolsa Ave.
Huntington Beach, CA 92647
Mr. Jim Rogan

Meridian Corporation
5113 Leesburg Pike
Suite 700
Falls Church, VA 22041
Mr. Dinesh Kumar

NASA Lewis Research Center
21000 Brookpark Road
Cleveland, OH 44135
Dr. Dennis Flood

NASA-Johnson Space Center
NASA Road One - EPS
Houston, TX 77058
Mr. William Simon

Pacific Gas and Electric Company
3400 Crow Canyon Rd.
San Ramon, CA 94583
Mr. Gerry Braun
Mr. Joe Iannucci

Power Kinetics, Inc.
1223 Peoples Ave.
Troy, NY 12180
Mr. Bob Rogers

Rockwell International
Energy Systems Group
8900 DeSoto Ave.
Canoga Park, CA 91304
Mr. Tom H. Springer

Rockwell International Corp
Energy Technology Center
P.O. Box 1449
Canoga Park, CA 91304
Mr. W. L. Bigelow

Sandia National Laboratories
Solar Department 8453
Livermore, CA 94550
Mr. A Skinrood
Dr. R. A. Rinne

Sandia National Laboratories
Solar Energy Department 6220
P.O. Box 5800
Albuquerque, NM 87185
Mr. John Otts
Mr. James Leonard
Dr. Donald Schuler
Dr. Tom Mancini

Science Applications, Inc.
10401 Roselle Street
San Diego, CA 92121
Dr. Barry Butler

Solar Energy Industries Association
1717 Massachusetts Ave., NW, No. 503
Washington, DC 20036
Mr. Carlo La Porta
Mr. David Goren
Mr. Hal Seilstad

Solar Energy Research Institute
1617 Cole Blvd.
Golden, CO 80401
Mr. B. P. Gupta
Mr. G. Groff

Solar Kinetics, Inc.
P.O. Box 47045
Dallas, TX 75247
Mr. Gus Hutchison
Mr. David White

Southern California Edison
2244 Walnut Grove Avenue
Rosemead, CA 91770
Mr. Joe Reeves

Texas Tech University
Dept. of Electrical Engineering
Lubbock, TX 79409
Mr. Edgar A. O'Hair
Physics Department
Ms. Virginia K. Agarwal

University of Arizona
College of Engineering
Tucson, AZ 85721
Dr. Kumar Ramohalli

University of Houston
4800 Calhoun
106 SPA Building
Houston, TX 77004
Dr. Alvin Hildebrandt
Dr. Lorin Vant-Hull

☆U.S. GOVERNMENT PRINTING OFFICE:1987 -773 -098/ 60042

Document Control Page	1. SERI Report No. SERI/STR-253-3212	2. NTIS Accession No.	3. Recipient's Accession No.

4. Title and Subtitle Mean and Peak Wind Load Reduction on Heliostats	5. Publication Date September 1987
	6.
7. Author(s) J. A. Peterka, L. Tan, B. Bienkiewicz, J. E. Cermak	8. Performing Organization Rept. No.
9. Performing Organization Name and Address Fluid Mechanics & Wind Eng. Program Colorado State University Fort Collins, CO 80523	10. Project/Task/Work Unit No. 5131.311
	11. Contract (C) or Grant (G) No. (C) XK-6-06034-1 (G)
12. Sponsoring Organization Name and Address Solar Energy Research Institute A Division of Midwest Research Institute 1617 Cole Boulevard Golden, CO 80401-3393	13. Type of Report & Period Covered Technical Report
	14.

15. Supplementary Notes

Technical Monitor: A. Lewandowski

16. Abstract (Limit: 200 words)

This report presents the results of wind-tunnel tests supported through the Solar Energy Research Institute (SERI) by the Office of SolarThermal Technology of the U.S. Department of Energy as part of the SERI research effort on innovative concentrators. As gravity loads on drive mechanisms are reduced through stretched-membrane technology, the wind-load contribution of the required drive capacity increases in percentage. Reduction of wind loads can provide economy in support structure and heliostat drive. Wind-tunnel tests have been directed at finding methods to reduce wind loads on heliostats. The tests investigated both mean and peak forces, and moments. A significant increase in ability to predict heliostat wind loads and their reduction within a heliostat field was achieved. In addition, a preliminary review of wind loads on parabolic dish collectors was conducted, resulting in a recommended research program for these type collectors.

17. Document Analysis

a. Descriptors Dynamic Loads; Heliostats; Solar Concentrators, Stresses; Wind; Wind Loads, Wind Load Reduction; Dishes

b. Identifiers/Open-Ended Terms

c. UC Categories
62a

18. Availability Statement National Technical Information Service U.S. Department of Commerce 5285 Port Royal Road Springfield, Virginia 22161	19. No. of Pages 240
	20. Price A11

Form No. 0069 (6-30-87)